

Chaos Synchronization and Its Application to Secure Communication

by

Hongtao Zhang

A thesis

presented to the University of Waterloo

in fulfillment of the

thesis requirement for the degree of

Doctor of Philosophy

in

Electrical and Computer Engineering

Waterloo, Ontario, Canada, 2010

©Hongtao Zhang 2010

I hereby declare that I am the sole author of this thesis. This is a true copy of the thesis, including any required final revisions, as accepted by my examiners.

I understand that my thesis may be made electronically available to the public.

Abstract

Chaos theory is well known as one of three revolutions in physical sciences in 20th-century, as one physicist called it: "Relativity eliminated the Newtonian illusion of absolute space and time; quantum theory eliminated the Newtonian dream of a controllable measurable process; and chaos eliminates the Laplacian fantasy of deterministic predictability". Specially, when chaos synchronization was found in 1991, chaos theory becomes more and more attractive. Chaos has been widely applied to many scientific disciplines: mathematics, programming, microbiology, biology, computer science, economics, engineering, finance, philosophy, physics, politics, population dynamics, psychology, and robotics. One of most important engineering applications is secure communication because of the properties of random behaviours and sensitivity to initial conditions of chaos systems. Noise-like dynamical behaviours can be used to mask the original information in symmetric cryptography. Sensitivity to initial conditions and unpredictability make chaotic systems very suitable to construct one-way function in public-key cryptography. In chaos-based secure communication schemes, information signals are masked or modulated (encrypted) by chaotic signals at the transmitter and the resulting encrypted signals are sent to the corresponding receiver across a public channel (unsafe channel). Perfect chaos synchronization is usually expected to recover the original information signals. In other words, the recovery of the information signals requires the receiver's own copy of the chaotic signals which are synchronized with the transmitter ones. Thus, chaos synchronization is the key technique throughout this whole process.

Due to the difficulties of generating and synchronizing chaotic systems and the limit of digital computer precision, there exist many challenges in chaos-based secure communica-

tion. In this thesis, we try to solve chaos generation and chaos synchronization problems. Starting from designing chaotic and hyperchaotic system by first-order delay differential equation, we present a family of novel cell attractors with multiple positive Lyapunov exponents. Compared with previously reported hyperchaos systems with complex mathematic structure (more than 3 dimensions), our system is relatively simple while its dynamical behaviours are very complicated. We present a systemic parameter control method to adjust the number of positive Lyapunov exponents, which is an index of chaos degree. Furthermore, we develop a delay feedback controller and apply it to Chen system to generate multi-scroll attractors. It can be generalized to Chua system, Lorenz system, Jerk equation, etc.

Since chaos synchronization is the critical technique in chaos-based secure communication, we present corresponding impulsive synchronization criteria to guarantee that the receiver can generate the same chaotic signals at the receiver when time delay and uncertainty emerge in the transmission process. Aiming at the weakness of general impulsive synchronization scheme, i.e., there always exists an upper boundary to limit impulsive intervals during the synchronization process, we design a novel synchronization scheme, intermittent impulsive synchronization scheme (IISS). IISS can not only be flexibly applied to the scenario where the control window is restricted but also improve the security of chaos-based secure communication via reducing the control window width and decreasing the redundancy of synchronization signals. Finally, we propose chaos-based public-key cryptography algorithms which can be used to encrypt synchronization signals and guarantee their security across the public channel.

Acknowledgments

First and foremost, I would like to express my deepest gratitude to my advisors, Professor Xuemin (Sherman) Shen and Professor Xinzhi Liu. Thank them for expert guidance, help and encouragement throughout my PH.D. studies. From them, I have learned not only how to do research but also how to achieve a brilliant life. Also, from them, I have learned the ability to find problems, define problems and solve problems. Most importantly, from them, I find out the key to success: diligence, confidence and patience.

I would like to express my extreme appreciation to my thesis committee members: Professor N. U. Ahmed, Professor Wei-Chau Xie, Professor Liang-Liang Xie and Professor Zhou Wang. Thank them for their precious time to read my thesis and their valuable suggestions and comments are greatly appreciated, which are very important for improving the quality of this thesis.

I would like to express the special gratitude to Professor Lin Cai, Dr. Jun Liu, Dr. Lijun Wang, Dr. Rongxing Lu and Dr. Hoting (Anderson) Cheng, who gave me many advices and help on my research. Also, thank my friends and all members in BBCR group and Applied Mathematics for their support and friendship. I am very lucky and happy to work with so many great talents. Thank them for enriching my life with pleasure and sunshine.

Thanks to the administrative and technical supporting staffs at the Department of Electrical and Computer Engineering. I was very impressed by their enthusiasm and patience. I am also grateful to University of Waterloo for providing such a friendly research environment throughout my studies.

I would never get so far without the support of my dear parents, sisters and girlfriend. Thank them for standing by my side all the time. One day, I will repay them with success for their unchanging love and encouragement.

To my dear parents

Table of Contents

List of Tables	xi
List of Figures	xii
1 Introduction	1
1.1 Chaotic System	1
1.2 Secure Communication	5
1.3 Motivation	7
1.4 Research Contributions	8
1.5 Thesis Outline	9
2 Related Work	11
2.1 Existing Chaotic Systems	11
2.2 Related Mathematical Background	21
2.3 Chaos-Based Secure Communication Scheme	27
2.4 Chaos-Based Public-Key Cryptography	31
3 Generating New Chaos and Hyperchaos	33
3.1 Generating New Chaos and Hyperchaos from Delay Differential Equation . .	33

3.1.1	Background	33
3.1.2	New Chaotic Attractor	34
3.1.3	General Form of DDE Generating Chaos	45
3.1.4	Summary	52
3.2	Generating Multi-Scroll Chaos and Hyperchaos from Chen System	52
3.2.1	System Statement	52
3.2.2	Dynamical Analysis	53
3.2.3	Generalized More-Scroll Chaos	56
3.2.4	Generalized More Complex Chaos and Hyperchaos	63
3.2.5	Summary	72
4	Impulsive Synchronization of Chaotic Systems with Delay	73
4.1	Synchronization of Two Chaotic Systems with Delay	73
4.1.1	Background	73
4.1.2	System Statement and Synchronization Scheme	74
4.1.3	Main Results	76
4.1.4	Numerical Example	80
4.1.5	Summary	83
4.2	Synchronization of Chaotic Dynamical Networks with Delay	85
4.2.1	Background	85
4.2.2	Preliminaries and Problem Formulation	86
4.2.3	Main Results	87
4.2.4	Numerical Example	96
4.2.5	Summary	97

5	Adaptive Network Synchronization Subject to Different Network Nodes	100
5.1	Introduction	100
5.2	Preliminaries	102
5.3	Adaptive Controller Design for Network Synchronization	103
5.4	Numerical Examples	111
5.5	Summary	119
6	A Novel Synchronization Approach: Intermittent Impulsive Synchronization	122
6.1	Intermittent Impulsive Synchronization of Two Chaotic Systems with Delay .	122
6.1.1	Introduction	122
6.1.2	Preliminaries	123
6.1.3	Synchronization Criteria	127
6.1.4	Numeral Examples	135
6.1.5	Summary	138
6.2	Intermittent Impulsive Synchronization of Delayed Chaotic Neural Networks	142
6.2.1	Introduction	142
6.2.2	Preliminaries	142
6.2.3	Synchronization Criteria	145
6.2.4	Numeral Example	157
6.2.5	Summary	161
7	Chaos-Based Public-Key Cryptography	163
7.1	Kocarev's Algorithm	163
7.2	Bergamo's Attack	165
7.3	Chaos-Based Public-Key Cryptography with Modified Chebyshev Polynomials	166

7.3.1	ElGamal Encryption with Modified Chebyshev Polynomials	166
7.3.2	RSA Public-Key Encryption with Modified Chebyshev Polynomials	168
7.3.3	An Example	169
7.4	Summary	170
8	Conclusions and Future Work	171
8.1	Contributions	171
8.2	Future Work	172
8.2.1	Synchronization Error Problem	173
8.2.2	Computer Realization of Chaos-Based Algorithms	173
	Bibliography	174

List of Tables

- 3.1 List of equilibrium points and responding roots of characteristic equations. . 55

List of Figures

1.1	(a)-(b): The phase portrait $x - z$ of the Lorenz attractor, respectively starting at $(15.00000, 15.00000, 30.00000)$ and $(15.00001, 15.00000, 30.00000)$; (c)-(d): The trajectory portrait of state variables z_1, z_2 and $z_2 - z_1$, starting at two initial points that differ only by 10^{-5} in the x-coordinate.	3
2.1	The portrait of the Lorenz attractor with $a = 10, b = 28$ and $c = 8/3$	12
2.2	The portrait of the Rössler attractor with $a = 0.2, b = 5.7$ and $c = 0.2$	13
2.3	The portrait of the Chen attractor with $a = 35, b = 3$ and $c = 28$	13
2.4	The portrait of the Jerk system $J = -ax'' - ax' + a \sin(2\pi bx)$ with $a = 0.3$ and $b = 0.25$	14
2.5	The trajectory of the Logistic map with $A = 4$ starting from $X(0) = 0.73$	15
2.6	The trajectory of the Tent map with $r = 0.9$ starting from $X(0) = 0.75$	15
2.7	The trajectory of the Gaussian map with $b = 7.5$ and $c = -0.3$ starting from $X(0) = 0.75$	16
2.8	The portrait of the Hénon attractor with $a = 1.4$ and $b = 0.3$ starting from $(0.25, 0.25)$	17
2.9	The portrait of the Chua circuit with $a_1 = 9, a_2 = 14.286, a_3 = 1, m_0 = -1/7$ and $m_1 = 1.5/7$	17

2.10	The portrait of the chaotic attractor by switching two linear systems starting from $(10, 0, 0)$	19
2.11	The portrait of the Mackey-Glass system with $\tau = 8$	20
2.12	The portrait of the Ikeda equation with $\mu = 20$ and $\tau = 2$	20
2.13	Two trajectories in phase space with initial separation Z_1	26
2.14	The principle diagram of chaos-based secure communication.	27
2.15	The principle diagram of state feedback control synchronization.	28
2.16	The principle diagram of impulsive control synchronization.	30
3.1	The trajectory portrait of vector $x(t)$, when $a = 0.8, b = 0.2, c = 0.5, d = 1.8$, and $\tau = 4.8$	35
3.2	The phase of $x(t - \tau) - x(t)$, when $a = 0.8, b = 0.2, c = 0.5, d = 1.8$, and $\tau = 4.8$	35
3.3	The phase of $x(t - \tau) - x(t)$, when (a): $\tau = 5$, (b): $\tau = 5.5$, (c): $\tau = 6$, (d): $\tau = 8$	36
3.4	The roots of the characteristic equations of system (3.1) at the equilibrium points (a) $x^* = 0$ and (b) $x^* = \pm 1.4119$	37
3.5	The Lyapunov spectrum of system (3.1) with parameters $N = 100$ and initial condition $x_0 = rand(100)$	38
3.6	The bifurcation diagram for the responding discretized system of (3.1) vs the parameter c with $a = 0.8, b = 0.2, d = 1.8$ and $\tau = 4.8$	38
3.7	The bifurcation diagram for the responding discretized system of (3.1) vs the delayed time τ with $a = 0.8, b = 0.2, c = 0.5$ and $d = 1.8$	39
3.8	The phase of $x(t - \tau) - x(t)$, when (a): $\tau = 4$, (b): $\tau = 8$	43

3.9	The phase of $x(t - \tau) - x(t)$, when (a): $\tau = 2.5$, (b): $\tau = 4$, (c): $\tau = 6$, (d): $\tau = 8$	44
3.10	The phase of $x(t - \tau) - x(t)$ with $c = 3.0$, when (a): $\tau = 1.5$, (b): $\tau = 3$, (c): $\tau = 4$, (d): $\tau = 5$, (e): $\tau = 6$, (f): $\tau = 8$	46
3.11	The first six Lyapunov exponents vs parameter c in $[0.5 \quad 3]$ with $a = 0.8$, $b = 0.2$, $d = 1.8$ and $\tau = 8.0$	47
3.12	The phase of $x(t) - x(t - \tau_2)$, when (a): $\tau_2 = 4$; (b): $\tau_2 = 8$	48
3.13	The phase of $x(t) - x(t - \tau_1) - x(t - \tau_2)$, when $\tau_1 = 4, \tau_2 = 6$	48
3.14	The phase of $x(t) - x(t - \tau_1) - x(t - \tau_2)$, when $\tau_1 = 4, \tau_2 = 8$	49
3.15	The phase of $x(t) - x(t - \tau_1) - x(t - \tau_2)$, when $\tau_1 = 1, \tau_2 = 10$	50
3.16	The phase of $x(t - \tau_2) - x(t - \tau_1) - x(t)$, when $\tau_1 = 2, \tau_2 = 4$	51
3.17	Chen chaotic attractor with $a = 35$, $b = 3$ and $c = 28$, starting from $[1, 1, 1]$	53
3.18	The phase portraits of controlled Chen system. (a) z-x-y; (b) x-y; (c) x-z; (d) y-z.	54
3.19	The roots of the characteristic equations of system (3.22) responding to equilibrium points $(\pm 6.9995, \pm 6.9995, 16.3311)$	56
3.20	The Lyapunov spectrum of system (3.22) with parameters $t = 1000$, starting from $(1, 1, 30)$	57
3.21	The phase portraits of system (3.22) with $d_2 = 5$, starting from $(1, 1, 30)$. (a) z-x-y; (b) x-y; (c) x-z; (d) y-z.	58
3.22	The phase portraits of system (3.22) with $d_2 = 14$, starting from $(1, 1, 30)$. (a) z-x-y; (b) x-y; (c) x-z; (d) y-z.	59
3.23	The phase portraits of system (3.22) with $d_2 = 22$, starting from $(1, 1, 30)$. (a) z-x-y; (b) x-y; (c) x-z; (d) y-z.	60

3.24	The phase portraits of system (3.22) with $d_2 = 28$, starting from $(1, 1, 30)$. (a) z-x-y; (b) x-y; (c) x-z; (d) y-z.	61
3.25	All Lyapunov exponents vs parameter d_2 in $[5 \ 25]$ with $a = 35$, $b = 3$, $c = 28$ and $d_1 = 1$	62
3.26	The phase portraits of system (3.24) with $d_0 = 1$, $d_1 = 1$, $d_2 = 5$ and $\tau = 0.1$.	64
3.27	The phase portraits of system (3.24) with $d_0 = 1$, $d_1 = 1$, $d_2 = 5$ and $\tau = 0.8$.	65
3.28	The phase portraits of system (3.24) with $d_0 = 1$, $d_1 = 1$, $d_2 = 30$ and $\tau = 0.05$	66
3.29	The phase portraits of system (3.24) with $d_0 = 1$, $d_1 = 1$, $d_2 = 30$ and $\tau = 0.8$.	67
3.30	The phase portraits of system (3.24) with $d_0 = 0.2$, $d_1 = 2$, $d_2 = 5$ and $\tau = 5$.	68
3.31	The phase portraits of system (3.24) with $d_0 = 0.2$, $d_1 = 2$, $d_2 = 40$ and $\tau = 5$.	69
3.32	The phase portraits of system (3.24) with $d_0 = 1$, $d_1 = -0.2$, $d_2 = 20$ and $\tau = 5$	70
3.33	The phase portraits of system (3.24) with $d_0 = 1$, $d_1 = -0.8$, $d_2 = 5$ and $\tau = 5$	71
4.1	(x_1, x_2, x_3) of the master system.	82
4.2	e_1 of the error system without delay.	82
4.3	e_1 of the error system with $\gamma_i = 0.05$	83
4.4	e_1 of the error system with $\tilde{\gamma} = 0.04$, $\gamma_i = 0.02$	84
4.5	e_1 of the error system without delay.	84
4.6	(x_1, x_2, x_3) of the isolate node of Chua's circuit starting from $(1, 1, 2)$	97
4.7	the portrait of (e_{11}, e_{21}, e_{31}) of the error system.	98
4.8	the portrait of (e_{12}, e_{22}, e_{23}) of the error system.	98
4.9	the portrait of (e_{13}, e_{23}, e_{33}) of the error system.	99

5.1	Synchronization errors, (a) e_{i1} , (b) e_{i2} , (c) e_{i3} for unknown constant parameters.	115
5.2	System parameters and their estimates: (a) nodes (1) – (10), (b) nodes (11) – (20), (c) nodes (21) – (30), and (d) the isolated oscillator, for unknown constant parameters.	116
5.3	Synchronization errors, (a) e_{i1} , (b) e_{i2} , (c) e_{i3} for unknown bounded parameters with $\Theta_i = 0.5$ and $\Psi = 1$.	117
5.4	System parameters and their estimates: (a) nodes (1) – (10), (b) nodes (11) – (20), (c) nodes (21) – (30), and (d) the isolated oscillator, for unknown bounded parameters with $\Theta_i = 0.5$ and $\Psi = 1$.	118
5.5	Synchronization errors, (a) e_{i1} , (b) e_{i2} , (c) e_{i3} for $\tilde{\Theta}_i = 0.01$ and $\tilde{\Psi} = 0.1$.	120
5.6	System parameters and their estimates: (a) nodes (1) – (10), (b) nodes (11) – (20), (c) nodes (21) – (30), and (d) the isolated oscillator, for $\tilde{\Theta}_i = 0.01$ and $\tilde{\Psi} = 0.1$.	121
6.1	Phase portrait $x(t - 5) - x(t)$ of the hyperchaotic system with $a = 0.8$, $b = 0.2$, $c = 3$, $d = 1.8$ and $\tau = 5$.	136
6.2	Synchronization error $e(t)$ with $\tau \leq \omega - \delta$, starting from initial conditions $\phi = rand$ and $\psi = 2 * rand$.	137
6.3	Synchronization error $e(t)$ with $\tau > \omega - \delta$, starting from initial conditions $\phi = rand$ and $\psi = 2 * rand$.	138
6.4	Phase portrait $x_1(t) - x_2(t)$ of Lu oscillator with system parameters $a = 0.8$, $b = 0.2$, $c = 3$, $d = 1.8$ and $\tau = 5$.	139
6.5	Synchronization errors (a) $e_1(t)$ and (b) $e_2(t)$ with $\Delta_{k,i} = 1.0$ and $B_{k,i} = 0.95I$.	140
6.6	Synchronization errors (a) $e_1(t)$ and (b) $e_2(t)$ with $\Delta_{k,i} = 1.3$ and $B_{k,i} = 0.95I$.	141

6.7	Phase portrait $x_1(t) - x_2(t)$ of DNNs (6.90) with system parameters $\Delta_{k,i} = 1.1$ and $B_k = 0.90I$	158
6.8	State trajectories of the master system (left) and the slave system in GISS. . .	159
6.9	Synchronization errors in GISS: (a) $e_1(t)$ and (b) $e_2(t)$ with $\Delta_{k,i} = 1.1$ and $B_k = 0.90I$	159
6.10	State trajectories of the master system (left) and the slave system in IISS. . .	160
6.11	Synchronization errors in IISS: (a) $e_1(t)$ and (b) $e_2(t)$ with $\Delta_{k,i} = 1.1$ and $B_k = 0.90I$	161
6.12	The relationship between the impulsive interval and the free window width to guarantee synchronization.	162
7.1	The framework diagram of symmetric chaos-based secure communication scheme.	164

Chapter 1

Introduction

1.1 Chaotic System

Henri Poincaré was the first discoverer of chaos. In 1890, while studying the three-body problem, he found that there existed some orbits which are non-periodic, and yet not forever increasing nor approaching a fixed point [1]. The main catalyst for the development of chaos theory is the electronic computer. Computers allow one to solve the nonlinear differential equations numerically that was impossible before. Computer graphics provides an easy way to visualize the behaviors of nonlinear systems.

In 1961, Edward Lorenz, the MIT meteorologist, whose interest in chaos came accidentally from his work on weather prediction, used a simple digital computer, a Royal McBee LGP-30, to run his weather simulation. He wanted to see a sequence of data again and to save time he started the simulation in the middle of his course. He was able to do this by entering a printout of the data corresponding to conditions in the middle of his simulation which he had calculated last time. To his surprise the weather that the machine began to predict was completely different from the weather calculated before. Lorenz tracked this down to the computer printout. The computer worked with 6-digit precision, but the printout rounded variables off to a 3-digit number, so a value like 0.506127 was printed as 0.506.

This difference is tiny and the consensus at the time would have been that it should have had practically no effect. However, Lorenz had discovered that small changes in initial conditions produced large changes in the long-term outcome. Lorenz’s discovery, which gave its name to Lorenz attractors, proved that meteorology could not reasonably predict weather beyond a weekly period. The Lorenz equation [2], which was derived from the simplified equations of convection rolls arising in the equations of the atmosphere by Edward Lorenz, is a nonlinear autonomous deterministic three-dimensional system as follows.

$$\begin{cases} \dot{x} = a(y - x) \\ \dot{y} = rx - xz - y \\ \dot{z} = xy - bz \end{cases} \quad (1.1)$$

where a is called the Prandtl number and r is called the Rayleigh number. All $a, b, r > 0$, but usually $a = 10$, $b = 8/3$ and r is varied. Fig. 1.1(a)-(b) show the phase portraits $x - z$ for the same period of time $t = 30$, respectively starting at $(15.00000, 15.00000, 30.00000)$ and $(15.00001, 15.00000, 30.00000)$. Fig. 1.1(c)-(d) show the trajectory of state variable z , starting at two initial points that differ only by 10^{-5} in the x -coordinate. Initially, the two trajectories seem coincident, as indicated by the small difference between the z coordinate of the blue and magenta trajectories, but for $t > 15$ the difference is as large as the value of the trajectory. This phenomenon is called as butterfly effect. ”Predictability: does the flap of a butterfly’s wings in Brazil set off a tornado in Texas?” was presented by Edward Lorenz in 1972. The butterfly effect is a phrase that encapsulates the more technical notion of sensitive dependence on initial conditions in chaos theory. Small variations of the initial condition of a dynamical system may produce large variations in the long term behavior of the system. So this is sometimes presented as esoteric behavior.

It is a milestone in the development of chaos theory that Lorenz attractor was presented. Since then, chaos research has become a very hot issue. Numerous chaos analysis methods were achieved such as Lyapunov exponents, bifurcation analysis, boundedness, equilibrium points analysis, etc. Specially, to control chaos to stable periodic orbits attracted lots of in-

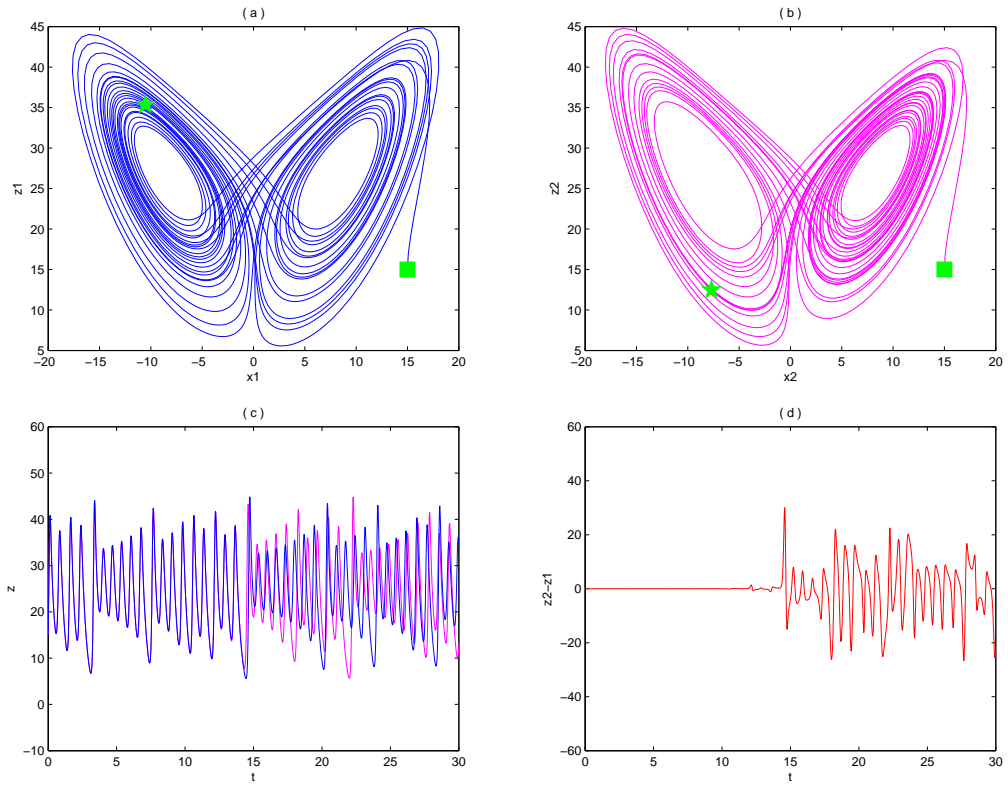


Figure 1.1: (a)-(b): The phase portrait $x - z$ of the Lorenz attractor, respectively starting at $(15.00000, 15.00000, 30.00000)$ and $(15.00001, 15.00000, 30.00000)$; (c)-(d): The trajectory portrait of state variables z_1, z_2 and $z_2 - z_1$, starting at two initial points that differ only by 10^{-5} in the x -coordinate.

terest of researchers and expects. Several techniques have been devised for chaos control, but most are developments of two basic approaches: the OGY (Ott, Grebogi and Yorke) method [3] and Pyragas continuous control [4]. Both methods require a previous determination of the unstable periodic orbits of the chaotic system before the control algorithm can be designed.

In 1990, Pecora and Carroll reported that two autonomous chaotic systems can be synchronized [5]. It is another milestone in chaos research. Subsequently, many synchronization methods were presented such as state feedback synchronization [6–12], impulsive synchronization [13–20]. Chaos theory was applied to many engineering areas. Specially, secure communication based chaos rapidly developed [21–39]. In 1993, Cuomo and Oppenheim presented the first scheme of a communications device made by two identical Lorenz oscillators [22]. In 1997, Kolumban, Kennedy and Chua realized digital communications based on chaos synchronization [24, 25]. After that, symmetric cryptography based on chaos grew up fast. In 2003, Kocarev and Tasev presented a public-key cryptography based on Chebyshev chaotic maps [37]. It rapidly became a new direction of chaos communications and attracted lots of attentions.

Chaos is used to describe the behavior of certain dynamical systems, i.e., systems whose state variables evolve with time, which may exhibit dynamics that are highly sensitive to initial conditions. As a result of this sensitivity, which manifests itself as an exponential growth of perturbations in the initial conditions, the behavior of chaotic systems appears to be random. This happens even though these systems are deterministic, meaning that their future dynamics are fully defined by their initial conditions, with no random elements involved. This behavior is known as deterministic chaos. For a dynamical system to be classified as chaotic, it must have the following properties:

1. it is sensitive to initial conditions;
2. it is topologically mixing;
3. its periodic orbits are dense.

Chaos has become 20th-century's third great revolution in physical sciences [40]. Like the first two revolutions, the relativity theory of Albert Einstein, which introduced the relativity of space and time, the quantum theory of Max Planck, which introduced the indeterminism to the description of nature, chaos cuts away the tenets of Newton's physics. As one physicist called it: "Relativity eliminates the Newtonian illusion of absolute space and time; quantum theory eliminates the Newtonian dream of a controllable measurable process; and chaos eliminates the Laplacian fantasy of deterministic predictability."

1.2 Secure Communication

Cryptography is the practice and study of hiding information. The modern field of cryptography can be divided into two areas of study, symmetric cryptography and public-key cryptography.

Symmetric cryptography refers to encryption methods in which both the sender and receiver share the same key (or, less commonly, in which their keys are different, but related in an easily computable way).

The modern study of symmetric ciphers relates mainly to the study of block ciphers and stream ciphers and to their applications. A block cipher is, in a sense, a modern embodiment of Alberti's polyalphabetic cipher: block ciphers take a block of plain-text and a key as input, and output a block of cipher-text of the same size. Since messages are almost always longer than a single block, some method of knitting together successive blocks is required. Several have been developed, some with better security in one aspect or another than others. They are the mode of operations and must be carefully considered when using a block cipher in a cryptosystem.

The Data Encryption Standard (DES) and the Advanced Encryption Standard (AES) are block cipher designs which have been designated cryptography standards by the US government (though DES's designation was finally withdrawn after the AES was adopted). Despite

its deprecation as an official standard, DES (especially its still-approved and much more secure triple-DES variant) remains quite popular; it is used across a wide range of applications, from ATM encryption to email privacy and secure remote access. Many other block ciphers have been designed and released, with considerable variation in quality. Many have been thoroughly broken.

Stream ciphers, in contrast to the 'block' type, create an arbitrarily long stream of key material, which is combined with the plain-text bit-by-bit or character-by-character, somewhat like the one-time pad. In a stream cipher, the output stream is created based on an internal state which changes as the cipher operates. That state change is controlled by the key and, in some stream ciphers, by the plain-text stream as well. RC4 is an example of a well-known and widely used stream cipher.

Symmetric cryptosystems use the same key for encryption and decryption of a message, though a message or group of messages may have a different key than others. A significant disadvantage of symmetric ciphers is the key management necessary to use them securely. Each distinct pair of communicating parties must, ideally, share a different key, and perhaps each cipher-text exchanged as well. The number of keys required increases as the square of the number of network members, which very quickly requires complex key management schemes to keep them all straight and secret. The difficulty of securely establishing a secret key between two communicating parties, when a secure channel doesn't already exist between them, also presents a chicken-and-egg problem which is a considerable practical obstacle for cryptography users in the real world.

In a ground-breaking 1976 paper [41], Whitfield Diffie and Martin Hellman proposed the notion of public-key (also, more generally, called asymmetric key) cryptography in which two different but mathematically related keys are used as a public key and a private key. A public key system is so constructed that calculation of one key (the private key) is computationally infeasible from the other (the public key), even though they are necessarily related. Instead, both keys are generated secretly, as an interrelated pair. The historian David Kahn

described public-key cryptography as "the most revolutionary new concept in the field since polyalphabetic substitution emerged in the Renaissance".

In public-key cryptosystems, the public key may be freely distributed, while its paired private key must remain secret. The public key is typically used for encryption, while the private or secret key is used for decryption. Diffie and Hellman showed that public-key cryptography was possible by presenting the Diffie-Hellman key exchange protocol [42].

In 1978, Ronald Rivest, Adi Shamir, and Len Adleman invented RSA, another public-key system [43]. In 1997, it finally became publicly known that asymmetric key cryptography had been invented by James H. Ellis at GCHQ, a British intelligence organization, and that, in the early 1970s, both the Diffie-Hellman and RSA algorithms had been previously developed (by Malcolm J. Williamson and Clifford Cocks, respectively) [44]. The Diffie-Hellman and RSA algorithms, in addition to being the first publicly known examples of high quality public-key algorithms, have been among the most widely used. Others include the Cramer-Shoup cryptosystem, ElGamal encryption, and various elliptic curve techniques.

1.3 Motivation

It is well known that deterministic chaos systems have random behaviors which look like noise. In symmetric chaos-based secure communication schemes, two chaotic oscillators are required as a transmitter (or master) and receiver (or slave). One can use chaotic signals to mask the plain-text at the transmitter and then the cipher-text is sent to the receiver across public channels. Because of the property of noise-like dynamics, it is very difficult for the eavesdropper to distinguish the cipher-text from noise. At the receiver, by chaos synchronization, one can achieve almost identical chaotic signals. Then, using this chaotic signals, one can easily recover the plain-text from cipher-text.

Chaos systems have another important property: sensitivity to initial conditions. It is natural for public-key cryptography. In chaos-based public-key cryptography, one can use

chaotic systems to construct one-way function. In term of the non-prediction, it is almost impossible to inversely computer the private key from the public key. In addition, theoretically, the trajectory of autonomous chaos is not intersected forever, thus there does not exist collision for attackers. In chaos-based secure communication schemes, we need chaos-based public-key cryptography to guarantee the security of synchronization signals across public channel.

There still exist some problems in chaos-based secure communication. Firstly, due to the non-perfect of chaos theory and the limit of the methods of generating chaos, sometimes the attackers can find out the chaos system used in encryption by state reconstruction. Secondly, due to the time delay in transmission and sample process, chaos synchronization is hard to be achieved. Finally, due to the limit of digital computer precision, computer chaotic maps are always periodic: all trajectories are eventually periodic. Therefore, there exist collisions for attackers to break down the chaos-based public-key cryptography. Based on the above three existing challenges, our research goals are:

1. to design more complex chaotic and hyperchaotic systems to avoid chaos carriers to be reconstructed;
2. to achieve new synchronization criteria to overcome the impact of time delay and uncertainty in chaos synchronization and network synchronization; and
3. to apply suitable public-key algorithms to chaos-based secure communication schemes to guarantee the security of synchronization signals across the public channel.

1.4 Research Contributions

This research focuses on studying two most critical problems in chaos-based secure communication: generation of chaos and chaos synchronization. In addition, we introduce the development of chaos-based public-key algorithms, which can be used to encrypt the synchronization signals across the public channel. Specifically, the main contributions of this

thesis are:

(1) A family of chaos and hyperchaos attractors from first-order delay differential equation are presented. With adjusting some system parameters, the system can exhibit a set of very interesting dynamical behaviors such as Hopf bifurcation and chaos. Furthermore, we introduce this kind of delay feedback control to well-known Chen system and then multi-scroll chaotic attractors are achieved.

(2) In chaos-based secure communication scheme, chaos synchronization is the critical issue. Aiming at the time delay in transmission and sample process, we present corresponding impulsive synchronization criteria and generalize them to dynamical networks. Specifically, some adaptive network synchronization criteria are achieved subject to different network nodes and uncertain system parameters. In the end, one new synchronization scheme, intermittent impulsive synchronization scheme, is presented to overcome the limit of general impulsive synchronization scheme, which is that there always exists an upper boundary to limit impulsive intervals.

(3) In chaos-based secure communication scheme, another important problem is how to guarantee the security of synchronization signals across the public channel. Chaos-based public-key cryptography plays a key role in this process. We introduce some proposed algorithms and their weaknesses. To construct new chaotic maps and to design new algorithms to improve the security of chaos-based public-key cryptography will have a promising perspective.

1.5 Thesis Outline

The remainder of this thesis is organized as follows. In chapter 2, we introduce some background knowledge and related works on chaos-based secure communication scheme. In chapter 3, we present two systematical methods to construct multi-scroll chaotic and hyperchaotic systems. In chapter 4, we study impulsive synchronization criteria of two identical

chaos with delay and generalize them to chaotic dynamical networks. In chapter 5, we study adaptive network synchronization subject to different network nodes and uncertain system parameters. In chapter 6, a novel synchronization scheme, called intermittent impulsive synchronization scheme, is presented. In chapter 7, chaos-based public-key cryptography is proposed to guarantee the security of synchronization signals across public channel. Conclusions and future work are followed in chapter 8.

Chapter 2

Related Work

2.1 Existing Chaotic Systems

Since the Lorenz attractor was found in 1963, chaos research attracted lots of attentions of scholars and experts. Many kind of new chaotic and hyperchaotic systems were presented subsequently. In term of different mathematic models and properties, chaotic systems can be classed as continuous chaos, discrete chaotic maps, switched chaos, delay chaos, hyperchaos and so on. Some representative systems are introduced as follows.

1. Continuous chaos. Besides the Lorenz system [2] referred before, the well-known Rössler chaos [45], Chen attractor [46] and Jerk function [47] also are continuous chaotic systems.

(a) Lorenz system. The mathematic equation is given as follows

$$\begin{cases} \dot{x}_1 = a(x_2 - x_1) \\ \dot{x}_2 = bx_1 - x_2 - x_1x_3 \\ \dot{x}_3 = -cx_3 + x_1x_2 \end{cases} \quad (2.1)$$

and the portrait of state vectors is shown in Fig. 2.1.

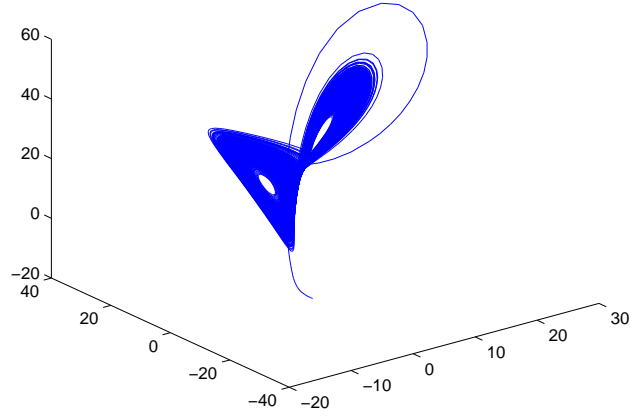


Figure 2.1: The portrait of the Lorenz attractor with $a = 10$, $b = 28$ and $c = 8/3$.

(b) Rössler system. The mathematic equation is given as follows

$$\begin{cases} \dot{x}_1 = -x_2 - x_3 \\ \dot{x}_2 = x_1 + ax_2 \\ \dot{x}_3 = x_1x_3 - bx_3 + c \end{cases} \quad (2.2)$$

and the portrait of state vectors is shown in Fig. 2.2.

(c) Chen system. The mathematic equation is given as follows

$$\begin{cases} \dot{x}_1 = a(x_2 - x_1) \\ \dot{x}_2 = (c - a)x_1 - x_1x_3 + cx_2 \\ \dot{x}_3 = -bx_3 + x_1x_2 \end{cases} \quad (2.3)$$

and the portrait of state vectors is shown in Fig. 2.3.

(d) Jerk equation (time derivative of acceleration). The mathematic equation is given as follows

$$x''' = J(x'', x', x) \quad (2.4)$$

and the portrait of state vectors is shown in Fig. 2.4.

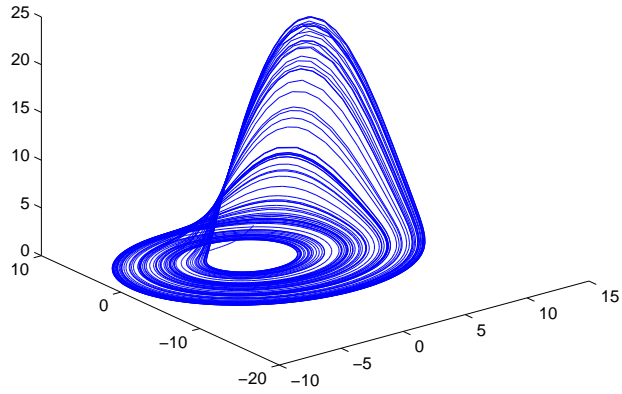


Figure 2.2: The portrait of the Rössler attractor with $a = 0.2$, $b = 5.7$ and $c = 0.2$.

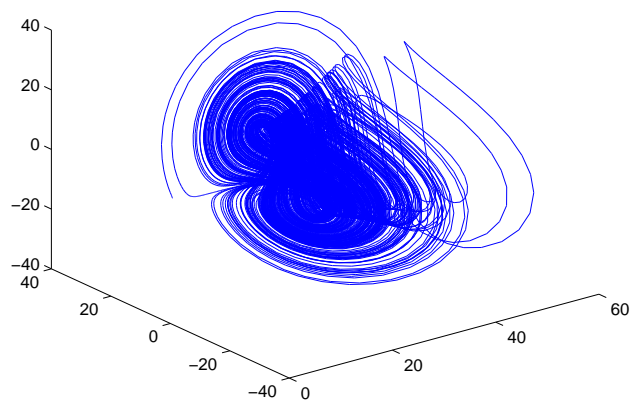


Figure 2.3: The portrait of the Chen attractor with $a = 35$, $b = 3$ and $c = 28$.

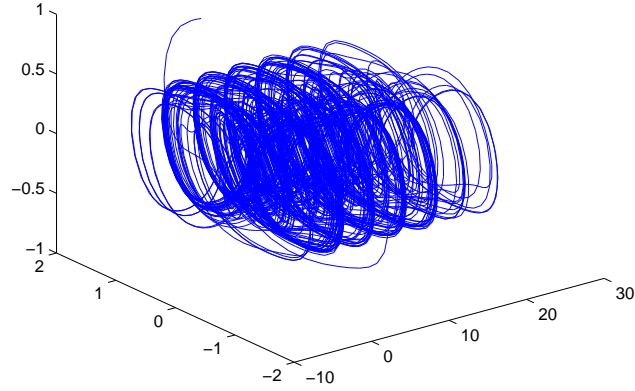


Figure 2.4: The portrait of the Jerk system $J = -ax'' - ax' + a \sin(2\pi bx)$ with $a = 0.3$ and $b = 0.25$.

2. Discrete chaos. The most famous discrete chaotic system is the logistic map, which is one of Chebyshev maps. Also there exist many other discrete chaotic maps such as Tent map, Gaussian map, Hénon map and so on.

(a) Logistic map. The mathematic equation is given as follows

$$x_{n+1} = Ax_n(1 - x_n), \quad x_0 \in [0, 1]. \quad (2.5)$$

and the trajectory is shown in Fig. 2.5.

(b) Tent map. The mathematic equation is given as follows

$$x_{n+1} = r(1 - 2|x_n - 1/2|), \quad x_0 \in [0, 1]. \quad (2.6)$$

and the trajectory is shown in Fig. 2.6.

(c) Gaussian map. The mathematic equation is given as follows

$$x_{n+1} = e^{-bx_n^2} + c, \quad x_0 \in [0, 1]. \quad (2.7)$$

and the trajectory is shown in Fig. 2.7.

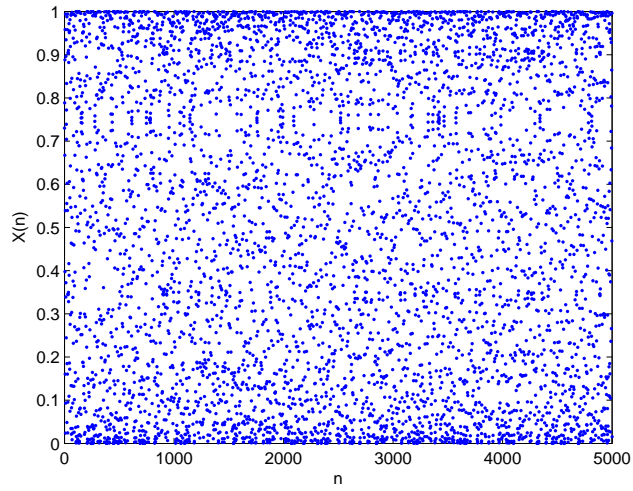


Figure 2.5: The trajectory of the Logistic map with $A = 4$ starting from $X(0) = 0.73$.

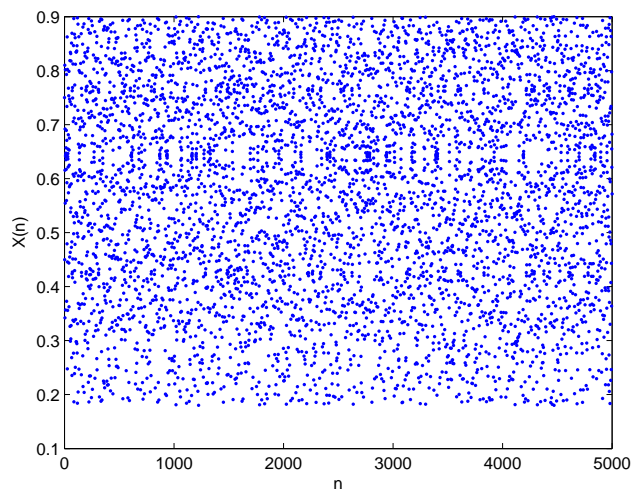


Figure 2.6: The trajectory of the Tent map with $r = 0.9$ starting from $X(0) = 0.75$.

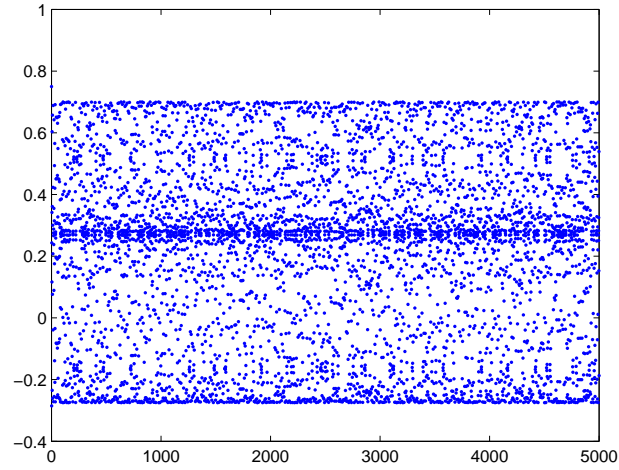


Figure 2.7: The trajectory of the Gaussian map with $b = 7.5$ and $c = -0.3$ starting from $X(0) = 0.75$.

(d) Hénon map. The mathematic equation is given as follows

$$\begin{cases} x_{n+1} = 1 - ax_n^2 + y_n \\ y_{n+1} = bx_n \end{cases} \quad (2.8)$$

and the portrait of state vectors is shown in Fig. 2.8.

3. Switched chaos. The Chua system is the first chaos realized by simple circuits, which is one of switched systems. By switching two linear 3-dimensional systems, we also presented a method to generate new chaotic systems.

(a) Chua circuit. The mathematic equation is given as follows

$$\begin{cases} \dot{x}_1 = a_1(x_2 - h(x_1)) \\ \dot{x}_2 = x_1 - x_2 + x_3 \\ \dot{x}_3 = -a_2x_2 \end{cases} \quad (2.9)$$

where $h(x_1) = m_1x_1 + 0.5(m_0 - m_1)(|x_1 + a_3| - |x_1 - a_3|)$, $a_1 = 9$, $a_2 = 14.286$, $a_3 = 1$, $m_0 = -1/7$ and $m_1 = 1.5/7$. The portrait of state vectors is shown in Fig. 2.9.

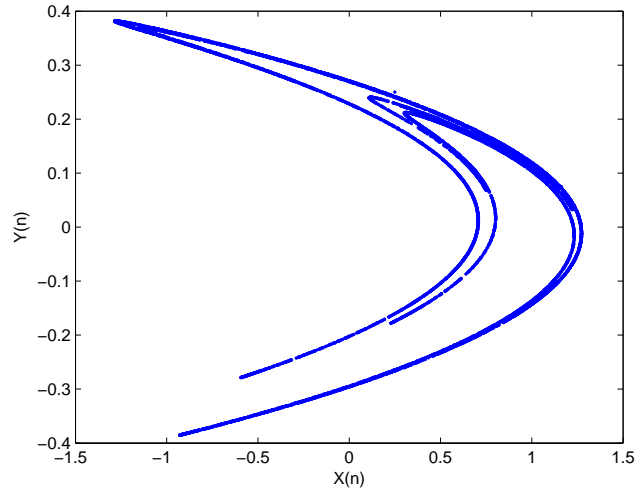


Figure 2.8: The portrait of the Hénon attractor with $a = 1.4$ and $b = 0.3$ starting from $(0.25, 0.25)$.

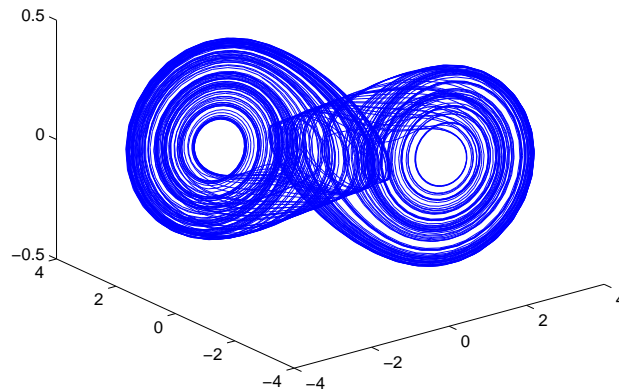


Figure 2.9: The portrait of the Chua circuit with $a_1 = 9$, $a_2 = 14.286$, $a_3 = 1$, $m_0 = -1/7$ and $m_1 = 1.5/7$.

(b) Linear switched chaos. The mathematic equation is given as follows

$$\dot{x} = A_1x + b_1 \quad (2.10)$$

$$\dot{x} = A_2x + b_2 \quad (2.11)$$

where x is an n -dimensional state vector, A_1, A_2 are $n \times n$ constant matrices, and b_1, b_2 are n -dimensional constant vectors. The portrait of state vectors is shown in Fig. 2.10.

Assume that system (2.10) has an unstable equilibrium x_1^* , and system (2.11) has a stable equilibrium x_2^* . Let

$$x_0^* = 1/2(x_1^* + x_2^*), \text{ and } l = 1/2\|x_1^* - x_2^*\|.$$

Define the following three regions:

$$\Sigma_1 = \{x \mid \|x - x_0^*\| \leq k\},$$

$$\Sigma_2 = \{x \mid k < \|x - x_0^*\| < m\},$$

$$\Sigma_3 = \{x \mid \|x - x_0^*\| \geq m\}.$$

where k and m are such that $l < k < m < +\infty$.

Switching rule: When system (2.10) is active, it will switch to system (2.11) at time t_1 if $X(t_1) \in \Sigma_3$. Similarly, when system (2.11) is active, it will switch to system (2.10) at time t_2 if $X(t_2) \in \Sigma_1$.

With this switching rule, the switched system will generate chaos or chaos-like behavior

if the system parameters are properly chosen. For example, choose $A_1 = \begin{pmatrix} a & b & 0 \\ -b & a & 0 \\ 0 & 0 & c \end{pmatrix}$,

$A_2 = \begin{pmatrix} f & 0 & 0 \\ 0 & g & h \\ 0 & -h & g \end{pmatrix}$, $b_1 = \begin{pmatrix} 0 \\ 0 \\ d \end{pmatrix}$, $b_2 = \begin{pmatrix} 0 \\ 0 \\ 0 \end{pmatrix}$ with $a = 0.9$, $b = 11.5$, $c = 0.5$,
 $d = 1.0$, $f = -0.5$, $g = -1$, $h = 20$, $k = 3$ and $m = 10$.

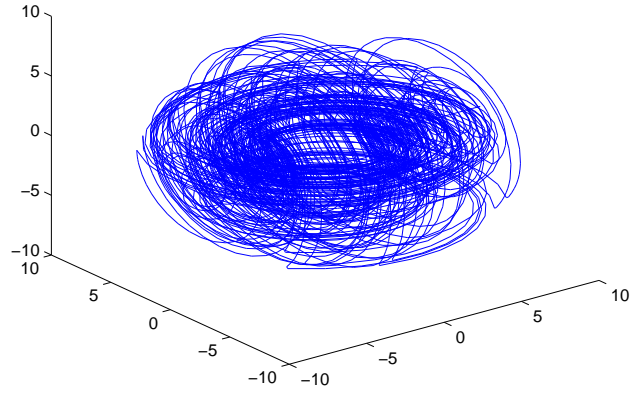


Figure 2.10: The portrait of the chaotic attractor by switching two linear systems starting from $(10, 0, 0)$.

4. Delay chaos. Mackey-Glass system is the first delay chaos found in 1977, which is a physiological model. Another one is Ikeda Equation which is obtained as a model of a passive optical resonator system.

(a) Mackey-Glass system. The mathematic equation is given as follows

$$\dot{x}(t) = -x(t) + \frac{2x(t - \tau)}{1 + x(t - \tau)^{10}} \quad (2.12)$$

and the portrait is shown in Fig. 2.11.

(b) Ikeda equation [48]. The mathematic equation is given as follows

$$\dot{x}(t) = -x(t) + \mu \sin(x(t - \tau)) \quad (2.13)$$

and the portrait is shown in Fig. 2.12.

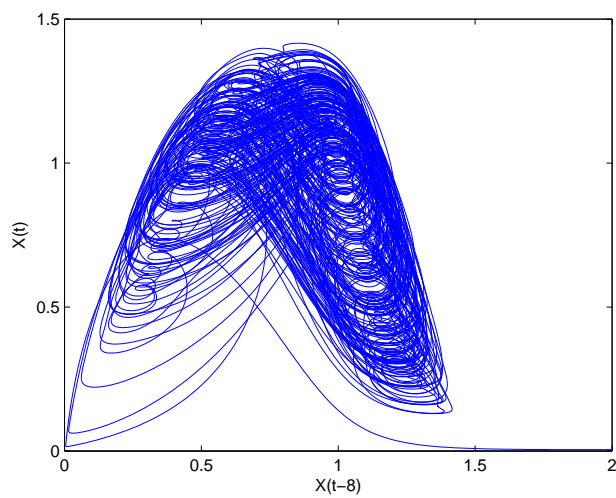


Figure 2.11: The portrait of the Mackey-Glass system with $\tau = 8$.

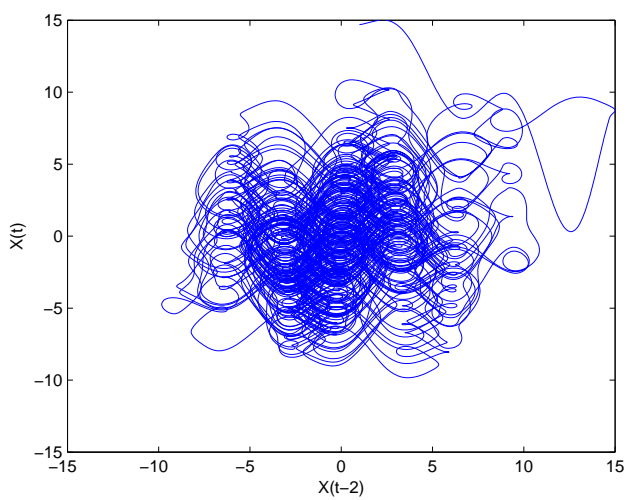


Figure 2.12: The portrait of the Ikeda equation with $\mu = 20$ and $\tau = 2$.

2.2 Related Mathematical Background

In this subsection, some basic concepts, definitions and mathematical background are introduced, which will be used in the following chapters.

Consider the systems of ordinary differential equations (ODEs) having the following form,

$$\dot{x}(t) = f(x(t)), \quad x(0) = x_0,$$

where $x(t) = (x_1(t), \dots, x_n(t))^T$, $f : D \rightarrow R^n$, $f(x(t)) = (f_1(x_1, \dots, x_n), \dots, f_n(x_1, \dots, x_n))$, D is an open and connected subset of R^n , and f is a locally Lipschitz function mapping D into R^n .

Equilibrium Points: A point $\bar{x} \in R^n$ is said to be an equilibrium point of the system

$$\dot{x}(t) = f(x(t)),$$

if $f(\bar{x}) = 0$. Clearly \bar{x} is an equilibrium point iff $x(t) = \bar{x}$ is a constant solution of the system.

Linearization system: The idea is to consider the linear approximation of f at an equilibrium point. Assume that f has continuous partial derivatives with respect to x . The derivatives of f is an $n \times n$ matrix Df defined by

$$Df = \left(\frac{\partial f_i}{\partial x_j} \right), \quad i, j = 1, 2, \dots, n.$$

Let x be close to the equilibrium point \bar{x} . Then by Taylor's theorem we have

$$\begin{aligned} f(x) &= f(\bar{x}) + Df(\bar{x})(x - \bar{x}) + R(\bar{x}, x) \\ &= Df(\bar{x})(x - \bar{x}) + R(\bar{x}, x), \end{aligned}$$

where $\lim_{x \rightarrow \bar{x}} \frac{R(\bar{x}, x)}{\|x - \bar{x}\|} = 0$.

The linear system:

$$\dot{y} = Df(\bar{x})y, \quad \text{where } y = x - \bar{x}$$

is called the linearization of the system $\dot{x}(t) = f(x(t))$.

Remark: Any non-zero equilibrium point can be transformed into a zero equilibrium point by making the change of variable $y = x - \bar{x}$. Thus we often assume that $\bar{x} = 0$ is an equilibrium point of the system $\dot{x}(t) = f(x(t))$.

Lyapunov Stability: The equilibrium point $\bar{x} = 0$ is said to be

- stable if for any $\epsilon > 0$, there exists a $\delta = \delta(\epsilon) > 0$ such that $\|x_0\| < \delta$ implies $\|x(t)\| < \epsilon, \forall t > 0$;
- asymptotically stable if it is stable and there exists a constant $\delta > 0$ such that $\|x_0\| < \delta$ implies $\lim_{t \rightarrow \infty} \|x(t)\| = 0$;
- unstable if it is not stable.

The First Method of Lyapunov: Consider the following system

$$\dot{x}(t) = f(x(t)) \quad \text{with} \quad f(0) = 0.$$

If the linearization of this system exists, its stability determines the local stability of the original nonlinear equation.

Positive Definite Function: Let D be an open subset of R^n containing the origin. A function $V : D \rightarrow R$ is said to be positive definite (positive semi-definite, negative definite, negative semi-definite) on D if it satisfies the following inequality

- (i) $V(0) = 0$;
- (ii) $V(x) > (\geq, <, \leq) 0, \quad \forall x \in D - \{0\}$.

A positive definite function V defined on R^n is said to be radially unbounded if the following condition holds:

$$\lim_{\|x\| \rightarrow \infty} V(x) \rightarrow \infty.$$

The Second Method of Lyapunov: Let $\bar{x} = 0$ be the equilibrium point of nonlinear system $\dot{x}(t) = f(x(t))$ where $f : D \rightarrow R$. If there exists a continuously differentiable function

$V : D \rightarrow R$ such that

- (i) $V(0) = 0$,
- (ii) $V(x) > 0, \quad \forall x \in D - \{0\}$,
- (iii) $\dot{V} \leq 0, \quad \forall x \in D - \{0\}$,

then the equilibrium point $\bar{x} = 0$ is stable.

If condition (iii) is replaced by

- (iii) $\dot{V} < 0, \quad \forall x \in D - \{0\}$,

then $\bar{x} = 0$ is asymptotically stable. Moreover, if $D = R^n$ and V is radially unbounded, then $\bar{x} = 0$ is globally asymptotically stable.

Consider a general delay differential equation, described by

$$\dot{x}(t) = f(t, x_t)$$

with the initial condition $x_{t_0} = \phi(t)$ for $t \in [t_0 - \tau, t_0]$, where $x(t) = x(t_0, t, \phi)$ is its solution, $x_t = x(t + \theta)$ for $\theta \in [-\tau, 0]$, and τ is a positive scalar. Define $\|\phi\|_\tau = \sup_{-\tau \leq \theta \leq 0} \|\phi(\theta)\|$ with $\|\cdot\|$ is the Euclidean norm on R^n .

Lyapunov-Razumikhin Theorem: For the above delay differential equation, the equilibrium point $\bar{x} = 0$ is stable if there exists a positive definite function $V(x)$ satisfies

$$\dot{V} \leq 0$$

whenever $V(x) \geq V(x_t(\theta))$, for all $\theta \in [-\tau, 0]$.

It is said to be asymptotically stable if there exist a function α , with $\alpha(s) > 0$ for $s > 0$, such that

$$\dot{V} \leq -\alpha(|x|)$$

whenever $\beta(V(x)) \geq V(x_t(\theta))$, for all $\theta \in [-\tau, 0]$, where the continuous nondecreasing function $\beta : R^+ \rightarrow R^+$ satisfies $\beta(s) > s$ for all $s > 0$.

It is said to be globally asymptotically stable if it is asymptotically stable and V is a radially unbounded function.

Attractor [49]: A compact invariant subset of the state space $A \subset M$ is called **an attractor** if

- (a) its basin of attraction, or stable set $B(A) = \{x \in M | \omega(x) \subset A\}$, has strictly positive Lebesgue measure;
- (b) there is no strictly smaller closed set $A' \subset A$ so that $B(A')$ coincides with $B(A)$ up to a set of Lebesgue measure zero.

An attractor is a set towards which a dynamical system evolves over time. Any trajectory of the dynamical system in the attractor will remain on the attractor. An attractor can be a point, a curve, a manifold, or even a complicated set with a fractal structure known as a strange attractor. Describing the attractors of chaotic dynamical systems has been one of the achievements of chaos theory.

Chaotic Attractor [50]: An invariant A set is called a chaotic attractor provided it is an attractor and the dynamical system has sensitive dependence on initial conditions on A (sometimes people require the system has a positive Lyapunov exponent on A instead of sensitive dependence).

Bifurcation: Bifurcation theory is the mathematical study of changes in the qualitative or topological structure of a given dynamical system such as the solutions of a family of differential equations, the solutions of chaotic maps, etc. A bifurcation occurs when a small change made to the parameter values (the bifurcation parameters) of a system causes a sudden qualitative or topological change in its dynamical behavior. Bifurcations occur in both continuous dynamical systems (described by ODEs, DDEs or PDEs) and discrete systems (described by maps). In dynamical systems, a bifurcation diagram shows the possible long-term values (equilibrium points or periodic orbits) of a system as a function of a bifurcation parameter in the dynamical systems.

Hopf Bifurcation [49]: Consider a one-parameter family of differential equations

$$\dot{x} = f(x; \mu), \quad x \in U, \quad \mu \in R,$$

where U is an open subset of R^n and μ is a real scalar parameter varying in some open interval $I \subseteq R$. Assume that $\bar{x} = \bar{x}(\mu)$ is an equilibrium point and the Jacobian matrix of f with respect to x , evaluated at $(\bar{x}(\mu); \mu)$, has a pair of simple complex conjugate eigenvalues $\lambda_{1,2}(\mu)$ such that, at a critical value μ_c of the parameter, we have

$$\operatorname{Re}\lambda_{1,2}(\mu_c) = 0, \quad \operatorname{Im}\lambda_{1,2}(\mu_c) \neq 0, \quad \frac{d}{d\mu}\lambda_{1,2}(\mu_c) \neq 0,$$

while $\operatorname{Re}\rho(\mu_c) < 0$ for any other eigenvalue ρ . This is called Hopf bifurcation.

Hopf bifurcation is a local bifurcation in which a fixed point of a dynamical system loses its stability as a pair of complex conjugate eigenvalues of the linearization around the fixed point cross the imaginary axis of the complex plane.

Lyapunov Exponent [50]: Let $f : R \rightarrow R$ be a C^1 function. For each point x_0 , define the Lyapunov (characteristic) exponent of x_0 , $\lambda(x_0)$, as follows:

$$\begin{aligned} \lambda(x_0) &= \limsup_{n \rightarrow \infty} \frac{1}{n} \log(|(f^n)'(x_0)|) \\ &= \limsup_{n \rightarrow \infty} \frac{1}{n} \sum_{j=0}^{n-1} \log(|f'(x_j)|) \end{aligned}$$

where $x_j = f^j(x_0)$.

Lyapunov exponent of a dynamical system is a measure of exponential divergence of orbits, which characterizes the rate of separation of very close trajectories. For example, two trajectories in phase space with initial separation Z_1 diverge to Z_2 after time $\Delta t = t_2 - t_1$ (shown in Fig. 2.13). Thus,

$$|Z_2| \approx e^{\lambda \Delta t} |Z_1|,$$

where λ is the Lyapunov exponent.

Lyapunov Spectrum: The Lyapunov exponents describe the behavior of vectors in the tangent space of the phase space and are defined from the Jacobian matrix,

$$J(x_0) = \left. \frac{df(x)}{dx} \right|_{x_0},$$

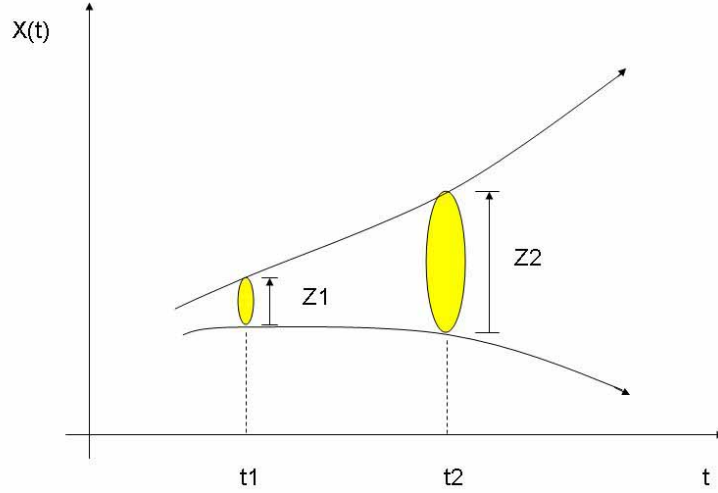


Figure 2.13: Two trajectories in phase space with initial separation Z_1 .

for dynamical system $\dot{x}(t) = f(x)$. The rate of separation can be different for different orientations of the initial separation vector. Thus, there is a spectrum of Lyapunov exponents the number of which equals to the dimensionality of the phase space, denoted by $\{\lambda_1, \lambda_2, \dots, \lambda_n\}$ in decreasing order. One of the most used and effective numerical techniques to calculate the Lyapunov spectrum for a smooth dynamical system is the periodic Gram-Schmidt orthonormalization of the Lyapunov vectors.

Lyapunov Dimension: Lyapunov Dimension is also called Kaplan-Yorke dimension, which gives an estimate of the rate of entropy production and of the fractal dimension of the considered dynamical system, defined by

$$D = k + \frac{\sum_{i=1}^k \lambda_i}{|\lambda_{k+1}|},$$

where k satisfies $\sum_{i=1}^k \lambda_i \geq 0$ and $\sum_{i=1}^{k+1} \lambda_i < 0$.

2.3 Chaos-Based Secure Communication Scheme

In 1990, Louis M. Pecora and Thomas L. Carroll firstly found synchronization phenomenon of two identical chaotic systems. We know that deterministic chaos can generate random dynamical behaviors. therefore, chaotic signals are very suitable for masked carriers. In 1993, Cuomo and Oppenheim presented the first scheme of a communication device made by two identical Lorenz oscillators [22]. In 1997, Kolumban, Kennedy and Chua realized digital communications based on synchronization of two identical Chua circuits [24, 25]. After that, chaos field attracted tremendous interests of scholars from various different areas and several symmetric chaos-based secure communication schemes were presented. The principle diagram of symmetric chaos-based secure communication schemes is shown in Fig. 2.14.

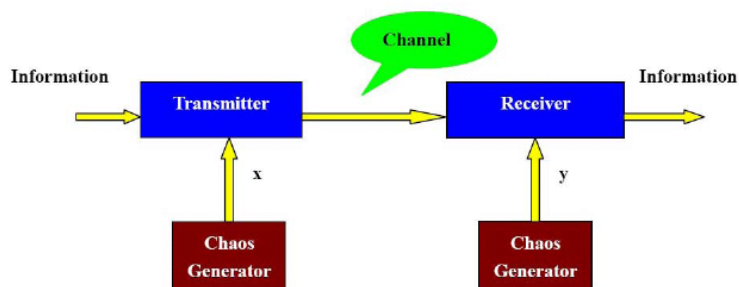


Figure 2.14: The principle diagram of chaos-based secure communication.

Principle: Information is masked by chaotic signals at the transmitter, and then sent to the receiver by the public channel. Finally the encrypted signals are decrypted at the receiver. In this scheme, the key issue is that the two identical chaos generators in the transmitter end and the receiver end need to be synchronized. That is, $x = y$.

Synchronization of chaos: Synchronization of chaotic systems is the key issue in symmetric chaos-based secure communication schemes. It is a phenomenon that may occur when two, or more, chaotic oscillators are coupled, or when a chaotic oscillator drives another chaotic oscillator. Because of the butterfly effect, which causes the exponential di-

vergence of the trajectories of two identical chaotic systems starting with the nearly same initial conditions, having two chaotic system evolving in synchrony might appear quite surprising. However, synchronization of coupled or driven chaotic oscillators is a phenomenon well established experimentally and reasonably understood theoretically.

The main synchronization methods of chaotic systems are state feedback control synchronization and impulsive control synchronization. We'll introduce them respectively.

(a) **State feedback control synchronization.** The most representative example of this synchronization is Peroca-Carroll scheme. The basic idea is that a chaotic system is self-synchronizing if it can be decomposed into subsystems: a drive system and a stable response subsystem that synchronize when coupled with a common drive signal. They showed numerically that synchronization occurs if all of the Lyapunov exponents for the response subsystems are negative.

The principle diagram is shown in Fig. 2.15. The master chaotic system and slave chaotic system are identical. We use the state variable z of the master system to drive the slave system such that the error system converges to zero. Information is encrypted at transmitter end by (x_1, y_1, z) , and then the ciphertexts $U(t)$ is sent to receiver end by public channel.

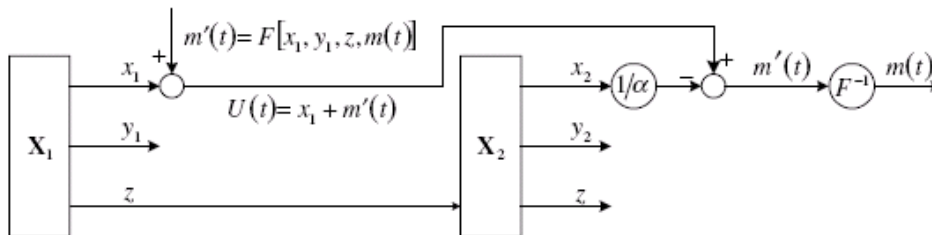


Figure 2.15: The principle diagram of state feedback control synchronization.

The mathematic model is followed as Eq. 2.14:

$$\begin{aligned}
 M & : \begin{cases} \dot{x}_1 = F_1(x_1, y_1, z) \\ \dot{y}_1 = F_2(x_1, y_1, z) \\ \dot{z} = F_3(x_1, y_1, z) \end{cases} \\
 S & : \begin{cases} \dot{x}_2 = F_1(x_2, y_2, z) \\ \dot{y}_2 = F_2(x_2, y_2, z) \\ \dot{z} = F_3(x_1, y_1, z) \end{cases}
 \end{aligned} \tag{2.14}$$

where M is the master system and S is the slave system. Let $e_1 = x_1 - x_2$ and $e_2 = y_1 - y_2$. We obtain the error system E followed as Eq. 2.15.

$$E : \begin{cases} \dot{e}_1 = F_1(x_1, y_1, z) - F_1(x_2, y_2, z) \\ \dot{e}_2 = F_2(x_1, y_1, z) - F_2(x_2, y_2, z) \end{cases} \tag{2.15}$$

If the error system is stable and converges to zero, we have $(x_1, y_1) = (x_2, y_2)$. Then we can decrypt the cipher-texts using (x_2, y_2, z) and recover the plain-texts. The stable conditions of the error system can be obtained by Lyapunov stability theory.

(b) **Impulsive control synchronization.**

Impulsive control means that at some select moments, the system states are changed suddenly. The principle diagram of impulsive control synchronization is shown in Fig. 2.16.

The mathematic model is followed as Eq. 2.16:

$$\begin{aligned}
 M & : \dot{X} = F(X) \\
 S & : \begin{cases} \dot{Y} = F(Y), & t \neq t_k \\ \Delta Y = B(X - Y), & t = t_k \end{cases} \\
 E & : \begin{cases} \dot{e} = F(X) - F(Y), & t \neq t_k \\ \Delta e = -Be, & t = t_k \end{cases}
 \end{aligned} \tag{2.16}$$

where $e = X - Y$. t_k ($k = 1, 2, \dots$) are the impulsive control points. If the error system E is stable and converges to zero, the two chaos systems are said to be synchronous. Here the

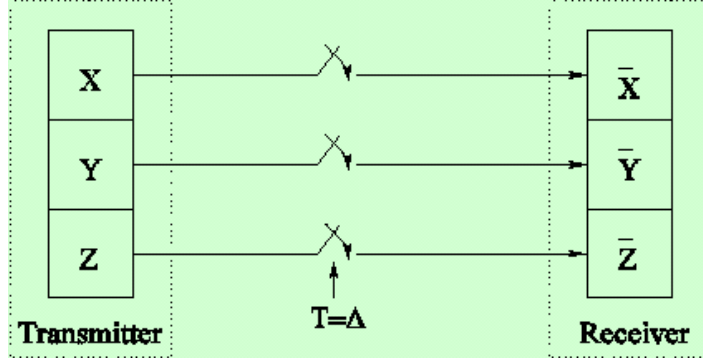


Figure 2.16: The principle diagram of impulsive control synchronization.

error system E is an impulsive differential equation [51]. Its stable conditions can be derived from the following Theorem 2.1.

A general form of impulsive differential equation with fixed time instants of impulsive effect can be expressed in the following form.

$$\begin{cases} \dot{x} = f(t, x), & t \neq \tau_k, \\ \Delta x = I_k(x), & t = \tau_k, \\ x(t_0) = x_0, & k = 1, 2, \dots \end{cases}$$

where $f : R_+ \times \Omega \rightarrow R^d$; $I_k : \Omega \rightarrow R^d$; Ω is a domain in R^d ; $\tau_k, k = 1, 2, \dots$, are time instants of impulsive effects and satisfy $0 < \tau_1 < \tau_2 < \dots, \tau_k \rightarrow +\infty$ as $k \rightarrow +\infty$.

We define

$$K_0 : = \{g \in C[R_+, R_+] : g(s) > 0 \text{ if } s > 0 \text{ and } g(0) = 0\};$$

$$K : = \{g \in K_0 : g(s) \text{ is strictly increasing in } s\};$$

$$PC : = \{p : R_+ \rightarrow R_+ : P \text{ is continuous on } (\tau_k, \tau_{k+1}] \text{ and } p(\tau_k^+) \text{ exit for } k = 1, 2, \dots\};$$

$$v_0 : = \{V : R_+ \times \Omega \rightarrow R_+ : V(t, x) \text{ is continuous on } (\tau_k, \tau_{k+1}] \times \Omega, \text{ locally Lipschitzian in } x \text{ and } V(\tau_k^+, x) \text{ exit for } k = 1, 2, \dots\}.$$

For $V \in v_0, (t, x) \in R_+ \times \Omega$ and $t \neq \tau_k$, we define $D^+V(t, x)$ by

$$D^+V(t, x) = \limsup_{\delta \rightarrow 0} [V(t + \delta, x + \delta f(t, x)) - V(t, x)].$$

Theorem 2.1 [52]: Assume that

- (i) there exists ρ and ρ_0 , with $0 < \rho_0 < \rho$, such that $x \in s(\rho_0)$ implies that $x + I_k(x) \in s(\rho)$ for all $k = 1, 2, \dots$;
- (ii) $V \in v_0$, $V(t, x)$ is positive definite and decrescent, and there exists $\psi_k \in K_0$ such that

$$V(\tau_k^+, x + I_k(x)) \leq \psi_k(V(\tau_k, x)), \quad k = 1, 2, \dots;$$

- (iii) there exist $c \in K$ and $p \in PC$ such that

$$D^+V(t, x) \leq p(t)c(V(t, x)), \quad x \in s(\rho), \quad t \neq \tau_k;$$

- (iv) there exists a constant $\sigma > 0$ such that for all $z \in (0, \sigma)$

$$\int_{\tau_k}^{\tau_{k+1}} p(s)ds + \int_z^{\psi_k(z)} \frac{ds}{c(s)} \leq -\gamma_k,$$

for some constants γ_k and $k = 1, 2, \dots$;

- (v) $\sum_{k=1}^{\infty} \gamma_k = \infty$.

Then any solution of the system, $x(t, t_0, x_0)$, converges to 0, i.e., $\lim_{t \rightarrow \infty} \|x(t, t_0, x_0)\| = 0$.

2.4 Chaos-Based Public-Key Cryptography

In 2003, Ljupco Kocarev and Zarko Tasev presented a kind of new public-key cryptography based on discrete chaotic map. Subsequently, a lot of algorithms based on discrete chaotic maps were presented. Also, some researchers used chaotic systems to construct Hash functions. Here, we will simply introduce a public-key cryptography system based on Chebyshev map.

Chebyshev polynomial of degree p is defined recurrently,

$$T_{p+1}(x) = 2xT_p(x) - T_{p-1}(x), \quad (2.17)$$

where $p = 1, 2, 3, \dots, T_0 = 1, T_1 = x$ and $x \in [-1, 1]$. We know that when $p > 1$, Chebyshev polynomial T_p is a chaotic map with positive Lyapunov exponent $LE = \ln(p)$. One of the most remarkable properties of the Chebyshev polynomials is the semi-group property:

$$T_r(T_s(x)) = T_{rs}(x). \quad (2.18)$$

Now we describe the algorithm. In a public key encryption system, an entity Alice has a public key e and a private key d . The public key defines an encryption transformation E_e , while the private key defines the associated decryption transform D_d . An entity Bob wishing to send a message M to Alice obtains an authentic copy of Alice's public key e , uses the encryption transform to obtain the cipher-text $c = E_e(M)$, and transmits c to Alice. To decrypt c , Alice applies the decryption transformation to obtain the plain-text $M = D_d(c)$.

Key Generation Algorithm:

Alice, in order to generate the keys, does the following:

1. Generates a large integer s ;
2. selects a random number $x \in [-1, 1]$ and computes $T_s(x)$;
3. sets her public key to $(x, T_s(x))$ and her private key to s .

Encryption Algorithm:

Bob, in order to encrypt a message, does the following:

1. Obtains Alice's authentic public key $(x, T_s(x))$;
2. Represents the message as a number $M \in [-1, 1]$.
3. Generates a large integer r ;
4. Computes $T_r(x), T_{rs}(x) = T_r(T_s(x))$ and $X = MT_{rs}(x)$;
5. Sends the cipher-text $C = (T_r(x), X)$ to Alice.

Decryption Algorithm:

Alice, to recover the plain-text M from the cipher-text C , does the following:

1. Uses her private key s to compute $T_{sr}(x) = T_s(T_r(x))$;
2. Recovers M by computing $M = X/T_{sr}(x)$.

Chapter 3

Generating New Chaos and Hyperchaos

3.1 Generating New Chaos and Hyperchaos from Delay Differential Equation

In this section, we construct a new chaotic attractor generated by a delay differential equation and its dynamical behavior is analyzed. Specially, the Lyapunov spectrum and Lyapunov dimension are calculated, the bifurcation diagram is shown and the boundedness is studied. Then, by changing the parameters to increase the number of equilibrium points, we obtain a set of more complex hyperchaotic attractors. Furthermore, we present a general form of this family of chaos, and simulate different chaotic phase portraits of these systems. Finally, some remarks and conclusions are given.

3.1.1 Background

Over the past two decades, generation of chaotic or hyperchaotic systems and their applications have attracted a great deal of attention [5, 21, 22, 46, 53–57]. Recently, multi-scroll attractors and hyperchaos systems have been presented [58–66]. In addition, a nonautonomous technique to generate multi-scroll attractors and hyperchaos has been introduced [67, 68].

Using switching systems some new chaotic attractors have been achieved [66, 69–71]. Some fractional differential systems have been presented to generate chaos [62, 72–74]. simultaneously, some simple circuits have been developed to realize chaos [64, 66, 75–77].

Most recently, delayed differential equation generating chaos has received considerable attention. Since Mackey-Glass system which is a physiological model was found to have chaotic behavior, several modified chaotic systems have been reported [78–81]. some experimental observation of multi-scroll attractors have been confirmed [80–82]. motivated by this, we present a family of delayed chaotic attractors by sine function. and a set of new complex attractors have been found by choosing suitable parameters and time delay.

3.1.2 New Chaotic Attractor

Consider the following delay differential equation:

$$\dot{x}(t) = a[-bx(t - \tau) + c \sin(dx(t - \tau))]. \quad (3.1)$$

where $a = 0.8$, $b = 0.2$, $c = 0.5$, $d = 1.8$, and $\tau = 4.8$. Fig. 3.1 shows the portrait of vector $x(t)$ and the phase of $x(t) - x(t - \tau)$ is shown in Fig. 3.2.

When different delayed times are chosen, Fig. 3.3 shows the phase portraits of $x(t) - x(t - \tau)$.

3.1.2.1 Dynamical Analysis

The system (3.1) has three equilibrium points: -1.4119 , 0 , 1.4119 . At the equilibrium point x^* , the characteristic equation of the system is

$$\lambda + abe^{-\lambda\tau} - acd \cos(dx^*)e^{-\lambda\tau} = 0. \quad (3.2)$$

At the equilibrium points $x^* = \pm 1.4119$, the system has the same characteristic equation

$$\lambda + 1.5083e^{-\lambda\tau} = 0. \quad (3.3)$$

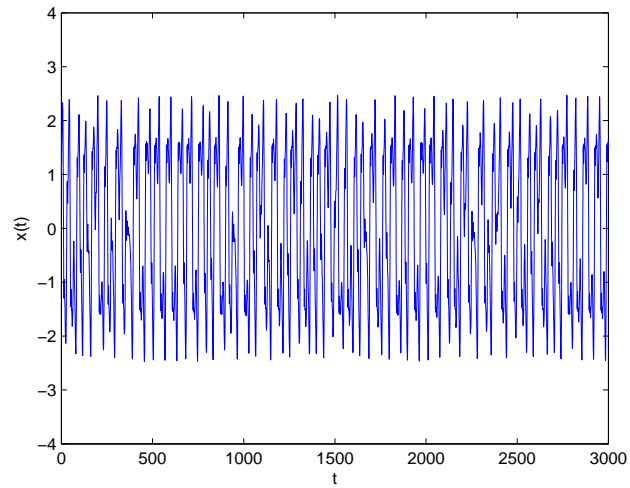


Figure 3.1: The trajectory portrait of vector $x(t)$, when $a = 0.8$, $b = 0.2$, $c = 0.5$, $d = 1.8$, and $\tau = 4.8$.

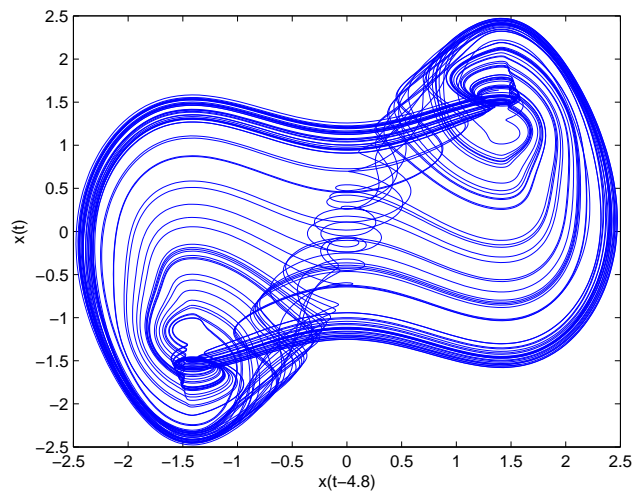


Figure 3.2: The phase of $x(t - \tau) - x(t)$, when $a = 0.8$, $b = 0.2$, $c = 0.5$, $d = 1.8$, and $\tau = 4.8$.

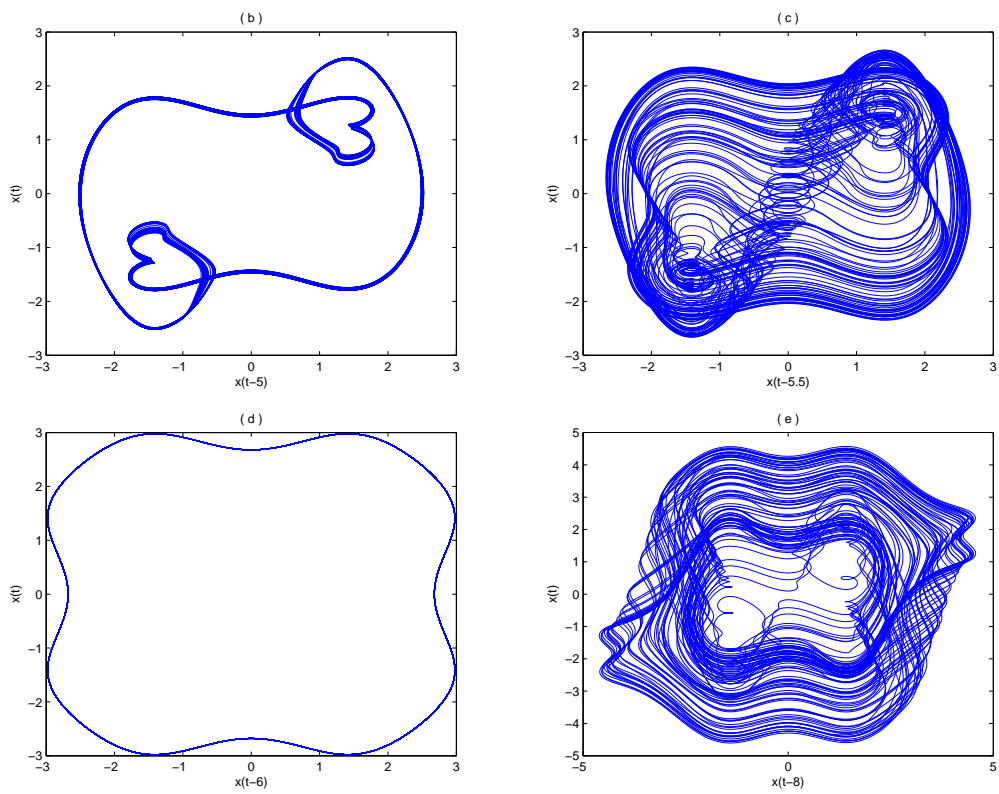


Figure 3.3: The phase of $x(t - \tau) - x(t)$, when (a): $\tau = 5$, (b): $\tau = 5.5$, (c): $\tau = 6$, (d): $\tau = 8$.

At the equilibrium point $x^* = 0$, the characteristic equation is

$$\lambda - 1.1200e^{-\lambda\tau} = 0. \quad (3.4)$$

The roots of characteristic equation at the equilibrium points $x^* = \pm 1.4119$ and $x^* = 0$ are shown in Fig. 3.4(a) and Fig. 3.4(b), respectively. It is clear that Hopf bifurcation occurs at $x^* = \pm 1.4119$ when suitable parameters are chosen. Furthermore, we calculate the maximal

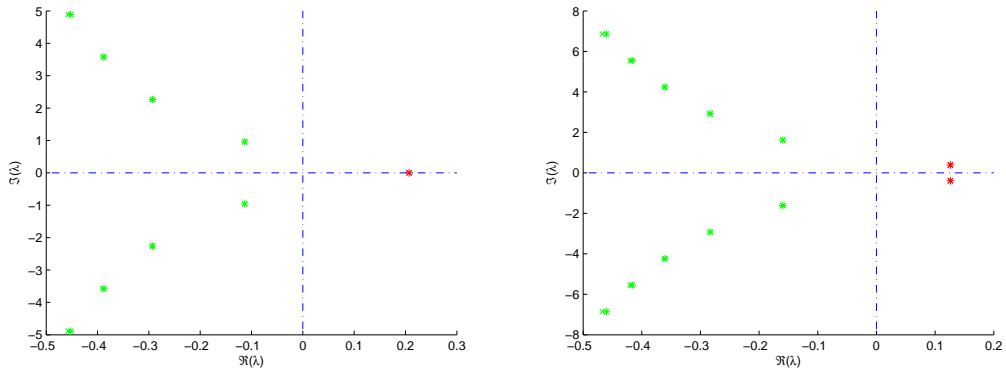


Figure 3.4: The roots of the characteristic equations of system (3.1) at the equilibrium points (a) $x^* = 0$ and (b) $x^* = \pm 1.4119$.

Lyapunov exponent $\lambda_{max} = 0.0211$ and Lyapunov dimension $d = 2.2718$ using the method in [83] and the Matlab LET toolbox. The Lyapunov spectrum is shown in Fig. 3.5. The bifurcation diagrams vs the parameters c and τ are respectively shown in Fig. 3.6 and Fig. 3.7. We find that there exist some strange bifurcations nearby $\tau = 6$ and $c = 0.8$.

3.1.2.2 Boundedness Analysis

Consider the following general delay differential equation:

$$\dot{x}(t) = Ax(t) + Bx(t - r) + f(x(t), x(t - r)), \quad (3.5)$$

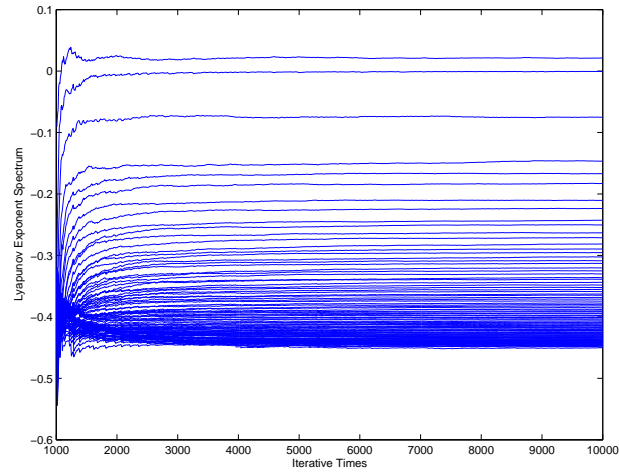


Figure 3.5: The Lyapunov spectrum of system (3.1) with parameters $N = 100$ and initial condition $x_0 = rand(100)$.

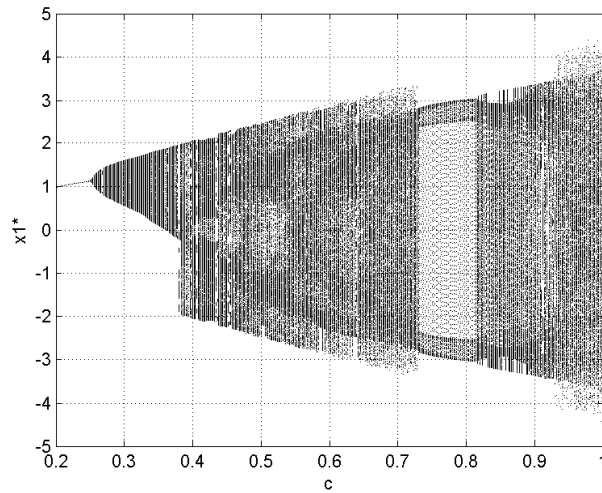


Figure 3.6: The bifurcation diagram for the responding discretized system of (3.1) vs the parameter c with $a = 0.8$, $b = 0.2$, $d = 1.8$ and $\tau = 4.8$.

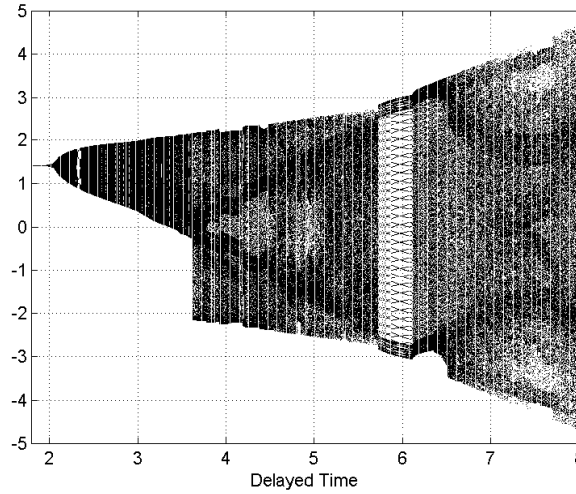


Figure 3.7: The bifurcation diagram for the responding discretized system of (3.1) vs the delayed time τ with $a = 0.8$, $b = 0.2$, $c = 0.5$ and $d = 1.8$.

where A , B and r are constants with $r > 0$. f is a nonlinear perturbation and x is scalar. Without the perturbation, (3.5) reduces to the linear homogeneous DDE,

$$\dot{x}(t) = Ax(t) + Bx(t - r). \quad (3.6)$$

Lemma 3.1: The solution $x = x(\phi)$ of Equation (3.5) with initial data ϕ on $[-r, 0]$ is given by

$$x(t) = y(t) + \int_0^t X(t-s)f(x(s), x(s-r))ds, \quad (3.7)$$

where $y = y(\phi)$ is the solution of the homogeneous equation (3.6) with initial data ϕ on $[-r, 0]$ and X is the fundamental solution of (3.6), i.e. the solution of (3.6) with initial data

$$\psi(t) = \begin{cases} 0, & -r \leq t < 0, \\ 1, & t = 0. \end{cases}$$

Proof: It is easy to check that $x(t)$ given by (3.7) satisfies the initial data ϕ on $[-r, 0]$. By uniqueness, it suffices to show that $x(t)$ given by (3.7) satisfies Equation (3.5). Actually, by

(3.7), we have

$$\begin{aligned}
\dot{x}(t) &= \dot{y}(t) + f(x(t), x(t-r)) + \int_0^t \dot{X}(t-s)f(x(s), x(s-r))ds \\
&= Ay(t) + By(t-r) + f(x(t), x(t-r)) \\
&\quad + \int_0^t [AX(t-s) + BX(t-s-r)]f(x(s), x(s-r))ds \\
&= A[y(t) + \int_0^t X(t-s)f(x(s), x(s-r))ds] \\
&\quad + B[y(t-r) + \int_0^{t-r} X(t-s-r)f(x(s), x(s-r))ds] \\
&= Ax(t) + Bx(t-r) + f(x(t), x(t-r)),
\end{aligned}$$

where the fact that $X(t-s-r) \equiv 0$ for $s \in (t-r, t]$ is used. The proof completes.

Define the characteristic equation of system (3.6) as follows,

$$h(\lambda) \stackrel{\text{def}}{=} \lambda - A - Be^{-\lambda r}. \quad (3.8)$$

Let $Re(\lambda)$ designate the real part of λ .

Lemma 3.2: For the homogeneous equation (3.6), if $\varepsilon_0 = \max\{Re(\lambda) : h(\lambda) = 0\}$, then, for any $\varepsilon_1 > \varepsilon_0$, there is a constant $k_1 = k_1(\varepsilon_1)$ such that the fundamental solution $X(t)$ satisfies the inequality

$$|X(t)| \leq k_1 e^{\varepsilon_1 t}, \quad t \geq 0. \quad (3.9)$$

The detailed proof can be seen in **Theorem 5.2** in Chapter 1 of [84].

Lemma 3.3: Suppose $\varepsilon_0 = \max\{Re(\lambda) : h(\lambda) = 0\}$ and $x(\phi)$ is the solution of the homogeneous equation (3.6), which coincides with ϕ on the $[-r, 0]$. Then, for any $\varepsilon_2 > \varepsilon_0$, there is a constant $k_2 = k_2(\varepsilon_2, \phi)$ such that

$$|x(\phi)| \leq k_2 e^{\varepsilon_2 t}, \quad t \geq 0.$$

The detailed proof can be seen in **Theorem 6.2** in Chapter 1 of [84].

Lemma 3.4: All roots of the equation $(z + a)e^z + b = 0$, where a and b are real, have negative real parts if and only if

$$a > -1$$

$$a + b > 0$$

$$b < \zeta \sin \zeta - a \cos \zeta$$

where ζ is the root of $\zeta = -a \tan \zeta$, $0 < \zeta < \pi$, if $a \neq 0$ and $\zeta = \pi/2$ if $a = 0$.

The detailed proof can be seen in **Theorem A.5** in Appendix of [84].

Theorem 3.1: For system (3.5), if the nonlinear perturbation is bounded, that is $|f| \leq M$ ($M > 0$), and the following inequalities are satisfied, then the solutions of system (3.5) are bounded.

$$Ar < 1, \tag{3.10}$$

$$A + B < 0, \tag{3.11}$$

$$-Br < \zeta \sin \zeta + Ar \cos \zeta. \tag{3.12}$$

where ζ is the root of $\zeta = Ar \tan \zeta$, $0 < \zeta < \pi$, if $A \neq 0$ and $\zeta = \pi/2$ if $A = 0$.

Proof: By inequalities (3.10), (3.11), (3.12) and **Lemma 3.4**, we have that all roots of the characteristic equation $\lambda - A - Be^{-\lambda r} = 0$ have negative real parts. So the conditions of **Lemma 3.2** and 3.3 are satisfied. By **Lemma 3.2** and 3.3, we have

$$|y(t)| \leq k_1 e^{\varepsilon_1 t}, \quad |X(t)| \leq k_2 e^{\varepsilon_2 t}, \quad t \geq 0. \tag{3.13}$$

where k_1 and k_2 are positive constants, ε_1 and ε_2 are negative constants, $y(t)$ is the solution of (3.6) with the initial data ϕ and $X(t)$ is the fundamental solution of (3.6).

Let $x(t)$ be the solution of (3.5). By **Lemma 3.1**, one obtains

$$\begin{aligned}
|x(t)| &\leq |y(t)| + M \int_0^t |X(t-s)| ds \\
&\leq k_1 + M \int_0^t e^{\varepsilon_2(t-s)} ds \\
&\leq k_1 + \frac{Mk_2}{-\varepsilon_2} (1 - e^{\varepsilon_2 t}) \\
&\leq k_1 - \frac{Mk_2}{\varepsilon_2}, \quad t \geq 0.
\end{aligned}$$

The proof completes.

Theorem 3.2: The solutions of system (3.1) are bounded, for arbitrary c and d , provided that

$$0 < ab\tau < \pi/2. \quad (3.14)$$

proof: It follows from **Theorem 3.1** by letting $A = 0$, $B = -ab$ and $r = \tau$.

3.1.2.3 Generalized Hyperchaotic Attractors

By increasing the number of Hopf bifurcation points, we can generalize system (3.1) to complex hyperchaotic attractors.

When $a = 0.8$, $b = 0.2$, $c = 1$, $d = 1.8$, system (3.1) has seven equilibrium points $(0, \pm 1.5681, \pm 4.0071, \pm 4.5899)$. Hopf bifurcation occurs at points $(\pm 1.5681, \pm 4.5899)$. Fig. 3.8 shows that system (3.1) can achieve more complex cell chaos when τ increases. When $\tau = 4.0$, the system has only one positive Lyapunov exponent $\lambda = 0.0493$ and Lyapunov dimension $d = 3.1035$. When $\tau = 8.0$, system (3.1) has two positive Lyapunov exponents $\lambda_1 = 0.0718$, $\lambda_2 = 0.0189$ and Lyapunov dimension $d = 5.0807$. It becomes a hyperchaos system.

When $a = 0.8$, $b = 0.2$, $c = 2$, $d = 1.8$, system (3.1) has eleven equilibrium points $(0, \pm 1.6531, \pm 3.7013, \pm 4.9484, \pm 7.4481, \pm 8.1932)$. Hopf bifurcation occurs at points $(\pm 1.6531, \pm 4.9484, \pm 8.1932)$. The phase of $x(t) - x(t - \tau)$ is shown in Fig. 3.9. When

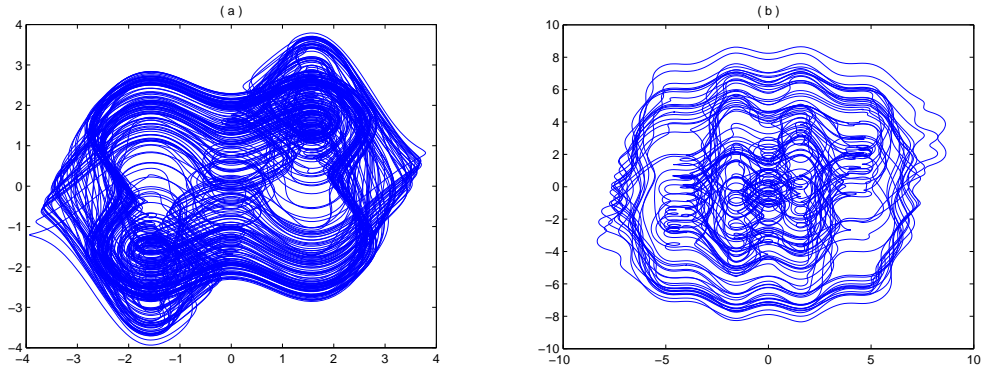


Figure 3.8: The phase of $x(t - \tau) - x(t)$, when (a): $\tau = 4$, (b): $\tau = 8$.

$\tau = 2.5$, the system has only one positive Lyapunov exponent $\lambda = 0.0627$ and Lyapunov dimension $d = 3.5655$. When $\tau = 4.0$, the system has two positive Lyapunov exponents $\lambda_1 = 0.0795$, $\lambda_2 = 0.0319$ and Lyapunov dimension $d = 5.4147$. When $\tau = 6.0$, the system has three positive Lyapunov exponents $\lambda_1 = 0.0912$, $\lambda_2 = 0.0630$, $\lambda_3 = 0.0156$ and Lyapunov dimension $d = 7.8406$. When $\tau = 8.0$, the system has four positive Lyapunov exponents $\lambda_1 = 0.1061$, $\lambda_2 = 0.0705$, $\lambda_3 = 0.0339$, $\lambda_4 = 0.0078$ and Lyapunov dimension $d = 10.0316$. With τ increasing it also turns into a hyperchaos.

When $a = 0.8$, $b = 0.2$, $c = 3$, $d = 1.8$, system (3.1) has fourteen equilibrium points $(0, \pm 1.6786, \pm 3.6366, \pm 5.0317, \pm 7.2854, \pm 8.3706, \pm 10.9723, \pm 11.6698)$. Hopf bifurcation occurs at points $(\pm 1.6786, \pm 5.0317, \pm 8.3706, \pm 11.6698)$. The phase of $x(t) - x(t - \tau)$ is shown in Fig. 3.10. When $\tau = 1.5$, the system has only one positive Lyapunov exponent $\lambda = 0.0577$ and Lyapunov dimension $d = 3.2522$. When $\tau = 3.0$, the system has two positive Lyapunov exponents $\lambda_1 = 0.0807$, $\lambda_2 = 0.0422$ and Lyapunov dimension $d = 6.0047$. When $\tau = 4.0$, the system has three positive Lyapunov exponents $\lambda_1 = 0.0925$, $\lambda_2 = 0.0593$, $\lambda_3 = 0.0259$ and Lyapunov dimension $d = 7.8487$. When $\tau = 5.0$, the system has four positive Lyapunov exponents $\lambda_1 = 0.1042$, $\lambda_2 = 0.0685$, $\lambda_3 = 0.0151$, $\lambda_4 = 0.0685$ and Lyapunov dimension $d = 9.6047$. When $\tau = 6.0$, the system has five positive Lyapunov exponents $\lambda_0 = 0.1086$, $\lambda_2 = 0.0786$, $\lambda_3 = 0.0498$, $\lambda_4 = 0.0262$, $\lambda_5 = 0.0046$ and Lyapunov

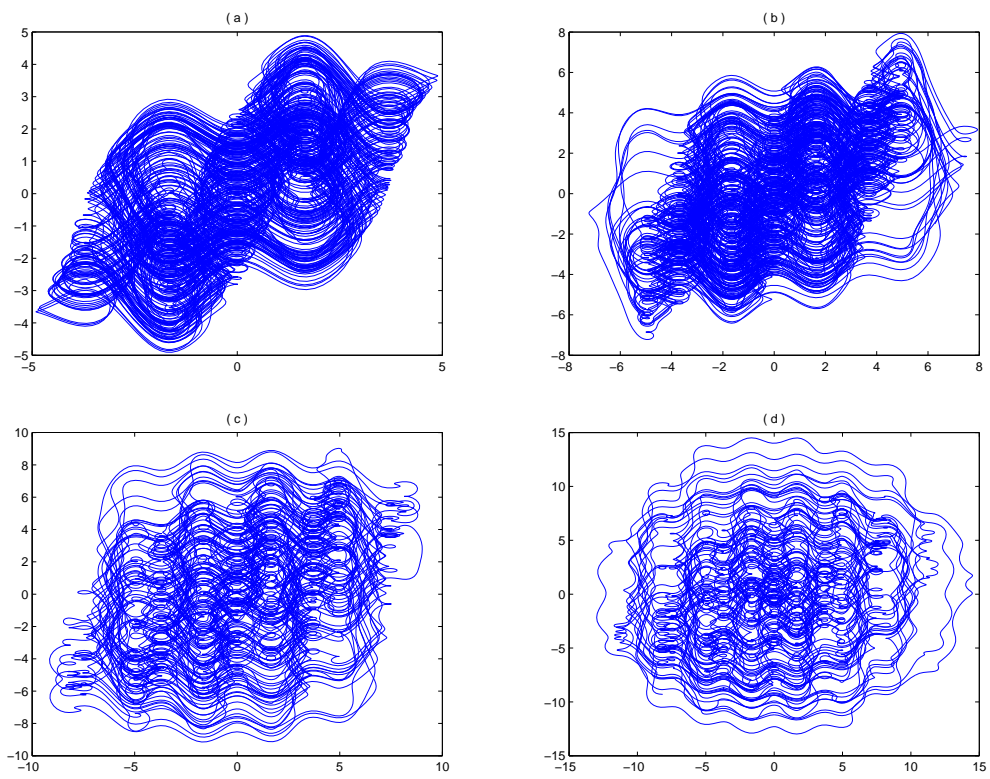


Figure 3.9: The phase of $x(t - \tau) - x(t)$, when (a): $\tau = 2.5$, (b): $\tau = 4$, (c): $\tau = 6$, (d): $\tau = 8$.

dimension $d = 11.4108$. When $\tau = 8.0$, the system has six positive Lyapunov exponents $\lambda_1 = 0.1210$, $\lambda_2 = 0.0927$, $\lambda_3 = 0.0634$, $\lambda_4 = 0.0410$, $\lambda_5 = 0.0191$, $\lambda_6 = 0.0067$ and Lyapunov dimension $d = 14.8941$. With τ increasing, it also turns into a hyperchaos.

Furthermore, by increasing c , we can increase the number of equilibrium points and the one of Hopf bifurcation points of system (3.1). With the number of positive Lyapunov exponents and Lyapunov dimension increasing, the system can turn into more complex hyperchaotic attractors by choosing suitable delayed time. Fig. 3.11 shows the maximal ten Lyapunov exponents change as c ranges in $[0.5 \quad 3]$ with fixed parameters $a = 0.8$, $b = 0.2$, $d = 1.8$ and $\tau = 8.0$.

3.1.3 General Form of DDE Generating Chaos

Consider the following general form of delay differential equation:

$$\dot{x}(t) = a[b_0x(t) + b_1x(t - \tau_1) + c \sin(dx(t - \tau_2))]. \quad (3.15)$$

Theorem 3.3: The solutions of system (3.15) are bounded, for arbitrary c , d and τ_2 , provided that

$$ab_0\tau_1 < 1, \quad (3.16)$$

$$ab_0 + ab_1 < 0, \quad (3.17)$$

$$-ab_1\tau_1 < \zeta \sin \zeta + ab_0\tau_1 \cos \zeta. \quad (3.18)$$

where ζ is the root of $\zeta = ab_0\tau_1 \tan \zeta$, $0 < \zeta < \pi$, if $ab_0 \neq 0$ and $\zeta = \pi/2$ if $ab_0 = 0$. **Proof:** It follows from **Theorem 3.1** by letting $A = ab_0$, $B = ab_1$ and $r = \tau_1$.

Corollary 1: If $b_1 = 0$, the solutions of system (3.16) which turns into some like the famous Ikeda Equation [48] are bounded, for arbitrary c and d , provided that

$$ab_0 < 0. \quad (3.19)$$

Proof: It follows from **Theorem 3.3** with $b_1 = 0$. Actually, condition (3.19) implies conditions (3.16) and (3.17) when $b_1 = 0$. Moreover, $ab_0 < 0$ implies $\zeta \in (\frac{\pi}{2}, \pi)$, and then

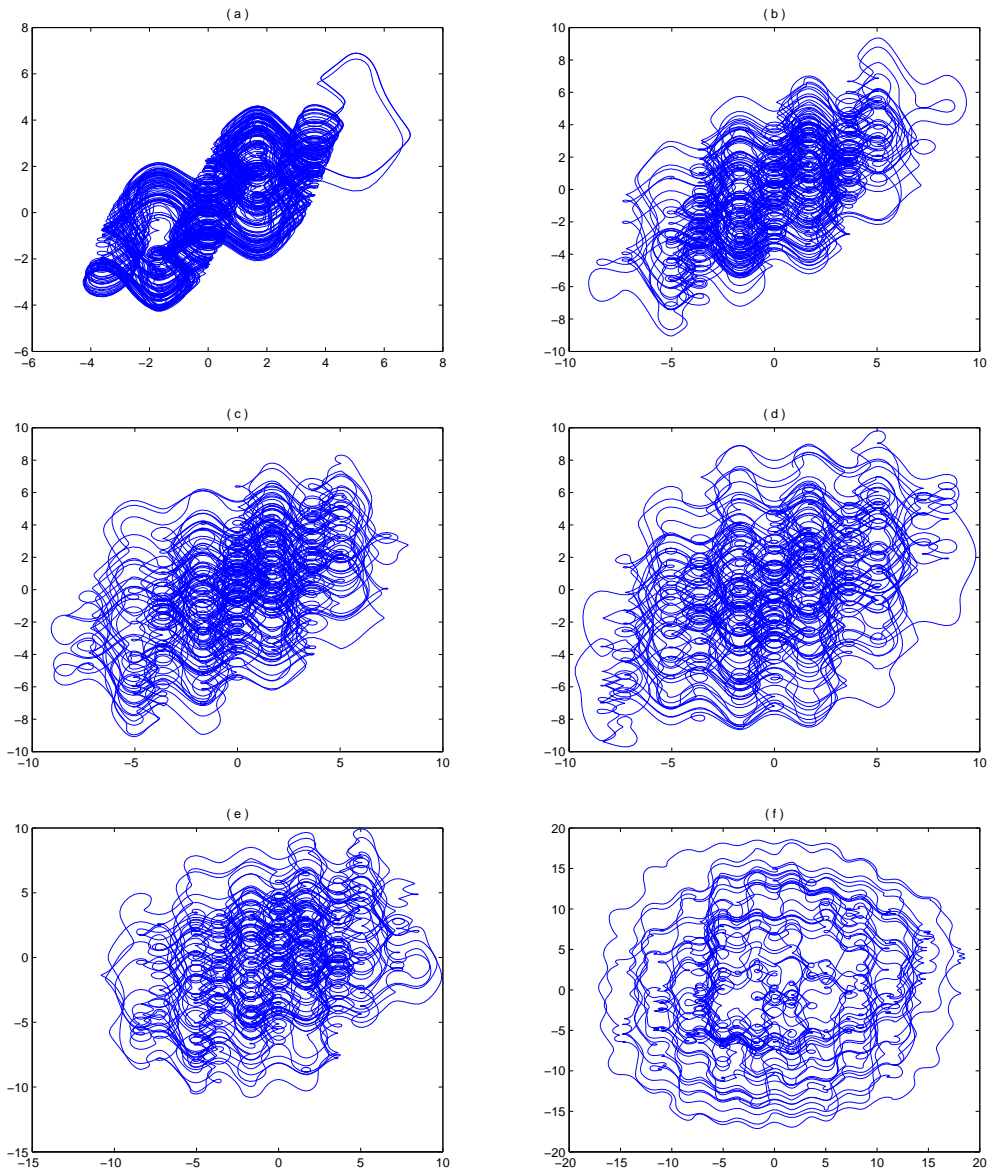


Figure 3.10: The phase of $x(t - \tau) - x(t)$ with $c = 3.0$, when (a): $\tau = 1.5$, (b): $\tau = 3$, (c): $\tau = 4$, (d): $\tau = 5$, (e): $\tau = 6$, (f): $\tau = 8$.

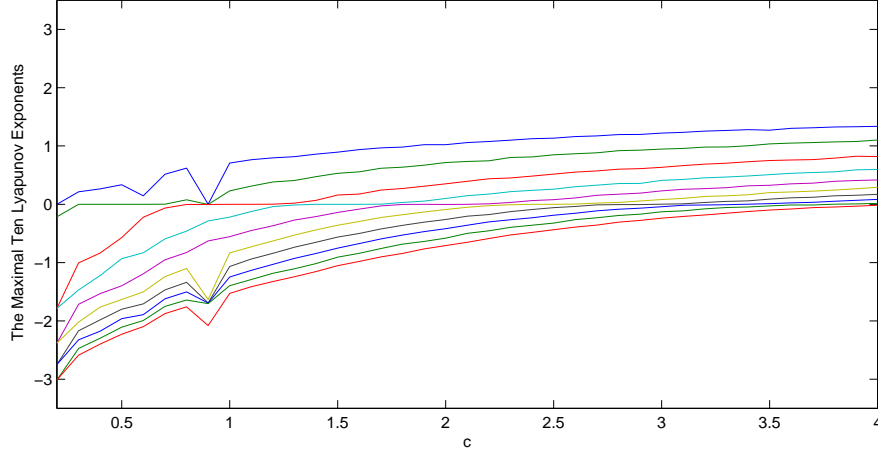


Figure 3.11: The first six Lyapunov exponents vs parameter c in $[0.5 \ 3]$ with $a = 0.8$, $b = 0.2$, $d = 1.8$ and $\tau = 8.0$.

condition (3.18) is always satisfied as

$$\zeta \sin \zeta + ab_0\tau_1 \cos \zeta = \frac{ab_0\tau_1 \sin^2 \zeta + ab_0\tau_1 \cos^2 \zeta}{\cos \zeta} = \frac{ab_0\tau_1}{\cos \zeta} > 0, \quad \zeta \in \left(\frac{\pi}{2}, \pi\right). \quad (3.20)$$

3.1.3.1 Special Case I: Ikeda Equation

When we choose $a = 0.8$, $b_0 = -0.4$, $b_1 = 0$, $c = 1$, $d = 1.8$, system (3.15) transforms to the Ikeda equation. Fig. 3.12 shows the phase portraits of $x(t)-x(t - \tau_2)$ when τ_2 chooses different values. The phase portraits are similar with the figures in [80].

3.1.3.2 Special Case II

We choose $a = 0.8$, $b_0 = 0$, $b_1 = -0.2$, $c = 0.5$, $d = 1.8$, $\tau_1 = 4$, $\tau_2 = 6$. System (3.15) still generates chaotic attractor. Fig. 3.13 shows the phase of $x(t)-x(t - \tau_1)-x(t - \tau_2)$.

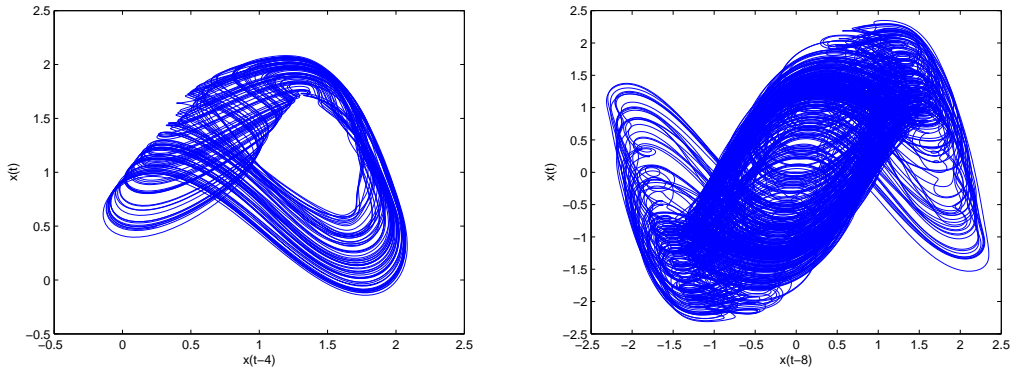


Figure 3.12: The phase of $x(t) - x(t - \tau_2)$, when (a): $\tau_2 = 4$; (b): $\tau_2 = 8$.

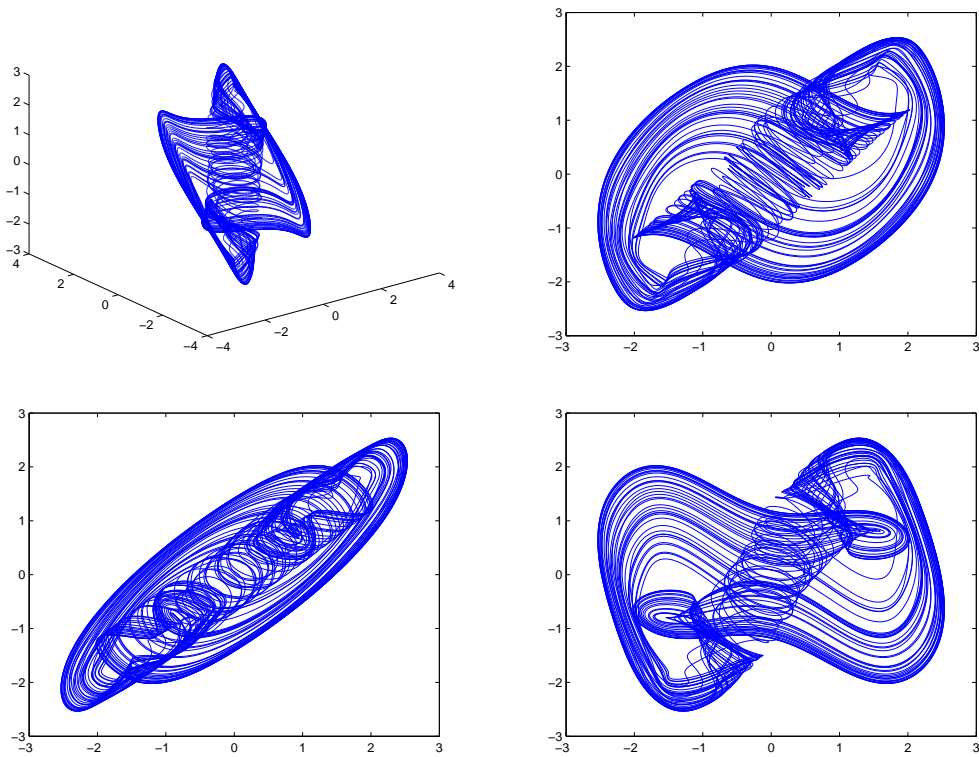


Figure 3.13: The phase of $x(t) - x(t - \tau_1) - x(t - \tau_2)$, when $\tau_1 = 4, \tau_2 = 6$.

3.1.3.3 Special Case III

We choose $a = 0.8$, $b_1 = -0.1$, $b_2 = -0.1$, $c = 0.5$, $d = 1.8$. System (3.15) still generates chaotic attractor. Fig. 3.14 shows the phase of $x(t)-x(t-\tau_1)-x(t-\tau_2)$ when suitable delayed times are chosen.

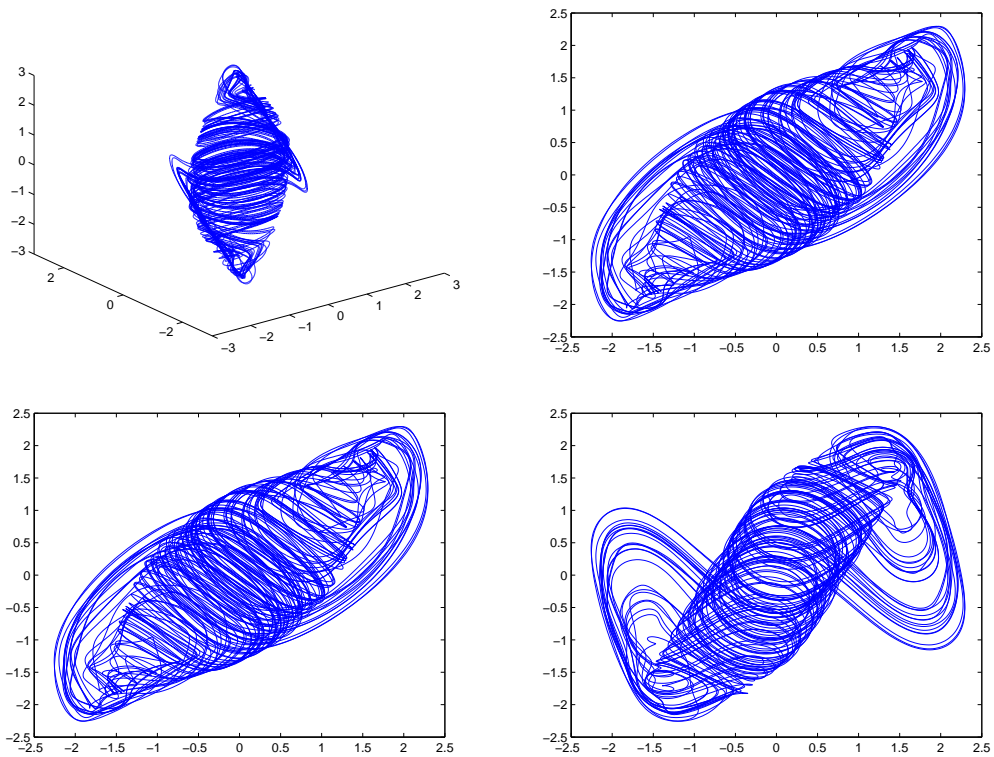


Figure 3.14: The phase of $x(t)-x(t-\tau_1)-x(t-\tau_2)$, when $\tau_1 = 4, \tau_2 = 8$.

3.1.3.4 Special Case IV

We choose $a = 0.8$, $b_1 = -0.4$, $b_2 = 0.2$, $c = 0.5$, $d = 1.8$. System (3.15) still generates chaotic attractor. Fig. 3.15 shows the phase of $x(t)-x(t-\tau_1)-x(t-\tau_2)$ when suitable delayed times are chosen.

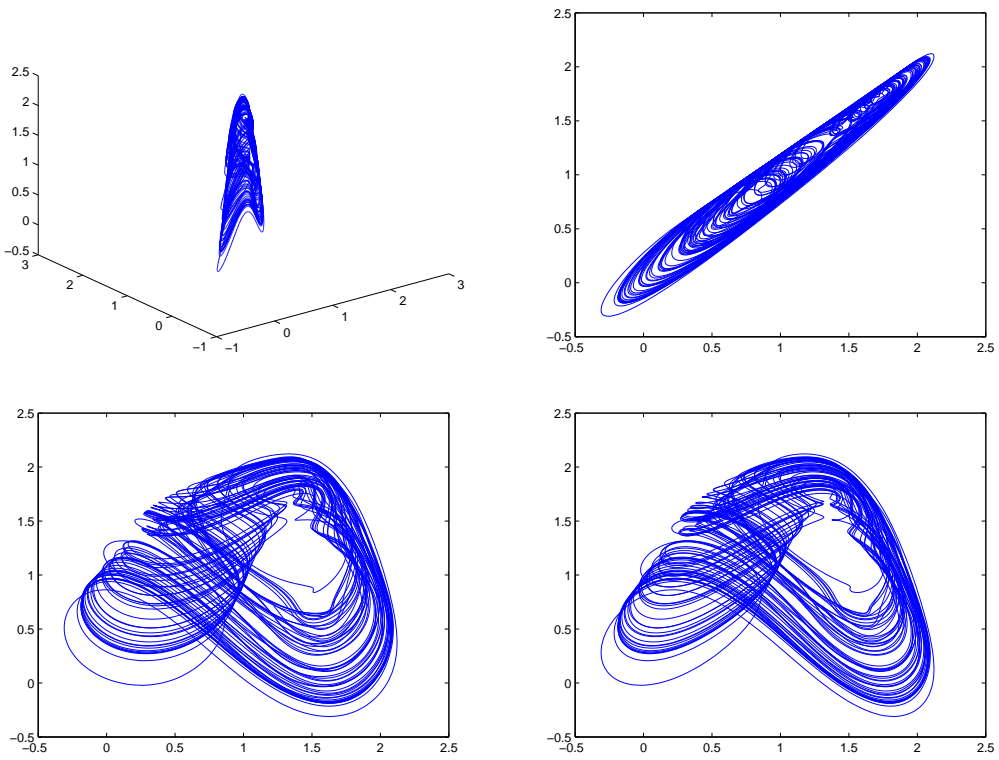


Figure 3.15: The phase of $x(t)-x(t-\tau_1)-x(t-\tau_2)$, when $\tau_1 = 1, \tau_2 = 10$.

3.1.3.5 Special Case V

We choose $a = 0.8$, $b_1 = 0.4$, $b_2 = -0.8$, $c = 0.5$, $d = 1.8$. System (3.15) still generates chaotic attractor. Fig. 3.16 shows the phase of $x(t)-x(t-\tau_1)-x(t-\tau_2)$ when suitable delayed times are chosen.

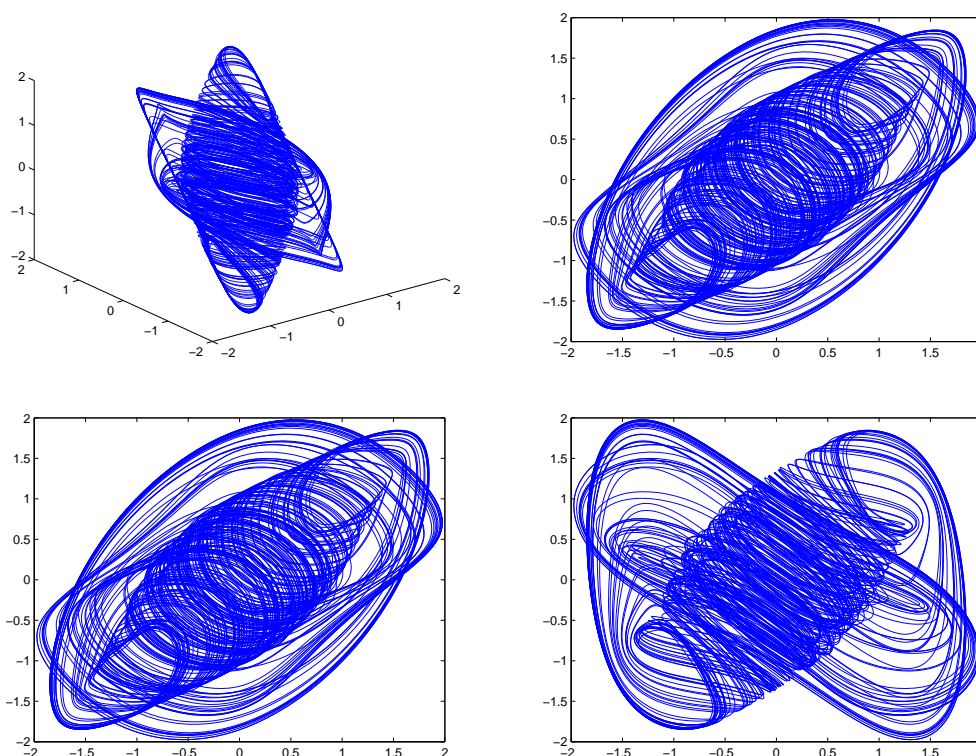


Figure 3.16: The phase of $x(t - \tau_2) - x(t - \tau_1) - x(t)$, when $\tau_1 = 2, \tau_2 = 4$.

Remark: Because of choosing the different signs of parameter values b_0 and b_1 , special cases I-V have different dynamical behaviors. And all these special cases can generate more complex chaotic attractors by increasing the number of Hopf bifurcation points of system (3.15).

3.1.4 Summary

This section has presented a family of new chaos from delayed differential equations with sine function. And the chaotic behavior and the boundedness of the system have been analyzed. A method to generalize the system to more complex chaotic attractors has been presented. Furthermore, a general form of DDE has been discussed and various chaotic behaviors have been simulated on different parameter conditions. We conclude that the general form of DDE can be generalized to more complex hyperchaotic attractors by increasing the number of Hopf bifurcations.

3.2 Generating Multi-Scroll Chaos and Hyperchaos from Chen System

3.2.1 System Statement

Chen system was presented in 1999, when he studied in controlling Lorenz system. It has been proved that Chen system is not topologically equivalent to the Lorenz system. The mathematic model is followed.

$$\begin{cases} \dot{x} = a(y - x) \\ \dot{y} = (c - a)x - xz + cy \\ \dot{z} = xy - bz \end{cases} \quad (3.21)$$

where $a = 35$, $b = 3$ and $c = 28$ (see Fig. 3.17).

We consider the following feedback control system,

$$\begin{cases} \dot{x} = a(y - x) \\ \dot{y} = (c - a)x - xu + cy \\ \dot{z} = xy - bz \end{cases} \quad (3.22)$$

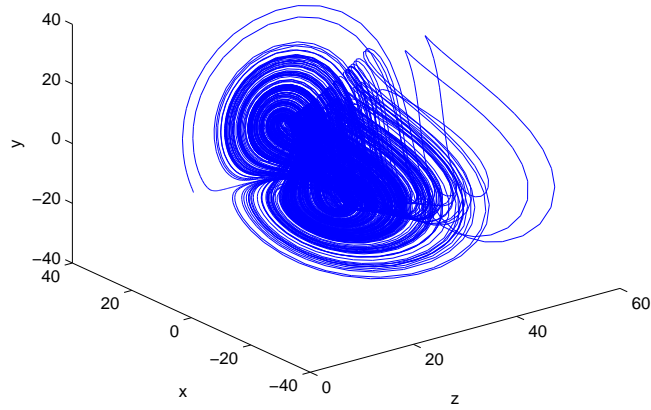


Figure 3.17: Chen chaotic attractor with $a = 35$, $b = 3$ and $c = 28$, starting from $[1, 1, 1]$.

where control function $u(t) = d_1 z(t) - d_2 \sin(z(t))$ with $a = 35$, $b = 3$, $c = 28$, $d_1 = 1$ and $d_2 = 8$. Fig.3.18 shows the phase portraits of state variables of the controlled Chen system, which is a 6-scroll attractor.

3.2.2 Dynamical Analysis

System (3.22) has 11 equilibrium points $(0, 0, 0)$, $(\pm 6.9995, \pm 6.9995, 16.3311)$, $(\pm 7.4572, \pm 7.4572, 18.5365)$, $(\pm 8.1020, \pm 8.1020, 21.8808)$, $(\pm 8.7929, \pm 8.7929, 25.7719)$ and $(\pm 9.0592, \pm 9.0592, 27.3561)$. At the equilibrium point (x^*, y^*, z^*) , the characteristic equation of the linearized system is

$$\begin{vmatrix} -a - \lambda & a & 0 \\ c - a - (d_1 z^* - d_2 \sin z^*) & c - \lambda & -d_1 x^* + d_2 x^* \cos z^* \\ y & x & -b - \lambda \end{vmatrix} = 0 \quad (3.23)$$

All equilibrium points and responding roots are shown in Table 3.1.

Therefore, all these equilibrium points are unstable. Fig. 3.19 shows the responding eigenvalues of points $(\pm 6.9995, \pm 6.9995, 16.3311)$. A pair of complex conjugate eigenval-

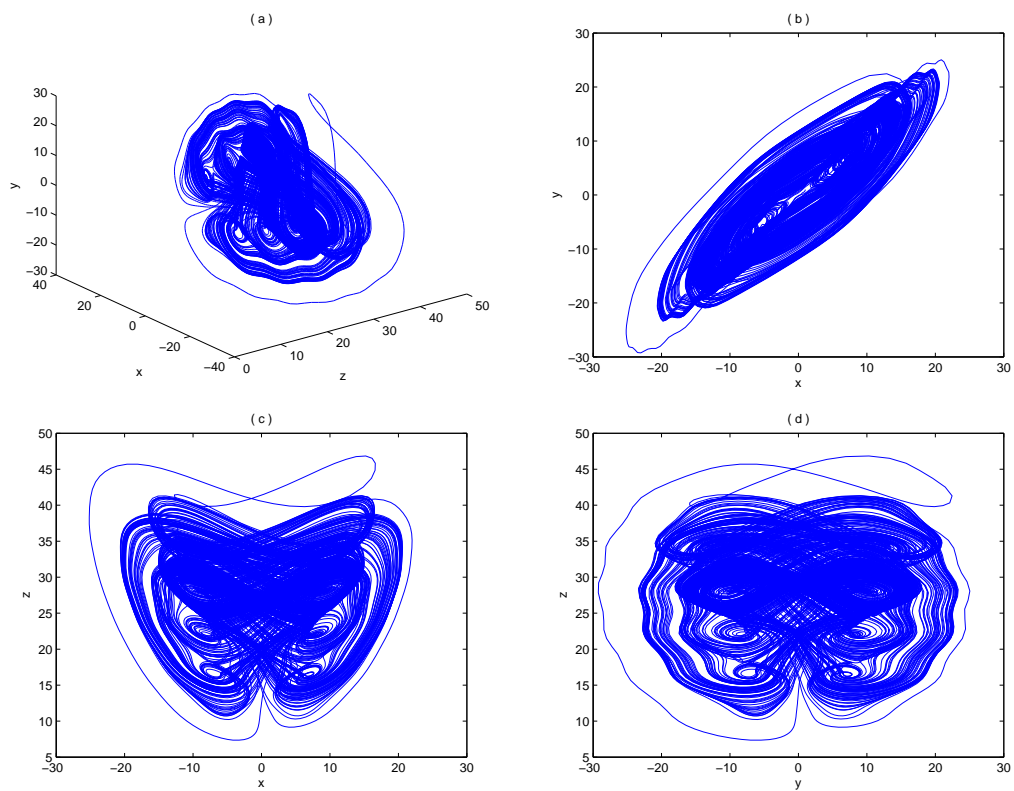


Figure 3.18: The phase portraits of controlled Chen system. (a) z - x - y ; (b) x - y ; (c) x - z ; (d) y - z .

Table 3.1: List of equilibrium points and responding roots of characteristic equations.

No.	Equilibrium Point	Roots of Characteristic Equation
1	(0, 0, 0)	$\lambda_1 = -30.8359$ $\lambda_2 = -3.0000$ $\lambda_3 = 23.8359$
2	(-6.9995, -6.9995, 16.3311)	$\lambda_1 = -28.3291$ $\lambda_2 = 9.1646 + 28.6971i$ $\lambda_3 = 9.1646 - 28.6971i$
3	(6.9995, 6.9995, 16.3311)	$\lambda_1 = -28.3291$ $\lambda_2 = 9.1646 + 28.6971i$ $\lambda_3 = 9.1646 - 28.6971i$
4	(-7.4572, -7.4572, 18.5365)	$\lambda_1 = -20.0227 + 21.3456i$ $\lambda_2 = -20.0227 - 21.3456i$ $\lambda_3 = 30.0454$
5	(7.4572, 7.4572, 18.5365)	$\lambda_1 = -20.0227 + 21.3456i$ $\lambda_2 = -20.0227 - 21.3456i$ $\lambda_3 = 30.0454$
6	(-8.1020, -8.1020, 21.8808)	$\lambda_1 = -31.7110$ $\lambda_2 = 10.8555 + 34.3397i$ $\lambda_3 = 10.8555 - 34.3397i$
7	(8.1020, 8.1020, 21.8808)	$\lambda_1 = -31.7110$ $\lambda_2 = 10.8555 + 34.3397i$ $\lambda_3 = 10.8555 - 34.3397i$
8	(-8.7929, -8.7929, 25.7719)	$\lambda_1 = -20.8583 + 22.1342i$ $\lambda_2 = -20.8583 - 22.1342i$ $\lambda_3 = 31.7166$
9	(8.7929, 8.7929, 25.7719)	$\lambda_1 = -20.8583 + 22.1342i$ $\lambda_2 = -20.8583 - 22.1342i$ $\lambda_3 = 31.7166$
10	(-9.0592, -9.0592, 27.3561)	$\lambda_1 = -30.2290$ $\lambda_2 = 10.1145 + 31.7952i$ $\lambda_3 = 10.1145 - 31.7952i$
11	(9.0592, 9.0592, 27.3561)	$\lambda_1 = -30.2290$ $\lambda_2 = 10.1145 + 31.7952i$ $\lambda_3 = 10.1145 - 31.7952i$

ues of the linearization around these equilibrium points cross the imaginary axis of the complex plane. It is clear that Hopf bifurcation will occur when suitable parameters are chosen. Similarly, at points $(\pm 8.1020, \pm 8.1020, 21.8808)$ and $(\pm 9.0592, \pm 9.0592, 27.3561)$, there exist Hopf bifurcations when suitable parameters are chosen.

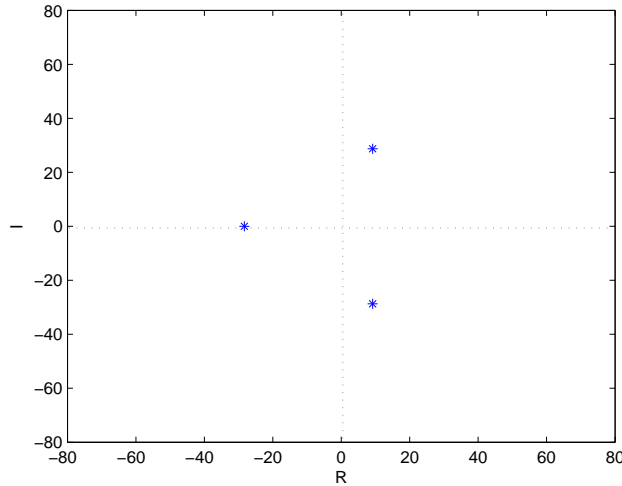


Figure 3.19: The roots of the characteristic equations of system (3.22) responding to equilibrium points $(\pm 6.9995, \pm 6.9995, 16.3311)$.

Furthermore, we calculate the maximal Lyapunov exponent $LE_{max} = 4.7859$ and Lyapunov dimension $d = 2.3236$ using the Matlab LET toolbox. The Lyapunov spectrum is shown in Fig. 3.20.

3.2.3 Generalized More-Scroll Chaos

From Fig. 3.18, we know the above new chaos is a 6-scroll Chen attractor. Furthermore, by choosing different values of parameter d_2 , we can control the number of equilibrium points of system (3.22). Subsequently, by controlling the number of Hopf bifurcation points, we will design complex chaotic systems with different topological structures.

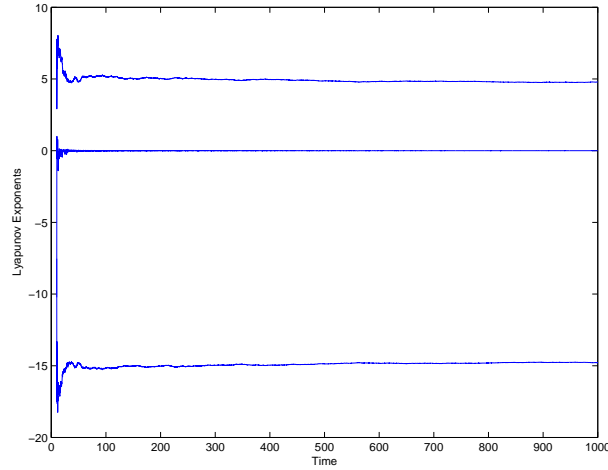


Figure 3.20: The Lyapunov spectrum of system (3.22) with parameters $t = 1000$, starting from $(1, 1, 30)$.

When $d_2 = 5$, system (3.22) has 7 equilibrium points $(0, 0, 0)$, $(\pm 7.0847, \pm 7.0847, 16.7311)$, $(\pm 7.4039, \pm 7.4039, 18.2726)$ and $(\pm 8.0917, \pm 8.0917, 21.8253)$. At points $(\pm 7.0847, \pm 7.0847, 16.7311)$ and $(\pm 8.0917, \pm 8.0917, 21.8253)$, there exist Hopf bifurcations when suitable parameters are chosen. Fig. 3.21 shows the phase portraits of state variables of system (3.22) with $d_2 = 5$, which is a 4-scroll attractor. The maximal Lyapunov exponent is $LE_{max} = 0.4015$ and Lyapunov dimension $d = 2.0316$.

When $d_2 = 14$, system (3.22) has 19 equilibrium points $(0, 0, 0)$, $(\pm 5.5575, \pm 5.5575, 10.2952)$, $(\pm 5.9635, \pm 5.9635, 11.8545)$, $(\pm 6.9429, \pm 6.9429, 16.0680)$, $(\pm 7.4867, \pm 7.4867, 18.6833)$, $(\pm 8.1102, \pm 8.1102, 21.9250)$, $(\pm 8.7390, \pm 8.7390, 25.4567)$, $(\pm 9.1274, \pm 9.1274, 27.7696)$, $(\pm 9.8534, \pm 9.8534, 32.3629)$ and $(\pm 10.0190, \pm 10.0190, 33.4602)$. At points $(\pm 5.5575, \pm 5.5575, 10.2952)$, $(\pm 6.9429, \pm 6.9429, 16.0680)$, $(\pm 8.1102, \pm 8.1102, 21.9250)$, $(\pm 9.1274, \pm 9.1274, 27.7696)$ and $(\pm 10.0190, \pm 10.0190, 33.4602)$, there exist Hopf bifurcations when suitable parameters are chosen. Fig. 3.22 shows the phase portraits of state variables of system (3.22) with $d_2 = 10$, which is a 8-scroll attractor. The maximal Lyapunov exponent is

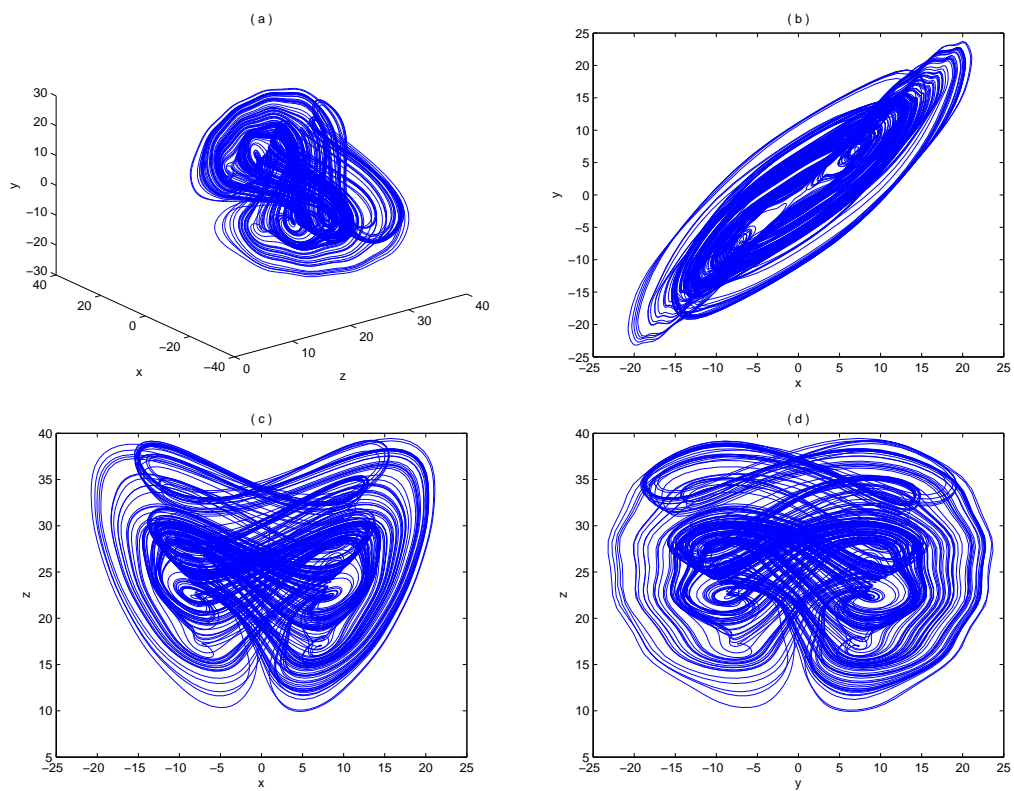


Figure 3.21: The phase portraits of system (3.22) with $d_2 = 5$, starting from $(1, 1, 30)$. (a) z - x - y ; (b) x - y ; (c) x - z ; (d) y - z .

$LE_{max} = 7.0722$ and Lyapunov dimension $d = 2.4142$.

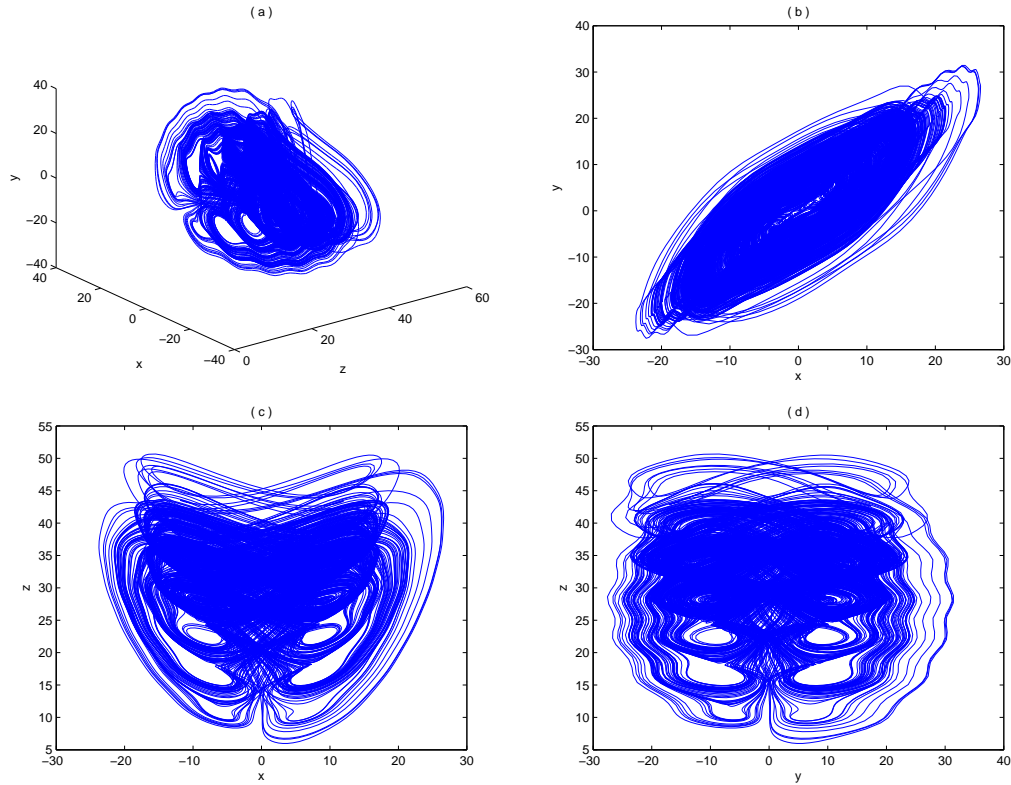


Figure 3.22: The phase portraits of system (3.22) with $d_2 = 14$, starting from $(1, 1, 30)$. (a) z-x-y; (b) x-y; (c) x-z; (d) y-z.

When $d_2 = 22$, system (3.22) has 27 equilibrium points $(0, 0, 0)$, $(\pm 3.4741, \pm 3.4741, 4.0231)$, $(\pm 4.0626, \pm 4.0626, 5.5015)$, $(\pm 5.4638, \pm 5.4638, 9.9510)$, $(\pm 6.0380, \pm 6.0380, 12.1525)$, $(\pm 6.9152, \pm 6.9152, 15.9400)$, $(\pm 7.4994, \pm 7.4994, 18.7470)$, $(\pm 8.1144, \pm 8.1144, 21.9480)$, $(\pm 8.7174, \pm 8.7174, 25.3309)$, $(\pm 9.1574, \pm 9.1574, 27.9528)$, $(\pm 9.7882, \pm 9.7882, 31.9362)$, $(\pm 10.0890, \pm 10.0890, 33.9293)$, $(\pm 10.7650, \pm 10.7650, 38.6286)$ and $(\pm 10.9291, \pm 10.9291, 39.8147)$. At points $(\pm 3.4741, \pm 3.4741, 4.0231)$, $(\pm 5.4638, \pm 5.4638, 9.9510)$, $(\pm 6.9152, \pm 6.9152, 15.9400)$, $(\pm 8.1144, \pm 8.1144, 21.9480)$, $(\pm 9.1574, \pm 9.1574, 27.9528)$, $(\pm 10.0890, \pm 10.0890, 33.9293)$ and $(\pm 10.9291, \pm 10.9291, 39.8147)$, there exist Hopf bifurcations when

suitable parameters are chosen. Fig. 3.23 shows the phase portraits of state variables of system (3.22) with $d_2 = 22$, which is a 14-scroll attractor. The maximal Lyapunov exponent is $LE_{max} = 8.6318$ and Lyapunov dimension $d = 2.4632$.

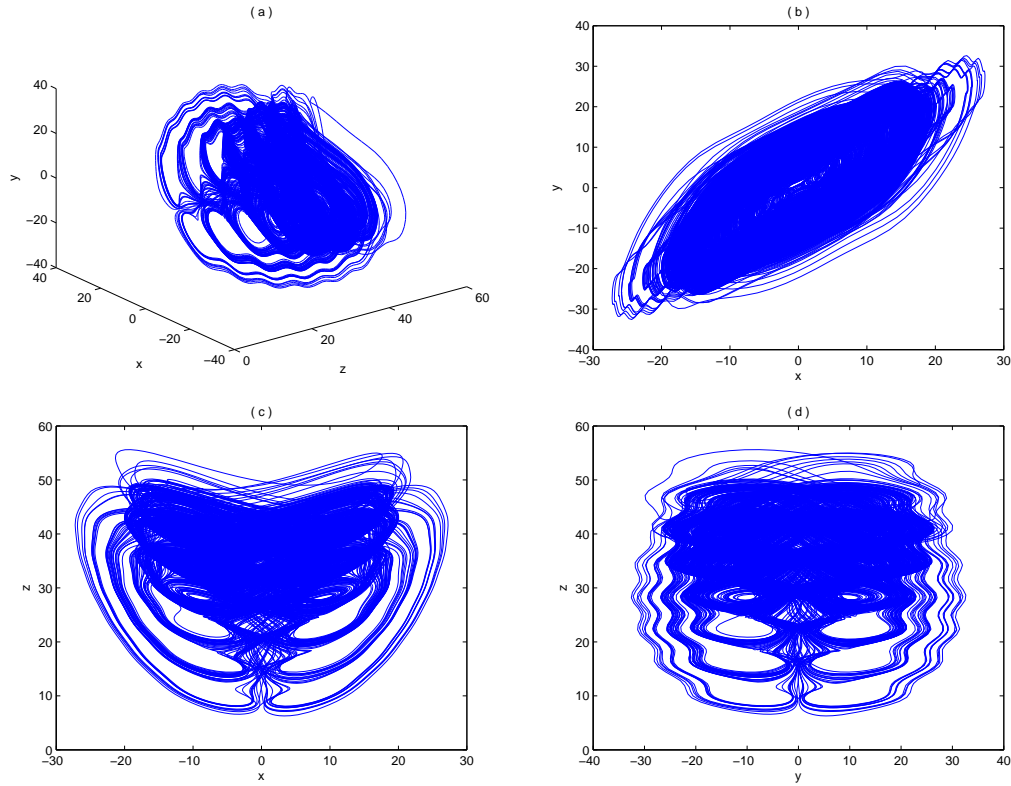


Figure 3.23: The phase portraits of system (3.22) with $d_2 = 22$, starting from $(1, 1, 30)$. (a) z-x-y; (b) x-y; (c) x-z; (d) y-z.

When $d_2 = 28$, system (3.22) has 31 equilibrium points $(0, 0, 0)$, $(\pm 3.3777, \pm 3.3777, 3.8029)$, $(\pm 4.1371, \pm 4.1371, 5.7053)$, $(\pm 5.4318, \pm 5.4318, 9.8349)$, $(\pm 6.0618, \pm 6.0618, 12.2485)$, $(\pm 6.9047, \pm 6.9047, 15.8914)$, $(\pm 7.5040, \pm 7.5040, 18.7698)$, $(\pm 8.1161, \pm 8.1161, 21.9570)$, $(\pm 8.7097, \pm 8.7097, 25.2864)$, $(\pm 9.1686, \pm 9.1686, 28.0209)$, $(\pm 9.7692, \pm 9.7692, 31.8124)$, $(\pm 10.1102, \pm 10.1102, 34.0718)$, $(\pm 10.7287, \pm 10.7287, 38.3682)$, $(\pm 10.9668, \pm 10.9668, 40.0905)$, $(\pm 11.6206, \pm 11.6206, 45.0129)$ and $(\pm 11.7497, \pm 11.7497, 46.0188)$. At points $(\pm 3.3777,$

$\pm 3.3777, 3.8029$), $(\pm 5.4318, \pm 5.4318, 9.8349)$, $(\pm 6.9047, \pm 6.9047, 15.8914)$, $(\pm 8.1161, \pm 8.1161, 21.9570)$, $(\pm 9.1686, \pm 9.1686, 28.0209)$, $(\pm 10.1102, \pm 10.1102, 34.0718)$, $(\pm 10.9668, \pm 10.9668, 40.0905)$ and $(\pm 11.7497, \pm 11.7497, 46.0188)$, there exist Hopf bifurcations when suitable parameters are chosen. Fig. 3.24 shows the phase portraits of state variables of system (3.22) with $d_2 = 28$, which is a 16-scroll attractor. The maximal Lyapunov exponent is $LE_{max} = 8.7869$ and Lyapunov dimension $d = 2.4677$.

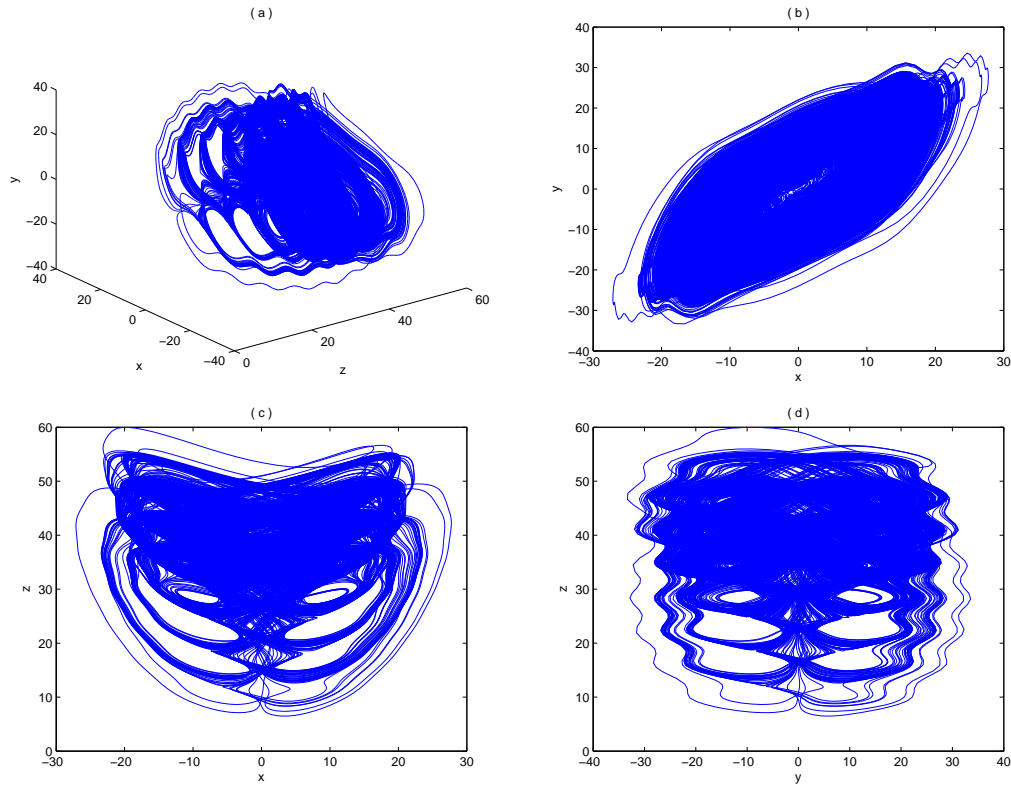


Figure 3.24: The phase portraits of system (3.22) with $d_2 = 28$, starting from $(1, 1, 30)$. (a) z-x-y; (b) x-y; (c) x-z; (d) y-z.

Fig. 3.25 shows all three Lyapunov exponents change as d_2 ranges in $[5 \ 25]$ with fixed parameters $a = 35, b = 3, c = 28$ and $d_1 = 1$.

Remark 1: when parameter d_2 increases, the number of equilibrium points increases cor-

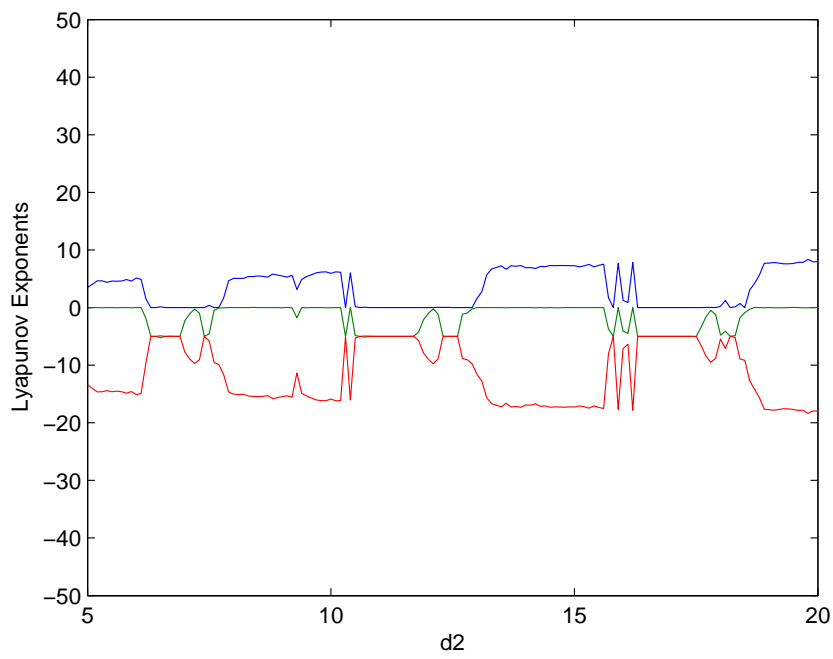


Figure 3.25: All Lyapunov exponents vs parameter d_2 in $[5 \ 25]$ with $a = 35$, $b = 3$, $c = 28$ and $d_1 = 1$.

respondingly. With Hopf bifurcation occurring over and over again, system (3.22) generates new attractors with more scrolls.

3.2.4 Generalized More Complex Chaos and Hyperchaos

We know one order delay differential equation can generate hyperchaotic dynamic behavior. In order to generalize system (3.22) to more complex chaos and hyperchaos, we introduce delay to control function, $u(t) = d_0z(t) + d_1z(t - \tau) - d_2\sin(z(t - \tau))$, system (3.22) transforms to the following.

$$\begin{cases} \dot{x} = a(y - x) \\ \dot{y} = (c - a)x - x(d_0z(t) + d_1z(t - \tau) - d_2\sin(z(t - \tau))) + cy \\ \dot{z} = xy - bz \end{cases} \quad (3.24)$$

where d_0, d_1, d_2 are constants and τ is delay time. When suitable parameters are chosen, system (3.24) can generate different chaotic and hyperchaotic attractors as follows.

3.2.4.1 Special Case I: $d_0 = d_1$

When $d_0 = 1, d_1 = 1, d_2 = 5$ and $\tau = 0.1$, system (3.24) generates different chaotic dynamic behaviors. The phase portraits are shown in Fig. 3.26.

When $d_0 = 1, d_1 = 1, d_2 = 5$ and $\tau = 0.8$, system (3.24) generates different chaotic dynamic behaviors. The phase portraits are shown in Fig. 3.27.

When $d_0 = 1, d_1 = 1, d_2 = 30$ and $\tau = 0.05$, system (3.24) generates hyperchaotic dynamic behaviors. The phase portraits are shown in Fig. 3.28.

When $d_0 = 1, d_1 = 1, d_2 = 30$ and $\tau = 0.8$, system (3.24) generates hyperchaotic dynamic behaviors. The phase portraits are shown in Fig. 3.29.

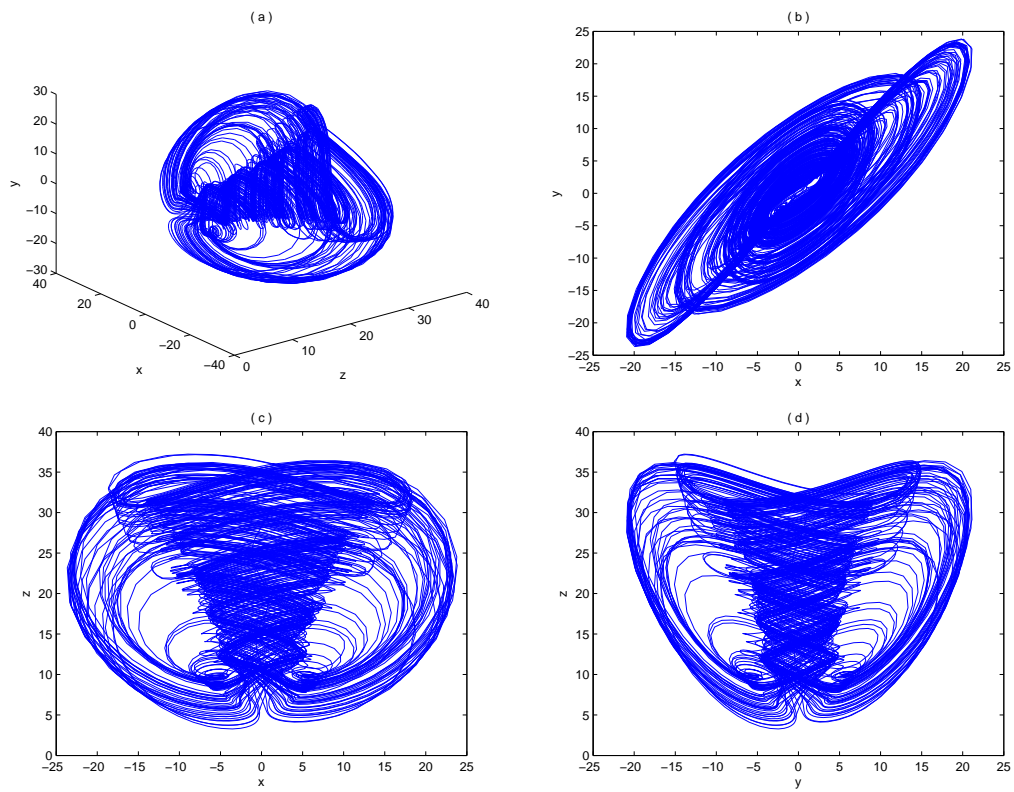


Figure 3.26: The phase portraits of system (3.24) with $d_0 = 1$, $d_1 = 1$, $d_2 = 5$ and $\tau = 0.1$.

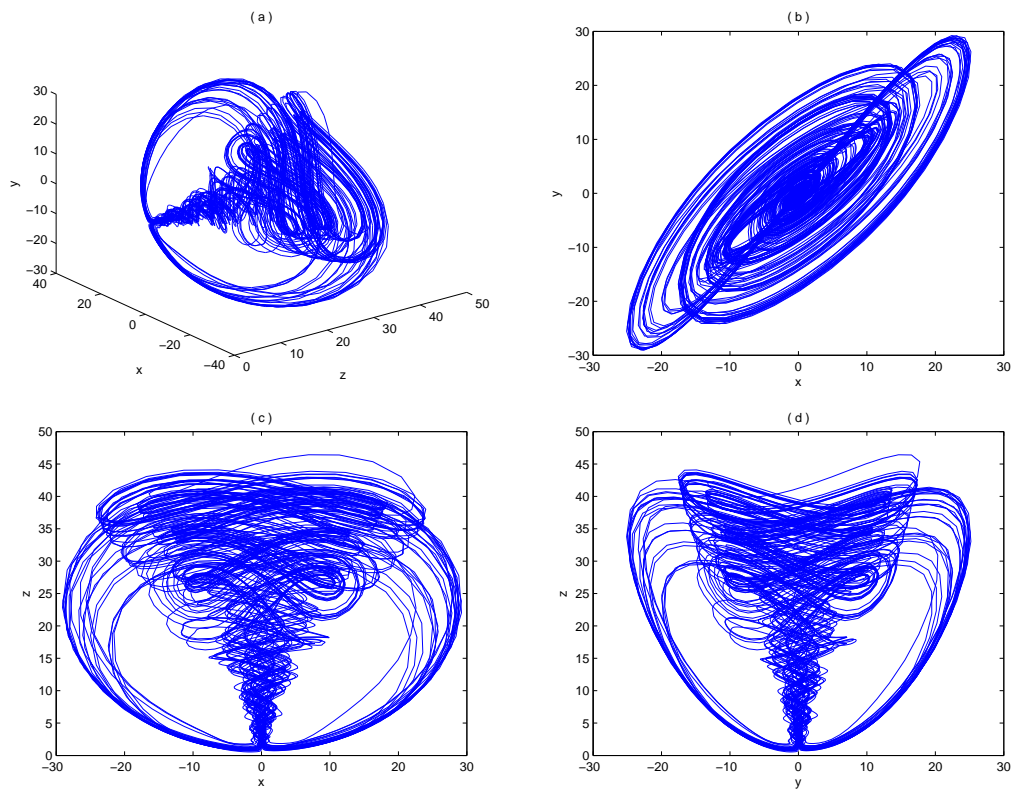


Figure 3.27: The phase portraits of system (3.24) with $d_0 = 1$, $d_1 = 1$, $d_2 = 5$ and $\tau = 0.8$.

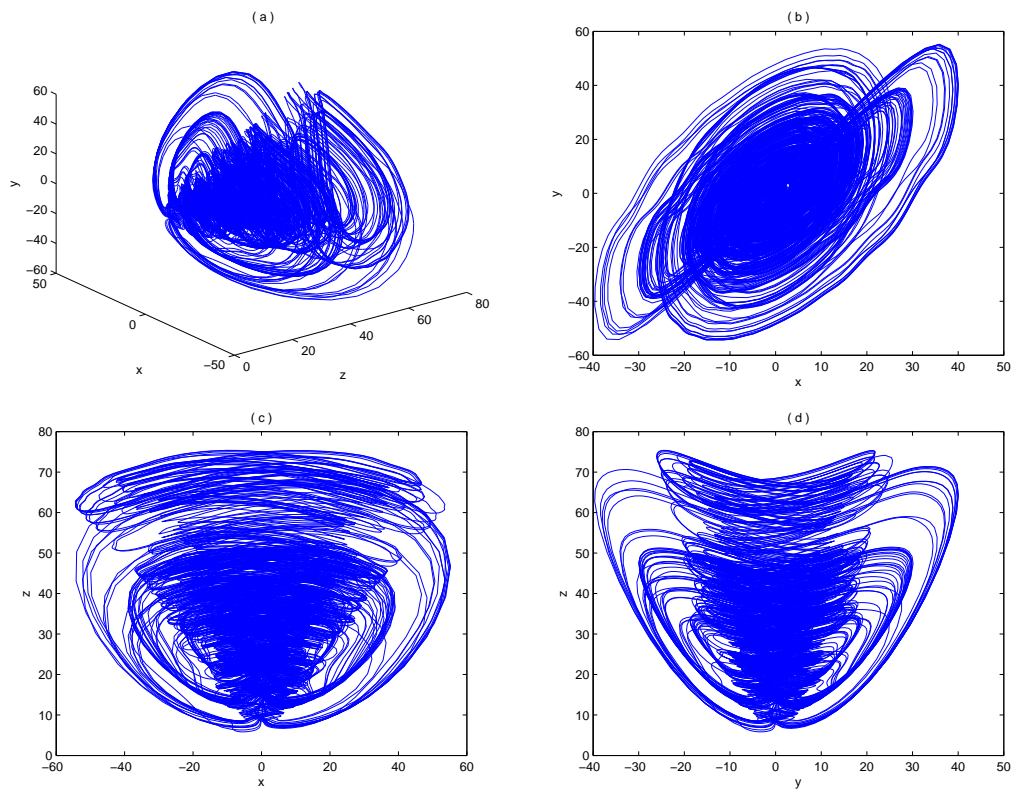


Figure 3.28: The phase portraits of system (3.24) with $d_0 = 1$, $d_1 = 1$, $d_2 = 30$ and $\tau = 0.05$.

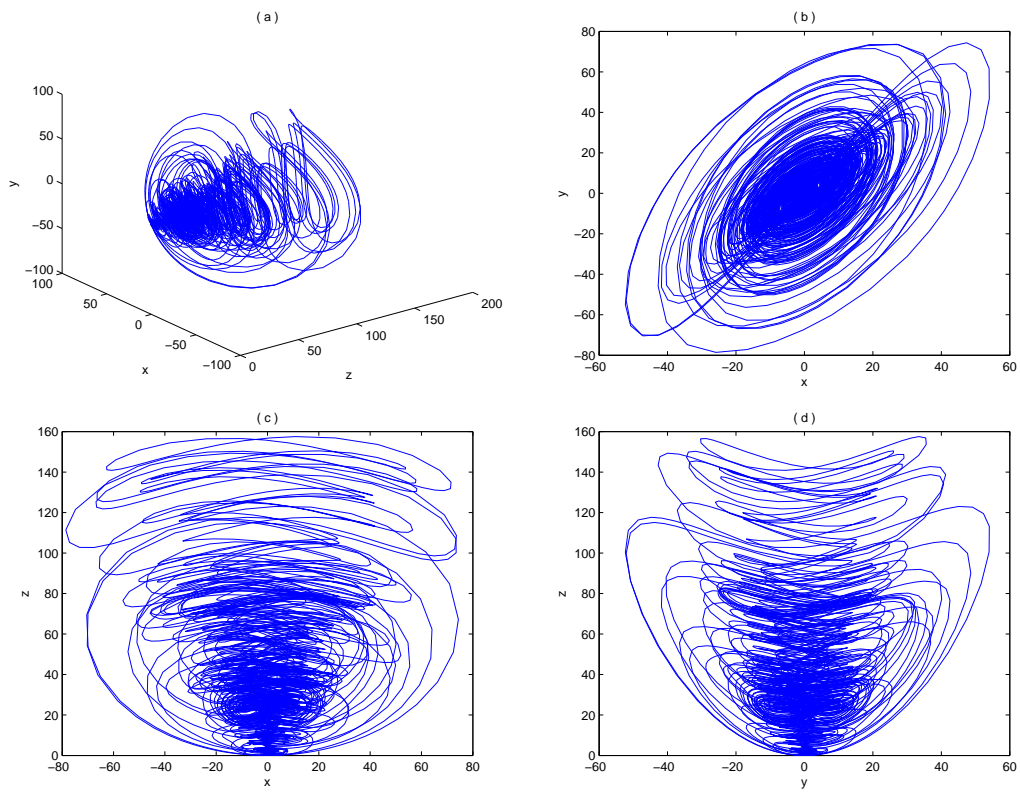


Figure 3.29: The phase portraits of system (3.24) with $d_0 = 1$, $d_1 = 1$, $d_2 = 30$ and $\tau = 0.8$.

3.2.4.2 Special Case II: $d_0 \neq d_1$

When $d_0 = 0.2$, $d_1 = 2$, $d_2 = 5$ and $\tau = 5$, system (3.24) generates different hyperchaotic dynamic behavior. The phase portraits are shown in Fig. 3.30.

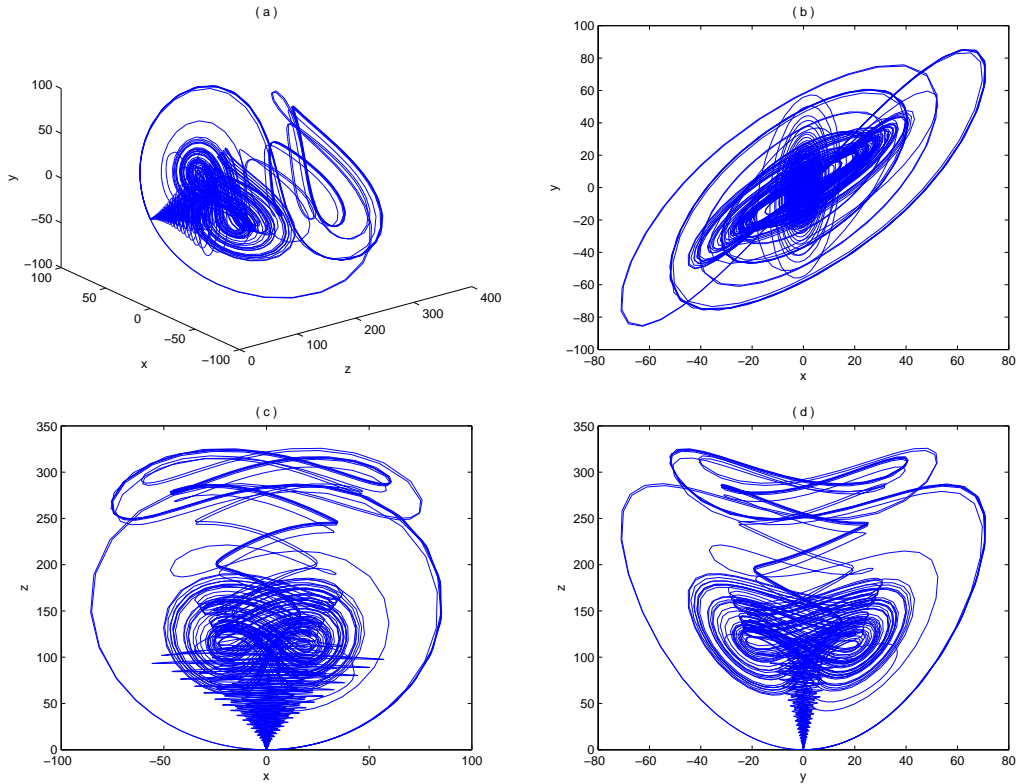


Figure 3.30: The phase portraits of system (3.24) with $d_0 = 0.2$, $d_1 = 2$, $d_2 = 5$ and $\tau = 5$.

When $d_0 = 0.2$, $d_1 = 2$, $d_2 = 40$ and $\tau = 5$, system (3.24) generates different hyperchaotic dynamic behavior. The phase portraits are shown in Fig. 3.31.

When $d_0 = 1$, $d_1 = -0.2$, $d_2 = 20$ and $\tau = 5$, system (3.24) generates different hyperchaotic dynamic behavior. The phase portraits are shown in Fig. 3.32.

When $d_0 = 1$, $d_1 = -0.8$, $d_2 = 5$ and $\tau = 5$, system (3.24) generates different hyperchaotic dynamic behavior. The phase portraits are shown in Fig. 3.33.

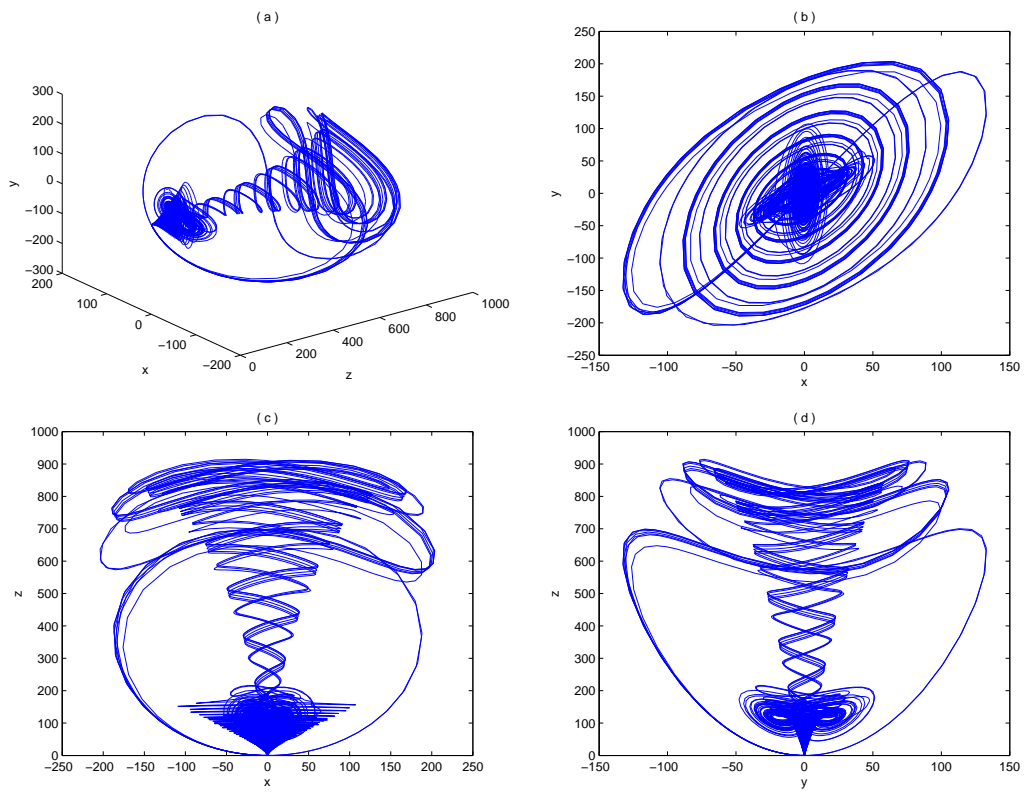


Figure 3.31: The phase portraits of system (3.24) with $d_0 = 0.2$, $d_1 = 2$, $d_2 = 40$ and $\tau = 5$.

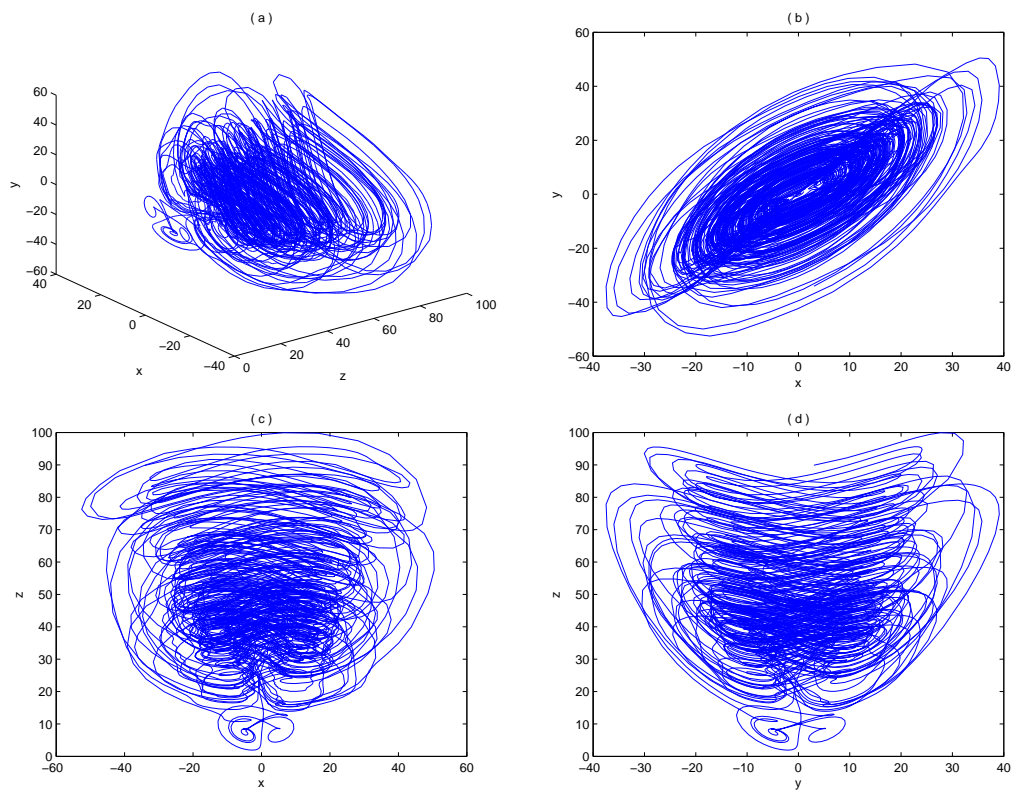


Figure 3.32: The phase portraits of system (3.24) with $d_0 = 1$, $d_1 = -0.2$, $d_2 = 20$ and $\tau = 5$.

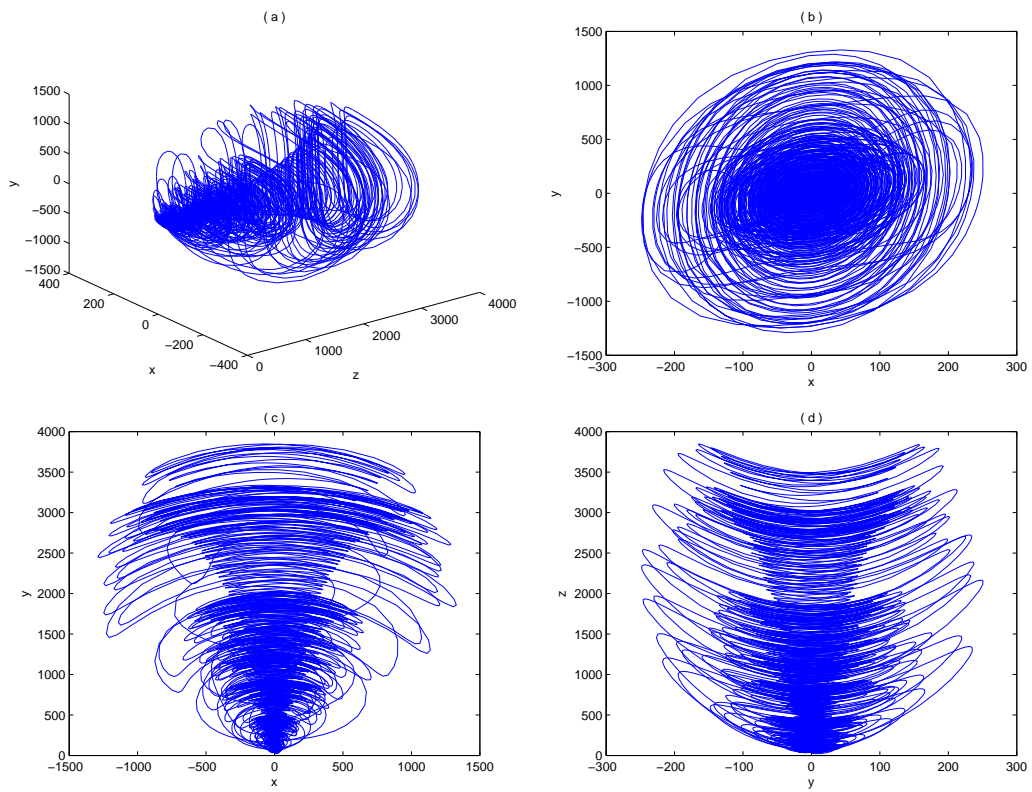


Figure 3.33: The phase portraits of system (3.24) with $d_0 = 1$, $d_1 = -0.8$, $d_2 = 5$ and $\tau = 5$.

3.2.5 Summary

This section has presented a feedback control function to generate multi-scroll attractors from Chen system. we have analyzed the dynamical behavior of this new attractor. By controlling the control parameters, we have achieved a set of new attractors with different scrolls. After that, we introduced time delay to control function $u(t)$ to generalize the multi-scroll attractors to more complex chaos and hyperchaos. This kind of control method can also be used to other chaotic system, such as Lorenz system, Jerk equation and so on.

Chapter 4

Impulsive Synchronization of Chaotic Systems with Delay

4.1 Synchronization of Two Chaotic Systems with Delay

In this section, we consider the impulsive synchronization of chaotic Lur'e systems with output feedback. The presence of transmission delay and sampling delay in the output feedback and impulsive control is studied. Based on LMI method, four sufficient condition for global asymptotic synchronization are derived. Finally, a numerical example is given to illuminate the validity of main results.

4.1.1 Background

Over the past decade, synchronization of chaotic or hyperchaotic systems and its applications to security communication have attracted a great deal of attention. In communication security schemes, information signals are masked by chaotic signal and then recovered in the receiver end. The recovery of the information signals requires that the receiver's chaotic signal is synchronized with the transmitter's one. There are two kind of methods to achieve synchronization which are state feedback and impulsive control. Firstly, synchronization is

done through driving the system at the receiver end by one of the state variables of the system at the transmitter end [5, 21, 22]. Furthermore, a linear combination of the state variables of the system at the transmitter end is applied [61, 85]. The hyperchaos synchronization between higher dimensional chaotic systems, possessing more than one positive Lyapunov exponent has been studied [61, 85]. Impulsive synchronization allows synchronization of chaotic systems using only small impulses generated by samples of the state variables of the driving system at discrete time instances. It has been developed [86, 87] and applied to a number of chaos-based communication systems which exhibit good performance for the synchronization purposes and for security purposes [18, 53].

Recently, the transmission and sampling delays in communication security systems become a hot issue which is a very challenging problem in both theory and application. Some results have been achieved [54–56]. Motivated by the above comments, we further study the chaos synchronization by both output feedback and impulsive control with delay in this paper. In particular, we analyze how much delay such systems can endure by a numerical example which reflect the robustness of impulsive synchronization and the ability to overcome the delay problem.

4.1.2 System Statement and Synchronization Scheme

Consider the following master-slave synchronization scheme:

$$\begin{aligned}
M & : \begin{cases} \dot{x}(t) = Ax(t) + B\sigma(Dx(t)) \\ p(t) = Cx(t) \end{cases} \\
S & : \begin{cases} \dot{z}(t) = Az(t) + B\sigma(Dz(t)) + u, t \neq \tau_i \\ q(t) = Cz(t) \end{cases} \\
C & : \Delta z(t) = K_3(p(t) - q(t)) + K_4(p(t - \gamma_i) - q(t - \gamma_i)), t = \tau_i
\end{aligned} \tag{4.1}$$

which consists of master system M , slave system S , output feedback $u = K_1(p(t) - q(t)) + K_2(p(t - \tilde{\gamma}) - q(t - \tilde{\gamma}))$, $\tilde{\gamma} \leq \gamma$, $\gamma_i \leq \gamma$, $\gamma \leq \Delta_i = \tau_{i+1} - \tau_i$ and impulsive control C .

M and S are identical Lur'e chaotic system with state vectors $x(t), z(t) \in R^n$ and matrices $A \in R^{n \times n}$, $B \in R^{n \times n_h}$, $D \in R^{n_h \times n}$. The diagonal nonlinearity $\sigma(\cdot) : R^{n_h} \mapsto R^{n_h}$ is assumed to belong to sector $[0, k]$. The output vectors of M and S are $p(t), q(t) \in R^l$ with $l \leq n$ and matrix $C \in R^{l \times n}$. For the impulsive control law C , a set of discrete time instants τ_i is considered where $0 < \tau_1 < \tau_2 < \dots < \tau_i < \dots$ with $\tau_i \rightarrow \infty$ as $i \rightarrow \infty$. K_1, K_3 are the matrices of output feedback and impulsive control respectively. K_2, K_4 are the delay perturbation matrices of output feedback and impulsive control respectively. $\tilde{\gamma}$ is the output feedback delay due to the presence of transmission delay in the process, and γ_i is the impulsive delay due to sample the impulses in the receiver end.

At the time instants τ_i , jumps in the state variable $z(t)$ are imposed

$$\Delta z(t)|_{t=\tau_i} = z(\tau_i^+) - z(\tau_i^-). \quad (4.2)$$

Let $e(t) = x(t) - z(t)$. From the synchronization scheme (4.1), the error dynamics $e(t)$ is given by

$$E : \begin{cases} \dot{e}(t) &= (A - K_1 C)e(t) + B\eta(De(t); z(t)) - K_2 C e(t - \tilde{\gamma}), t \neq \tau_i \\ \Delta e(t) &= -K_3 C e(t) - K_4 C e(t - \gamma_i), t = \tau_i \end{cases} \quad (4.3)$$

where $\eta(De(t); z(t)) = \sigma(De(t) + Dz(t)) - \sigma(Dz(t))$ and $\Delta e(t) = \Delta x(t) - \Delta z(t)$ with $\Delta x(t) = 0$. Assume that the nonlinearity $\eta(De(t); z(t))$ belongs to sector $[0, k]$:

$$0 \leq \frac{\eta_i(d_i^T e(t); z(t))}{d_i^T e(t)} = \frac{\sigma_i(d_i^T e(t) + d_i^T z(t)) - \sigma_i(d_i^T z(t))}{d_i^T e(t)} \leq k, \quad \forall e(t), z(t); i = 1, 2, \dots, n_h (d_i^T e(t) \neq 0), \quad (4.4)$$

where d_i^T denotes the i th row vector of D .

Then, the following inequality holds:

$$\eta_i(d_i^T e(t); z(t))[\eta_i(d_i^T e(t); z(t)) - kd_i^T e(t)] \leq 0, \quad \forall e(t), z(t); i = 1, 2, \dots, n_h. \quad (4.5)$$

4.1.3 Main Results

In this subsection, we shall obtain some criteria for global asymptotical synchronization of system (4.1). Lemma 4.1 firstly is introduced which will be used in the proof of the theorems.

Lemma 4.1 [13]: Let $\gamma > 0$ and $m \in C^1[J, R_+]$, where $J = [a - \gamma, b)$, $0 < b - a \leq \Delta_i$. Assume that there exist constants $l > 0$ and $\beta \in (0, 1)$ such that

$$m'(t) \leq lm(t), \quad \text{whenever} \quad m(t) \geq \beta m(t + s), \quad s \in [-\gamma, 0]; \quad (4.6)$$

and there exists a constant $\eta > 0$ such that $m(s) \leq \eta$, $s \in [a - \gamma, a)$, $m(a) \leq \beta\eta$, and

$$l\Delta_i + \ln \beta < 0. \quad (4.7)$$

Then there exists an $d = d(\eta)$, $0 < d < \eta$ such that $m(t) \leq \eta - d$, $t \geq a$.

Theorem 4.1: For $K_2 \neq 0$, $K_4 \neq 0$, if there exist a diagonal positive definite matrix $\Lambda = \text{diag}\{\lambda_i\} \in R^{n_h \times n_h}$, a symmetric positive definite matrix $P \in R^{n \times n}$, matrices $K_1, K_3 \in R^{n \times l}$, $F_1 = -K_1 C$, $F_2 = -K_2 C$, $G_1 = -K_3 C$, $G_2 = -K_4 C$, and real constants $\alpha_1, \alpha_2 > 0$, $\beta_1 > 0$, $\beta_2 > 0$, $\beta_1 + \beta_2 \leq \beta < 1$ such that the following matrix inequalities

$$\begin{bmatrix} (A + F_1)^T P + P(A + F_1) - \alpha_1 P & PB + kD^T \Lambda & PF_2 \\ B^T P + k\Lambda D & -2\Lambda & 0 \\ F_2^T P & 0 & -\alpha_2 P \end{bmatrix} \leq 0, \quad (4.8)$$

$$\begin{bmatrix} (I + G_1^T)P(I + G_1) - \beta_1 P & (I + G_1^T)PG_2 \\ G_2^T P(I + G_1) & G_2^T PG_2 - \beta_2 P \end{bmatrix} \leq 0, \quad (4.9)$$

$$\frac{\Delta_i}{\beta}(\beta\alpha_1 + \alpha_2) + \ln \beta < 0, \quad i = 1, 2, \dots \quad (4.10)$$

are satisfied, then the origin of the synchronization error system (4.3) is globally asymptotically stable. In other words, the master system M and the slave system S are of global asymptotical synchronization.

Proof: Construct a Lyapunov function in the form of

$$V(e(t)) = e^T(t)Pe(t), \quad (4.11)$$

where P is a symmetric positive definite matrix. Let $V(t) =: V(e(t))$.

When $t \in (\tau_i, \tau_{i+1})$, taking the time derivative of the Lyapunov function (4.11) along the trajectories of (4.3) and using the inequalities (4.5), (4.8), one obtains

$$\begin{aligned} & \dot{V}(t) \\ &= \dot{e}(t)^T Pe(t) + e(t)^T P\dot{e}(t) \\ &= e(t)^T ((A + F_1)^T P + P(A + F_1))e(t) + \eta^T B^T Pe(t) + e(t)^T PB\eta + e(t - \tilde{\gamma})^T F_2^T Pe(t) \\ & \quad + e(t)^T PF_2e(t - \tilde{\gamma}) \\ &\leq e(t)^T ((A + F_1)^T P + P(A + F_1))e(t) + \eta^T B^T Pe(t) + e(t)^T PB\eta + e(t - \tilde{\gamma})^T F_2^T Pe(t) \\ & \quad + e(t)^T PF_2e(t - \tilde{\gamma}) - \sum_i 2\lambda_i \eta_i (\eta_i - kd_i^T e(t)) \\ &\leq \xi_1^T Y_1 \xi_1 + \alpha_1 e(t)^T Pe(t) + \alpha_2 e(t - \tilde{\gamma})^T Pe(t - \tilde{\gamma}) \\ &\leq \alpha_1 V(t) + \alpha_2 V(t - \tilde{\gamma}). \end{aligned} \quad (4.12)$$

$$\text{where } \xi_1 = \begin{bmatrix} e(t) \\ \eta \\ e(t - \tilde{\gamma}) \end{bmatrix}, Y = \begin{bmatrix} (A + F_1)^T P + P(A + F_1) - \alpha_1 P & PB + kD^T \Lambda & PF_2 \\ B^T P + k\Lambda D & -2\Lambda & 0 \\ F_2^T P & 0 & -\alpha_2 P \end{bmatrix}.$$

(4.12) implies, if $V(t) \geq \beta m(t + s)$, $s \in [-\gamma, 0]$,

$$V\dot{(t)} \leq \frac{1}{\beta}(\beta\alpha_1 + \alpha_2)V(t), t \neq \tau_i. \quad (4.13)$$

When $t = \tau_i$, in terms of (4.9), we have

$$\begin{aligned} & V(\tau_i) \\ &= ((I + G_1)e(\tau_i^-) + G_2e(\tau_i - \gamma_i))^T P((I + G_1)e(\tau_i^-) + G_2e(\tau_i - \gamma_i)) \\ &= e(\tau_i^-)^T (I + G_1)^T P(I + G_1)e(\tau_i^-) + e(\tau_i - \gamma_i)^T G_2^T P(I + G_1)e(\tau_i^-) \\ & \quad + e(\tau_i^-)^T (I + G_1)^T PG_2e(\tau_i - \gamma_i) + e(\tau_i - \gamma_i)^T G_2^T PG_2e(\tau_i - \gamma_i) \\ &\leq \zeta_1^T Y S_1 \zeta_1 + \beta_1 e(\tau_i^-)^T Pe(\tau_i^-) + \beta_2 e(\tau_i - \gamma_i)^T Pe(\tau_i - \gamma_i) \\ &\leq \beta_1 V(\tau_i^-) + \beta_2 V(\tau_i - \gamma_i), i = 1, 2, \dots \end{aligned} \quad (4.14)$$

where $\zeta_1 = \begin{bmatrix} e(\tau_i^-) \\ e(\tau_i - \gamma_i) \end{bmatrix}$, $Y = \begin{bmatrix} (I + G_1^T)P(I + G_1) - \beta_1 P & (I + G_1^T)PG_2 \\ G_2^T P(I + G_1) & G_2^T PG_2 - \beta_2 P \end{bmatrix}$.
 Suppose that the original condition $V(t_0) \leq \eta$, $t_0 \in [\tau_1 - \gamma, \tau_1)$, by (14), we have

$$V(\tau_1) \leq \beta_1 V(\tau_1^-) + \beta_2 V(\tau_1 - \gamma_1) \leq \beta \eta, \quad (4.15)$$

in view of (4.10), (4.13), (4.15) and lemma 4.1, one obtains

$$V(t) \leq \rho \eta, \quad \rho \in (0, 1), t \in (\tau_1, \tau_2). \quad (4.16)$$

Continuing this process, we get

$$V(\tau_i) \leq \beta_1 V(\tau_i^-) + \beta_2 V(\tau_i - \gamma_i) \leq \beta \rho^{i-1} \eta, \quad (4.17)$$

and

$$V(t) \leq \rho^{i-1} \eta, \quad \rho \in (0, 1), t \in (\tau_i, \tau_{i+1}). \quad (4.18)$$

which yields $V(t) \mapsto 0$, as $i \mapsto +\infty$. Thus, $e(t) \mapsto 0$, as $t \mapsto +\infty$.

Therefore, the origin of the synchronization error system (4.3) is globally asymptotically stable. In other words, the master system M and the slave system S are of global asymptotical synchronization.

When $K_4 = 0$, i.e., there exists no delay perturbation in the impulsive control, we have the following theorem:

Theorem 4.2 [57]: For $K_2 \neq 0$, $K_4 = 0$, For $K_2 \neq 0$, $K_4 \neq 0$, if there exist a diagonal positive definite matrix $\Lambda = \text{diag}\{\lambda_i\} \in R^{n_h \times n_h}$, a symmetric positive definite matrix $P \in R^{n \times n}$, matrices $K_1, K_3 \in R^{n \times l}$, $F_1 = -K_1 C$, $F_2 = -K_2 C$, $G_1 = -K_3 C$, and real constants $\alpha_1, \alpha_2 > 0$, $0 < \beta < 1$ such that the following matrix inequalities

$$\begin{bmatrix} (A + F_1)^T P + P(A + F_1) - \alpha_1 P & PB + kD^T \Lambda & PF_2 \\ B^T P + k\Lambda D & -2\Lambda & 0 \\ F_2^T P & 0 & -\alpha_2 P \end{bmatrix} \leq 0, \quad (4.19)$$

$$\begin{bmatrix} -\beta P & (I + G_1)^T P \\ P(I + G_1) & -P \end{bmatrix} \leq 0, \quad (4.20)$$

$$\frac{\Delta_i}{\beta}(\beta\alpha_1 + \alpha_2) + \ln \beta < 0, i = 1, 2, \dots \quad (4.21)$$

are satisfied, then the origin of the synchronization error system (4.3) is globally asymptotically stable. In other words, the master system M and the slave system S are of global asymptotical synchronization.

The proof is similar to that of Theorem 4.1. and thus is omitted.

When $K_2 = 0$, i.e., there exists no delay perturbation in feedback control, we get the following theorem:

Theorem 4.3: For $K_2 = 0$, $K_4 \neq 0$, if there exist a diagonal positive definite matrix $\Lambda = \text{diag}\{\lambda_i\} \in R^{n_h \times n_h}$, a symmetric positive definite matrix $P \in R^{n \times n}$, matrices $K_1, K_3 \in R^{n \times l}$, $F_1 = -K_1 C$, $G_1 = -K_3 C$, $G_2 = -K_4 C$, and real constants $\alpha_1, \beta_1 > 0$, $\beta_2 > 0$, $\beta_1 + \beta_2 \leq \beta < 1$ such that the following matrix inequalities

$$\begin{bmatrix} (A + F_1)^T P + P(A + F_1) - \alpha_1 P & PB + kD^T \Lambda \\ B^T P + k\Lambda D & -2\Lambda \end{bmatrix} \leq 0, \quad (4.22)$$

$$\begin{bmatrix} (I + G_1^T)P(I + G_1) - \beta_1 P & (I + G_1^T)PG_2 \\ G_2^T P(I + G_1) & G_2^T PG_2 - \beta_2 P \end{bmatrix} \leq 0, \quad (4.23)$$

$$\Delta_i \alpha_1 + \ln \beta < 0, i = 1, 2, \dots \quad (4.24)$$

are satisfied, then the origin of the synchronization error system (4.3) is globally asymptotically stable. In other words, the master system M and the slave system S are of global asymptotical synchronization.

The proof is similar to that of Theorem 4.1. and thus is omitted.

When $K_2 = K_4 = 0$, i.e., there exists no delay perturbation in both feedback control and impulsive control, we get the following theorem:

Theorem 4.4: For $K_2 = 0$, $K_4 = 0$, if there exist a diagonal positive definite matrix $\Lambda = \text{diag}\{\lambda_i\} \in R^{n_h \times n_h}$, a symmetric positive definite matrix $P \in R^{n \times n}$, matrices $K_1, K_3 \in R^{n \times l}$, $F_1 = -K_1 C$, $G_1 = -K_3 C$, and real constants α , $0 < \beta < 1$ such that the following matrix inequalities

$$\begin{bmatrix} (A + F_1)^T P + P(A + F_1) - \alpha_1 P & PB + kD^T \Lambda \\ B^T P + k\Lambda D & -2\Lambda \end{bmatrix} \leq 0, \quad (4.25)$$

$$\begin{bmatrix} -\beta P & (I + G_1)^T P \\ P(I + G_1) & -P \end{bmatrix} \leq 0, \quad (4.26)$$

$$\Delta_i \alpha_1 + \ln \beta < 0, i = 1, 2, \dots \quad (4.27)$$

are satisfied, then the origin of the synchronization error system (4.3) is globally asymptotically stable. In other words, the master system M and the slave system S are of global asymptotical synchronization.

The proof is similar to that of Theorem 4.1. and thus is omitted.

Remark 4.1: In Theorem 4.1, the constant α_1 (if $\alpha_1 > 0$) measures the degree of instability of the error system with only feedback control and is determined by the eigenvalues of the matrix $A + F_1$. α_2 is determined by the matrix F_2 . The positive constants β_1, β_2 measure the amplitude of the control impulses, the smaller the β_1, β_2 are and the larger the amplitude. If $\alpha_1 < 0$, i.e., the error system with only feedback control is stable, then a larger interval length of consecutive impulses is allowed.

4.1.4 Numerical Example

In this subsection, we illustrate the synchronization based on two identical chua's circuits. We take the following representation for Chua's circuit:

$$\begin{cases} \dot{x}_1 = a_1[x_2 - h(x_1)] \\ \dot{x}_2 = x_1 - x_2 + x_3 \\ \dot{x}_3 = -a_2x_2 \end{cases} \quad (4.28)$$

with nonlinear characteristic

$$h(x_1) = m_1x_1 + \frac{1}{2}(m_0 - m_1)(|x_1 + a_3| - |x_1 - a_3|)$$

where $a_1 = 9$, $a_2 = 14.286$, $a_3 = 1$, $m_0 = -1/7$, $m_1 = 1.5/7$ in order to obtain the double scroll attractor shown in Fig. 4.1. The nonlinearity $\psi(x_1) = 1/2(|x_1 + a_3| - |x_1 - a_3|)$ (linear characteristic with saturation) belongs to sector $[0, 1]$. Therefore, Chua's circuit can be interpreted as the Lur'e system $\dot{x} = Ax + B\psi(Dx)$ where

$$A = \begin{bmatrix} -a_1m_1 & a_1 & 0 \\ 1 & -1 & 1 \\ 0 & -a_2 & 0 \end{bmatrix}, B = \begin{bmatrix} -a_1(m_0 - m_1) \\ 0 \\ 0 \end{bmatrix}, \\ D = \begin{bmatrix} 1 & 0 & 0 \end{bmatrix}. \quad (4.29)$$

We define the output matrix $C = [1 \ 0 \ 0]$. Firstly, suppose that there exists no delay perturbation and choose the real constants $\alpha_1 = 2$, $\beta = 0.3$, $\Lambda = 2$, $P = I$ by Theorem 4.4, we obtain output feedback matrix and impulsive matrix as follows:

$$K_1 = [1.5379 \ 0.2841 \ -0.3648]^T, K_3 = [0.5 \ 0.5 \ 0.5]^T.$$

The impulsive intervals satisfy $\tau_{i+1} - \tau_i \leq 0.3010$. The simulation results of error system $e(t)$ are shown in Fig. 4.2. We can find that $e(t)$ is asymptotically tending to zero. When some delays in impulses occur $\gamma_i = 0.05$, the error system $e(t)$ becomes unstable as shown in Fig. 4.3.

If we suppose the transmission delay $\tilde{\gamma} = 0.04$, $\gamma_i = 0.02$, $K_2 = [2 \ 2 \ 2]^T$, $K_4 = [0.1 \ 0.1 \ 0.1]^T$ and choose the real constants $\alpha = -0.2$, $\beta_1 = 1.1$, $\beta_2 = 0.4$, $\Lambda = 3I$, $P =$

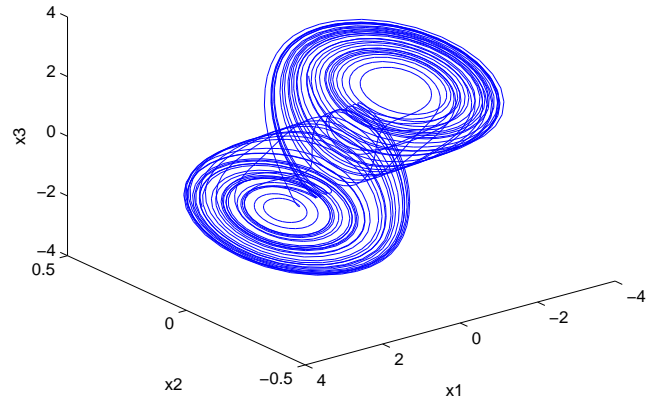


Figure 4.1: (x_1, x_2, x_3) of the master system.

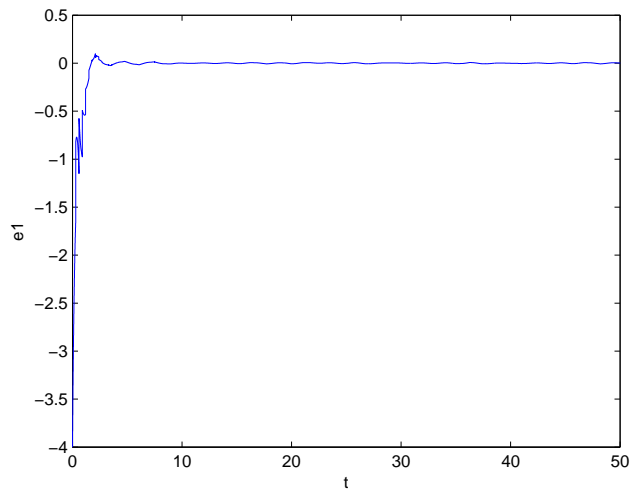


Figure 4.2: e_1 of the error system without delay.

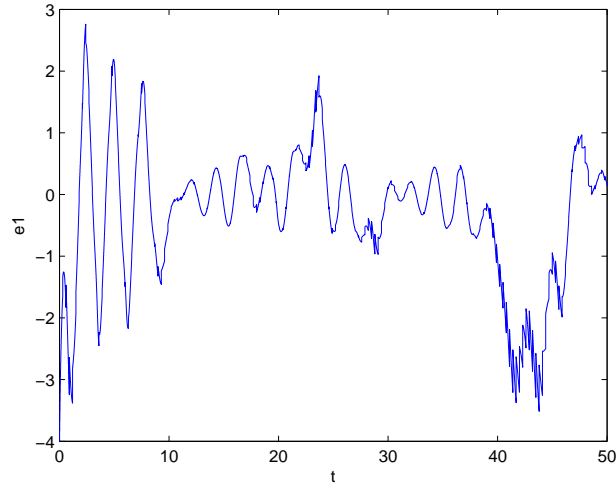


Figure 4.3: e_1 of the error system with $\gamma_i = 0.05$.

$Q = I$ By Theorem 4.1, we obtain the output feedback matrix and impulsive matrix as follows:

$$K_1 = [4.6911 \quad 1.5356 \quad -0.2775]^T, \quad K_3 = [0.95 \quad 0.95 \quad 0.95]^T,$$

and the impulsive interval $\tau_{i+1} - \tau_i \leq 0.12$. The simulation results of error system $e(t)$ are shown in Fig.4. In this condition, let $\tilde{\gamma} = 0$, $\gamma_i = 0$, the error system $e(t)$ still converge to zero. It is shown in Fig.5.

4.1.5 Summary

We investigated the synchronization of two identical Lur'e chaotic systems by impulsive control and output feedback control. Some sufficient conditions for global asymptotical synchronization have been achieved. By comparison, we find out the delay in impulses is terrible. A numerical example has been given to show the effectiveness of the main results.

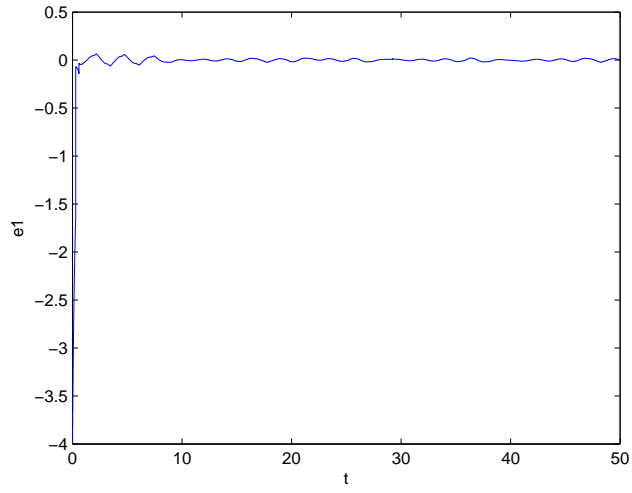


Figure 4.4: e_1 of the error system with $\tilde{\gamma} = 0.04$, $\gamma_i = 0.02$.

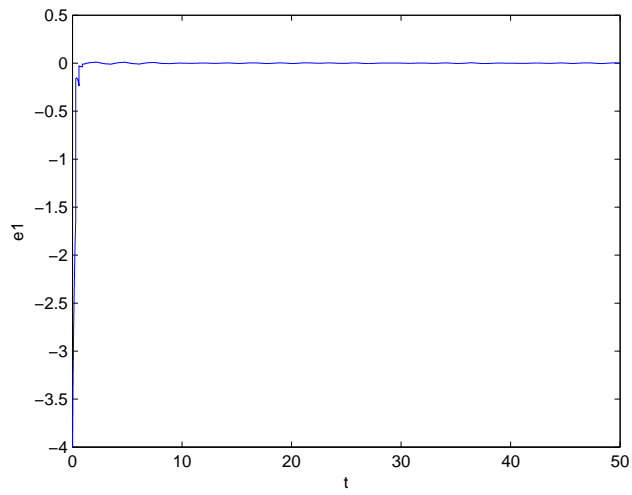


Figure 4.5: e_1 of the error system without delay.

4.2 Synchronization of Chaotic Dynamical Networks with Delay

In this section, we consider the impulsive synchronization of uncertain dynamical networks. The presence of coupling delay and impulsive delay in the network coupling and impulsive control is studied. Based on LMI method, several criteria for global impulsive synchronization are derived for complex dynamical networks. Finally, a numerical example is given to illuminate the validity of main results.

4.2.1 Background

Recently, synchronization of dynamical networks has become a hot issue [88–92]. A dynamical network is made up of coupled nodes, which may be chaotic systems such as Chua’s circuit, Chen’s system and so on. The network coupling functions which could be linear or nonlinear may be unknown, but they are bounded. It is noticed that the network coupling may affect heavily on the synchronization scheme when some synchronization techniques [88, 89] are applied. Although adaptive synchronization [91] is relatively relatively efficient method for uncertain dynamical networks, it is very complex to design the controller. Impulsive synchronization [18, 54–57, 87, 92], which allows synchronization of chaotic systems using only small impulses generated by samples of the state variables of the driving system at the discrete time instances, has been proved to be a very effective method in chaos synchronization. It can induce the information redundancy in the transmitted signal and increase the robustness against the disturbances. It has been applied to network synchronization without delay [92]. However, coupling delay and impulsive delay always occur in the synchronization process and sometime cause catastrophic results. It is a very challenging problem in both theory and application.

In this section, motivated by the above comments, we further study the network synchronization with coupling delay and impulsive delay. some criteria for global impulsive

synchronization are derived for complex dynamical networks. In particular, we analyze how much delay such systems can endure by a numerical example which reflect the robustness of impulsive synchronization and the ability to overcome the delay problem.

4.2.2 Preliminaries and Problem Formulation

Consider the following dynamical network consisting of N identical nodes, which are n -dimensional dynamical systems, with uncertain coupling :

$$\begin{aligned} \dot{X}_i(t) = & AX_i(t) + \varphi(t, X_i(t)) + G_i(X_1(t), X_2(t), \dots, X_N(t)) \\ & + H_i(X_1(t - \tilde{\gamma}), X_2(t - \tilde{\gamma}), \dots, X_N(t - \tilde{\gamma})), \quad i = 1, 2, \dots, N. \end{aligned} \quad (4.30)$$

where $X_i(t) = (x_{i1}(t), x_{i2}(t), \dots, x_{in}(t))^T \in R^n$, represents the state vector of the i th node, $A \in R^{n \times n}$, $\varphi : R_+ \times R^n \rightarrow R^n$ is a smooth nonlinear vector functions, $G_i, H_i : R^m \rightarrow R^n$ are smooth but unknown coupling functions, where $m = nN$. It is assumed that when the network achieves synchronization, namely, when $X_1(t) = X_2(t) = \dots = X_N(t)$ as $t \rightarrow \infty$, the coupling terms should vanish, ie., $G_i(X_1(t), X_2(t), \dots, X_N(t)) = 0$, $H_i(X_1(t - \tilde{\gamma}), X_2(t - \tilde{\gamma}), \dots, X_N(t - \tilde{\gamma})) = 0$, $i = 1, 2, \dots, N$. $\tilde{\gamma}$ is the coupling delay.

Let $Y(t)$ be a solution of the isolate node of the network, i.e.,

$$\dot{Y}(t) = AY(t) + \varphi(t, Y(t)) \quad (4.31)$$

existing for all $t \in R_+$. Here, $Y(t)$ may be an equilibrium point, a periodic orbit or even a chaotic orbit.

An impulsive control law of system (4.30) is given by a sequence $\{\tau_k, U_{ik}\}$ such that the state of network (4.30) synchronizes with the state of node (4.31). The controlled network (4.30) satisfies the following system:

$$\begin{cases} \dot{X}_i(t) = & AX_i(t) + \varphi(t, X_i(t)) + G_i(X_1(t), X_2(t), \dots, X_N(t)) \\ & + H_i(X_1(t - \tilde{\gamma}), X_2(t - \tilde{\gamma}), \dots, X_N(t - \tilde{\gamma})), t \neq \tau_k \\ \Delta X_{ik} = & U_{ik}, \quad t = \tau_k, k = 1, 2, \dots \end{cases} \quad (4.32)$$

where $i = 1, 2, \dots, N$, $\Delta X_{ik} = X_i(\tau_k^+) - X_i(\tau_k^-)$, where $X_i(\tau_k^+)$ is the right limit of X_{ik} at $t = \tau_k$, $X_{ik} = X_i(\tau_k^+)$ and $X_i(\tau_k^-)$ is the left limit. $U_{ik} = B_{ik}(X_i(\tau_k^-) - Y(\tau_k)) + D_{ik}(X_i(\tau_k^- - \gamma_k) - Y(\tau_k - \gamma_k))$, where B_{ik}, D_{ik} are the impulsive control matrices and γ_k is the impulsive delay. The sequence $\{\tau_i\}$ satisfies $0 < \tau_1 < \tau_2 < \dots < \tau_k < \dots, \tau_k \rightarrow \infty$ as $k \rightarrow \infty$. $\max\{\tilde{\gamma}, \gamma_{k-1}\} \leq \min\{\tau_{k+1} - \tau_k\}$.

Let $e_i(t) = X_i(t) - Y(t)$, we obtain the error system:

$$\begin{cases} \dot{e}_i(t) = Ae_i(t) + \tilde{\varphi}(t, X_i(t), Y(t)) + \tilde{G}_i(X(t), Y(t)) \\ \quad + \tilde{H}_i(X(t - \tilde{\gamma}), Y(t - \tilde{\gamma})), t \neq \tau_k \\ \Delta e_{ik} = B_{ik}e_i(\tau_k^-) + D_{ik}e_i(\tau_k - \gamma_k), \quad t = \tau_k, k = 1, 2, \dots \end{cases} \quad (4.33)$$

where $\tilde{\varphi}(t, X_i(t), Y(t)) = \varphi(t, X_i(t)) - \varphi(t, Y(t))$, $\tilde{G}_i(X(t), Y(t)) = G_i(X_1(t), X_2(t), \dots, X_N(t)) - G_i(Y(t), Y(t), \dots, Y(t))$, and $\tilde{H}_i(X(t - \tilde{\gamma}), Y(t - \tilde{\gamma})) = G_i(X_1(t - \tilde{\gamma}), X_2(t - \tilde{\gamma}), \dots, X_N(t - \tilde{\gamma})) - G_i(Y(t - \tilde{\gamma}), Y(t - \tilde{\gamma}), \dots, Y(t - \tilde{\gamma}))$. Clearly, network (4.30) synchronizes with node (4.31) by impulsive control $\{\tau_k, U_{ik}\}$ if and only if the error system (4.33) is globally asymptotically stable about zero.

Assumption 4.1: There exist positive constants $\mu_{ij}, \nu_{ij}, i, j = 1, 2, \dots, N$, such that

$$\|G_i(X_1(t), X_2(t), \dots, X_N(t)) - G_i(Y(t), Y(t), \dots, Y(t))\| \leq \sum_{j=1}^N \mu_{ij} \|e_j(t)\| \quad (4.34)$$

$$\|H_i(X_1(t), X_2(t), \dots, X_N(t)) - H_i(Y(t), Y(t), \dots, Y(t))\| \leq \sum_{j=1}^N \nu_{ij} \|e_j(t)\|. \quad (4.35)$$

Assumption 4.2: There exist positive constants L_i such that for any $t \in [\tau_k, \tau_{k+1})$,

$$\begin{aligned} \|\varphi(t, X_i(t)) - \varphi(t, Y(t))\| &\leq L_i \|X_i(t) - Y(t)\|, \\ i = 1, 2, \dots, N; k = 1, 2, \dots \end{aligned} \quad (4.36)$$

4.2.3 Main Results

In this subsection, we shall obtain some criteria for global asymptotical stability of error system (4.33).

Theorem 4.5: For error system (4.33), let Assumption 4.1, 4.2 hold. Assume that for an impulsive control law $\{\tau_k, U_{ik}\}$

(i) there exist positive definite matrices P_i and constants $\alpha_1, \alpha_2 > 0, \theta_{i1} > 0, \theta_{i2} > 0$ such that

$$Q_1 = \begin{bmatrix} A^T P_i + P_i A + C_{i1} I - \alpha_1 P_i & 0 \\ 0 & C_{i2} I - \alpha_2 P_i \end{bmatrix} \leq 0; \quad (4.37)$$

where $C_{i1} = 2L_i \lambda_{\max}(P_i) + \theta_{i1} \lambda_{\max}(P_i) \sum_{j=1}^N \mu_{ij} + \theta_{i2} \lambda_{\max}(P_i) \sum_{j=1}^N \nu_{ij} + \frac{1}{\theta_{i1}} \sum_{j=1}^N \lambda_{\max}(P_j) \mu_{ji}$, $C_{i2} = \frac{1}{\theta_{i2}} \sum_{j=1}^N \lambda_{\max}(P_j) \nu_{ji}$, $\lambda_{\max}(\cdot)$ represents the maximum eigenvalue.

(ii) there exist real numbers $\beta_{i1} > 0, \beta_{i2} > 0, \beta_{i1} + \beta_{i2} \leq \beta < 1$ such that for $i = 1, 2, \dots, N$,

$$Q_2 = \begin{bmatrix} (I + B_{ik})^T P_i (I + B_{ik}) - \beta_1 P_i & (I + B_{ik})^T P_i D_{ik} \\ D_{ik}^T P_i (I + B_{ik}) & D_{ik}^T P_i D_{ik} - \beta_2 P_i \end{bmatrix} \leq 0, \quad (4.38)$$

(iii) there exist a positive τ such that $\tau_k - \tau_{k-1} \leq \tau, k = 1, 2, \dots$, and

$$\frac{\tau}{\beta} (\beta \alpha_1 + \alpha_2) + \ln \beta < 0. \quad (4.39)$$

Then the error system (4.33) is globally asymptotically stable about zero. In other words, network (4.30) synchronizes with node (4.31) by impulsive control $\{\tau_k, U_{ik}\}$.

Proof: Construct a Lyapunov function in the form of

$$V(t) = \sum_{i=1}^N e_i^T(t) P_i e_i, \quad (4.40)$$

When $t \in [\tau_k, \tau_{k+1})$, taking the time derivative of the Lyapunov function (4.40) along the trajectories of (4.33) and using the inequality (4.37), one obtains

$$\begin{aligned}
& \dot{V}(t) \\
&= \sum_{i=1}^N [\dot{e}_i(t)^T P_i e_i(t) + e_i(t)^T P_i \dot{e}_i(t)] \\
&= \sum_{i=1}^N \left[e_i(t)^T (A^T P_i + P_i A) e_i(t) + e_i(t)^T P_i (\tilde{\varphi}_i + \tilde{G}_i + \tilde{H}_i) \right. \\
&\quad \left. + (\tilde{\varphi}_i + \tilde{G}_i + \tilde{H}_i)^T P_i e_i(t) \right] \\
&\leq \sum_{i=1}^N \left[e_i(t)^T (A^T P_i + P_i A) e_i(t) + \|e_i(t)^T P_i\| (\|\tilde{\varphi}_i\| + \|\tilde{G}_i\| + \|\tilde{H}_i\|) \right. \\
&\quad \left. + (\|\tilde{\varphi}_i\| + \|\tilde{G}_i\| + \|\tilde{H}_i\|) \|P_i e_i(t)\| \right] \\
&\leq \sum_{i=1}^N \left[e_i(t)^T (A^T P_i + P_i A) e_i(t) + 2L_i \lambda_{\max}(P_i) e_i(t)^T e_i(t) \right. \\
&\quad \left. + 2\|e_i(t)^T P_i\| \sum_{j=1}^N (\mu_{ij} \|e_j(t)\|) + 2\|e_i(t)^T P_i\| \sum_{j=1}^N (\nu_{ij} \|e_j(t - \tilde{\gamma})\|) \right] \\
&\leq \sum_{i=1}^N \left[e_i(t)^T (A^T P_i + P_i A) e_i(t) + 2L_i \lambda_{\max}(P_i) e_i(t)^T e_i(t) \right. \\
&\quad \left. + 2\lambda_{\max}(P_i) \sum_{j=1}^N (\mu_{ij} \|e_i(t)\| \|e_j(t)\|) + 2\lambda_{\max}(P_i) \sum_{j=1}^N (\nu_{ij} \|e_i(t)\| \|e_j(t - \tilde{\gamma})\|) \right] \\
&\leq \sum_{i=1}^N \left[e_i(t)^T (A^T P_i + P_i A) e_i(t) + 2L_i \lambda_{\max}(P_i) e_i(t)^T e_i(t) \right. \\
&\quad \left. + \lambda_{\max}(P_i) \sum_{j=1}^N \mu_{ij} (\theta_{i1} e_i(t)^T e_i(t) + \frac{1}{\theta_{i1}} e_j(t)^T e_j(t)) \right. \\
&\quad \left. + \lambda_{\max}(P_i) \sum_{j=1}^N \nu_{ij} (\theta_{i2} e_i(t)^T e_i(t) + \frac{1}{\theta_{i2}} e_j(t - \tilde{\gamma})^T e_j(t - \tilde{\gamma})) \right] \\
&\leq \sum_{i=1}^N \left[e_i(t)^T (A^T P_i + P_i A) e_i(t) + 2L_i \lambda_{\max}(P_i) e_i(t)^T e_i(t) \right. \\
&\quad \left. + \theta_{i1} \lambda_{\max}(P_i) \sum_{j=1}^N \mu_{ij} e_i(t)^T e_i(t) + \theta_{i2} \lambda_{\max}(P_i) \sum_{j=1}^N \nu_{ij} e_i(t)^T e_i(t) \right. \\
&\quad \left. + \frac{1}{\theta_{i1}} \sum_{j=1}^N \lambda_{\max}(P_j) \mu_{ji} e_i(t)^T e_i(t) + \frac{1}{\theta_{i2}} \sum_{j=1}^N \lambda_{\max}(P_j) \mu_{ji} e_i(t - \tilde{\gamma})^T e_i(t - \tilde{\gamma}) \right] \\
&\leq \sum_{i=1}^N \left[e_i(t)^T (A^T P_i + P_i A + C_1 I - \alpha_1 P_i) e_i(t) + e_i(t - \tilde{\gamma})^T (C_2 I - \alpha_2 P_i) e_i(t - \tilde{\gamma}) \right] \\
&= \sum_{i=1}^N \left[\xi_1^T Q_1 x_{i1} + \alpha_1 e_i(t)^T P_i e_i(t) + \alpha_2 e_i(t - \tilde{\gamma})^T P_i e_i(t - \tilde{\gamma}) \right] \\
&\leq \alpha_1 V(t) + \alpha_2 V(t - \tilde{\gamma}). \tag{4.41}
\end{aligned}$$

where $\varphi_i = \varphi(t, X_i(t), Y(t))$, $\tilde{G}_i = \tilde{G}_i(X_i(t), Y(t))$, and $\tilde{H}_i = \tilde{H}_i(X_i(t), Y(t))$, $\xi_1 = \begin{bmatrix} e_i(t) \\ e_i(t - \tilde{\gamma}) \end{bmatrix}$.

(4.41) implies, if $V(t) \geq \beta V(t+s)$, $s \in [-\tilde{\gamma}, 0]$,

$$V(t) \leq \frac{1}{\beta}(\beta\alpha_1 + \alpha_2)V(t), t \neq \tau_k. \quad (4.42)$$

When $t = \tau_k$, in terms of (4.38), we have

$$\begin{aligned} & V(\tau_k) \\ &= \sum_{i=1}^N [((I + B_{ik})e(\tau_k^-) + D_{ik}e(\tau_k - \gamma_k))^T P_i ((I + B_{ik})e(\tau_k^-) + D_{ik}e(\tau_k - \gamma_k))] \\ &= \sum_{i=1}^N [e(\tau_k^-)^T (I + B_{ik})^T P_i (I + B_{ik})e(\tau_k^-) + e(\tau_k - \gamma_k)^T D_{ik}^T P_i (I + B_{ik})e(\tau_k^-) \\ &\quad + e(\tau_k^-)^T (I + B_{ik})^T P_i D_{ik} e(\tau_k - \gamma_k) + e(\tau_k - \gamma_k)^T D_{ik}^T P_i D_{ik} e(\tau_k - \gamma_k)] \\ &= \sum_{i=1}^N [\xi_2^T Q_2 \xi_1 + \beta_{i1} e(\tau_k^-)^T P_i e(\tau_k^-) + \beta_{i2} e(\tau_k - \gamma_k)^T P_i e(\tau_k - \gamma_k)] \\ &\leq \beta_{i1} V(\tau_k^-) + \beta_{i2} V(\tau_k - \gamma_k), i = 1, 2, \dots \end{aligned} \quad (4.43)$$

where $\xi_2 = \begin{bmatrix} e(\tau_k^-) \\ e(\tau_k - \gamma_k) \end{bmatrix}$.

Suppose that the initial condition $V(t_0) \leq \eta$, $t_0 \in [\tau_1 - \gamma_0, \tau_1)$, by (4.43), we have

$$V(\tau_1) \leq \beta_{i1} V(\tau_1^-) + \beta_{i2} V(\tau_1 - \gamma_1) \leq \beta \eta, \quad (4.44)$$

in view of (4.39), (4.42), (4.44) and lemma 4.1, one obtains

$$V(t) < \eta \leq \rho \eta, \quad \rho \in (0, 1), t \in [\tau_1, \tau_2). \quad (4.45)$$

Continuing this process, we get

$$V(\tau_k) \leq \beta_{i1} V(\tau_k^-) + \beta_{i2} V(\tau_k - \gamma_k) \leq \beta \rho^{k-1} \eta, \quad (4.46)$$

and

$$V(t) \leq \rho^k \eta, \quad \rho \in (0, 1), t \in ([\tau_k, \tau_{k+1}). \quad (4.47)$$

which yields $V(t) \mapsto 0$, as $k \mapsto +\infty$. Thus, $e(t) \mapsto 0$, as $t \mapsto +\infty$.

Therefore, the error system (4.33) is globally asymptotically stable about zero. In other words, network (4.30) synchronizes with node (4.31) by impulsive control $\{\tau_k, U_{ik}\}$. The proof is hence completed.

Remark 4.2: By **Theorem 4.5**, the maximum interval of impulses for globally synchronization can be estimated as

$$\tau = -\frac{\beta \ln \beta}{\beta \alpha_1 + \alpha_2}. \quad (4.48)$$

When $H_i \equiv 0$, i.e., there exists no coupling delay in the dynamical network, we have the following theorem:

Theorem 4.6: For error system (4.33), let Assumption 4.1, 4.2 hold. Assume that for an impulsive control law $\{\tau_k, U_{ik}\}$

(i) there exist positive definite matrices P_i and constants $\alpha_1, \theta_{i1} > 0$ such that

$$Q_1 = A^T P_i + P_i A + C_{i1} I - \alpha_1 P_i \leq 0; \quad (4.49)$$

where $C_{i1} = 2L_i \lambda_{max}(P_i) + \theta_{i1} \lambda_{max}(P_i) \sum_{j=1}^N \mu_{ij} + \frac{1}{\theta_{i1}} \sum_{j=1}^N \lambda_{max}(P_j) \mu_{ji}$, $\lambda_{max}(\cdot)$ represents the maximum eigenvalue.

(ii) there exist real numbers $\beta_{i1} > 0$, $\beta_{i2} > 0$, $\beta_{i1} + \beta_{i2} \leq \beta < 1$ such that for $i = 1, 2, \dots, N$,

$$Q_2 = \begin{bmatrix} (I + B_{ik})^T P_i (I + B_{ik}) - \beta_1 P_i & (I + B_{ik})^T P_i D_{ik} \\ D_{ik}^T P_i (I + B_{ik}) & D_{ik}^T P_i D_{ik} - \beta_2 P_i \end{bmatrix} \leq 0, \quad (4.50)$$

(iii) there exist a positive τ such that $\tau_k - \tau_{k-1} \leq \tau$, $k = 1, 2, \dots$, and

$$\tau \alpha_1 + \ln \beta < 0. \quad (4.51)$$

Then the error system (4.33) is globally asymptotically stable about zero. In other words, network (4.30) synchronizes with node (4.31) by impulsive control $\{\tau_k, U_{ik}\}$.

Proof: Construct a Lyapunov function in the form of

$$V(t) = \sum_{i=1}^N e_i^T(t) P_i e_i, \quad (4.52)$$

When $t \in [\tau_k, \tau_{k+1})$, taking the time derivative of the Lyapunov function (4.52) along the trajectories of (4.33) and using the inequality (4.49), one obtains

$$\begin{aligned}
& \dot{V}(t) \\
&= \sum_{i=1}^N [\dot{e}_i(t)^T P_i e_i(t) + e_i(t)^T P_i \dot{e}_i(t)] \\
&= \sum_{i=1}^N \left[e_i(t)^T (A^T P_i + P_i A) e_i(t) + e_i(t)^T P_i (\tilde{\varphi}_i + \tilde{G}_i) \right. \\
&\quad \left. + (\tilde{\varphi}_i + \tilde{G}_i)^T P_i e_i(t) \right] \\
&\leq \sum_{i=1}^N \left[e_i(t)^T (A^T P_i + P_i A) e_i(t) + \|e_i(t)^T P_i\| (\|\tilde{\varphi}_i\| + \|\tilde{G}_i\|) \right. \\
&\quad \left. + (\|\tilde{\varphi}_i\| + \|\tilde{G}_i\|) \|P_i e_i(t)\| \right] \\
&\leq \sum_{i=1}^N \left[e_i(t)^T (A^T P_i + P_i A) e_i(t) + 2L_i \lambda_{\max}(P_i) e_i(t)^T e_i(t) \right. \\
&\quad \left. + 2\|e_i(t)^T P_i\| \sum_{j=1}^N (\mu_{ij} \|e_j(t)\|) \right] \\
&\leq \sum_{i=1}^N \left[e_i(t)^T (A^T P_i + P_i A) e_i(t) + 2L_i \lambda_{\max}(P_i) e_i(t)^T e_i(t) \right. \\
&\quad \left. + \lambda_{\max}(P_i) \sum_{j=1}^N \mu_{ij} (\theta_{i1} e_i(t)^T e_i(t) + \frac{1}{\theta_{i1}} e_j(t)^T e_j(t)) \right] \\
&\leq \sum_{i=1}^N [e_i(t)^T (A^T P_i + P_i A + C_1 I - \alpha_1 P_i) e_i(t)] \\
&\leq \alpha_1 V(t). \tag{4.53}
\end{aligned}$$

where $\varphi_i = \varphi(t, X_i(t), Y(t))$, $\tilde{G}_i = \tilde{G}_i(X_i(t), Y(t))$.

(4.53) implies, if $V(t) \geq \beta V(t+s)$, $s \in [-\tilde{\gamma}, 0]$,

$$\dot{V}(t) \leq \alpha_1 V(t), t \neq \tau_k. \tag{4.54}$$

The rest of the proof is similar to that of Theorem 4.5 and thus is omitted.

When $D_{ik} \equiv 0$, i.e., there exists no impulsive delay in the impulsive control, we have the following theorem:

Theorem 4.7: For error system (4.33), let Assumption 4.1, 4.2 hold. Assume that for an impulsive control law $\{\tau_k, U_{ik}\}$

(i) there exist positive definite matrices P_i and constants $\alpha_1, \alpha_2 > 0, \theta_{i1} > 0, \theta_{i2} > 0$ such that

$$Q_1 = \begin{bmatrix} A^T P_i + P_i A + C_{i1} I - \alpha_1 P_i & 0 \\ 0 & C_{i2} I - \alpha_2 P_i \end{bmatrix} \leq 0; \tag{4.55}$$

where $C_{i1} = 2L_i \lambda_{max}(P_i) + \theta_{i1} \lambda_{max}(P_i) \sum_{j=1}^N \mu_{ij} + \theta_{i2} \lambda_{max}(P_i) \sum_{j=1}^N \nu_{ij} + \frac{1}{\theta_{i1}} \sum_{j=1}^N \lambda_{max}(P_j) \mu_{ji}$, $C_{i2} = \frac{1}{\theta_{i2}} \sum_{j=1}^N \lambda_{max}(P_j) \nu_{ji}$, $\lambda_{max}(\cdot)$ represents the maximum eigenvalue.

(ii) there exist real numbers $0 < \beta < 1$ such that for $i = 1, 2, \dots, N$,

$$Q_2 = (I + B_{ik})^T P_i (I + B_{ik}) - \beta P_i \leq 0, \quad (4.56)$$

(iii) there exist a positive τ such that $\tau_k - \tau_{k-1} \leq \tau$, $k = 1, 2, \dots$, and

$$\frac{\tau}{\beta} (\beta \alpha_1 + \alpha_2) + \ln \beta < 0. \quad (4.57)$$

Then the error system (4.33) is globally asymptotically stable about zero. In other words, network (4.30) synchronizes with node (4.31) by impulsive control $\{\tau_k, U_{ik}\}$.

Proof: Construct a Lyapunov function in the form of

$$V(t) = \sum_{i=1}^N e_i^T(t) P_i e_i, \quad (4.58)$$

When $t = \tau_k$, in terms of (4.56), we have

$$\begin{aligned} & V(\tau_k) \\ &= \sum_{i=1}^N [((I + B_{ik})e(\tau_k^-))^T P_i ((I + B_{ik})e(\tau_k^-))] \\ &= \sum_{i=1}^N [e(\tau_k^-)^T (I + B_{ik})^T P_i (I + B_{ik}) e(\tau_k^-)] \\ &\leq \beta V(\tau_k^-), i = 1, 2, \dots \end{aligned} \quad (4.59)$$

The rest of the proof is similar to that of Theorem 4.5 and thus is omitted.

When $H_i \equiv 0$ and $D_{ik} \equiv 0$, i.e., there exists no impulsive delay in the impulsive control, we have the following theorem:

Theorem 4.8: For error system (4.33), let Assumption 4.1, 4.2 hold. Assume that for an impulsive control law $\{\tau_k, U_{ik}\}$

(i) there exist positive definite matrices P_i and constants $\alpha_1, \theta_{i1} > 0$ such that

$$Q_1 = A^T P_i + P_i A + C_{i1} I - \alpha_1 P_i \leq 0; \quad (4.60)$$

where $C_{i1} = 2L_i\lambda_{max}(P_i) + \theta_{i1}\lambda_{max}(P_i)\sum_{j=1}^N\mu_{ij} + \frac{1}{\theta_{i1}}\sum_{j=1}^N\lambda_{max}(P_j)\mu_{ji}$, $\lambda_{max}(\cdot)$ represents the maximum eigenvalue.

(ii) there exist real numbers $0 < \beta < 1$ such that for $i = 1, 2, \dots, N$,

$$Q_2 = (I + B_{ik})^T P_i (I + B_{ik}) - \beta P_i \leq 0, \quad (4.61)$$

(iii) there exist a positive τ such that $\tau_k - \tau_{k-1} \leq \tau$, $k = 1, 2, \dots$, and

$$\tau\alpha_1 + \ln \beta < 0. \quad (4.62)$$

Then the error system (4.33) is globally asymptotically stable about zero. In other words, network (4.30) synchronizes with node (4.31) by impulsive control $\{\tau_k, U_{ik}\}$.

Proof: Construct a Lyapunov function in the form of

$$V(t) = \sum_{i=1}^N e_i^T(t) P_i e_i, \quad (4.63)$$

When $t \in [\tau_k, \tau_{k+1})$, taking the time derivative of the Lyapunov function (4.63) along the trajectories of (4.33) and using the inequality (4.60), one obtains

$$\begin{aligned}
& \dot{V}(t) \\
&= \sum_{i=1}^N [\dot{e}_i(t)^T P_i e_i(t) + e_i(t)^T P_i \dot{e}_i(t)] \\
&= \sum_{i=1}^N \left[e_i(t)^T (A^T P_i + P_i A) e_i(t) + e_i(t)^T P_i (\tilde{\varphi}_i + \tilde{G}_i) \right. \\
&\quad \left. + (\tilde{\varphi}_i + \tilde{G}_i)^T P_i e_i(t) \right] \\
&\leq \sum_{i=1}^N \left[e_i(t)^T (A^T P_i + P_i A) e_i(t) + \|e_i(t)^T P_i\| (\|\tilde{\varphi}_i\| + \|\tilde{G}_i\|) \right. \\
&\quad \left. + (\|\tilde{\varphi}_i\| + \|\tilde{G}_i\|) \|P_i e_i(t)\| \right] \\
&\leq \sum_{i=1}^N \left[e_i(t)^T (A^T P_i + P_i A) e_i(t) + 2L_i \lambda_{\max}(P_i) e_i(t)^T e_i(t) \right. \\
&\quad \left. + 2\|e_i(t)^T P_i\| \sum_{j=1}^N (\mu_{ij} \|e_j(t)\|) \right] \\
&\leq \sum_{i=1}^N \left[e_i(t)^T (A^T P_i + P_i A) e_i(t) + 2L_i \lambda_{\max}(P_i) e_i(t)^T e_i(t) \right. \\
&\quad \left. + \lambda_{\max}(P_i) \sum_{j=1}^N \mu_{ij} (\theta_{i1} e_i(t)^T e_i(t) + \frac{1}{\theta_{i1}} e_j(t)^T e_j(t)) \right] \\
&\leq \sum_{i=1}^N [e_i(t)^T (A^T P_i + P_i A + C_1 I - \alpha_1 P_i) e_i(t)] \\
&\leq \alpha_1 V(t). \tag{4.64}
\end{aligned}$$

where $\varphi_i = \varphi(t, X_i(t), Y(t))$, $\tilde{G}_i = \tilde{G}_i(X_i(t), Y(t))$.

(4.66) implies, if $V(t) \geq \beta V(t+s)$, $s \in [-\tilde{\gamma}, 0]$,

$$V(t) \leq \alpha_1 V(t), t \neq \tau_k. \tag{4.65}$$

When $t = \tau_k$, in terms of (4.61), we have

$$\begin{aligned}
& V(\tau_k) \\
&= \sum_{i=1}^N [((I + B_{ik})e(\tau_k^-))^T P_i ((I + B_{ik})e(\tau_k^-))] \\
&= \sum_{i=1}^N [e(\tau_k^-)^T (I + B_{ik})^T P_i (I + B_{ik}) e(\tau_k^-)] \\
&\leq \beta V(\tau_k^-), i = 1, 2, \dots \tag{4.66}
\end{aligned}$$

The rest of the proof is similar to that of Theorem 4.5 and thus is omitted.

4.2.4 Numerical Example

In this subsection, we illustrate the synchronization based on three identical Chua's circuits.

We take the following representation for Chua's circuit:

$$\begin{cases} \dot{x}_1 = a_1[x_2 - h(x_1)] \\ \dot{x}_2 = x_1 - x_2 + x_3 \\ \dot{x}_3 = -a_2x_2 \end{cases} \quad (4.67)$$

with nonlinear characteristic

$$h(x_1) = m_1x_1 + \frac{1}{2}(m_0 - m_1)(|x_1 + a_3| - |x_1 - a_3|)$$

where $a_1 = 9$, $a_2 = 14.286$, $a_3 = 1$, $m_0 = -1/7$, $m_1 = 1.5/7$ in order to obtain the double scroll attractor as shown in Fig 4.6. Chua's circuit can be interpreted as $\dot{y} = Ay + \varphi(y)$ where

$$A = \begin{bmatrix} 0 & a_1 & 0 \\ 1 & -1 & 1 \\ 0 & -a_2 & 0 \end{bmatrix}, \varphi = \begin{bmatrix} -a_1h(y_1) \\ 0 \\ 0 \end{bmatrix}.$$

The functions G_i, H_i satisfy

$$\begin{aligned} G_1 &= \begin{bmatrix} -x_{11} + 2x_{21} - x_{31} \\ 0 \\ 0 \end{bmatrix}, H_1 = \begin{bmatrix} -x_{11}(t - \tilde{\gamma}) + 2x_{21}(t - \tilde{\gamma}) - x_{31}(t - \tilde{\gamma}) \\ 0 \\ 0 \end{bmatrix}; \\ G_2 &= \begin{bmatrix} -x_{21} + 2x_{31} - x_{11} \\ 0 \\ 0 \end{bmatrix}, H_2 = \begin{bmatrix} -x_{21}(t - \tilde{\gamma}) + 2x_{31}(t - \tilde{\gamma}) - x_{11}(t - \tilde{\gamma}) \\ 0 \\ 0 \end{bmatrix}; \\ G_3 &= \begin{bmatrix} -x_{31} + 2x_{11} - x_{21} \\ 0 \\ 0 \end{bmatrix}, H_3 = \begin{bmatrix} -x_{31}(t - \tilde{\gamma}) + 2x_{11}(t - \tilde{\gamma}) - x_{21}(t - \tilde{\gamma}) \\ 0 \\ 0 \end{bmatrix}. \end{aligned}$$

where $\tilde{\gamma} = 0.2s$.

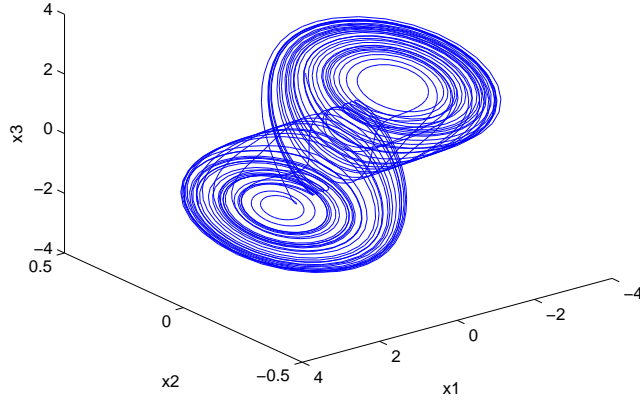


Figure 4.6: (x_1, x_2, x_3) of the isolate node of Chua's circuit starting from $(1, 1, 2)$.

Impulsive control matrices are followed,

$$B_{ik} = -0.9I, D_{ik} = 0.1I, \gamma_k = 0.08s.$$

Let $P = I, \theta_{i1} = \theta_{i2} = 1, N = 3$. By Theorem 4.5, we obtain $\tau = 0.53s$. The trajectories of error system (4.33) is shown in Fig.4.7-4.9.

Remark 4.3: By the theorem 4.5, we obtain the maximum impulsive interval $\tau = 0.53s$. In fact, when $\tau \leq 0.80s$, the error system (4.33) always is globally asymptotically stable about zero. Hence the main results, in some sence, are conservative.

4.2.5 Summary

We have investigated the synchronization of dynamical network by impulsive control. Considering the effect of coupling delay and impulsive delay, we have achieved some sufficient conditions for global asymptotical synchronization. A numerical example has been given to show the effectiveness of the main results.

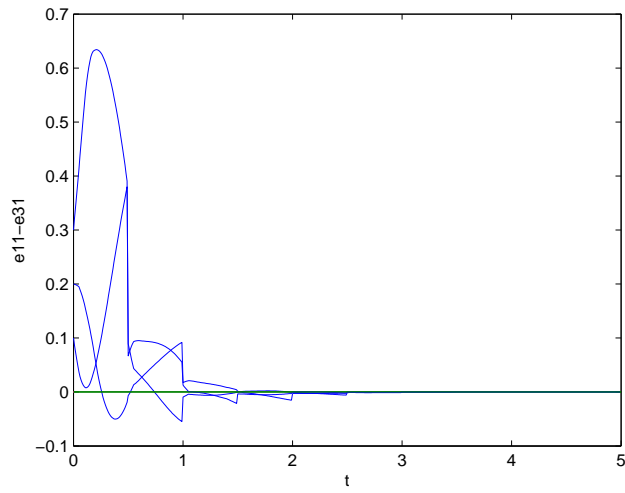


Figure 4.7: the portrait of (e_{11}, e_{21}, e_{31}) of the error system.

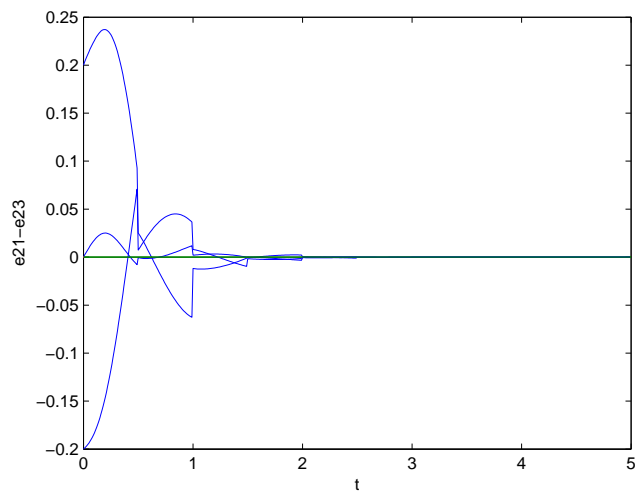


Figure 4.8: the portrait of (e_{12}, e_{22}, e_{23}) of the error system.

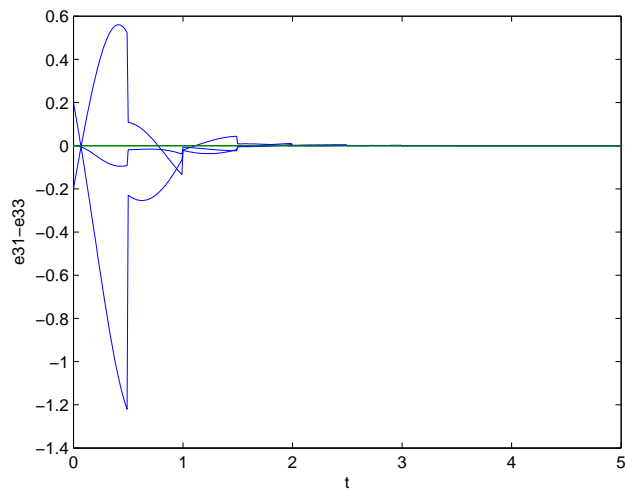


Figure 4.9: the portrait of (e_{13}, e_{23}, e_{33}) of the error system.

Chapter 5

Adaptive Network Synchronization Subject to Different Network Nodes

5.1 Introduction

Over the past decade, complex dynamical networks have attracted a lot of attention and been intensively studied in various areas. A complex dynamical network consists of a large set of network nodes, which can be convergent systems, periodic systems, aperiodic systems, chaotic oscillators, etc. Among these nodes, there exist some uncertain connections, called diffusive couplings, which may be linear or nonlinear, and may be unknown sometimes. An interesting and significant phenomenon in studying complex dynamical networks is network synchronization, i.e., all network nodes are synchronized with a desired isolated oscillator. Network synchronization has been widely utilized in biological science, chemical reaction, secret communication and cryptography, nonlinear oscillation synchronization and many other fields [93–95].

Since the introduction of synchronizing two identical chaotic systems with different initial condition by Pecora and Carroll [5], synchronization techniques have been rapidly improved. Chaotic synchronization includes master-slave synchronization and network syn-

chronization. For the master-slave pattern, a number of active and nonlinear control approaches have been proposed to synchronize two identical oscillators, such as active control between two Lorenz systems [96], a backstepping approach between two Genesio systems [97, 98], an adaptive control between two uncertain Liu systems [99], impulsive synchronization [18, 55–57, 92], delay feedback synchronization [100], a variable structure method [101] and a sliding model control [102]. On the other hand, synchronization between two different chaotic systems using nonlinear control schemes has been studied [103–106]. Specially, [107] studies the adaptive synchronization of two different chaotic systems with unknown constant parameters. And [108] studies the adaptive synchronization of two different chaotic system with unknown time varying parameters.

For network synchronization, due to the complexity and characteristics of dynamical networks, most of the existing works only consider dynamical networks including identical nodes. However, in reality, the network nodes are usually different and uncertain. How to realize network synchronization subjected to different nodes with unknown parameters becomes a challenging and significant open issue. To the best of our knowledge, there is no existing work deriving network synchronization based on this kind of complex dynamical network. In this paper, we consider a complex dynamical network with three features: (1) all network nodes and the desired isolated oscillator can have different structures; (2) the diffusive couplings among network nodes are uncertain and bounded; and (3) some parameters in network nodes and the isolated oscillator are unknown, which can be constant, time varying but bounded, or bounded in the rate of their variations. Several adaptive controllers and upgrade laws are presented and synchronization criteria based on Lyapunov stability theorem are derived to guarantee network synchronization under different kind of unknown system parameters. Compared with [109–111], our network model is more general and uncertain, and our adaptive controllers and synchronization criteria hold for different node networks. For networks subjected to unknown system parameters, our results will be very useful for practical engineering applications.

5.2 Preliminaries

In this section, we introduce a complex dynamical network model and an adaptive synchronization scheme. Some preliminary definition and hypothesis are given.

Consider a complex dynamical system consisting of N different nonlinear network nodes with unknown parameters. In addition, among these nodes, there exist some uncertain nonlinear diffusive couplings. The mathematical model can be described by

$$\dot{x}_i = f_i(t, x_i) + F_i(t, x_i)\theta_i + h_i(x_1, x_2, \dots, x_N) + u_i, \quad t \geq 0 \quad (5.1)$$

where $i = 1, 2, \dots, N$, $x_i = (x_{i1}, x_{i2}, \dots, x_{in}) \in \mathfrak{R}^n$ is the state vector of the i th node, $\theta_i \in \mathfrak{R}^m$ is the system parameter vector of the i th node, which is unknown, $u_i \in \mathfrak{R}^n$ is the control input, $f_i \in C^1(\mathfrak{R}^+ \times \mathfrak{R}^n, \mathfrak{R}^n)$, $F_i \in C^1(\mathfrak{R}^+ \times \mathfrak{R}^n, \mathfrak{R}^{n \times m_i})$ and $h_i \in C^1(\mathfrak{R}^n \times \dots \times \mathfrak{R}^n, \mathfrak{R}^n)$. The functions f_i and F_i are known, which are not necessarily the same for all i , i.e., the structures of nodes could be different. h_i is the uncertain nonlinear diffusive coupling function and satisfies $h_i(x_1, x_2, \dots, x_N) = 0$ as $x_1 = x_2 = \dots = x_N$.

The isolated oscillator is described by

$$\dot{s} = g(t, s) + G(t, s)\xi, \quad t \geq 0 \quad (5.2)$$

where $s \in \mathfrak{R}^n$ is the state vector of the isolated node, $\xi \in \mathfrak{R}^l$ is the unknown system parameter, $g \in C^1(\mathfrak{R}^+ \times \mathfrak{R}^n, \mathfrak{R}^n)$ and $G \in C^1(\mathfrak{R}^+ \times \mathfrak{R}^n, \mathfrak{R}^{n \times l})$.

Network Synchronization: Let $x_i(t; t_0, x_0)$ and $s(t; t_0, s_0)$ be the solutions of the complex dynamical network (5.1) and the isolated oscillator (5.2), respectively, where $x_0 = (x_1^0, x_2^0, \dots, x_N^0)$ and s_0 are the initial conditions. If there exists some control input u_i such that

$$\lim_{t \rightarrow \infty} \|x_i(t; t_0, x_0) - s(t; t_0, s_0)\| = 0, \quad i = 1, 2, \dots, N,$$

then all network nodes of dynamical network (5.1) are said to realize synchronization with

isolated oscillator (5.2), where $\|\cdot\|$ is the Euclidean norm of vectors and matrices, i.e.,

$$X = [x_1 \ x_2 \ \dots \ x_n]^T, \quad \|X\| = \left(\sum_{i=1}^n x_i^2 \right)^{1/2};$$

$$A = [a_{ij}]_{n \times m}, \quad \|A\| = \left(\sum_{i,j} a_{ij}^2 \right)^{1/2}.$$

Denote $x_i(t) =: x_i(t; t_0, x_0)$, $s(t) = s(t; t_0, s_0)$. Let $e_i(t) = x_i(t) - s(t)$, $i=1,2,\dots,N$. We obtain the following error system

$$\dot{e}_i = f_i(t, x_i) - g(t, s) + F_i(t, x_i)\theta_i - G(t, s)\xi + H_i(x_1, x_2, \dots, x_N, s) + u_i, \quad (5.3)$$

where $H_i(x_1, x_2, \dots, x_N, s) = h_i(x_1, x_2, \dots, x_N) - h_i(s, s, \dots, s)$.

From the definition of network synchronization, if there exist adaptive controllers u_i such that

$$\lim_{t \rightarrow +\infty} \|e_i(t)\| = 0, \quad i = 1, 2, \dots, N,$$

then network synchronization is achieved.

Hypothesis 5.1: Assume that there exist non-negative constants γ_{ij} ($1 \leq i, j \leq N$) such that

$$H_i(x_1, x_2, \dots, x_N, s) \leq \sum_{j=1}^N \gamma_{ij} \|e_j\|, \quad \text{for } 1 \leq i \leq N.$$

5.3 Adaptive Controller Design for Network Synchronization

It is assumed that all states of the network nodes and the isolated oscillator are measurable or available. If the system parameters θ_i and ξ are unknown constants, we have the following synchronization criterion.

Theorem 5.1: Consider complex dynamical network (5.1) and isolated oscillator (5.2). Suppose that system parameters θ_i and ξ are unknown constants and the nonlinear diffusive

coupling functions h_i satisfy **Hypothesis 5.1**. Then the following adaptive controllers and updating laws will synchronize all network nodes of complex dynamical network (5.1) with isolated oscillator (5.2),

$$u_i = -f_i(t, x_i) + g(t, s) - F_i(t, x_i)\alpha_i + G(t, s)\beta - k_i e_i, \quad (5.4)$$

$$\dot{\alpha}_i = P_i^{-1} F_i(t, x_i)^T e_i, \quad (5.5)$$

$$\dot{\beta} = -Q^{-1} G(t, s)^T \sum_{i=1}^N e_i, \quad (5.6)$$

where α_i and β are estimates of θ_i and ξ , respectively, k_i ($1 \leq i \leq N$) are suitable positive constants to be determined, and P_i, Q are positive definite matrices.

Proof: Define a Lyapunov function as

$$V = \frac{1}{2} \sum_{i=1}^N e_i^T e_i + \frac{1}{2} \sum_{i=1}^N (\alpha_i - \theta_i)^T P_i (\alpha_i - \theta_i) + \frac{1}{2} (\beta - \xi)^T Q (\beta - \xi). \quad (5.7)$$

Taking derivative of V with respect to t , we get

$$\dot{V} = \sum_{i=1}^N e_i^T \dot{e}_i + \sum_{i=1}^N \dot{\alpha}_i^T P_i (\alpha_i - \theta_i) + \dot{\beta}^T Q (\beta - \xi). \quad (5.8)$$

Substituting Eqs. (5.3), (5.4), (5.5) and (5.6) into (5.8), we have

$$\begin{aligned}
\dot{V} &= \sum_{i=1}^N e_i^T [f(t, x_i) - g(t, s) + F_i(t, x_i)\theta_i - G(t, s)\xi \\
&\quad + H_i(x_1, x_2, \dots, x_N, s) + u_i] \\
&\quad + \sum_{i=1}^N \dot{\alpha}_i^T P_i(\alpha_i - \theta_i) + \dot{\beta}^T Q(\beta - \xi) \\
&= \sum_{i=1}^N e_i^T [F_i(t, x_i)(\theta_i - \alpha_i) - G(t, s)(\xi - \beta) \\
&\quad + H_i(x_1, x_2, \dots, x_N, s) - k_i e_i] \\
&\quad + \sum_{i=1}^N [P_i^{-1} F_i(t, x_i)^T e_i]^T P_i(\alpha_i - \theta_i) \\
&\quad + [-Q^{-1} G(t, s)^T \sum_{i=1}^N e_i]^T Q(\beta - \xi) \\
&= \sum_{i=1}^N e_i^T [H_i(x_1, x_2, \dots, x_N, s) - k_i e_i] \\
&\leq \sum_{i=1}^N \|e_i\| \sum_{j=1}^N (\gamma_{ij} \|e_j\|) - k_i \sum_{i=1}^N \|e_i\|^2
\end{aligned} \tag{5.9}$$

Define $\eta = [\|e_1\| \|e_2\| \dots \|e_N\|]^T$, $\Gamma = [\gamma_{ij}]_{N \times N}$, we obtain

$$\dot{V} \leq \eta^T (\Gamma - \text{diag}\{k_1, k_2, \dots, k_N\}) \eta. \tag{5.10}$$

Since Γ is a constant matrix, we can select suitable positive constants k_i such that $\Gamma - \text{diag}\{k_1, k_2, \dots, k_N\}$ is a negative definite matrix. Thus, V is positive definite and \dot{V} is negative definite along the trajectories of error systems, which implies $\lim_{t \rightarrow \infty} e_i = 0$. In other words, all network nodes of dynamical network (5.1) are synchronized with isolated oscillator (5.2) using adaptive controllers (5.4)-(5.6).

The proof is complete.

Remark 5.1: It is not true that, under adaptive controllers (5.4)-(5.6), the estimates α_i and β will converge to unknown parameters θ_i and ξ , respectively. However, from **Theorem 5.1**,

the state vectors $x_i(t)$ of network nodes will converge to the state vector $s(t)$ of the isolated oscillator.

If the unknown system parameters θ_i and ξ are not constants, but time varying and bounded by known bounds, i.e.,

$$\|\theta_i - \tilde{\theta}_i\| < \Theta_i, \quad \|\xi - \tilde{\xi}\| < \Psi, \quad (5.11)$$

we have the following synchronization criterion.

Theorem 5.2: Consider complex dynamical network (5.1) and isolated oscillator (5.2). Suppose that system parameters θ_i and ξ are time varying and bounded, satisfying (5.11) and the nonlinear diffusive coupling functions h_i satisfy **Hypothesis 5.1**. Then the following adaptive controllers and updating laws will synchronize all network nodes of complex dynamical network (5.1) with isolated oscillator (5.2),

$$\begin{aligned} u_i &= -f_i(t, x_i) + g(t, s) - F_i(t, x_i)\alpha_i + G(t, s)\beta - k_i e_i, \\ &\quad -\|F_i(t, x_i)\|\Theta_i \text{sign}(e_i) - \|G(t, s)\|\Psi \text{sign}(e_i), \end{aligned} \quad (5.12)$$

$$\dot{\alpha}_i = P_i^{-1} F_i(t, x_i)^T e_i, \quad (5.13)$$

$$\dot{\beta} = -Q^{-1} G(t, s)^T \sum_{i=1}^N e_i, \quad (5.14)$$

where α_i and β are estimates of θ_i and ξ , respectively, k_i ($1 \leq i \leq N$) are suitable positive constants to be determined, P_i, Q are positive definite matrices, and Θ_i and Ψ are the bounds of system parameters θ_i and ξ , respectively.

Proof: Define a Lyapunov function as

$$V = \frac{1}{2} \sum_{i=1}^N e_i^T e_i + \frac{1}{2} \sum_{i=1}^N (\alpha_i - \tilde{\theta}_i)^T P_i (\alpha_i - \tilde{\theta}_i) + \frac{1}{2} (\beta - \tilde{\xi})^T Q (\beta - \tilde{\xi}). \quad (5.15)$$

Differentiating the Lyapunov function (5.15) with respect to t , we get

$$\begin{aligned}
\dot{V} &= \sum_{i=1}^N e_i^T \dot{e}_i + \sum_{i=1}^N \dot{\alpha}_i^T P_i(\alpha_i - \tilde{\theta}_i) + \dot{\beta}^T Q(\beta - \tilde{\xi}) \\
&= \sum_{i=1}^N e_i^T [f_i(t, x_i) - g(t, s) + F_i(t, x_i)\theta_i - G(t, s)\xi \\
&\quad + H_i(x_1, x_2, \dots, x_N, s) + u_i] \\
&\quad + \sum_{i=1}^N \dot{\alpha}_i^T P_i(\alpha_i - \tilde{\theta}_i) + \dot{\beta}^T Q(\beta - \tilde{\xi}) \\
&= \sum_{i=1}^N e_i^T [F_i(t, x_i)((\theta_i - \tilde{\theta}_i) - (\alpha_i - \tilde{\theta}_i)) \\
&\quad - G(t, s)((\xi - \tilde{\xi}) - (\beta - \tilde{\xi})) \\
&\quad - \|F_i(t, x_i)\| \Theta_i \text{sign}(e_i) - \|G(t, s)\| \Psi \text{sign}(e_i) \\
&\quad + H_i(x_1, x_2, \dots, x_N, s) - k_i e_i] \\
&\quad + \sum_{i=1}^N [P_i^{-1} F_i(t, x_i)^T e_i]^T P_i(\alpha_i - \tilde{\theta}_i) \\
&\quad + [-Q^{-1} G(t, s)^T \sum_{i=1}^N e_i]^T Q(\beta - \tilde{\xi}) \\
&= \sum_{i=1}^N e_i^T [F_i(t, x_i)(\theta_i - \tilde{\theta}_i) - G(t, s)(\xi - \tilde{\xi}) \\
&\quad - \|F_i(t, x_i)\| \Theta_i \text{sign}(e_i) - \|G(t, s)\| \Psi \text{sign}(e_i) \\
&\quad + H_i(x_1, x_2, \dots, x_N, s) - k_i e_i]. \tag{5.16}
\end{aligned}$$

Since

$$\|e_i\| = \left(\sum_{j=1}^n e_{ij}^2 \right)^{1/2} \leq \sum_{j=1}^n |e_{ij}|,$$

we have

$$\begin{aligned}
\|e_i^T F_i(t, x_i)(\theta_i - \tilde{\theta}_i)\| &\leq \|e_i\| \|F_i(t, x_i)\| \Theta_i \\
&\leq \left(\sum_{j=1}^n |e_{ij}| \right) \|F_i(t, x_i)\| \Theta_i \\
&= e_i^T \|F_i(t, x_i)\| \Theta_i \text{sign}(e_i).
\end{aligned} \tag{5.17}$$

Similarly,

$$\|e_i^T G(t, s)(\xi - \tilde{\xi})\| \leq e_i^T \|G(t, s)\| \Psi \text{sign}(e_i). \tag{5.18}$$

Substituting Eqs. (5.17) and (5.18) into Eq. (5.16), we have

$$\begin{aligned}
\dot{V} &\leq \sum_{i=1}^N [\|e_i^T F_i(t, x_i)(\theta_i - \tilde{\theta}_i)\| + \|e_i^T G(t, s)(\xi - \tilde{\xi})\| \\
&\quad - e_i^T \|F_i(t, x_i)\| \Theta_i \text{sign}(e_i) - e_i^T \|G(t, s)\| \Psi \text{sign}(e_i) \\
&\quad + e_i^T H_i(x_1, x_2, \dots, x_N, s) - e_i^T k_i e_i] \\
&\leq \sum_{i=1}^N [e_i^T H_i(x_1, x_2, \dots, x_N, s) - e_i^T k_i e_i] \\
&\leq \eta^T (\Gamma - \text{diag}\{k_1, k_2, \dots, k_N\}) \eta,
\end{aligned} \tag{5.19}$$

where $\eta = [\|e_1\| \|e_2\| \dots \|e_N\|]^T$, $\Gamma = [\gamma_{ij}]_{N \times N}$.

We can select suitable positive constants k_i ($i = 1, 2, \dots, N$) such that $\Gamma - \text{diag}\{k_1, k_2, \dots, k_N\}$ is a negative matrix. It implies $\lim_{t \rightarrow \infty} e_i = 0$. In other words, all network nodes of dynamical network (5.1) are synchronized with isolated oscillator (5.2) using adaptive controllers (5.12)-(5.14).

The proof is complete.

Remark 5.2: *Theorem 5.2* is an extension of *Theorem 5.1*. Let $\Theta_i = 0$ and $\Psi = 0$, then the adaptive controllers (5.12)-(5.14) in *Theorem 5.2* become (5.4)-(5.6) in *Theorem 5.1*. In addition, when the network synchronization is completely achieved, the estimates α_i and β are not necessary to converge to θ_i and ξ .

If system parameters θ_i and ξ are time varying and unknown, but the rates of their variations are bounded, i.e.,

$$|\dot{\theta}_i| \leq \tilde{\Theta}_i, \quad |\dot{\xi}| \leq \tilde{\Psi}, \quad (5.20)$$

we have the following criterion to guarantee network synchronization.

Theorem 5.3: Consider dynamical network (5.1) and isolated oscillator (5.2). Suppose that the system parameters are time varying and unknown, but the rates of their variations are bounded, satisfying condition (5.20) and the nonlinear diffusive coupling functions h_i satisfy **Hypothesis 5.1**. Then the following adaptive controllers and updating laws will synchronize all network nodes of complex dynamical network (5.1) with isolated oscillator (5.2),

$$\begin{aligned} u_i &= -f_i(t, x_i) + g(t, s) - F_i(t, x_i)\alpha_i + G(t, s)\beta - k_i e_i, \\ &\quad - \|F_i(t, x_i)\| \text{sign}(e_i) \tilde{\Theta}_i(t - t_0) \\ &\quad - \|G(t, s)\| \text{sign}(e_i) \tilde{\Psi}(t - t_0), \quad t \geq t_0, \end{aligned} \quad (5.21)$$

$$\dot{\alpha}_i = P_i^{-1} F_i(t, x_i)^T e_i, \quad (5.22)$$

$$\dot{\beta} = -Q^{-1} G(t, s)^T \sum_{i=1}^N e_i, \quad (5.23)$$

where α_i and β are estimates of θ_i and ξ , respectively, k_i ($1 \leq i \leq N$) are suitable positive constants to be determined, P_i , Q are positive definite matrices, and $\tilde{\Theta}_i$ and $\tilde{\Psi}$ are the bounds of $\dot{\theta}_i$ and $\dot{\xi}$, respectively.

Proof: Denote the initial conditions $\theta_i(t_0)$ and $\xi(t_0)$ as θ_i^0 and ξ^0 , which are unknown. We construct a Lyapunov function in the form of

$$\begin{aligned} V &= \frac{1}{2} \sum_{i=1}^N e_i^T e_i + \frac{1}{2} \sum_{i=1}^N (\alpha_i - \theta_i^0)^T P_i (\alpha_i - \theta_i^0) \\ &\quad + \frac{1}{2} (\beta - \xi^0)^T Q (\beta - \xi^0). \end{aligned} \quad (5.24)$$

Differentiating (5.24) with respect to t , we get

$$\begin{aligned}
\dot{V} &= \sum_{i=1}^N e_i^T [F_i(t, x_i)(\theta_i - \theta_i^0) - \|F_i(t, x_i)\| \mathbf{sign}(e_i) \tilde{\Theta}_i(t - t_0) \\
&\quad - G(t, s)(\xi - \xi^0) - \|G(t, s)\| \mathbf{sign}(e_i) \tilde{\Psi}(t - t_0) \\
&\quad + H_i(x_1, x_2, \dots, x_N, s) - k_i e_i].
\end{aligned} \tag{5.25}$$

Since

$$\begin{aligned}
&\|e_i^T F_i(t, x_i)(\theta_i - \theta_i^0)\| \\
&\leq \|e_i\| \|F_i(t, x_i)\| \|\dot{\theta}_i(t - t_0)\| \\
&\leq \left(\sum_{j=1}^n |e_{ij}| \right) \|F_i(t, x_i)\| \tilde{\Theta}_i(t - t_0) \\
&= e_i^T \|F_i(t, x_i)\| \mathbf{sign}(e_i) \tilde{\Theta}_i(t - t_0)
\end{aligned} \tag{5.26}$$

and

$$\|e_i^T G(t, s)(\xi - \xi^0)\| \leq e_i^T \|G(t, s)\| \mathbf{sign}(e_i) \tilde{\Psi}(t - t_0), \tag{5.27}$$

substituting Eqs. (5.26) and (5.27) into Eq. (5.25), we have

$$\begin{aligned}
\dot{V} &\leq \sum_{i=1}^N [e_i^T H_i(x_1, x_2, \dots, x_N, s) - e_i^T k_i e_i] \\
&\leq \eta^T (\Gamma - \mathbf{diag}\{k_1, k_2, \dots, k_N\}) \eta,
\end{aligned} \tag{5.28}$$

where $\eta = [\|e_1\| \|e_2\| \dots \|e_N\|]^T$, $\Gamma = [\gamma_{ij}]_{N \times N}$.

One can select suitable positive constants k_i ($i = 1, 2, \dots, N$) such that $\Gamma - \mathbf{diag}\{k_1, k_2, \dots, k_N\}$ is a negative matrix. It implies $\lim_{t \rightarrow \infty} e_i = 0$. In other words, all network nodes of dynamical network (5.1) are synchronized with isolated oscillator (5.2) using adaptive controllers (5.21)-(5.23).

The proof is complete.

5.4 Numerical Examples

In this section, several examples are presented to verify the correctness of the above synchronization criteria.

Consider a complex dynamical network consisting of 30 different nodes, where nodes (1)-(10) are identical Lorenz systems [2], nodes (11)-(20) are identical Chen systems [46] and nodes (21)-(30) are identical Rössler systems [45]. The isolated oscillator is a modified Chua's circuit [112].

Nodes (1)-(10) are described by

$$\begin{cases} \dot{x}_{i1} = \theta_{i1}(x_{i2} - x_{i1}) \\ \dot{x}_{i2} = \theta_{i2}x_{i1} - x_{i1}x_{i3} - x_{i2} \\ \dot{x}_{i3} = x_{i1}x_{i2} - \theta_{i3}x_{i3} \end{cases}, \quad (5.29)$$

where $i = 1, 2, \dots, 10$, θ_{i1} , θ_{i2} and θ_{i3} are unknown system parameters.

Firstly, we rewrite (5.29) in the standard form as follows,

$$\dot{x}_i = f_i(t, x_i) + F_i(t, x_i)\theta_i, \quad (5.30)$$

where

$$f(t, x_i) = \begin{bmatrix} 0 \\ -x_{i1}x_{i3} - x_{i2} \\ x_{i1}x_{i2} \end{bmatrix}, \quad x_i = \begin{bmatrix} x_{i1} \\ x_{i2} \\ x_{i3} \end{bmatrix},$$

$$F(t, x_i) = \begin{bmatrix} x_{i2} - x_{i1} & 0 & 0 \\ 0 & x_{i1} & 0 \\ 0 & 0 & -x_{i3} \end{bmatrix}, \quad \theta_i = \begin{bmatrix} \theta_{i1} \\ \theta_{i2} \\ \theta_{i3} \end{bmatrix}.$$

Nodes (11)-(20) are described by

$$\begin{cases} \dot{x}_{i1} = \theta_{i1}(x_{i2} - x_{i1}) \\ \dot{x}_{i2} = (\theta_{i2} - \theta_{i1})x_{i1} - x_{i1}x_{i3} + \theta_{i2}x_{i2} \\ \dot{x}_{i3} = x_{i1}x_{i2} - \theta_{i3}x_{i3} \end{cases}, \quad (5.31)$$

where $i = 11, 12, \dots, 20$, θ_{i1} , θ_{i2} and θ_{i3} are unknown system parameters.

Also, we rewrite (5.31) in the standard form (5.30), where

$$f(t, x_i) = \begin{bmatrix} 0 \\ -x_{i1}x_{i3} \\ x_{i1}x_{i2} \end{bmatrix}, \quad x_i = \begin{bmatrix} x_{i1} \\ x_{i2} \\ x_{i3} \end{bmatrix},$$

$$F(t, x_i) = \begin{bmatrix} x_{i2} - x_{i1} & 0 & 0 \\ -x_{i1} & x_{i1} + x_{i2} & 0 \\ 0 & 0 & -x_{i3} \end{bmatrix}, \quad \theta_i = \begin{bmatrix} \theta_{i1} \\ \theta_{i2} \\ \theta_{i3} \end{bmatrix}.$$

Nodes (21)-(30) are described by

$$\begin{cases} \dot{x}_{i1} = -(x_{i2} + x_{i3}) \\ \dot{x}_{i2} = x_{i1} + \theta_{i1}x_{i2} \\ \dot{x}_{i3} = \theta_{i2} + x_{i3}(x_{i1} - \theta_{i3}) \end{cases}, \quad (5.32)$$

where $i = 21, 12, \dots, 30$, θ_{i1} , θ_{i2} and θ_{i3} are unknown system parameters.

Also, we rewrite (5.32) in the standard form (5.30), where

$$f(t, x_i) = \begin{bmatrix} -x_{i2} - x_{i3} \\ x_{i1} \\ x_{i1}x_{i3} \end{bmatrix}, \quad x_i = \begin{bmatrix} x_{i1} \\ x_{i2} \\ x_{i3} \end{bmatrix},$$

$$F(t, x_i) = \begin{bmatrix} 0 & 0 & 0 \\ x_{i2} & 0 & 0 \\ 0 & 1 & -x_{i3} \end{bmatrix}, \quad \theta_i = \begin{bmatrix} \theta_{i1} \\ \theta_{i2} \\ \theta_{i3} \end{bmatrix}.$$

The diffusive coupling functions are given,

$$h_i(x_1, x_2, \dots, x_N) = \begin{bmatrix} -w_1(x_{i-1}) + 2w_1(x_i) - w_1(x_{i+1}) \\ -w_2(x_{i-1}) + 2w_2(x_i) - w_2(x_{i+1}) \\ -w_3(x_{i-1}) + 2w_3(x_i) - w_3(x_{i+1}) \end{bmatrix}, \quad (5.33)$$

where $w_1(x_i) = x_{i2} - x_{i1}$, $w_2(x_i) = 0$, $w_3(x_i) = x_{i1}x_{i2} - x_{i2}x_{i3}$, $x_0 = x_{30}$, $x_{31} = x_1$ and $1 \leq i \leq 30$.

Since it is confined that Lorenz system, Chen system and Rössler system all are bounded, there exists a constant M such that $x_{ij}, s_j \leq M$ for $1 \leq i \leq 30$ and $j = 1, 2, 3$. We have

$$\|H_i(x_1, x_2, \dots, x_N, s)\| \leq 3\sqrt{2(1 + 4M^2)}(\|e_{i-1}\| + \|e_i\| + \|e_{i+1}\|).$$

Therefore, **Hypothesis 5.1** is satisfied.

The desired isolated oscillator is a modified Chua's circuit, described by

$$\begin{cases} \dot{s}_1 = \xi_1(s_2 - \frac{2s_1^3 - s_1}{7}) \\ \dot{s}_2 = s_1 - s_2 + s_3 \\ \dot{s}_3 = -\xi_2 s_2 \end{cases}, \quad (5.34)$$

where ξ_1 and ξ_2 are unknown system parameters.

Represent (5.34) in the standard form as follows,

$$\dot{s} = g(t, s) + G(t, s)\xi, \quad (5.35)$$

where

$$g(t, s) = \begin{bmatrix} 0 \\ s_1 - s_2 + s_3 \\ 0 \end{bmatrix}, \quad s = \begin{bmatrix} s_1 \\ s_2 \\ s_3 \end{bmatrix},$$

$$G(t, s) = \begin{bmatrix} s_2 - \frac{2s_1^3 - s_1}{7} & 0 \\ 0 & 0 \\ 0 & -s_2 \end{bmatrix}, \quad \xi = \begin{bmatrix} \xi_1 \\ \xi_2 \end{bmatrix}.$$

System Parameters θ_i and ξ are Unknown Constants

Consider that system parameters θ_i, ξ are unknown constants,

$$\theta_i = \begin{cases} (10, 28, 8/3)^T, & 1 \leq i \leq 10; \\ (35, 28, 3)^T, & 11 \leq i \leq 20; \\ (0.2, 0.2, 5.7)^T, & 21 \leq i \leq 30. \end{cases}$$

$$\xi = (10, 100/7)^T.$$

According to **Theorem 5.1**, we choose the initial values as follows: $k_i = 10$, $\alpha_i = [3, 3, 3]^T$, $\beta = [4, 4]^T$, $x_i = [-8 + 0.5i, -5 + 0.3i, 4 - 0.2i]^T$ and $s = [1, 1, 1]^T$. The synchronous errors e_i are shown in Fig. 5.1. The system parameters and their estimates are in Fig. 5.2. Obviously, by the adaptive controllers (5.4)-(5.6), the network nodes such as Lorenz systems, Chen systems and Rössler systems all are synchronized with the desired modified Chua's circuit.

System Parameters θ_i and ξ are Unknown, Time Varying and Bounded

Consider that system parameters θ_i and ξ are time varying and bounded. $\Theta_i = 0.5$, and $\Psi = 1$.

$$\theta_i = \begin{cases} (10 + 0.5 \sin(t), 28, 8/3)^T, & 1 \leq i \leq 10; \\ (35 + 0.5 \sin(t), 28, 3)^T, & 11 \leq i \leq 20; \\ (0.2 + 0.5 \sin(t), 0.2, 5.7)^T, & 21 \leq i \leq 30. \end{cases}$$

and

$$\xi = (10 + \sin(t), 100/7)^T.$$

According to **Theorem 5.2**, we choose the initial conditions as follows: $k_i = 10$, $\alpha_i = [3, 3, 3]^T$, $\beta = [4, 4]^T$, $x_i = [-8 + 0.5i, -5 + 0.3i, 4 - 0.2i]^T$ and $s = [1, 1, 1]^T$. The synchronous errors e_i are shown in Fig. 5.3. The system parameters and their estimates are shown in Fig. 5.4. Obviously, by the adaptive controllers (5.12)-(5.14), the network nodes such as Lorenz systems, Chen systems and Rössler systems all are synchronized with the desired modified Chua's circuit.

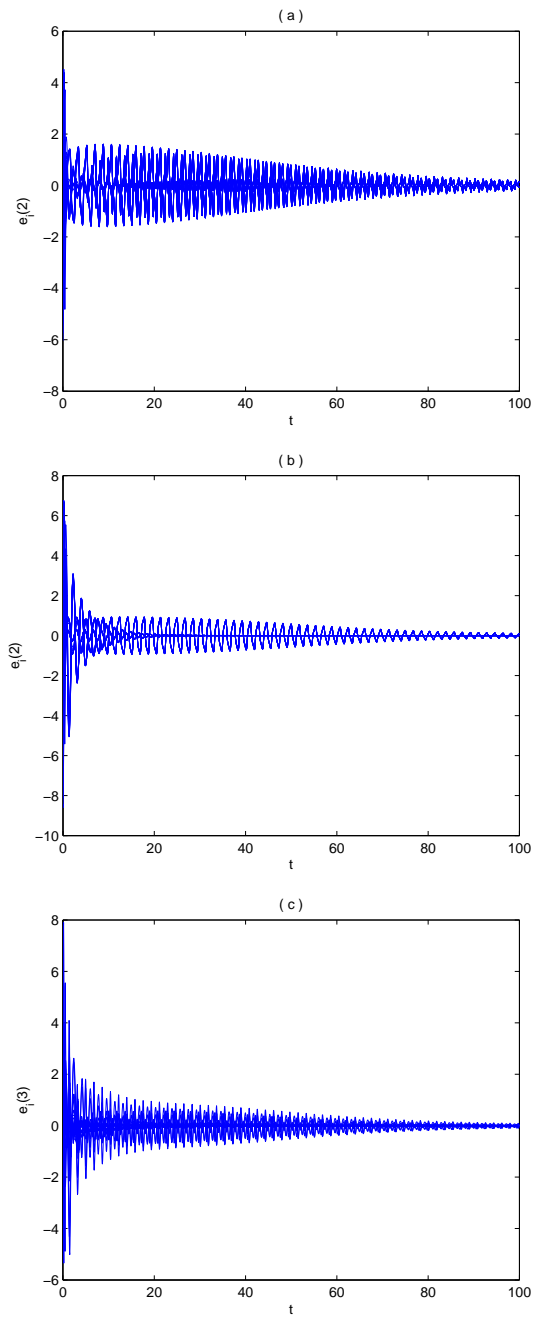


Figure 5.1: Synchronization errors, (a) e_{i1} , (b) e_{i2} , (c) e_{i3} for unknown constant parameters.

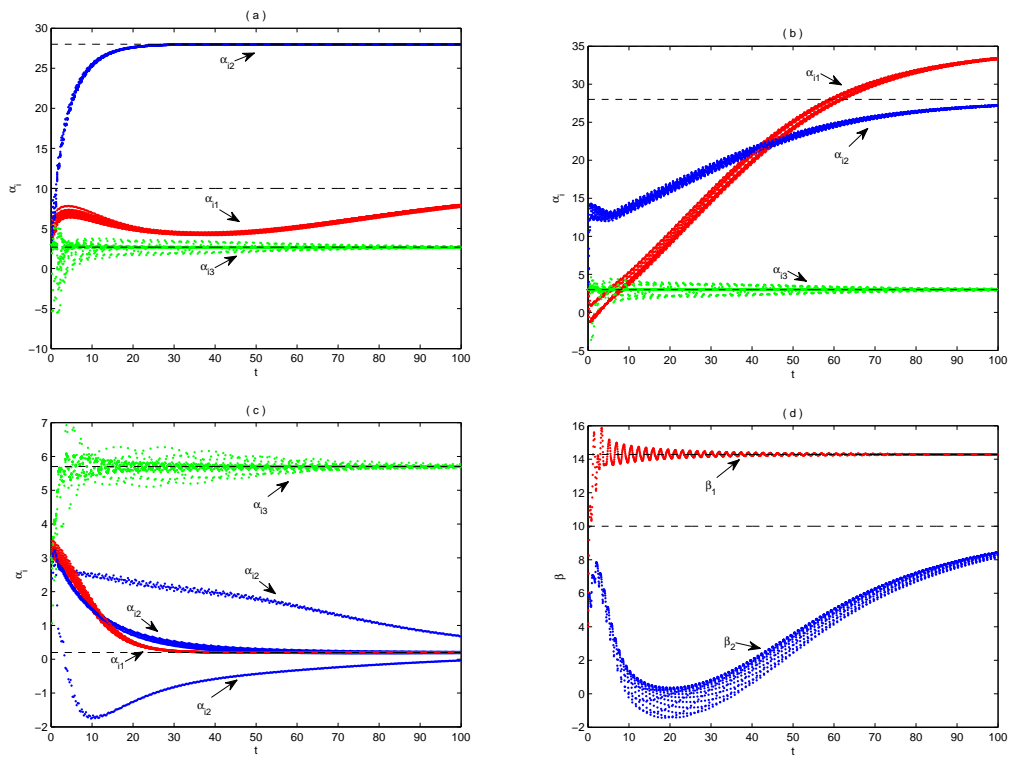


Figure 5.2: System parameters and their estimates: (a) nodes (1)–(10), (b) nodes (11)–(20), (c) nodes (21) – (30), and (d) the isolated oscillator, for unknown constant parameters.

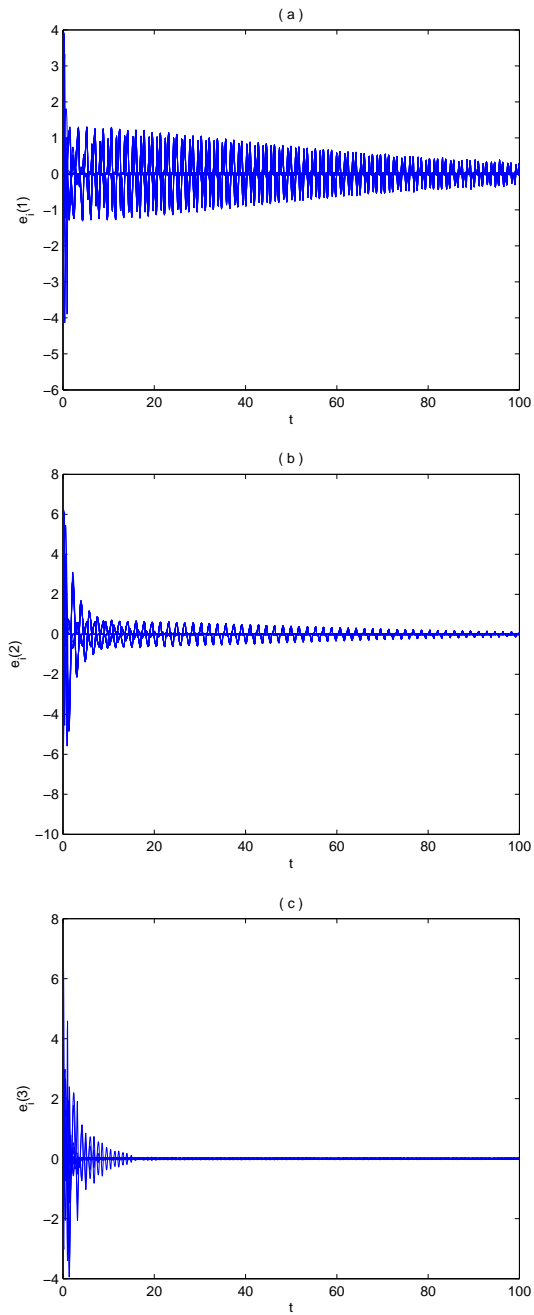


Figure 5.3: Synchronization errors, (a) e_{i1} , (b) e_{i2} , (c) e_{i3} for unknown bounded parameters with $\Theta_i = 0.5$ and $\Psi = 1$.

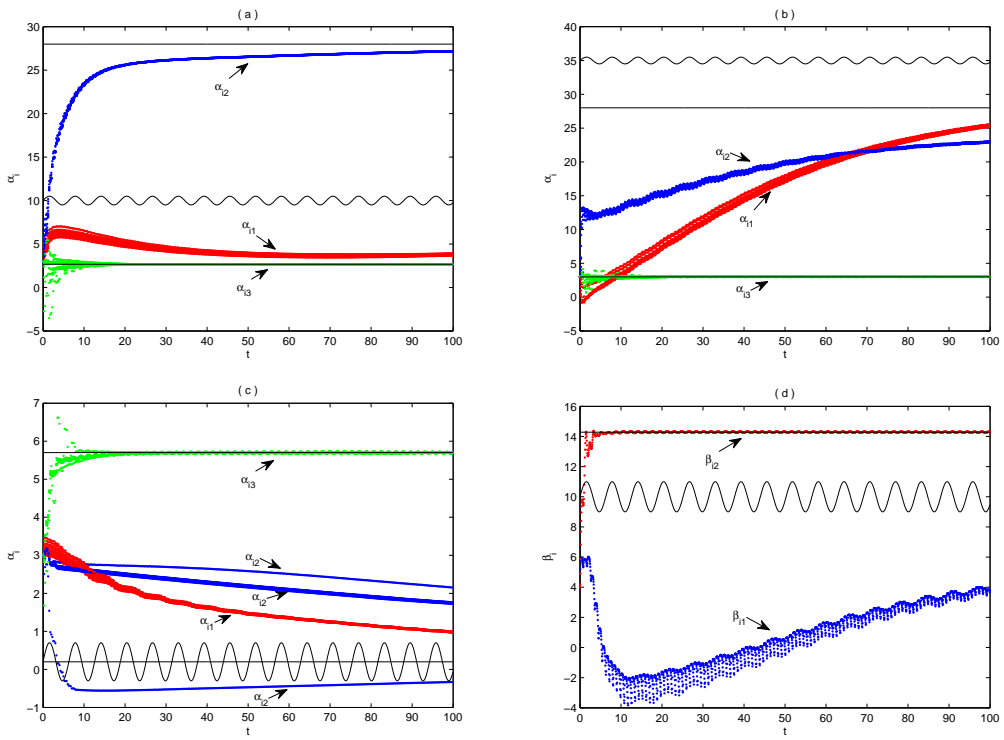


Figure 5.4: System parameters and their estimates: (a) nodes (1)–(10), (b) nodes (11)–(20), (c) nodes (21) – (30), and (d) the isolated oscillator, for unknown bounded parameters with $\Theta_i = 0.5$ and $\Psi = 1$.

System Parameters θ_i and ξ are Unknown, and $\dot{\theta}_i$ and $\dot{\xi}$ are Bounded

Consider that system parameters θ_i, ξ are unknown, but $\dot{\theta}_i, \dot{\xi}$ are bounded.

$$\theta_i = \begin{cases} (10 + 0.01t, 28, 8/3)^T, & 1 \leq i \leq 10; \\ (35 + 0.01t, 28, 3)^T, & 11 \leq i \leq 20; \\ (0.2 + 0.01t, 0.2, 5.7)^T, & 21 \leq i \leq 30. \end{cases}$$

and

$$\xi = (10 + 0.1t, 100/7)^T.$$

Thus, $\dot{\theta}_i = 0.01$ and $\dot{\Psi} = 0.1$. According to **Theorem 5.3**, we choose the initial conditions as follows: $k_i = 10$, $\alpha_i = [3, 3, 3]^T$, $\beta = [4, 4]^T$, $x_i = [-8 + 0.5i, -5 + 0.3i, 4 - 0.2i]^T$ and $s = [1, 1, 1]^T$. The synchronous errors e_i are shown in Fig. 5.5. The system parameters and their estimates are shown in Fig. 5.6. Obviously, by the adaptive controllers (5.21)-(5.23), the network nodes such as Lorenz systems, Chen systems and Rössler systems all are synchronized with the desired modified Chua's circuit.

5.5 Summary

We have investigated adaptive network synchronization subjected to different network nodes. Several adaptive controllers and updating laws have been designed to realize network synchronization respectively under different kind of system parameters. Numerical examples have verified the correctness of our synchronization criteria. It has been shown that the parameter estimates α_i and β are not necessary to converge to system parameters θ_i and ξ , i.e., our adaptive control approaches can guarantee network synchronization well without accurately tracking the unknown system parameters. How to track the unknown system parameters is our future research work.

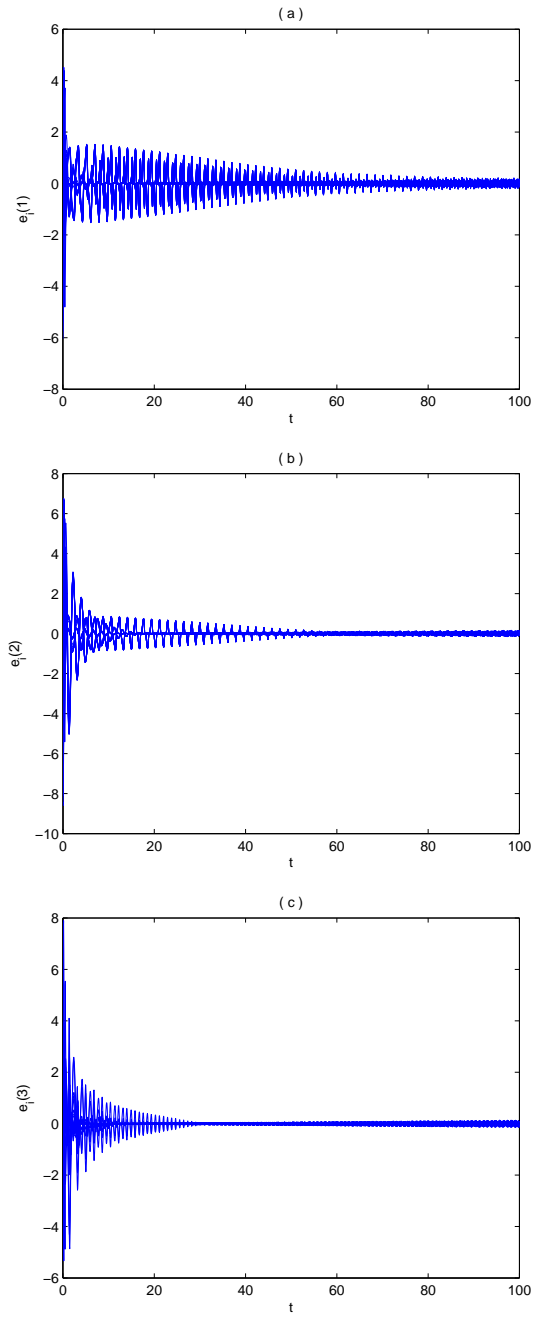


Figure 5.5: Synchronization errors, (a) e_{i1} , (b) e_{i2} , (c) e_{i3} for $\tilde{\Theta}_i = 0.01$ and $\tilde{\Psi} = 0.1$.

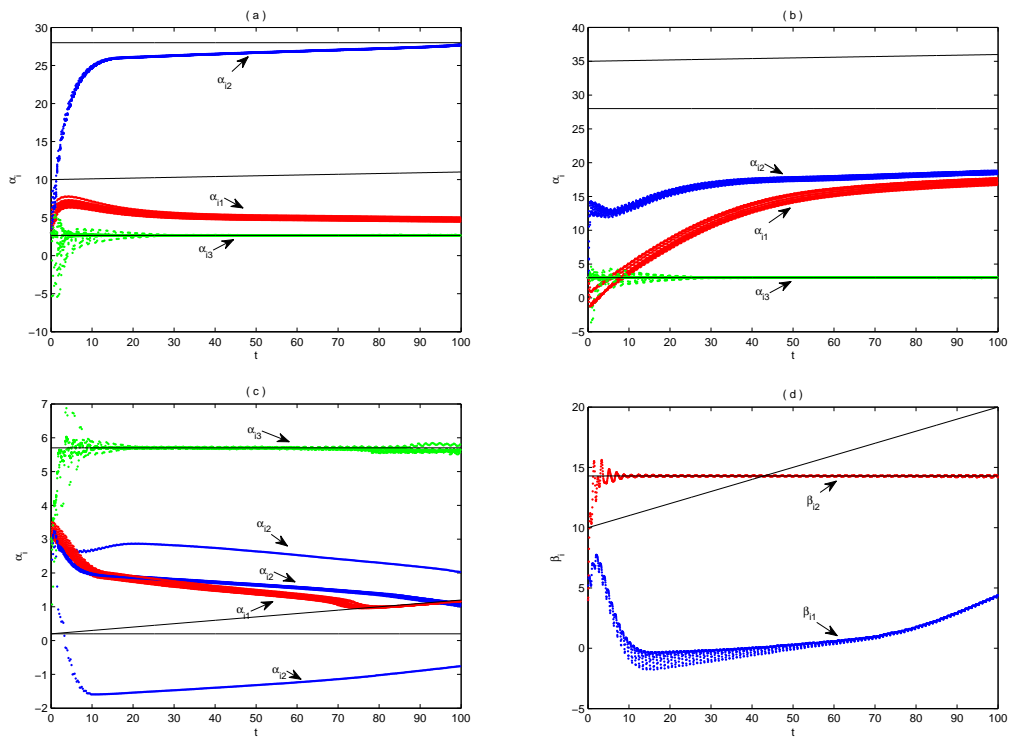


Figure 5.6: System parameters and their estimates: (a) nodes (1)–(10), (b) nodes (11)–(20), (c) nodes (21)–(30), and (d) the isolated oscillator, for $\tilde{\Theta}_i = 0.01$ and $\tilde{\Psi} = 0.1$.

Chapter 6

A Novel Synchronization Approach: Intermittent Impulsive Synchronization

6.1 Intermittent Impulsive Synchronization of Two Chaotic Systems with Delay

6.1.1 Introduction

Impulsive synchronization becomes a new trend in chaos-based secure communication. However, there always exists an upper boundary on the time intervals between the impulses (impulsive intervals) during the synchronization process [13, 20]. Usually, impulsive intervals are small, i.e., the controller in the slaver system needs to be activated frequently. But in some situations such as the orbital transfer of satellite, control of money supply in a financial market, etc., the control windows (the time periods the controller can work) are restricted. If the free windows (the time periods the controller can not be activated) are larger than the bound of the impulsive intervals, the general impulsive synchronization approach will fail. On the other hand, to reduce the control windows and to decrease the redundancy of synchronization signals is a new way to improve the security of chaos-based secure communication.

Therefore, in this section, we present intermittent impulsive synchronization, i.e., in our synchronization scheme, the impulsive control only acts in the control windows, not during the whole time. To the best of our knowledge, there is no existing work studying this challenging problem. Our synchronization criteria based on Lyapunov-Razumikhin theory can be used as a guideline for engineering applications.

6.1.2 Preliminaries

In this section, we introduce the intermittent impulsive synchronization scheme. Some preliminary lemmas and hypotheses are given.

Let R denote the set of real numbers, R_+ the set of nonnegative real numbers and R^n the n -dimensional Euclidean linear space equipped with the Euclidean norm $\|\cdot\|$. Throughout this paper, $P > 0$ (< 0 , ≤ 0 , ≥ 0) denotes a symmetrical positive (negative, semi-negative, semi-positive) definite matrix P , P^T the transpose of P and $\lambda_{M(m)}(P)$ the maximum (minimum) eigenvalue of P . Let $\varphi(t^+) = \lim_{s \rightarrow t^+} \varphi(s)$ and $\varphi(t^-) = \lim_{s \rightarrow t^-} \varphi(s)$.

Definition 6.1:

$$PC([a, b], R^n) = \{\varphi : [a, b] \rightarrow S \mid \varphi(t^+) = \varphi(t), \forall t \in [a, b]; \\ \varphi(t^-) \text{ exists in } S, \forall t \in (a, b] \text{ and } \varphi(t^-) = \varphi(t) \\ \text{for all but at most a finite number of points } t \in (a, b]\}.$$

where $a, b \in R$ with $a < b$ and $S \subset R^n$.

We equip the linear space $PC([-\tau, 0], R^n)$ with the norm $\|\cdot\|_\tau$ defined by $\|\varphi\|_\tau = \sup_{-\tau \leq s \leq 0} \|\varphi(s)\|$.

Consider a class of general chaotic systems with delay. In our synchronization scheme, the master system is given in the following form:

$$\begin{cases} \frac{dx(t)}{dt} = Ax(t) + Bf(x(t)) + Cg(x(t - \tau)), & t > 0, \\ x(t) = \phi, & -\tau \leq t \leq 0, \end{cases} \quad (6.1)$$

where $x(t) \in R^n$ is the state variable, A, B and C are $n \times n$ constant matrices, $f : R^n \rightarrow R^n$ and $g : R^n \rightarrow R^n$ both are continuous nonlinear functions satisfying $f(0) = 0$ and $g(0) = 0$, τ is the time delay, and $\phi \in PC([-\tau, 0], R^n)$ is the initial condition.

Define free windows $[k\omega, k\omega + \delta]$ and control windows $[k\omega + \delta, (k + 1)\omega]$ where $k = 0, 1, \dots$ and $0 < \delta < \omega < \infty$. Different from general impulsive control, intermittent impulsive control only works in control windows. The corresponding slave system is designed as follows.

When $t \in [k\omega, k\omega + \delta]$,

$$\frac{dy(t)}{dt} = Ay(t) + Bf(y(t)) + Cg(y(t - \tau)); \quad (6.2)$$

When $t \in [k\omega + \delta, (k + 1)\omega]$,

$$\begin{cases} \frac{dy(t)}{dt} = Ay(t) + Bf(y(t)) + Cg(y(t - \tau)), & t \neq T_{k,i}, \\ \Delta y(t) = U_{k,i}(x(t), y(t)), & t = T_{k,i}, \end{cases} \quad (6.3)$$

where $k = 0, 1, \dots, i = 1, 2, \dots, M_k, M_k$ is a positive integer related to $k, T_{k,i}$ denotes the i -th impulsive instant in the k -th control window, $k\omega + \delta = T_{k,1} < T_{k,2} < \dots < T_{k,M_k} \leq (k + 1)\omega$, $U_{k,i}(x(t), y(t)) = B_{k,i}(x(t) - y(t))$ is the impulsive control. Let $T_{k,M_k+1} = (k + 1)\omega$ and define $\Delta_{k,i} = T_{k,i+1} - T_{k,i}$.

The initial condition for slaver system (6.2)-(6.3) is given by

$$y(t) = \psi, \quad -\tau \leq t \leq 0,$$

where $\psi \in PC([-\tau, 0], R^n)$.

Let $e(t) = x(t) - y(t)$. We obtain the following error system.

When $t \in [k\omega, k\omega + \delta]$, we have

$$\frac{de(t)}{dt} = Ae(t) + B\tilde{f}(t) + C\tilde{g}(t - \tau). \quad (6.4)$$

When $t \in [k\omega + \delta, (k + 1)\omega]$, we have

$$\begin{cases} \frac{de(t)}{dt} = Ae(t) + B\tilde{f}(t) + C\tilde{g}(t - \tau), & t \neq T_{k,i}, \\ \Delta e(t) = -B_{k,i}e(t), & t = T_{k,i}, \end{cases} \quad (6.5)$$

where $\tilde{f}(t) = f(x(t)) - f(y(t))$ and $\tilde{g}(t) = g(x(t)) - g(y(t))$.

In this paper, we assume that f and g are Lipschitz continuous functions, i.e.,

Hypothesis 6.1: there exist positive constants L_f and L_g such that, for all $x, y \in R^n$,

$$\|f(x) - f(y)\| \leq L_f \|x - y\|, \quad \|g(x) - g(y)\| \leq L_g \|x - y\|. \quad (6.6)$$

Definition 6.2: Given a function $V(t, e(t)) : R_+ \times R^n \rightarrow R_+$, the upper right hand derivative of V with respect to the error system (6.4)-(6.5) is defined by

$$D^+V(t, e(t)) = \lim_{h \rightarrow 0^+} \sup \frac{1}{h} [V(t+h, e(t+h)) - V(t, e(t))],$$

for all $t \neq T_{k,i}$ in R_+ .

To prove the criteria of synchronization in the next section, we need the following lemmas.

Lemma 6.1 [113]: For any vectors $x, y \in R^n$ and positive constant ξ , the following matrix inequality holds:

$$2x^T y \leq \xi x^T x + \frac{1}{\xi} y^T y.$$

Lemma 6.2 [114]: Suppose that function $y(t)$ is non-negative when $t \in (-\tau, \infty)$ and satisfies the following:

$$\frac{dy(t)}{dt} \leq k_1 y(t) + k_2 y(t - \tau), \quad t \geq 0,$$

where k_1 and k_2 are positive constants. We then have the following inequality:

$$y(t) \leq \|y(0)\|_{\tau} e^{(k_1+k_2)t}, \quad t \geq 0.$$

Lemma 6.3 [57]: Let $\gamma > 0$ and $m \in C^1[J, R_+]$, where $J = [a - \gamma, b)$, $0 < b - a \leq \Delta$. Assume that there exist constants $l > 0$ and $\beta \in (0, 1)$ such that

$$D^+m(t) \leq lm(t), \quad \text{whenever } m(t) \geq \beta m(t+s), \quad s \in [-\gamma, 0];$$

and there exists a constant $\eta > 0$ such that $m(s) \leq \eta$, $s \in [a - \gamma, a)$, $m(a) \leq \beta\eta$, and

$$l\Delta + \ln \beta < 0.$$

Then $m(t) < \eta, t \geq a$.

Lemma 6.4: Let $\gamma > 0$ and $m \in C^1[J, R_+]$, where $J = [a - \gamma, b), 0 < b - a \leq \Delta$. Assume that there exist constants $l > 0$ and $\beta \in (0, 1)$ such that

$$D^+m(t) \leq lm(t), \quad \text{whenever } m(t) \geq \beta m(t + s), \quad s \in [-\gamma, 0]; \quad (6.7)$$

and there exist constants $\eta > 0$ and d ($\beta < d < 1$) such that $m(s) \leq \eta, s \in [a - \gamma, a), m(a) \leq \beta\eta$, and

$$l\Delta + \ln \beta < \ln d. \quad (6.8)$$

Then $m(t) < d\eta, t \geq a$.

Proof: Suppose that, for the sake of contradiction, there exists a $t^* > a$ such that

$$m(t^*) = d\eta \text{ and } m(t) < d\eta, \quad t \in [a, t^*).$$

Let $t^1 = \sup\{t \in [a, t^*], m(t) \leq \beta\eta\}$. Then $t^1 \in [a, t^*), m(t^1) = \beta\eta$ and $\beta\eta \leq m(t) \leq d\eta, \quad t \in [t^1, t^*]$. Thus for $t \in [t^1, t^*]$, we have

$$\beta m(t + s) \leq \beta\eta \leq m(t), \quad s \in [-\gamma, 0],$$

which implies

$$D^+m(t) \leq lm(t), \quad t \in [t^1, t^*].$$

Integrating from t^1 to t^* gives

$$\ln(m(t^*)) - \ln(m(t^1)) \leq l(t^* - t^1) \leq l\Delta.$$

But

$$\ln(m(t^*)) - \ln(m(t^1)) = \ln(d\eta) - \ln(\beta\eta) > l\Delta,$$

which is a contradiction. The proof completes.

6.1.3 Synchronization Criteria

In this section, based on Lyapunov-Razumikhin theorem and LMI approach, we derive some synchronization criteria via intermittent impulsive control.

Theorem 6.1: Assume that for an intermittent impulsive control law $\{T_{k,i}, U_{k,i}\}$

- (i) there exist a positive definite matrix P and constants $\alpha_1 > 0$, $\alpha_2 > 0$, $\xi_1 > 0$ and $\xi_2 > 0$ such that

$$PA + A^T P + \xi_1 P B B^T P + \xi_2 P C C^T P + \frac{1}{\xi_1} L_f^2 I - \alpha_1 P \leq 0; \quad (6.9)$$

and

$$\frac{1}{\xi_2} L_g^2 I - \alpha_2 P \leq 0; \quad (6.10)$$

- (ii) there exist real numbers $\beta_{k,i} \in (0, 1)$ such that

$$(I - B_{k,i}^T) P (I - B_{k,i}) - \beta_{k,i} P \leq 0; \quad (6.11)$$

- (iii) there exists a real number d ($\beta_{k,i} < d < 1$) such that for each k, i ,

$$\frac{\Delta_{k,i}}{\beta_{k,i}} (\beta_{k,i} \alpha_1 + \alpha_2) + \ln \beta_{k,i} \leq \ln d, \quad (6.12)$$

where $\Delta_{k,i} = T_{k,i+1} - T_{k,i}$ and $T_{k,M_k+1} = (k+1)\omega$.

- (iv) the time delay τ satisfies $\Delta \leq \tau \leq \omega - \delta$ and

$$d e^{(\alpha_1 + \alpha_2)\delta} < 1, \quad (6.13)$$

where $\Delta = \max_{k,i} \{\Delta_{k,i}\}$.

Then the trivial solution of error system (6.4)-(6.5) is asymptotically stable. It implies that slaver system (6.2)-(6.3) is synchronized with master system (6.1) by intermittent impulsive control $\{T_{k,i}, U_{k,i}\}$.

Proof: Define $V(t) = e(t)^T P e(t)$. When $t \in [k\omega, k\omega + \delta]$, the error system runs on subsystem (6.4). Thus, we have

$$\begin{aligned} D^+V(t) &= \dot{e}(t)^T P e(t) + e(t)^T P \dot{e}(t) \\ &= e(t)^T (A^T P + P A^T) e(t) + 2e(t)^T P B \tilde{f}(t) \\ &\quad + 2e(t)^T P C \tilde{g}(t - \tau) \end{aligned} \quad (6.14)$$

By **Lemma 6.1** and condition (6.6), we obtain

$$\begin{aligned} D^+V(t) &\leq e(t)^T (A^T P + P A^T) e(t) + \xi_1 e(t)^T P B B^T P e(t) \\ &\quad + \frac{1}{\xi_1} \|\tilde{f}(t)\|^2 + \xi_2 e(t)^T P C C^T P e(t) + \frac{1}{\xi_2} \|\tilde{g}(t - \tau)\|^2 \\ &\leq e(t)^T (A^T P + P A^T + \xi_1 P B B^T P + \xi_2 P C C^T P \\ &\quad + \frac{1}{\xi_1} L_f^2 I) e(t) + \frac{1}{\xi_2} L_g^2 e(t - \tau)^T e(t - \tau) \end{aligned} \quad (6.15)$$

By condition (i), we have

$$D^+V(t) \leq \alpha_1 V(t) + \alpha_2 V(t - \tau). \quad (6.16)$$

In term of **Lemma 6.2**, we have

$$V(t) \leq \|V(k\omega)\|_\tau e^{(\alpha_1 + \alpha_2)(t - k\omega)}, \quad t \in [k\omega, k\omega + \delta]. \quad (6.17)$$

Thus,

$$V(k\omega + \delta) \leq \|V(k\omega)\|_\tau e^{(\alpha_1 + \alpha_2)\delta}.$$

When $t \in [k\omega + \delta, (k + 1)\omega]$, the error system runs on subsystem (6.5). Thus the impulsive control works.

When $t \in (T_{k,1}, T_{k,2})$, we have

$$D^+V(t) \leq \alpha_1 V(t) + \alpha_2 V(t - \tau),$$

which implies, if $V(t) \geq \beta_{k,i} V(t + s)$, $s \in [-\tau, 0]$,

$$D^+V(t) \leq \frac{1}{\beta_{k,i}} (\beta_{k,i} \alpha_1 + \alpha_2) V(t). \quad (6.18)$$

When $t = T_{k,1}$, we get by condition (ii)

$$\begin{aligned}
V(T_{k,1}) &= e^T(T_{k,1}^-)(I - B_{k,1})^T P (I - B_{k,1}) e(T_{k,1}^-) \\
&\leq \beta_{k,i} e^T(T_{k,1}^-) P e(T_{k,1}^-) \\
&= \beta_{k,i} V(T_{k,1}^-) \\
&\leq \beta_{k,i} \|V(T_{k,1})\|_\tau.
\end{aligned} \tag{6.19}$$

By (6.18), (6.19), condition (iii) and Lemma 6.4, we have

$$V(t) < d \|V(T_{k,1})\|_\tau, \quad t \in [T_{k,1}, T_{k,2}). \tag{6.20}$$

Similarly, we have

$$V(t) < d \|V(T_{k,i})\|_\tau, \quad t \in [T_{k,i}, T_{k,i+1}), \text{ for } i = 2, 3, \dots, M_k, \tag{6.21}$$

where $T_{k,M_k+1} = (k+1)\omega$.

Since $d < 1$, we have

$$\|V(T_{k,i+1})\|_\tau \leq \|V(T_{k,i})\|_\tau \text{ for } i = 1, 2, \dots, M_k - 1.$$

Thus,

$$V(t) < d \|V(T_{k,1})\|_\tau, \quad t \in [k\omega + \delta, (k+1)\omega]. \tag{6.22}$$

When $k = 0$, by (6.17) and (6.22), we have

$$V(t) \leq \|V(0)\|_\tau e^{(\alpha_1 + \alpha_2)\delta}, \quad t \in [0, \delta],$$

and

$$V(t) < d \|V(\delta)\|_\tau, \quad t \in [\delta, \omega].$$

Since $\|V(\delta)\|_\tau \leq \|V(0)\|_\tau e^{(\alpha_1 + \alpha_2)\delta}$, by condition (iv), we have

$$V(t) < d \|V(0)\|_\tau e^{(\alpha_1 + \alpha_2)\delta} \leq \rho \|V(0)\|_\tau, \quad t \in [\delta, \omega],$$

where $0 < \rho = d e^{(\alpha_1 + \alpha_2)\delta} < 1$.

Similarly, when $k = 1$, we have

$$V(t) \leq \begin{cases} \|V(\omega)\|_{\tau} e^{(\alpha_1 + \alpha_2)\delta}, & t \in [\omega, \omega + \delta]; \\ \rho \|V(\omega)\|_{\tau}, & t \in [\omega + \delta, 2\omega]. \end{cases}$$

When $t \in [k\omega, (k+1)\omega]$, we have

$$V(t) \leq \begin{cases} \|V(k\omega)\|_{\tau} e^{(\alpha_1 + \alpha_2)\delta}, & t \in [k\omega, k\omega + \delta]; \\ \rho \|V(k\omega)\|_{\tau}, & t \in [k\omega + \delta, (k+1)\omega]. \end{cases}$$

Since $\tau \leq \omega - \delta$ in condition (iv), we have

$$\|V((k+1)\omega)\|_{\tau} \leq \|V((k+1)\omega)\|_{\omega - \delta} \leq \rho \|V(k\omega)\|_{\tau}.$$

Furthermore,

$$V(t) \leq \begin{cases} \rho^k \|V(0)\|_{\tau} e^{(\alpha_1 + \alpha_2)\delta}, & t \in [k\omega, k\omega + \delta]; \\ \rho^{k+1} \|V(0)\|_{\tau}, & t \in [k\omega + \delta, (k+1)\omega]. \end{cases}$$

Thus,

$$\lim_{t \rightarrow \infty} V(t) = 0.$$

Since $V(t) = e^T(t)Pe(t)$, we have

$$\frac{V(t)}{\lambda_M(P)} \leq \|e(t)\|^2 \leq \frac{V(t)}{\lambda_m(P)}.$$

For any $\epsilon > 0$, choose $\sigma = \sigma(\epsilon) > 0$ such that $\sigma < \sqrt{\frac{\lambda_M(P)}{\lambda_m(P)} e^{-(\alpha_1 + \alpha_2)\delta}} \epsilon$. When $e(0) < \sigma$, we have

$$\begin{aligned} \|e(t)\| &\leq \sqrt{\frac{V(t)}{\lambda_m(P)}} \leq \sqrt{\frac{\|V(0)\|_{\tau} e^{(\alpha_1 + \alpha_2)\delta}}{\lambda_m(P)}} \\ &\leq \sqrt{\frac{\lambda_M(P) e^{(\alpha_1 + \alpha_2)\delta} \|e(0)\|^2}{\lambda_m(P)}} \\ &< \epsilon. \end{aligned} \tag{6.23}$$

Also,

$$\lim_{t \rightarrow \infty} \|e(t)\| \leq \lim_{t \rightarrow \infty} \frac{V(t)}{\lambda_m(P)} = 0. \tag{6.24}$$

Therefore, the trivial solution $e(t)$ of error system (6.4)-(6.5) is asymptotically stable. It implies that slaver system (6.2)-(6.3) is synchronized with master system (6.1) by intermittent impulsive control $\{T_{k,i}, U_{k,i}\}$.

Define $\Delta_0 = \min_{k,i}\{\Delta_{k,i}\}$ and $M_0 = \min_k\{M_k\}$. If the time delay τ is small and satisfies $\tau < \Delta_0$, then we have the following synchronization criterion.

Theorem 6.2: Assume that for an intermittent impulsive control law $\{T_{k,i}, U_{k,i}\}$

- (i) there exist a positive definite matrix P and constants $\alpha_1 > 0$, $\alpha_2 > 0$, $\xi_1 > 0$ and $\xi_2 > 0$ such that

$$PA + A^T P + \xi_1 P B B^T P + \xi_2 P C C^T P + \frac{1}{\xi_1} L_f^2 I - \alpha_1 P \leq 0; \quad (6.25)$$

and

$$\frac{1}{\xi_2} L_g^2 I - \alpha_2 P \leq 0; \quad (6.26)$$

- (ii) there exist real numbers $\beta_{k,i} \in (0, 1)$ such that

$$(I - B_{k,i}^T) P (I - B_{k,i}) - \beta_{k,i} P \leq 0; \quad (6.27)$$

- (iii) there exists a real number d ($\beta_{k,i} < d < 1$) such that for each k, i ,

$$\frac{\Delta_{k,i}}{\beta_{k,i}} (\beta_{k,i} \alpha_1 + \alpha_2) + \ln \beta_{k,i} \leq \ln d, \quad (6.28)$$

where $\Delta_{k,i} = T_{k,i+1} - T_{k,i}$ and $T_{k,M_k+1} = (k+1)\omega$.

- (iv) the time delay τ satisfies $\tau \leq \Delta_0$ and

$$d^{M_0} e^{(\alpha_1 + \alpha_2)\delta} < 1, \quad (6.29)$$

where $\Delta = \max_{k,i}\{\Delta_{k,i}\}$.

Then the trivial solution of error system (6.4)-(6.5) is asymptotically stable. It implies that slaver system (6.2)-(6.3) is synchronized with master system (6.1) by intermittent impulsive control $\{T_{k,i}, U_{k,i}\}$.

Proof: Because conditions (i)-(iii) are same with that of Theorem 6.1, $V(t)$ still satisfies (6.21). We have

$$V(t) < d\|V(T_{k,i})\|_{\tau}, \quad t \in [T_{k,i}, T_{k,i+1}), \text{ for } i = 2, 3, \dots, M_k,$$

where $T_{k,M_k+1} = (k+1)\omega$.

Since $\tau \leq \Delta_0$, we have

$$\|V(T_{k,i+1})\|_{\tau} \leq \|V(T_{k,i+1})\|_{\Delta_{k,i}} < d\|V(T_{k,i})\|_{\tau},$$

for $i = 1, 2, \dots, M_k - 1$. Thus,

$$V(t) < d^i\|V(T_{k,1})\|_{\tau}, \quad t \in [T_{k,i}, T_{k,i+1}), \text{ for } i = 2, 3, \dots, M_k, \quad (6.30)$$

where $T_{k,M_k+1} = (k+1)\omega$.

When $k = 0$, by (6.17) and (6.30), we have

$$V(t) \leq \|V(0)\|_{\tau} e^{(\alpha_1 + \alpha_2)\delta}, \quad t \in [0, \delta],$$

and

$$V(t) < d^i\|V(0)\|_{\tau} e^{(\alpha_1 + \alpha_2)\delta}, \quad t \in [T_{1,i}, T_{1,i+1}).$$

Similarly, when $k = 1$, we have

$$V(t) \leq \begin{cases} \|V(\omega)\|_{\tau} e^{(\alpha_1 + \alpha_2)\delta}, & t \in [\omega, \omega + \delta]; \\ d^i\|V(\omega)\|_{\tau} e^{(\alpha_1 + \alpha_2)\delta}, & t \in [T_{2,i}, T_{2,i+1}). \end{cases}$$

When $t \in [k\omega, (k+1)\omega]$, we have

$$V(t) \leq \begin{cases} \|V(k\omega)\|_{\tau} e^{(\alpha_1 + \alpha_2)\delta}, & t \in [k\omega, k\omega + \delta]; \\ d^i\|V(k\omega)\|_{\tau} e^{(\alpha_1 + \alpha_2)\delta}, & t \in [T_{k,i}, T_{k,i+1}). \end{cases}$$

Since $\tau \leq \Delta_0$ in condition (iv), we have

$$\|V((k+1)\omega)\|_{\tau} \leq \|V((k+1)\omega)\|_{\Delta_0} \leq d^{M_k} \|V(k\omega)\|_{\tau} e^{(\alpha_1 + \alpha_2)\delta}.$$

In terms of condition (iv), we have

$$\|V((k+1)\omega)\|_\tau \leq d^{M_0} \|V(k\omega)\|_\tau e^{(\alpha_1+\alpha_2)\delta} \leq \theta \|V(k\omega)\|_\tau,$$

where $\theta = d^{M_0} e^{(\alpha_1+\alpha_2)\delta} < 1$.

Furthermore,

$$V(t) \leq \begin{cases} \theta^k \|V(0)\|_\tau e^{(\alpha_1+\alpha_2)\delta}, & t \in [k\omega, k\omega + \delta]; \\ \theta^k d^i \|V(0)\|_\tau, & t \in [[T_{k,i}, T_{k,i+1}). \end{cases}$$

Thus,

$$\lim_{t \rightarrow \infty} V(t) = 0.$$

Similarly, for any $\epsilon > 0$, choose $\sigma = \sigma(\epsilon) > 0$ such that $\sigma < \sqrt{\frac{\lambda_M(P)}{\lambda_m(P)}} e^{-(\alpha_1+\alpha_2)\delta} \epsilon$. When $e(0) < \sigma$, we have

$$\|e(t)\| < \epsilon. \quad (6.31)$$

Also,

$$\lim_{t \rightarrow \infty} \|e(t)\| = 0. \quad (6.32)$$

Therefore, the trivial solution $e(t)$ of error system (6.4)-(6.5) is asymptotically stable. It implies that slaver system (6.2)-(6.3) is synchronized with master system (6.1) by intermittent impulsive control $\{T_{k,i}, U_{k,i}\}$.

If the impulsive laws $\{T_{k,i}, U_{k,i}\}$ ($k = 1, 2, \dots$) are same in every control window, $\Delta_{k,i} = \Delta_1$ and $B_{k,i} = B$, then we have the following corollaries.

Corollary 6.1: Assume that for an intermittent impulsive control law $\{T_{k,i}, U_{k,i}\}$

- (i) there exist a positive definite matrix P and constants $\alpha_1 > 0$, $\alpha_2 > 0$, $\xi_1 > 0$ and $\xi_2 > 0$ such that

$$PA + A^T P + \xi_1 P B B^T P + \xi_2 P C C^T P + \frac{1}{\xi_1} L_f^2 I - \alpha_1 P \leq 0; \quad (6.33)$$

and

$$\frac{1}{\xi_2} L_g^2 I - \alpha_2 P \leq 0; \quad (6.34)$$

(ii) there exists a real number $\beta \in (0, 1)$ such that

$$(I - B^T)P(I - B) - \beta P \leq 0; \quad (6.35)$$

(iii) there exists a real number $d(\beta < d < 1)$ such that for each k, i ,

$$\frac{\Delta_1}{\beta}(\beta\alpha_1 + \alpha_2) + \ln \beta \leq \ln d. \quad (6.36)$$

(iv) the time delay τ satisfies $\Delta_1 \leq \tau \leq \omega - \delta$ and

$$de^{(\alpha_1 + \alpha_2)\delta} < 1. \quad (6.37)$$

Then slaver system (6.2)-(6.3) is synchronized with master system (6.1) by intermittent impulsive control $\{T_{k,i}, U_{k,i}\}$.

Corollary 6.2: Assume that for an intermittent impulsive control law $\{T_{k,i}, U_{k,i}\}$

(i) there exist a positive definite matrix P and constants $\alpha_1 > 0$, $\alpha_2 > 0$, $\xi_1 > 0$ and $\xi_2 > 0$ such that

$$PA + A^T P + \xi_1 P B B^T P + \xi_2 P C C^T P + \frac{1}{\xi_1} L_f^2 I - \alpha_1 P \leq 0; \quad (6.38)$$

and

$$\frac{1}{\xi_2} L_g^2 I - \alpha_2 P \leq 0; \quad (6.39)$$

(ii) there exists a real number $\beta \in (0, 1)$ such that

$$(I - B^T)P(I - B) - \beta P \leq 0; \quad (6.40)$$

(iii) there exists a real number $d(\beta < d < 1)$ such that for each k, i ,

$$\frac{\Delta_1}{\beta_1}(\beta_1\alpha_1 + \alpha_2) + \ln \beta \leq \ln d. \quad (6.41)$$

(iv) the time delay τ satisfies $\tau \leq \Delta_1$ and

$$d^{M_1} e^{(\alpha_1 + \alpha_2)\delta} < 1, \quad (6.42)$$

where $M_1 = \lfloor \frac{\omega - \delta}{\Delta_1} \rfloor + 1$ and $\lfloor a \rfloor$ denotes the nearest integers less than or equal to a .

Then slaver system (6.2)-(6.3) is synchronized with master system (6.1) by intermittent impulsive control $\{T_{k,i}, U_{k,i}\}$.

6.1.4 Numeral Examples

In this section, two numeral examples are given to show the effectiveness of the main result.

Example 6.1: Consider the following hyperchaotic attractor as the master system:

$$\frac{dx(t)}{dt} = a[-bx(t - \tau) + c \sin(dx(t - \tau))], \quad (6.43)$$

where $a = 0.8$, $b = 0.2$, $c = 3$, $d = 1.8$ and $\tau = 5$. This hyperchaotic system possesses four positive Lyapunov exponents $\lambda_1 = 0.1042$, $\lambda_2 = 0.0685$, $\lambda_3 = 0.0151$ and $\lambda_4 = 0.0685$ as shown in Fig. 6.1.

Assume that $\omega = 10$ and $\delta = 5$, then the free windows are $[10k, 10k + 5]$ and the control windows are $[10k + 5, 10k + 10]$. We design the impulsive laws are same in each control window with $\Delta_{k,i} = 0.1$ and $B_{k,i} = 0.95I$. Then the corresponding slave system is of the form:

When $t \in [10k, 10k + 5]$,

$$\frac{dy(t)}{dt} = -ay(t) + b \sin(y(t - \tau)), \quad (6.44)$$

When $t \in [10k + 5, 10k + 10]$,

$$\begin{cases} \frac{dy(t)}{dt} = -ay(t) + b \sin(y(t - \tau)), & t \neq T_{k,i}, \\ \Delta y(t) = 0.95(x(t) - y(t)), & t = T_{k,i}. \end{cases} \quad (6.45)$$

Let $e(t) = x(t) - y(t)$, we have the error system as follows,

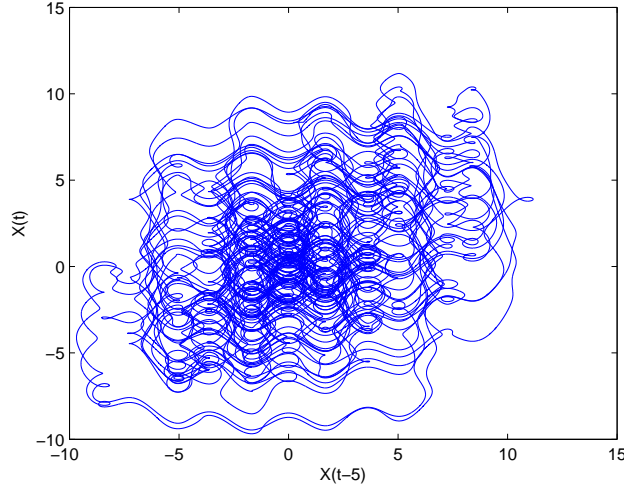


Figure 6.1: Phase portrait $x(t - 5) - x(t)$ of the hyperchaotic system with $a = 0.8$, $b = 0.2$, $c = 3$, $d = 1.8$ and $\tau = 5$.

When $t \in [10k, 10k + 5]$,

$$\frac{de(t)}{dt} = -ae(t) + b\tilde{g}(t - \tau),$$

When $t \in [10k + 5, 10k + 10]$,

$$\begin{cases} \frac{de(t)}{dt} = -ae(t) + b\tilde{g}(t - \tau), & t \neq T_{k,i}, \\ \Delta e(t) = -0.95e(t), & t = T_{k,i}, \end{cases}$$

where $\tilde{g}(t) = \sin(x(t)) - \sin(y(t))$.

Note that $A = 0$, $B = 0$, $C = 8$, $L_f = 0$ and $L_g = ab + ac = 2.56$. Let $P = I$. Thus, conditions (6.33)-(6.37) are satisfied. By Corollary 1, we know that slaver system (6.44)-(6.45) is synchronized with master system (6.43) by intermittent impulsive control with $\Delta_{k,i} = 0.1$ and $B_{k,i} = 0.95I$. The trajectory of synchronization error is shown in Fig. 6.2. Our simulation results show that when impulsive intervals satisfy $\Delta_{k,i} \leq 0.16$ the synchronization can be always achieved. If we choose $\delta = 6$, then $\tau > \omega - \delta$ breaks

condition (6.37). The synchronization error is shown in Fig. 6.3, which implies that the synchronization can not be achieved.

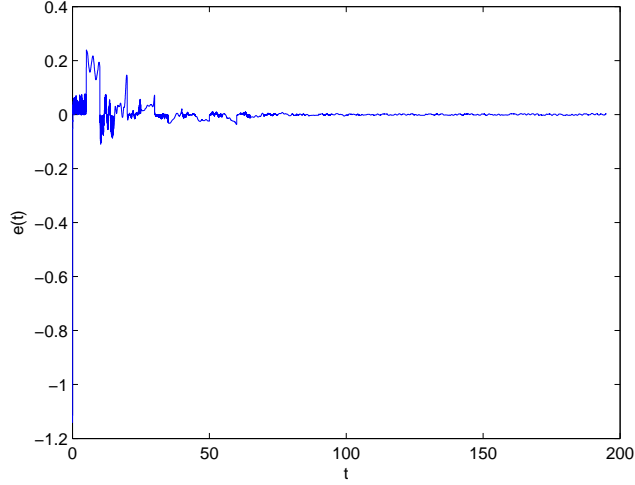


Figure 6.2: Synchronization error $e(t)$ with $\tau \leq \omega - \delta$, starting from initial conditions $\phi = rand$ and $\psi = 2 * rand$.

Example 6.2: Consider a 2-dimensional Lu oscillator, described by,

$$\frac{dx(t)}{dt} = -Ax(t) + f(x(t)) + g(x(t - \tau)), \quad (6.46)$$

where $\tau = 1$,

$$A = \begin{pmatrix} 1 & 0 \\ 0 & 1 \end{pmatrix}, \quad f(x) = \begin{pmatrix} 3.0 & 5.0 \\ 0.1 & 2.0 \end{pmatrix} \begin{pmatrix} \tanh(x_1) \\ \tanh(x_2) \end{pmatrix},$$

and

$$g(x) = \begin{pmatrix} -2.5 & 0.2 \\ 0.1 & -1.5 \end{pmatrix} \begin{pmatrix} \tanh(x_1) \\ \tanh(x_2) \end{pmatrix}.$$

The phase portrait of Lu oscillator is shown in Fig. 6.4. Assume that $\omega = 10$ and $\delta = 5$, then the free windows are $[10k, 10k+5]$ and the control windows are $[10k+5, 10k+10]$. We design the impulsive laws are same in each control window with $\Delta_{k,i} = 1.0$ and $B_{k,i} = 0.95I$.

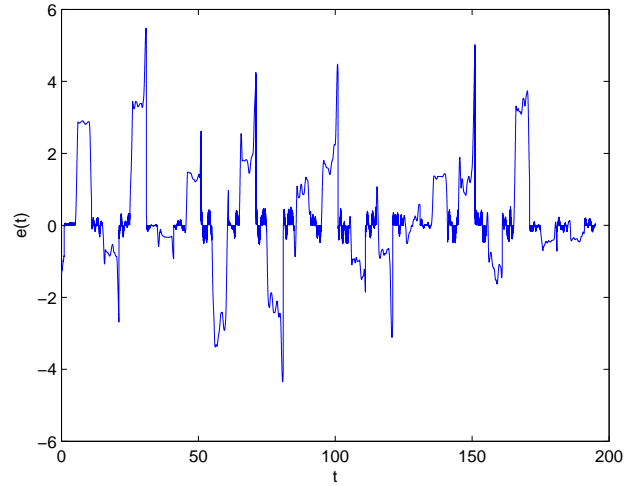


Figure 6.3: Synchronization error $e(t)$ with $\tau > \omega - \delta$, starting from initial conditions $\phi = rand$ and $\psi = 2 * rand$.

Let $P = I$. Thus, conditions (6.38)-(6.42) are satisfied. By Corollary 2, we know that the corresponding slaver system is synchronized with master system (6.46) by intermittent impulsive control with $\Delta_{k,i} = 1.0$ and $B_{k,i} = 0.95I$. The synchronization error is shown in Fig. 6.5. Our simulation results show that when impulsive intervals satisfy $\Delta_{k,i} \leq 1.2$ the synchronization can be always achieved. When $\Delta_{k,i} = 1.3$, the trajectory of synchronization error is shown in Fig. 6.6. It implies that the synchronization can not be achieved.

Remark 6.1: In both examples, the control window width $\omega - \delta$ is only a half of the whole period width ω . General impulsive synchronization approach is not suitable for these scenarios because the free window width δ is greater than the upper bound of the impulsive intervals.

6.1.5 Summary

In this section, we have investigated intermittent impulsive synchronization of two chaotic systems with delay. In our synchronization scheme, the impulsive controller is only acti-

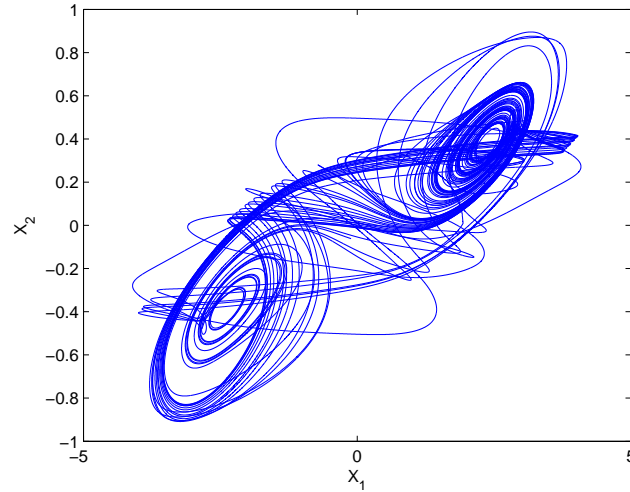


Figure 6.4: Phase portrait $x_1(t) - x_2(t)$ of Lu oscillator with system parameters $a = 0.8$, $b = 0.2$, $c = 3$, $d = 1.8$ and $\tau = 5$.

vated in the control windows, not during the whole time. Aiming for two different situations $\tau \leq \Delta_{k,i}$ and $\Delta_{k,i} < \tau \leq \omega - \delta$, we have presented corresponding synchronization criteria respectively. Compared with general impulsive synchronization, intermittent impulsive synchronization breaks through the limit of the upper bound of impulsive intervals. It can be flexibly applied to the scenario where the control window is restricted. On the other hand, by reducing the control window width and decreasing the redundancy of the synchronization signals, we can further improve the security of chaos-based secure communication. Thus, intermittent impulsive synchronization will have a great application and perspective.

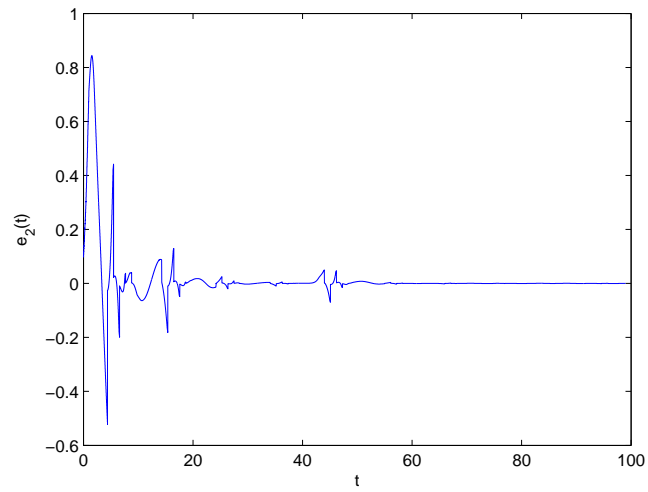
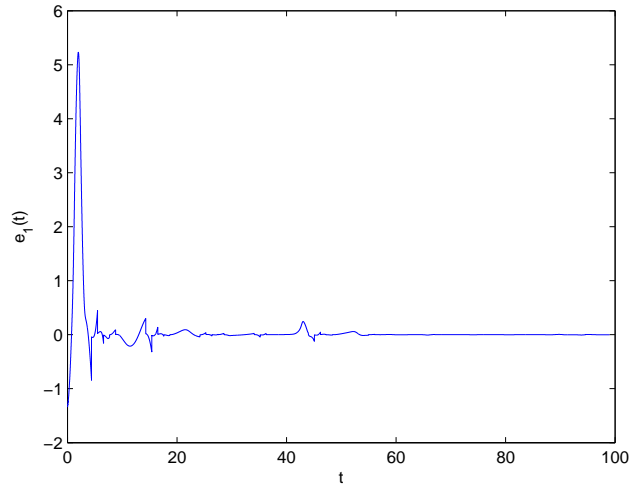


Figure 6.5: Synchronization errors (a) $e_1(t)$ and (b) $e_2(t)$ with $\Delta_{k,i} = 1.0$ and $B_{k,i} = 0.95I$.

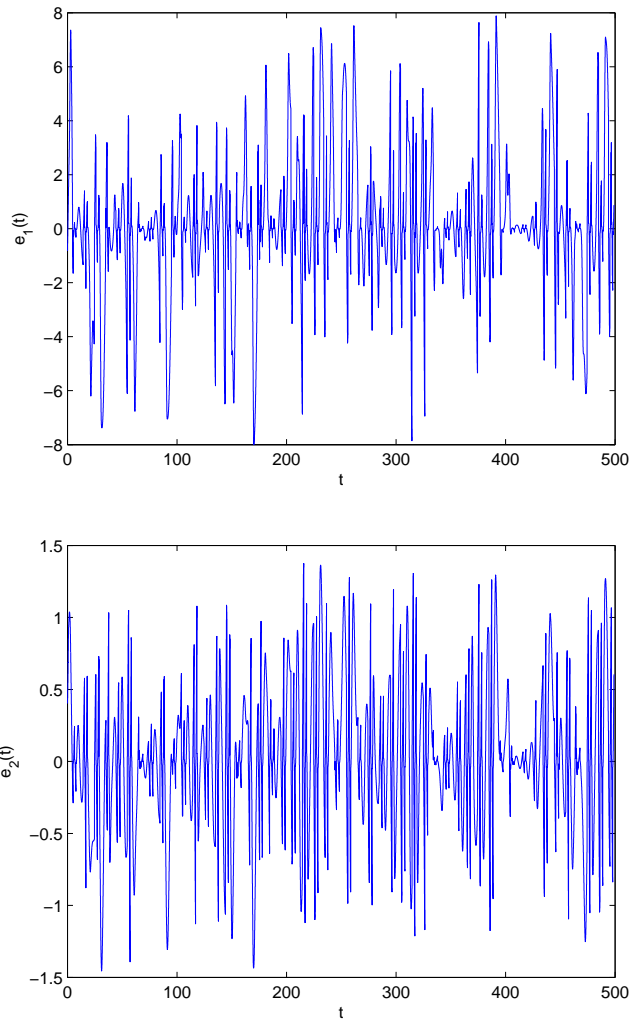


Figure 6.6: Synchronization errors (a) $e_1(t)$ and (b) $e_2(t)$ with $\Delta_{k,i} = 1.3$ and $B_{k,i} = 0.95I$.

6.2 Intermittent Impulsive Synchronization of Delayed Chaotic Neural Networks

6.2.1 Introduction

Delayed neural networks (DNNs) are concerned with stimulus-driven responses, internally generated in the brain. The neurons of the brain can generate complex patterns of activity with an extraordinarily rich spatial and temporal structure, and they remain highly sensitive to sensory input. Most related literature has mainly been devoted to the stability analysis and periodic oscillations of networks. However, it has been shown that such networks can exhibit chaotic behaviors [115–117]. Recently, chaos synchronization of coupled neural networks has attracted lots of attentions of scholars [118–122]. In this section, we generalize intermittent impulsive synchronization scheme to delayed chaotic neural networks.

6.2.2 Preliminaries

Some preliminary lemmas and hypotheses are given. Let R denote the set of real numbers, R_+ the set of nonnegative real numbers and R^n the n -dimensional Euclidean linear space equipped with the Euclidean norm $\|\cdot\|$. Throughout this paper, $P > 0$ (< 0 , ≤ 0 , ≥ 0) denotes a symmetrical positive (negative, semi-negative, semi-positive) definite matrix P , P^T the transpose of P and $\lambda_{M(m)}(P)$ the maximum (minimum) eigenvalue of P . Let $\varphi(t^+) = \lim_{s \rightarrow t^+} \varphi(s)$ and $\varphi(t^-) = \lim_{s \rightarrow t^-} \varphi(s)$.

Definition 6.3:

$$PC([a, b], R^n) = \{\varphi : [a, b] \rightarrow S | \varphi(t^+) = \varphi(t), \forall t \in [a, b]; \\ \varphi(t^-) \text{ exists in } S, \forall t \in (a, b] \text{ and } \varphi(t^-) = \varphi(t) \\ \text{for all but at most a finite number of points } t \in (a, b]\}.$$

where $a, b \in R$ with $a < b$ and $S \subset R^n$.

We equip the linear space $PC([-τ, 0], R^n)$ with the norm $\| \cdot \|_τ$ defined by $\|\varphi\|_τ = \sup_{-τ \leq s \leq 0} \|\varphi(s)\|$.

Consider a class of general delayed chaotic neural networks. In our synchronization scheme, the master system is given in the following form:

$$\begin{aligned} \frac{dx_i(t)}{dt} = & -c_i x_i(t) + \sum_{j=1}^n a_{ij} f_j(x_j(t)) \\ & + \sum_{j=1}^n b_{ij} f_j(x_j(t - \tau(t))) + J_i, \quad t > 0, \end{aligned} \quad (6.47)$$

where $i = 1, 2, \dots, n$, $x_i(t)$ is the state vector associated with the i -th neuron, f_i denotes the activation function, by which the neurons respond to each other, $c_i > 0$, $A = (a_{ij})_{n \times n}$ and $B = (b_{ij})_{n \times n}$ are the connection weight matrix and the delayed connection weight matrix, respectively, which indicate the strengths of the neuron interconnections within the network, J_i is a constant external input to set the desired equilibrium point, $\tau(t)$ is the time-varying delay, satisfying $r = \max_{t \in R^+} \{\tau(t)\}$ and the initial condition of (6.47) is given by $x_i(t) = \phi_i \in PC([-r, 0], R)$.

General Impulsive Synchronization Scheme (GISS):

The corresponding slave system is designed by

$$\begin{cases} \frac{dy_i(t)}{dt} = -c_i y_i(t) + \sum_{j=1}^n a_{ij} f_j(y_j(t)) \\ \quad + \sum_{j=1}^n b_{ij} f_j(y_j(t - \tau(t))) + J_i, \quad t \neq T_k, \\ \Delta y_i(t) = U_{k,i}(x_i(t), y_i(t)), \quad t = T_k, \end{cases} \quad (6.48)$$

where $k = 0, 1, \dots, T_k$ is the k -th impulsive instant, $U_{k,i}(x_i(t), y_i(t)) = B_{k,i}(x_i(t) - y_i(t))$ is the impulsive control of i -th neuron at the k -th impulsive instant and $\{T_k, U_{k,i}\}$ is called the impulsive law.

The initial condition for slaver system (6.48) is given by

$$y_i(t) = \psi(t), \quad -r \leq t \leq 0,$$

where $\psi \in PC([-r, 0], R)$.

Let $e_i(t) = x_i(t) - y_i(t)$. We obtain the following error system:

$$\begin{cases} \frac{de_i(t)}{dt} = -c_i e_i(t) + \sum_{j=1}^n a_{ij} \tilde{f}_j(e_j(t)) \\ \quad + \sum_{j=1}^n b_{ij} \tilde{f}_j(e_j(t - \tau(t))), & t \neq T_k, \\ \Delta e_i(t) = -B_{k,i} e_i(t), & t = T_k, \end{cases} \quad (6.49)$$

where $\tilde{f}_i(e_i(t)) = f_i(x_i(t)) - f_i(y_i(t))$.

In our intermittent impulsive synchronization scheme, impulsive control only occurs in control windows, not during the whole time. firstly define free windows $[m\omega, m\omega + \delta]$ and control windows $[m\omega + \delta, (m+1)\omega]$ where $m = 0, 1, \dots$ and $0 < \delta < \omega < \infty$.

Intermittent Impulsive Synchronization Scheme (IISS):

The corresponding slave system is designed as follows:

$$\begin{cases} \frac{dy_i(t)}{dt} = -c_i y_i(t) + \sum_{j=1}^n a_{ij} f_j(y_j(t)) \\ \quad + \sum_{j=1}^n b_{ij} f_j(y_j(t - \tau(t))) + J_i, & t \in [m\omega, m\omega + \delta], \\ \left\{ \begin{array}{l} \frac{dy_i(t)}{dt} = -c_i y_i(t) + \sum_{j=1}^n a_{ij} f_j(y_j(t)) \\ \quad + \sum_{j=1}^n b_{ij} f_j(y_j(t - \tau(t))) + J_i, & t \neq T_{m,l}, \\ \Delta y_i(t) = U_{m,l,i}(x_i(t), y_i(t)), & t = T_{m,l}, \end{array} \right. & t \in [m\omega + \delta, (m+1)\omega], \end{cases} \quad (6.50)$$

where $m = 0, 1, \dots, l = 1, 2, \dots, M_m$, M_m is a positive integer related to m , $T_{m,l}$ denotes the l -th impulsive instant in the m -th control window, $m\omega + \delta = T_{m,1} < T_{m,2} < \dots < T_{m,M_m} \leq (k+1)\omega$, $U_{m,l,i}(x_i(t), y_i(t)) = B_{m,l,i}(x_i(t) - y_i(t))$ is the impulsive control. Let $T_{k,M_{k+1}} = (k+1)\omega$ and define $\Delta_{k,i} = T_{k,i+1} - T_{k,i}$.

Let $e_i(t) = x_i(t) - y_i(t)$. Also, we obtain the following error system:

$$\left\{ \begin{array}{l} \frac{de_i(t)}{dt} = -c_i e_i(t) + \sum_{j=1}^n a_{ij} \tilde{f}_j(e_j(t)) \\ \quad + \sum_{j=1}^n b_{ij} \tilde{f}_j(e_j(t - \tau(t))), \\ \qquad \qquad \qquad t \in [m\omega, m\omega + \delta], \\ \left\{ \begin{array}{l} \frac{de_i(t)}{dt} = -c_i e_i(t) + \sum_{j=1}^n a_{ij} \tilde{f}_j(e_j(t)) \\ \quad + \sum_{j=1}^n b_{ij} \tilde{f}_j(e_j(t - \tau(t))), \quad t \neq T_{m,l}, \\ \Delta e_i(t) = -B_{m,l,i} e_i(t), \quad t = T_{m,l}, \\ \qquad \qquad \qquad t \in [m\omega + \delta, (m+1)\omega], \end{array} \right. \end{array} \right. \quad (6.51)$$

where $\tilde{f}_i(e_i(t)) = f_i(x_i(t)) - f_i(y_i(t))$.

Throughout this paper, we assume that f_i , ($i = 1, 2, \dots, n$) is bounded and satisfies the Lipschitz condition, i.e.,

H1: Each activation function f_i ($i = 1, 2, \dots, n$) is bounded and there exists a positive constant L_i such that, for all $x, y \in R$,

$$\|f_i(x) - f_i(y)\| \leq L_i \|x - y\|. \quad (6.52)$$

Definition 6.4: Given a function $V(t, e(t)) : R_+ \times R^n \rightarrow R_+$, the upper right hand derivative of V with respect to the error system (6.50)-(6.51) is defined by

$$D^+V(t, e(t)) = \lim_{h \rightarrow 0^+} \sup \frac{1}{h} [V(t+h, e(t+h)) - V(t, e(t))],$$

for all $t \neq T_{k,i}$ in R_+ .

6.2.3 Synchronization Criteria

In this section, based on Lyapunov-Razumikhin theorem and LMI approach, we derive some synchronization criteria via general impulsive control and intermittent impulsive control, respectively. Firstly, consider GISS, we have the following general impulsive synchronization criterion.

General Impulsive Synchronization Criterion

In GISS, error system (6.49) can be rewritten in the following compact form:

$$\begin{cases} \frac{de(t)}{dt} = -Ce(t) + A\tilde{f}(e(t)) + B\tilde{f}(e(t - \tau(t))), & t \neq T_k, \\ \Delta e(t) = -B_k e(t), & t = T_k, \end{cases} \quad (6.53)$$

where $e(t) = [e_1(t), \dots, e_n(t)]^T$, $C = \text{diag}\{c_1, \dots, c_n\}$, $A = (a_{ij})_{n \times n}$, $B = (b_{ij})_{n \times n}$, $\tilde{f}(e(t)) = [\tilde{f}_1(e_1(t)), \dots, \tilde{f}_n(e_n(t))]$ and $B_k = \text{diag}\{B_{k,1}, \dots, B_{k,n}\}$.

Theorem 6.3: In GISS, assume that for an impulsive control law $\{T_k, U_{k,i}\}$

- (i) there exist a positive definite matrix P and constants $\alpha_1 > 0$, $\alpha_2 > 0$, $\xi_1 > 0$ and $\xi_2 > 0$ such that

$$-2PC + \xi_1 PAA^T P + \xi_2 PBB^T P + \frac{1}{\xi_1} L_f - \alpha_1 P \leq 0, \quad (6.54)$$

and

$$\frac{1}{\xi_2} L_f - \alpha_2 P \leq 0, \quad (6.55)$$

where $L_f = \text{diag}\{L_1^2, L_2^2, \dots, L_n^2\}$.

- (ii) there exist a real number $\beta \in (0, 1)$ such that

$$(I - B_k^T)P(I - B_k) - \beta P \leq 0. \quad (6.56)$$

- (iii) there exists a positive number Δ , ($\Delta \geq \Delta_k$) such that

$$\frac{\Delta}{\beta}(\beta\alpha_1 + \alpha_2) + \ln \beta \leq 0, \quad (6.57)$$

where $\Delta_k = T_{k+1} - T_k$.

Then the trivial solution of error system (6.53) is asymptotically stable. It implies that slaver system (6.48) is synchronized with master system (6.47) by impulsive control $\{T_k, U_{k,i}\}$.

Proof: Define $V(t) = e(t)^T P e(t)$. When $t \in (T_k, T_{k+1})$, we have

$$\begin{aligned} D^+V(t) &= \dot{e}(t)^T P e(t) + e(t)^T P \dot{e}(t) \\ &= -2e(t)^T P C e(t) + 2e(t)^T P A \tilde{f}(e(t)) \\ &\quad + 2e(t)^T P B \tilde{f}(e(t - \tau(t))) \end{aligned} \quad (6.58)$$

By **Lemma 6.1** and condition (6.52), we obtain

$$\begin{aligned} D^+V(t) &\leq -2e(t)^T P C e(t) + \xi_1 e(t)^T P A A^T P e(t) \\ &\quad + \frac{1}{\xi_1} \|\tilde{f}(e(t))\|^2 + \xi_2 e(t)^T P B B^T P e(t) \\ &\quad + \frac{1}{\xi_2} \|\tilde{f}(e(t - \tau(t)))\|^2 \\ &\leq e(t)^T (-2PC + \xi_1 P A A^T P + \xi_2 P B B^T P \\ &\quad + \frac{1}{\xi_1} L_f) e(t) + \frac{1}{\xi_2} L_f e(t - \tau(t))^T e(t - \tau(t)) \end{aligned} \quad (6.59)$$

where $L_f = \text{diag}\{L_1^2, L_2^2, \dots, L_n^2\}$.

By condition (i), we have

$$D^+V(t) \leq \alpha_1 V(t) + \alpha_2 V(t - \tau). \quad (6.60)$$

which implies, if $V(t) \geq \beta V(t + s)$, $s \in [-r, 0]$,

$$D^+V(t) \leq \frac{1}{\beta} (\beta \alpha_1 + \alpha_2) V(t). \quad (6.61)$$

When $t = T_k$, we get by condition (ii)

$$\begin{aligned} V(T_k) &= e^T(T_k^-) (I - B_k)^T P (I - B_k) e(T_k^-) \\ &\leq \beta e^T(T_k^-) P e(T_k^-) \\ &= \beta V(T_k^-) \\ &\leq \beta \|V(T_k)\|_r. \end{aligned} \quad (6.62)$$

By (6.61), (6.62), condition (iii) and Lemma 6.3, we have

$$V(t) < \|V(T_k)\|_r \leq \rho \|V(T_k)\|_r, \quad t \in (T_k, T_{k+1}), \quad (6.63)$$

where $\beta \leq \rho < 1$.

From (6.62) and (6.63), we have

$$V(t) \leq \rho^k \|V(0)\|_r, \quad t \in [T_k, T_{k+1}]. \quad (6.64)$$

For any $\epsilon > 0$, choose $\sigma = \sigma(\epsilon) > 0$ such that $\sigma < \sqrt{\frac{\lambda_m(P)}{\lambda_M(P)\rho}}\epsilon$. When $\|e(0)\|_r < \sigma$, we have

$$\begin{aligned} \|e(t)\| &\leq \sqrt{\frac{V(t)}{\lambda_m(P)}} \leq \sqrt{\frac{\|V(0)\|_r \rho}{\lambda_m(P)}} \\ &\leq \sqrt{\frac{\lambda_M(P)\rho \|e(0)\|_r^2}{\lambda_m(P)}} \\ &< \epsilon. \end{aligned} \quad (6.65)$$

Also,

$$\lim_{t \rightarrow \infty} \|e(t)\| \leq \lim_{t \rightarrow \infty} \frac{V(t)}{\lambda_m(P)} = 0. \quad (6.66)$$

Therefore, the trivial solution $e(t)$ of error system (6.53) is asymptotically stable. It implies that slaver system (6.48) is synchronized with master system (6.47) by impulsive control $\{T_k, U_{k,i}\}$.

Remark 6.2: Conditions (6.54)-(6.56) of **Theorem 6.3** are related to impulsive controllers $U_{k,i}$ and condition (6.57) is about impulsive intervals Δ_k . If the controllers are strong enough (i.e., $B_k \approx I$) and the impulsive intervals are small enough (i.e., $\Delta_k \approx 0$), then all conditions of **Theorem 6.3** are always satisfied. It implies that we can always realize chaos synchronization by GISS.

If the impulsive laws $\{T_k, U_{k,i}\}$ ($k = 1, 2, \dots$) are same, $\Delta_k = \Delta_1$ and $B_k = B_s$, then we have the following corollary.

Corollary 6.3: In GISS, assume that for an impulsive control law $\{T_k, U_{k,i}\}$

- (i) there exist a positive definite matrix P and constants $\alpha_1 > 0$, $\alpha_2 > 0$, $\xi_1 > 0$ and $\xi_2 > 0$ such that

$$-2PC + \xi_1 PAA^T P + \xi_2 PBB^T P + \frac{1}{\xi_1} L_f - \alpha_1 P \leq 0,$$

and

$$\frac{1}{\xi_2} L_f - \alpha_2 P \leq 0,$$

where $L_f = \text{diag}\{L_1^2, L_2^2, \dots, L_n^2\}$.

(ii) there exist a real number $\beta \in (0, 1)$ such that

$$(I - B_s^T)P(I - B_s) - \beta P \leq 0;$$

(iii) the impulsive interval Δ_1 satisfies

$$\frac{\Delta_1}{\beta}(\beta\alpha_1 + \alpha_2) + \ln \beta \leq 0.$$

Then slaver system (6.48) is synchronized with master system (6.47) by impulsive control $\{T_k, U_{k,i}\}$.

Intermittent Impulsive Synchronization Criterion

In IISS, error system (6.51) can be rewritten in the following compact form:

$$\left\{ \begin{array}{l} \frac{de(t)}{dt} = -Ce(t) + A\tilde{f}(e(t)) + B\tilde{f}(e(t - \tau(t))), \\ \quad \quad \quad t \in [m\omega, m\omega + \delta], \\ \left\{ \begin{array}{l} \frac{de(t)}{dt} = -Ce(t) + A\tilde{f}(e(t)) \\ \quad \quad \quad + B\tilde{f}(e(t - \tau(t))), \quad t \neq T_{m,l}, \\ \Delta e(t) = -B_{m,l}e(t), \quad t = T_{m,l}, \\ \quad \quad \quad t \in [m\omega + \delta, (m+1)\omega], \end{array} \right. \end{array} \right. \quad (6.67)$$

where $e(t) = [e_1(t), \dots, e_n(t)]^T$, $C = \text{diag}\{c_1, \dots, c_n\}$, $A = (a_{ij})_{n \times n}$, $B = (b_{ij})_{n \times n}$, $\tilde{f}(e(t)) = [\tilde{f}_1(e_1(t)), \dots, \tilde{f}_n(e_n(t))]$ and $B_{m,l} = \text{diag}\{B_{m,l,1}, \dots, B_{m,l,n}\}$.

Theorem 6.4: In IISS, assume that for an intermittent impulsive control law $\{T_{m,l}, U_{m,l,i}\}$

(i) there exist a positive definite matrix P and constants $\alpha_1 > 0$, $\alpha_2 > 0$, $\xi_1 > 0$ and $\xi_2 > 0$ such that

$$-2PC + \xi_1 PAA^T P + \xi_2 PBB^T P + \frac{1}{\xi_1} L_f - \alpha_1 P \leq 0, \quad (6.68)$$

and

$$\frac{1}{\xi_2} L_f - \alpha_2 P \leq 0, \quad (6.69)$$

where $L_f = \text{diag}\{L_1^2, L_2^2, \dots, L_n^2\}$.

(ii) there exist real numbers $\beta_{m,l} \in (0, 1)$ such that

$$(I - B_{m,l}^T)P(I - B_{m,l}) - \beta_{m,l}P \leq 0. \quad (6.70)$$

(iii) there exists a real number $d(\beta_{m,l} < d < 1)$ such that for each m, l ,

$$\frac{\Delta_{m,l}}{\beta_{m,l}}(\beta_{m,l}\alpha_1 + \alpha_2) + \ln \beta_{m,l} \leq \ln d, \quad (6.71)$$

where $\Delta_{m,l} = T_{m,l+1} - T_{m,l}$ and $T_{m,M_m+1} = (m+1)\omega$.

(iv) the upper bound r of time delay satisfies $\Delta \leq r \leq \omega - \delta$ and

$$de^{(\alpha_1+\alpha_2)\delta} < 1, \quad (6.72)$$

where $\Delta = \max_{m,l}\{\Delta_{m,l}\}$.

Then the trivial solution of error system (6.67) is asymptotically stable. It implies that slaver system (6.50) is synchronized with master system (6.47) by intermittent impulsive control $\{T_{m,l}, U_{m,l,i}\}$.

Proof: Define $V(t) = e(t)^T P e(t)$. When $t \in [m\omega, m\omega + \delta]$, the slave system runs in free windows and the impulsive control does not work. Then we have

$$D^+V(t) \leq \alpha_1 V(t) + \alpha_2 V(t - \tau). \quad (6.73)$$

In term of **Lemma 6.2**, we have

$$V(t) \leq \|V(m\omega)\|_r e^{(\alpha_1+\alpha_2)(t-m\omega)}, \quad t \in [m\omega, m\omega + \delta]. \quad (6.74)$$

Thus,

$$V(m\omega + \delta) \leq \|V(m\omega)\|_r e^{(\alpha_1+\alpha_2)\delta}.$$

When $t \in [m\omega + \delta, (m+1)\omega]$, the slave system runs in control windows. Thus the impulsive control works.

When $t \in (T_{m,1}, T_{m,2})$, we have

$$D^+V(t) \leq \alpha_1 V(t) + \alpha_2 V(t - \tau),$$

which implies, if $V(t) \geq \beta_{m,l} V(t + s)$, $s \in [-r, 0]$,

$$D^+V(t) \leq \frac{1}{\beta_{m,l}} (\beta_{m,l} \alpha_1 + \alpha_2) V(t). \quad (6.75)$$

When $t = T_{m,1}$, we get by condition (ii)

$$\begin{aligned} V(T_{m,1}) &= e^T(T_{m,1}^-)(I - B_{m,1})^T P (I - B_{m,1}) e(T_{m,1}^-) \\ &\leq \beta_{m,l} e^T(T_{m,1}^-) P e(T_{m,1}^-) \\ &= \beta_{m,l} V(T_{m,1}^-) \\ &\leq \beta_{m,l} \|V(T_{m,1})\|_\tau. \end{aligned} \quad (6.76)$$

By (6.75), (6.76), condition (iii) and Lemma 6.4, we have

$$V(t) < d \|V(T_{m,1})\|_r, \quad t \in [T_{m,1}, T_{m,2}). \quad (6.77)$$

Similarly, we have

$$V(t) < d \|V(T_{m,l})\|_r, \quad t \in [T_{m,l}, T_{m,l+1}), \text{ for } i = 2, 3, \dots, M_m, \quad (6.78)$$

where $T_{m,M_m+1} = (m+1)\omega$.

Since $d < 1$, we have

$$\|V(T_{m,l+1})\|_r \leq \|V(T_{m,l})\|_r \text{ for } i = 1, 2, \dots, M_m - 1.$$

Thus,

$$V(t) < d \|V(T_{m,1})\|_r, \quad t \in [m\omega + \delta, (m+1)\omega]. \quad (6.79)$$

When $m = 0$, by (6.74) and (6.79), we have

$$V(t) \leq \|V(0)\|_r e^{(\alpha_1 + \alpha_2)\delta}, \quad t \in [0, \delta],$$

and

$$V(t) < d\|V(\delta)\|_r, \quad t \in [\delta, \omega].$$

Since $\|V(\delta)\|_r \leq \|V(0)\|_r e^{(\alpha_1+\alpha_2)\delta}$, by condition (iv), we have

$$V(t) < d\|V(0)\|_r e^{(\alpha_1+\alpha_2)\delta} \leq \rho\|V(0)\|_r, \quad t \in [\delta, \omega],$$

where $0 < \rho = de^{(\alpha_1+\alpha_2)\delta} < 1$.

Similarly, when $k = 1$, we have

$$V(t) \leq \begin{cases} \|V(\omega)\|_r e^{(\alpha_1+\alpha_2)\delta}, & t \in [\omega, \omega + \delta]; \\ \rho\|V(\omega)\|_r, & t \in [\omega + \delta, 2\omega]. \end{cases}$$

When $t \in [m\omega, (m+1)\omega]$, we have

$$V(t) \leq \begin{cases} \|V(m\omega)\|_r e^{(\alpha_1+\alpha_2)\delta}, & t \in [m\omega, m\omega + \delta]; \\ \rho\|V(m\omega)\|_r, & t \in [m\omega + \delta, (m+1)\omega]. \end{cases}$$

Since $r \leq \omega - \delta$ in condition (iv), we have

$$\|V((m+1)\omega)\|_r \leq \|V((m+1)\omega)\|_{\omega-\delta} \leq \rho\|V(m\omega)\|_r.$$

Furthermore,

$$V(t) \leq \begin{cases} \rho^m \|V(0)\|_r e^{(\alpha_1+\alpha_2)\delta}, & t \in [m\omega, m\omega + \delta]; \\ \rho^{m+1} \|V(0)\|_r, & t \in [m\omega + \delta, (m+1)\omega]. \end{cases}$$

Thus,

$$\lim_{t \rightarrow \infty} V(t) = 0.$$

Since $V(t) = e^T(t)Pe(t)$, we have

$$\frac{V(t)}{\lambda_M(P)} \leq \|e(t)\|^2 \leq \frac{V(t)}{\lambda_m(P)}.$$

For any $\epsilon > 0$, choose $\sigma = \sigma(\epsilon) > 0$ such that $\sigma < \sqrt{\frac{\lambda_m(P)}{\lambda_M(P)} e^{-(\alpha_1 + \alpha_2)\delta}} \epsilon$. When $\|e(0)\|_r < \sigma$, we have

$$\begin{aligned} \|e(t)\| &\leq \sqrt{\frac{V(t)}{\lambda_m(P)}} \leq \sqrt{\frac{\|V(0)\|_r e^{(\alpha_1 + \alpha_2)\delta}}{\lambda_m(P)}} \\ &\leq \sqrt{\frac{\lambda_M(P) e^{(\alpha_1 + \alpha_2)\delta} \|e(0)\|_r^2}{\lambda_m(P)}} \\ &< \epsilon. \end{aligned} \quad (6.80)$$

Also,

$$\lim_{t \rightarrow \infty} \|e(t)\| \leq \lim_{t \rightarrow \infty} \frac{V(t)}{\lambda_m(P)} = 0. \quad (6.81)$$

Therefore, the trivial solution $e(t)$ of error system (6.67) is asymptotically stable. It implies that slaver system (6.50) is synchronized with master system (6.47) by intermittent impulsive control $\{T_{m,l}, U_{m,l,i}\}$.

Remark 6.3: In the proof of **Theorem 6.4**, $V(t)$ converges exponentially to zero along the trajectory of error system (6.51). Also, synchronization error $e(t)$ converges exponentially to zero. It implies that chaos synchronization becomes better and better with synchronization time passing.

Define $\Delta_0 = \min_{m,l} \{\Delta_{m,l}\}$ and $M_0 = \min_m \{M_m\}$. If the time delay $\tau(t)$ is small and satisfies $\tau(t) \leq r < \Delta_0$, then we have the following synchronization criterion.

Theorem 6.5: Assume that for an intermittent impulsive control law $\{T_{m,l}, U_{m,l,i}\}$

- (i) there exist a positive definite matrix P and constants $\alpha_1 > 0$, $\alpha_2 > 0$, $\xi_1 > 0$ and $\xi_2 > 0$ such that

$$-2PC + \xi_1 PAA^T P + \xi_2 PBB^T P + \frac{1}{\xi_1} L_f - \alpha_1 P \leq 0, \quad (6.82)$$

and

$$\frac{1}{\xi_2} L_f - \alpha_2 P \leq 0, \quad (6.83)$$

where $L_f = \text{diag}\{L_1^2, L_2^2, \dots, L_n^2\}$.

- (ii) there exist real numbers $\beta_{m,l} \in (0, 1)$ such that

$$(I - B_{m,l}^T)P(I - B_{m,l}) - \beta_{m,l}P \leq 0. \quad (6.84)$$

(iii) there exists a real number $d(\beta_{m,l} < d < 1)$ such that for each m, l ,

$$\frac{\Delta_{m,l}}{\beta_{m,l}}(\beta_{m,l}\alpha_1 + \alpha_2) + \ln \beta_{m,l} \leq \ln d, \quad (6.85)$$

where $\Delta_{m,l} = T_{m,l+1} - T_{m,l}$ and $T_{m,M_m+1} = (m+1)\omega$.

(iv) the time delay $\tau(t)$ satisfies $\tau(t) \leq r \leq \Delta_0$ and

$$d^{M_0} e^{(\alpha_1 + \alpha_2)\delta} < 1, \quad (6.86)$$

where $\Delta = \max_{m,l} \{\Delta_{m,l}\}$, $\Delta_0 = \min_{m,l} \{\Delta_{m,l}\}$ and $M_0 = \min_m \{M_m\}$.

Then the trivial solution of error system (6.67) is asymptotically stable. It implies that slaver system (6.50) is synchronized with master system (6.47) by intermittent impulsive control $\{T_{m,l}, U_{m,l,i}\}$.

Proof: Because conditions (i)-(iii) are same with that of Theorem 6.4, $V(t)$ still satisfies (6.78). We have

$$V(t) < d \|V(T_{m,l})\|_r, \quad t \in [T_{m,l}, T_{m,l+1}), \text{ for } l = 2, 3, \dots, M_m,$$

where $T_{m,M_m+1} = (m+1)\omega$.

Since $r \leq \Delta_0$ in condition (iv), we have

$$\|V(T_{m,l+1})\|_r \leq \|V(T_{m,l+1})\|_{\Delta_{m,l}} < d \|V(T_{m,l})\|_r,$$

for $l = 1, 2, \dots, M_m - 1$. Thus,

$$V(t) < d^l \|V(T_{m,1})\|_r, \quad t \in [T_{m,l}, T_{m,l+1}), \text{ for } l = 2, 3, \dots, M_m, \quad (6.87)$$

where $T_{m,M_m+1} = (m+1)\omega$.

When $m = 0$, by (6.74) and (6.77), we have

$$V(t) \leq \|V(0)\|_r e^{(\alpha_1 + \alpha_2)\delta}, \quad t \in [0, \delta),$$

and

$$V(t) < d^l \|V(0)\|_r e^{(\alpha_1 + \alpha_2)\delta}, \quad t \in [T_{0,l}, T_{0,l+1}).$$

Similarly, when $m = 1$, we have

$$V(t) \leq \begin{cases} \|V(\omega)\|_r e^{(\alpha_1 + \alpha_2)\delta}, & t \in [\omega, \omega + \delta); \\ d^l \|V(\omega)\|_r e^{(\alpha_1 + \alpha_2)\delta}, & t \in [T_{1,l}, T_{1,l+1}). \end{cases}$$

When $t \in [m\omega, (m+1)\omega]$, we have

$$V(t) \leq \begin{cases} \|V(m\omega)\|_r e^{(\alpha_1 + \alpha_2)\delta}, & t \in [m\omega, m\omega + \delta); \\ d^l \|V(m\omega)\|_r e^{(\alpha_1 + \alpha_2)\delta}, & t \in [T_{m,l}, T_{m,l+1}). \end{cases}$$

Since $\tau(t) \leq r \leq \Delta_0$ in condition (iv), we have

$$\|V((m+1)\omega)\|_r \leq \|V((m+1)\omega)\|_{\Delta_0} \leq d^{M_m} \|V(m\omega)\|_r e^{(\alpha_1 + \alpha_2)\delta}.$$

In terms of condition (iv), we have

$$\|V((m+1)\omega)\|_r \leq d^{M_0} \|V(m\omega)\|_r e^{(\alpha_1 + \alpha_2)\delta} \leq \theta \|V(m\omega)\|_r,$$

where $\theta = d^{M_0} e^{(\alpha_1 + \alpha_2)\delta} < 1$.

Furthermore,

$$V(t) \leq \begin{cases} \theta^m \|V(0)\|_r e^{(\alpha_1 + \alpha_2)\delta}, & t \in [m\omega, m\omega + \delta); \\ \theta^m d^l \|V(0)\|_r, & t \in [T_{m,l}, T_{m,l+1}). \end{cases}$$

Thus,

$$\lim_{t \rightarrow \infty} V(t) = 0.$$

Similarly, for any $\epsilon > 0$, choose $\sigma = \sigma(\epsilon) > 0$ such that $\sigma < \sqrt{\frac{\lambda_m(P)}{\lambda_M(P)}} e^{-(\alpha_1 + \alpha_2)\delta} \epsilon$. When $\|e(0)\|_r < \sigma$, we have

$$\|e(t)\| < \epsilon. \quad (6.88)$$

Also,

$$\lim_{t \rightarrow \infty} \|e(t)\| = 0. \quad (6.89)$$

Therefore, the trivial solution $e(t)$ of error system (6.67) is asymptotically stable. It implies that slaver system (6.50) is synchronized with master system (6.47) by intermittent impulsive control $\{T_{m,l}, U_{m,l,i}\}$.

If the impulsive laws $\{T_{m,l}, U_{m,l,i}\}$ ($m = 0, 1, \dots$) are same in all control windows, $\Delta_{m,l} = \Delta_1$ and $B_{m,l} = B_s$, then we have the following corollaries.

Corollary 6.4: In IISS, assume that for an intermittent impulsive control law $\{T_{m,l}, U_{m,l,i}\}$

- (i) there exist a positive definite matrix P and constants $\alpha_1 > 0$, $\alpha_2 > 0$, $\xi_1 > 0$ and $\xi_2 > 0$ such that

$$-2PC + \xi_1 PAA^T P + \xi_2 PBB^T P + \frac{1}{\xi_1} L_f - \alpha_1 P \leq 0,$$

and

$$\frac{1}{\xi_2} L_f - \alpha_2 P \leq 0,$$

where $L_f = \text{diag}\{L_1^2, L_2^2, \dots, L_n^2\}$.

- (ii) there exists a real number $\beta \in (0, 1)$ such that

$$(I - B_s^T)P(I - B_s) - \beta P \leq 0.$$

- (iii) there exists a real number $d(\beta < d < 1)$ such that

$$\frac{\Delta_1}{\beta}(\beta\alpha_1 + \alpha_2) + \ln \beta \leq \ln d.$$

- (iv) the time delay upper bound r satisfies $\Delta_1 \leq r \leq \omega - \delta$ and

$$de^{(\alpha_1 + \alpha_2)\delta} < 1.$$

Then slaver system (6.50) is synchronized with master system (6.47) by intermittent impulsive control $\{T_{m,l}, U_{m,l,i}\}$.

Corollary 6.5: Assume that for an intermittent impulsive control law $\{T_{m,l}, U_{m,l,i}\}$

- (i) there exist a positive definite matrix P and constants $\alpha_1 > 0$, $\alpha_2 > 0$, $\xi_1 > 0$ and $\xi_2 > 0$ such that

$$-2PC + \xi_1 PAA^T P + \xi_2 PBB^T P + \frac{1}{\xi_1} L_f^2 I - \alpha_1 P \leq 0,$$

and

$$\frac{1}{\xi_2} L_f^2 I - \alpha_2 P \leq 0,$$

where $L_f = \text{diag}\{L_1^2, L_2^2, \dots, L_n^2\}$.

- (ii) there exists a real number $\beta \in (0, 1)$ such that

$$(I - B_s^T)P(I - B_s) - \beta P \leq 0.$$

- (iii) there exists a real number $d(\beta < d < 1)$ such that

$$\frac{\Delta_1}{\beta}(\beta\alpha_1 + \alpha_2) + \ln \beta \leq \ln d.$$

- (iv) the time delay $\tau(t)$ satisfies $\tau(t) \leq r \leq \Delta_1$ and

$$d^{M_1} e^{(\alpha_1 + \alpha_2)\delta} < 1,$$

where $M_1 = \lfloor \frac{\omega - \delta}{\Delta_1} \rfloor + 1$ and $\lfloor a \rfloor$ denotes the nearest integers less than or equal to a .

Then slaver system (6.50) is synchronized with master system (6.47) by intermittent impulsive control $\{T_{m,l}, U_{m,l,i}\}$.

6.2.4 Numeral Example

In this section, a numeral example is given to show the effectiveness of the main result.

Consider a typical Hopfield neural network as the master system, described by

$$\frac{dx(t)}{dt} = -Cx(t) + Af(x(t)) + Bf(x(t - \tau(t))) + J, \quad (6.90)$$

where

$$C = \begin{bmatrix} 1 & 0 \\ 0 & 1 \end{bmatrix}, A = \begin{bmatrix} 2.0 & -0.1 \\ -5.0 & 2.8 \end{bmatrix}, B = \begin{bmatrix} -1.6 & -0.1 \\ -0.3 & -2.5 \end{bmatrix}$$

$$f(x(t)) = \begin{bmatrix} \tanh x_1 \\ \tanh x_2 \end{bmatrix}, \quad \tau(t) = 1, \quad J = \begin{bmatrix} 0 \\ 0 \end{bmatrix}.$$

The chaotic behavior of system (6.90) is shown in Fig. 6.7. Firstly considering GISS, we choose impulsive control parameters: $\Delta_k = 1.1$ and $B_k = 0.90I$. Let $P = I$. Thus, conditions (6.54)-(6.57) are satisfied. By Theorem 6.3, we know that the corresponding slaver system is synchronized with master system (6.90) by general impulsive control with $\Delta_k = 1.1$ and $B_k = 0.90I$. The state trajectories of master and slave systems are shown in Fig. 6.8. The synchronization errors are shown in Fig. 6.9. Our simulation results show that when impulsive intervals satisfy $\Delta_k \leq 1.44$ the synchronization can be always achieved.

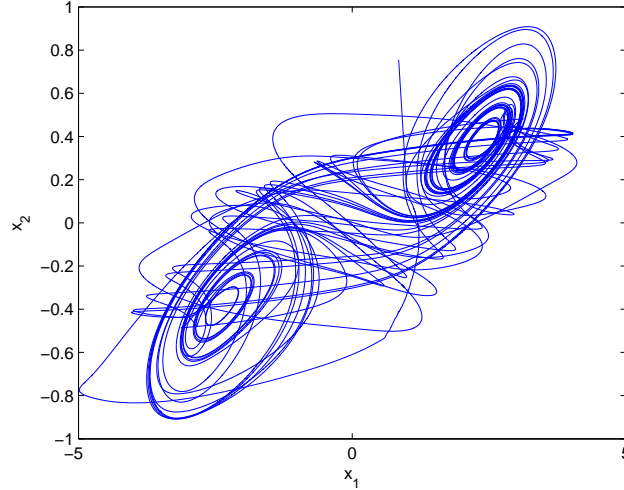


Figure 6.7: Phase portrait $x_1(t) - x_2(t)$ of DNNs (6.90) with system parameters $\Delta_{k,i} = 1.1$ and $B_k = 0.90I$.

Assume that $\omega = 10$ and $\delta = 5$, then the free windows are $[10m, 10m+5]$ and the control windows are $[10m + 5, 10m + 10]$. Since the free window width is greater than the impul-

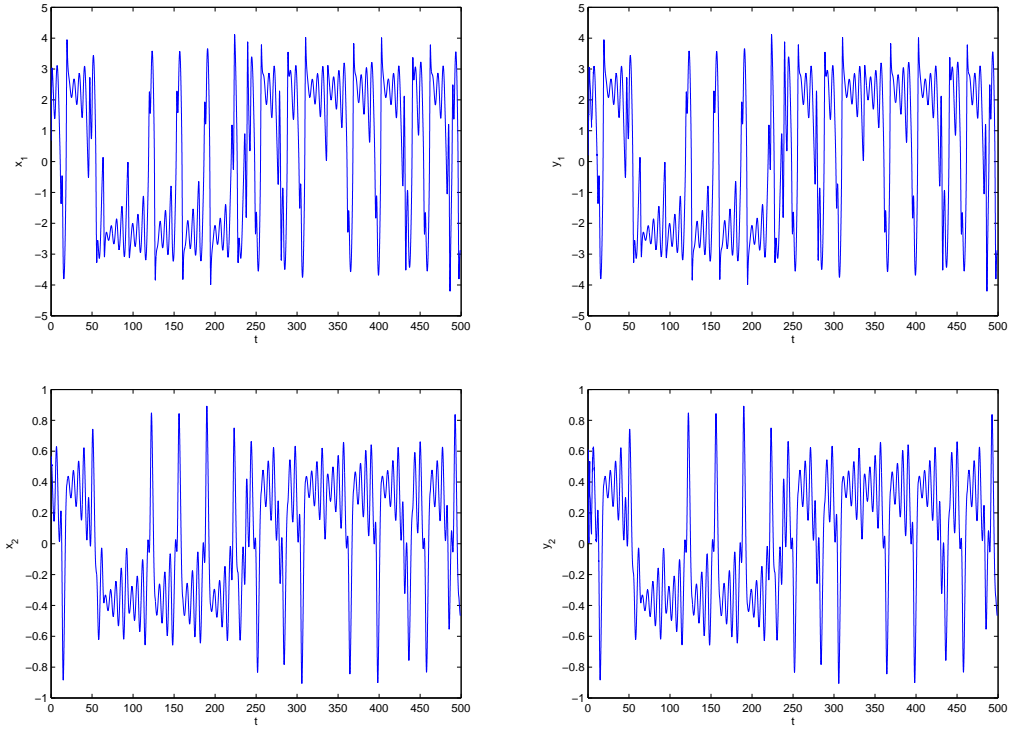


Figure 6.8: State trajectories of the master system (left) and the slave system in GISS.

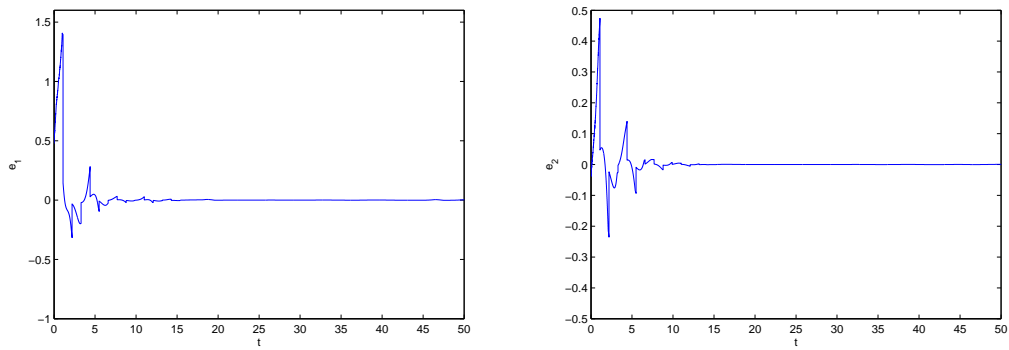


Figure 6.9: Synchronization errors in GISS: (a) $e_1(t)$ and (b) $e_2(t)$ with $\Delta_{k,i} = 1.1$ and $B_k = 0.90I$.

sive interval, GISS fails in this scenario. Now, considering IISS, choose control parameters $\Delta_{m,l} = 1.1$ and $B_{m,l} = 0.90I$. Let $P = I$. By Corollary 6.5, we know that the corresponding slaver system is synchronized with master system (6.90). The state trajectories of master and slave systems and synchronization errors are shown in Fig. 6.10-6.11. Simulation results show that when impulsive intervals satisfy $\Delta_k \leq 1.22$, the synchronization can be always achieved.

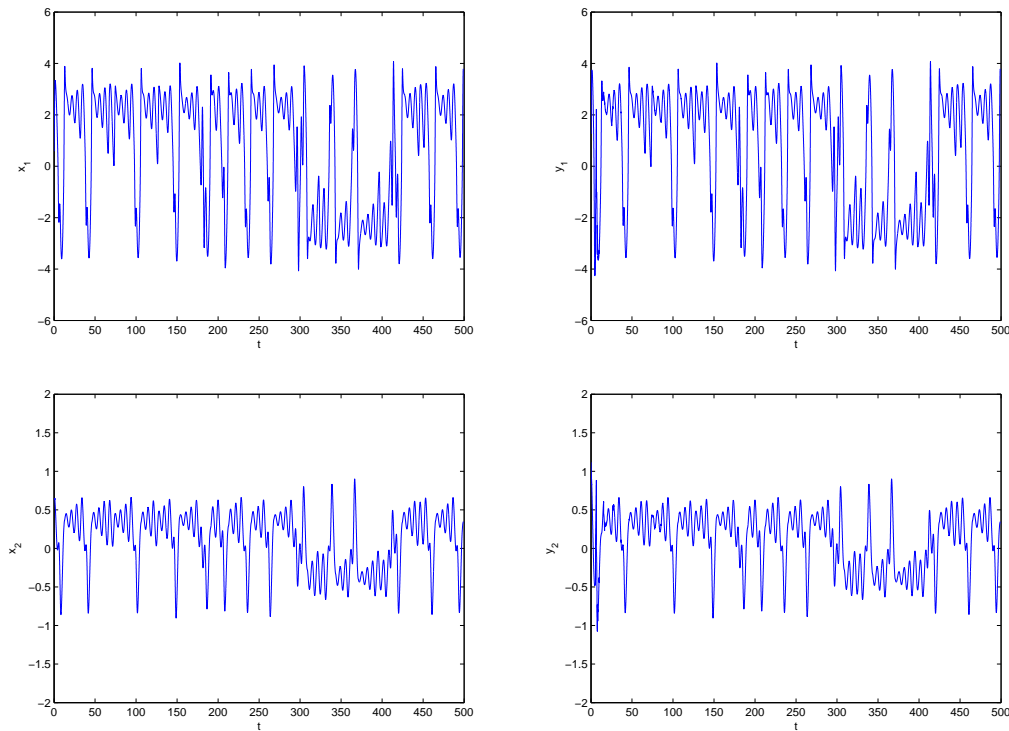


Figure 6.10: State trajectories of the master system (left) and the slave system in IISS.

Remark 6.4: In the above example, the control window width $\omega - \delta$ is a half of the whole period width ω . General impulsive synchronization approach is not applicable for this Scenario because the free window width δ is greater than the impulsive interval.

Next, fixing the control parameter $B_{m,l} = 0.90I$, we try to find out the relationship between the impulsive interval and the free window width to guarantee synchronization.

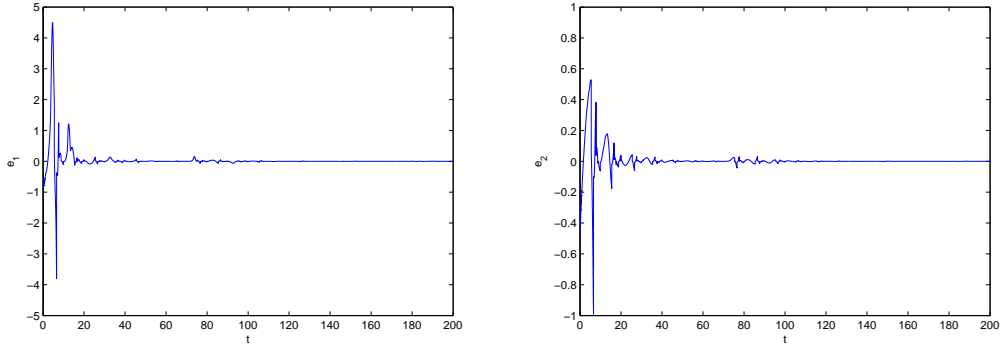


Figure 6.11: Synchronization errors in IISS: (a) $e_1(t)$ and (b) $e_2(t)$ with $\Delta_{k,i} = 1.1$ and $B_k = 0.90I$.

Simulation results are shown in Fig. 6.12.

Remark 6.5: Fig. 6.12 shows that the upper bound of the free window width will decrease with the impulsive interval increasing. In other words, to guarantee synchronization, if one wants to reduce the control window width, he needs to pay more frequent control in the control windows.

6.2.5 Summary

In this section, we have investigated intermittent impulsive synchronization of two delayed chaotic neural networks. We have presented a novel intermittent impulsive synchronization scheme to break through the limitation of the general impulsive synchronization scheme. In our synchronization scheme, the impulsive controller is only activated in the control windows, not in free windows. Several criteria to guarantee chaos synchronization of two coupled neural networks, based on Lyapunov-Razumikhin theory and LMI. One numeral example is given to shown how IISS breaks through the limit of the upper bound of impulsive intervals, different from GISS. IISS can be flexibly applied to the scenario where the control window is restricted. On the other hand, via reducing the control window width and decreasing the redundancy of the synchronization signals, one can further improve the secu-

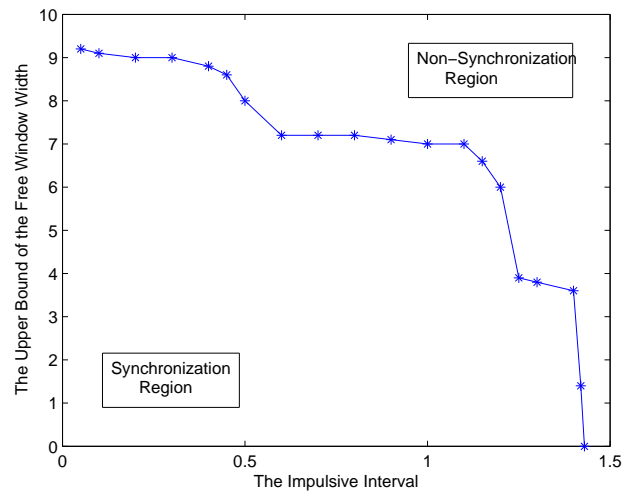


Figure 6.12: The relationship between the impulsive interval and the free window width to guarantee synchronization.

ity of chaos-based secure communication. Thus, IISS should have a great application and perspective.

Chapter 7

Chaos-Based Public-Key Cryptography

For chaos-based secure communication scheme, public-key cryptography is needed to encrypt synchronization signals and guarantee their security when synchronization signals are sent to the receiver across a public channel (unsafe channel). The whole framework is shown in Fig. 7.1. Issues 1 and 2 have been studied in detail in previous chapters. Issue 3, which is about encryption of synchronization signals, will be introduced in this chapter. Conventional public-key algorithms such as RSA, ElGamal and Elliptic Curve Cryptography are suitable for this encryption. Furthermore, we propose chaos-based public-key algorithms, which can be applied to our symmetric chaos-based secure communication to encrypt synchronization signals, and to analyze related security. Chaos-based public-key cryptography is becoming an active topic in public-key cryptography technology.

7.1 Kocarev's Algorithm

As mentioned before, Ljupco Kocarev and Zarko Tasev presented a public-key algorithm based on Chebyshev polynomials in 2003 [37], which is a milestone in chaos-based public-key cryptography research. The details are as follows.

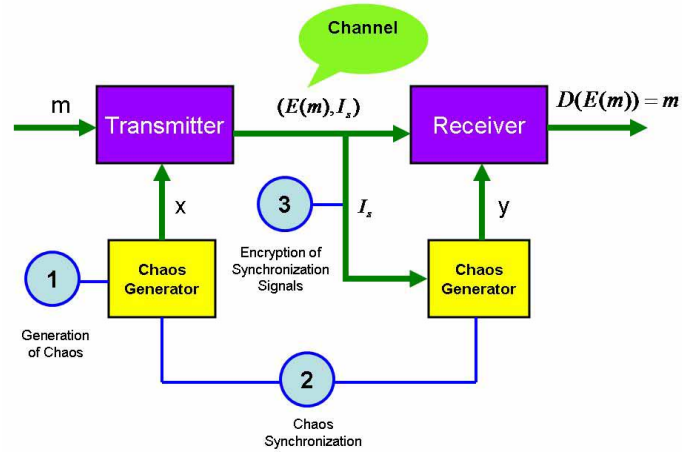


Figure 7.1: The framework diagram of symmetric chaos-based secure communication scheme.

Chebyshev maps: Chebyshev polynomial maps $T_p : R \rightarrow R$ with degree p is defined by

$$T_{p+1}(x) = 2xT_p(x) - T_{p-1}(x),$$

with $p = 1, 2, \dots$, $T_0 = 1$ and $T_1 = x$. Its domain is the interval $x \in [-1, 1]$. When $p > 1$, Chebyshev map is chaotic with positive Lyapunov exponent $\lambda = \ln(p)$.

Semi-group property:

$$T_r(T_s(x)) = T_{rs}(x).$$

An immediate consequence of this property is that Chebyshev polynomials commute under composition,

$$T_r(T_s(x)) = T_s(T_r(x)).$$

Kocarev's chaos-based public-key algorithm consists of three parts: key generation algorithm, encryption algorithm and decryption algorithm. The detail is followed. **Key Generation Algorithm:**

Key Generation Algorithm:

Alice, in order to generate the keys, does the following:

1. Generates a large integer s ;
2. Selects a random number $x \in [-1, 1]$ and computes $T_s(x)$;
3. Sets her public key to $(x, T_s(x))$ and her private key to s .

Encryption Algorithm:

Bob, in order to encrypt a message, does the following:

1. Obtains Alice's authentic public key $(x, T_s(x))$;
2. Represents the message as a number $m \in [-1, 1]$.
3. Generates a large integer r ;
4. Computes $T_r(x)$, $T_{rs}(x) = T_r(T_s(x))$ and $X = mT_{rs}(x)$;
5. Sends the cipher-text $C = (T_r(x), X)$ to Alice.

Decryption Algorithm:

Alice, to recover the plain-text m from the cipher-text C , does the following:

1. Uses her private key s to compute $T_{sr}(x) = T_s(T_r(x))$;
2. Recovers m by computing $m = X/T_{sr}(x)$.

7.2 Bergamo's Attack

Kocarev's chaos-based public-key algorithm looks perfect, which uses the semi-group property of Chebyshev maps to accomplish encryption and decryption by different keys. Specially, it is incomputable to derive the private key s from the public key $(x, T_s(x))$ because of the sensitivity of chaotic maps to initial conditions and system parameters. However, Chebyshev polynomials can be alternatively defined as follows,

$$T_p(x) = \cos(p \cdot \arccos(x)).$$

If an eavesdropper can find out an integer \bar{r} such that $T_{\bar{r}}(x) = T_r(x)$, he can recover m without secret key as follows.

Bergamo's Attack Algorithm [123]:

1. Computer an \bar{r} such that $T_{\bar{r}}(x) = T_r(x)$;

2. Evaluate $T_{\bar{r}s}(x) = T_{\bar{r}}(T_s(x))$;
3. Recover $m = X/T_{sr}(x)$.

Let Z be the set of integers and N the set of natural numbers. Define

$$P = \left\{ \frac{\pm \arccos(T_r(x)) + 2k\pi}{\arccos(x)} \mid k \in Z \right\}.$$

Thus, $\bar{r} \in P \cap N$.

7.3 Chaos-Based Public-Key Cryptography with Modified Chebyshev Polynomials

Bergamo's attack is built on the periodic property of Chebyshev polynomials, where cosine function is periodic. To avoid this kind of attack, Professor Kocarev extended his algorithms to modular arithmetic as follows.

Modified Chebyshev polynomials: Let $T_p: \{0, 1, \dots, N-1\} \rightarrow \{0, 1, \dots, N-1\}$ defined as

$$y = T_p(x)(\text{mod } N),$$

where x and N are integers.

Theorem 7.1 [124]: Modified Chebyshev polynomials commute under composition, i.e.,

$$T_p(T_q(x)(\text{mod } N))(\text{mod } N) = T_{pq}(x)(\text{mod } N).$$

Theorem 7.2 [124]: Let N be an odd prime and let $x \in Z$ such that $0 \leq x < N$. Then the period of the sequence $T_n(x)(\text{mod } N)$, for $n = 0, 1, \dots$, is a divisor of $N^2 - 1$.

7.3.1 ElGamal Encryption with Modified Chebyshev Polynomials

The ElGamal encryption is an asymmetric key encryption algorithm which can be viewed as a Diffie-Hellman key agreement in key transfer mode. Its security is based on the intractability

of the discrete logarithm problem. In the ElGamal encryption scheme, Alice generates a large random prime N and a generator x of the multiplicative group Z_N^* of integers modulo N . She also generates a random integer $s \leq N - 1$ and computes $A = x^s \pmod{N}$. Alice's public key is (x, N, A) ; Alice's private key is s . To encrypt a message m , Bob selects a random integer $r \leq N - 1$, computes $B = x^r \pmod{N}$ and $X = mA^r \pmod{N}$, and sends the cipher-text $c = (B, X)$ to Alice. To recover the original message m from c , Alice uses the private key s to recover m by computing $m = B^{-s}X \pmod{N}$. This decryption allows recovery of the original message because of $B^{-s}mA^r \equiv x^{-rs}mx^{rs} \equiv m \pmod{N}$.

ElGamal encryption with modified Chebyshev polynomials [124]:

Algorithm for key generation.

Alice does the following:

1. Generates a large random prime N and an initial integer x such that $x < N$;
2. Generates a random integer $s < N$ and compute $A = T_s(x) \pmod{N}$;
3. Alice's public key is (x, N, A) ; Alice's private key is s .

Algorithm for ElGamal encryption.

To encrypt a message m , Bob does the following:

- (a) Obtains Alice's public key (x, N, A) ;
- (b) Represents the message as an integer m in the range $0, 1, \dots, N - 1$;
- (c) Selects a random integer $r < N$;
- (d) Computes $B = T_r(x) \pmod{N}$ and $X = mT_r(A) \pmod{N}$;
- (e) Sends the cipher-text $c = (B, X)$ to Alice.

Algorithm for ElGamal decryption.

To recover the message m from c , Alice does the following:

- (a) Uses the private key s to compute $C = T_s(B) \pmod{N}$;
- (b) Recovers m by computing $m = XC^{-1} \pmod{N}$.

The proof of this algorithm follows from Theorem 7.1.

7.3.2 RSA Public-Key Encryption with Modified Chebyshev Polynomials

The RSA cryptosystem, named after its inventors, R. Rivest, A. Shamir, and L. Adleman, is the most widely used public-key cryptosystem. Its security is based on the intractability of the integer factorization problem. In the RSA algorithm, let $N = pq$ and $\phi = (p - 1)(q - 1)$, where p and q are two large random (and distinct) primes p and q . Alice selects a random integer e ($1 < e < \phi$) such that $\gcd(e, \phi) = 1$ and computes the unique integer d ($1 < d < \phi$) such that $ed \equiv 1 \pmod{\phi}$. Alice's public key is (N, e) ; Alice's private key is d . To encrypt a message m , Bob computes $c = m^e \pmod{N}$ and sends to Alice. To recover the message m from c , Alice should use the private key d to recover $m = c^d \pmod{N}$. Let $\pi_p(x) = x^p \pmod{N}$. The decryption in the RSA algorithm works because the functions π_e, π_d commute under composition and p is a periodic point of the function π_{ed} for each $m : m^{ed} \equiv m \pmod{N}$. The last follows from the following observation. Since $ed \equiv 1 \pmod{\phi}$, there exists an integer k such that $ed = 1 + k\phi$. Now, if $\gcd(m, p) = 1$, then by Fermat's little theorem $m^{p-1} \equiv 1 \pmod{p}$. Raising both sides of this congruence to the power of $k(q - 1)$ and then multiplying both sides by m yields $m^{ed} \equiv m \pmod{p}$. By the same argument $m^{ed} \equiv m \pmod{q}$. Finally, since p and q are distinct primes, it follows that $m^{ed} \equiv m \pmod{N}$ by Chinese remainder theorem.

RSA encryption with modified Chebyshev polynomials [125]:

Algorithm for key generation.

Alice does the following:

1. Generates two large distinct primes p and q , each roughly the same size;
2. Computes $N = pq$ and $\phi = (p - 1)(q - 1)$;
3. Selects a random integer e ($1 < e < \phi$) such that $\gcd(e, \phi) = 1$;
4. Computes the unique integer d ($1 < d < \phi$) such that $ed \equiv 1 \pmod{\phi}$;
5. Alice's public key is (N, e) ; Alice's private key is d .

Algorithm for encryption.

To encrypt a message m , Bob does the following:

- (a) Obtains Alice's public key (N, e) ;
- (b) Represents the message as an integer in the interval $[1, N - 1]$;
- (c) Computes $c = T_e(m)(\text{mod } N)$ and send to Alice.

Algorithm for decryption.

To recover the message m from c , Alice does the following:

- (a) Uses the private key d to recover $m = T_d(c)(\text{mod } N)$.

The proof of this algorithm follows from Theorem 7.1 and 7.2,

$$T_d(T_e(x)) \equiv T_{de}(x) \equiv T_{1+k\phi}(x) \equiv T_1(x) \equiv x(\text{mod } p).$$

7.3.3 An Example

In our chaos-based public-key secure communication system, suppose that the transmitter needs to send a synchronization signal $m = 11.223344$ with 6-digit precision (impulsive signal) to the receiver across a public channel. The following shows how the system works by RSA encryption with modified Chebyshev polynomials.

Firstly, the receiver selects two primes $p = 21787$ and $q = 3793$. Thus, $N = 82638091$ and $\phi = 6829053595064064$. Then he selects $e = 65537$, coprime with ϕ , and computes $d = 2150406320724737$. He publishes his public key $(N = 82638091, e = 65537)$ and keeps his private key $d = 2150406320724737$ secret.

To encrypt the synchronization signal m , the transmitter firstly maps m to integer set by $M = 10^6 m$. Then computes $c = T_{65537}(M)(\text{mod } N) = 12355612$ and send c to the receiver.

To decrypt this cipher c , the receiver computes $M = T_{2150406320724737}(c)(\text{mod } N) = 11223344$ and then recovers the original synchronization signal $m = 11.223344$ by the inverse map $m = 10^{-6} M$.

7.4 Summary

The two proposed chaos-based public-key algorithms with modified Chebyshev polynomials, ElGamal encryption with Chebyshev polynomials and RSA encryption with Chebyshev polynomials, possess the resistance to Bergamo's attack, which are both secure and practical and can be used to encrypt synchronization signals across the public channel in chaos-based secure communication.

Chapter 8

Conclusions and Future Work

In this chapter, the main contributions of this thesis are summarized, and followed by the future work.

8.1 Contributions

This thesis focus on studying chaos-based secure communication. The major contribution is to solve chaos synchronization. In addition, generation of chaotic and hyperchaotic systems is included and chaos-based public-key cryptography is introduced. The details can be summarized as follows:

- Firstly, we design a family of chaos and hyperchaos by first-order delay differential equation and present a systematical method to control this system to the cell attractors with desired number of positive Lyapunov exponents. By adjusting the corresponding system parameters, this system can generate complex chaotic behaviors. Furthermore, we introduce this kind of delay feedback control to well-known Chen system and generate multi-scroll Chen attractors. Also, this kind of control approach can be generalized to Chua system, Lorenz system, Jerk equation, etc.

- Secondly, aiming at the challenging problem, time delay in transmission and sample process, based on Lyapunov-Razumikhin technic, we achieve global asymptotical synchronization criteria by impulsive control. Furthermore, we generalize them to chaotic dynamical networks to realize network synchronization with delay. For general networks subject to different network nodes with uncertain system parameters, an adaptive synchronization approach is presented to guarantee network synchronization. Finally, to overcome the weakness of general impulsive synchronization scheme, i.e., there always exists an upper boundary to limit impulsive intervals during synchronization process, a novel synchronization scheme, intermittent impulsive synchronization scheme, is designed, which can not only be flexibly applied to the scenario where the control window is restricted and also improve the security of chaos-based secure communication, via reducing the control window width and decreasing the redundancy of the synchronization signals.
- Thirdly, chaos-based public-key cryptography is introduced to guarantee the security of synchronization signals across the public channel. Although the existing algorithms are not secure enough, compared to classic public-key algorithms such as RSA, ECC, etc, chaos-based public-key cryptography provides a new direction in modern cryptography technology. Thus, further research on new chaotic maps and new algorithms is required urgently.

8.2 Future Work

Our research has made a notable progress on chaos-based secure communication. Yet, there still exist some challenges between theoretical study and engineering application. This research is still a very wide-open field, and there are several new research directions to be explored to complement our efforts.

8.2.1 Synchronization Error Problem

In this thesis, we utilize Lyapunov method to prove chaos synchronization. i.e., synchronization errors converge to zero as time t goes to infinity. However, in reality, one usually requires that synchronization errors can decline to a desired level in a short time. In other words, the decreasing velocity of synchronization errors is a very important index in engineering application. Thus, exponential chaos synchronization, which implies that synchronization errors converge to zero at a constant exponential rate, becomes a very useful issue. In addition, there always exists stochastic disturbance in communication process. So stochastic synchronization is also a significant research topic.

8.2.2 Computer Realization of Chaos-Based Algorithms

In this thesis, we have introduced some chaos-based public-key cryptography algorithms and their drawbacks. However, the most challenging problem is that all chaotic maps represented on computer turn into periodic maps due to the limit of computer precision. Thus, how to design suitable chaotic maps with large enough period on computer to avoid collision is an important research issue. Without doubt, chaos-based public-key cryptography is a potential direction in future. However, up to now, there does not exist a perfect algorithm which can bear comparison with conventional public-key cryptography algorithms such as RSA, ElGamal, Elliptic Curve Cryptography, etc. There is much work on designing chaos-based public-key algorithms needed to be done. In addition, we will consider other latest research progresses such as chaos-based hash function, chaos-based pseudo-random number generator, chaos-based key agreement protocol and related security issues.

Bibliography

- [1] J. H. Poincaré, “Sur le problme des trois corps et les quations de la dynamique. divergence des sries de m. lindstedt,” *Acta Mathematica*, vol. 13, no. 3, pp. 1–270, 1890.
- [2] E. N. Lorenz, “Deterministic non-periodic flow,” *Journal of the Atmospheric Sciences*, vol. 20, pp. 130–141, 1963.
- [3] E. Ott, C. Grebogi, and J. A. Yorke, “Controlling chaos,” *Journal of the Atmospheric Sciences*, vol. 64, no. 11, pp. 1196–1199, 1990.
- [4] K. Pyragas, “Continuous control of chaos by self-controlling feedback,” *Physics Letters A*, vol. 170, pp. 421–428, Nov 1992.
- [5] L. M. Pecora and T. L. Carroll, “Synchronization in chaotic systems,” *Phys. Rev. Lett.*, vol. 64, no. 8, pp. 821–824, Feb 1990.
- [6] F. Liu, Y. Ren, X. Shan, and Z. Qiu, “A linear feedback synchronization theorem for a class of chaotic systems,” *Chaos, Solitons & Fractals*, vol. 13, pp. 723–730, March 2002.
- [7] Y. Wang, Z.-H. Guan, and H. O. Wang, “Feedback and adaptive control for the synchronization of chen system via a single variable,” *Physics Letters A*, vol. 312, no. 1, pp. 34–40, 2003.

- [8] Y. Hong, H. Qin, and G. Chen, “Adaptive synchronization of chaotic systems via state or output feedback control,” *International Journal of Bifurcation and Chaos in Applied Sciences and Engineering*, vol. 11, pp. 1149–1158, 2001.
- [9] J. Suykens, P. Curran, and L. Chua, “Master-slave synchronization using dynamic output feedback,” *International Journal of Bifurcation and Chaos*, vol. 7, no. 3, pp. 671–680, 1997.
- [10] J. A.-R. Ricardo Femat and G. Fernández-Anaya, “Adaptive synchronization of high-order chaotic systems: a feedback with low-order parametrization,” *Physica D: Non-linear Phenomena*, vol. 139, no. 3, pp. 231–246, May 2000.
- [11] J. Suykens, P. Curran, and L. Chua, “Robust synthesis for master-slave synchronization of lur’e systems,” *Circuits and Systems I: Fundamental Theory and Applications, IEEE Transactions on [see also Circuits and Systems I: Regular Papers, IEEE Transactions on]*, vol. 46, no. 7, pp. 841–850, Jul 1999.
- [12] G.-P. Jiang, G. Chen, and W.-S. Tang, “A new criterion for chaos synchronization using linear state feedback control,” *International Journal of Bifurcation and Chaos in Applied Sciences and Engineering*, vol. 13, pp. 2343–2352, 2003.
- [13] T. Yang and L. Chua, “Impulsive stabilization for control and synchronization of chaotic systems: theory and application to secure communication,” *Circuits and Systems I: Fundamental Theory and Applications, IEEE Transactions on [see also Circuits and Systems I: Regular Papers, IEEE Transactions on]*, vol. 44, no. 10, pp. 976–988, Oct 1997.
- [14] T. Yang, L.-B. Yang, and C.-M. Yang, “Impulsive synchronization of lorenz systems,” *Physics Letters A*, vol. 226, no. 6, pp. 349–354, March 1997.
- [15] J. Sun, Y. Zhang, and Q. Wu, “Impulsive control for the stabilization and synchronization of lorenz systems,” *Physics Letters A*, vol. 298, no. 2, pp. 153–160, June 2002.

- [16] W. Xie, C. Wen, and Z. Li, "Impulsive control for the stabilization and synchronization of lorenz systems," *Physics Letters A*, vol. 275, no. 1, pp. 67–72, October 2000.
- [17] A. I. Panas, T. Yang, and L. O. Chua, "Experimental results of impulsive synchronization between two chua's circuits," *International Journal of Bifurcation and Chaos*, vol. 8, no. 3, pp. 639–644, 1998.
- [18] J. Suykens, T. Yang, and L. Chua, "Impulsive synchronization of chaotic lur'e systems by measurement feedback," *International Journal of Bifurcation and Chaos*, vol. 8, no. 6, pp. 1371–1381, 1998.
- [19] M. Itoh, T. Yang, and L. Chua, "Conditions for impulsive synchronization of chaotic and hyperchaotic systems," *International Journal of Bifurcation and Chaos in Applied Sciences and Engineering*, vol. 11, pp. 551–560, 2001.
- [20] T. Yang and L. Chua, "Impulsive control and synchronization of nonlinear dynamical systems and application to secure communication," *International Journal of Bifurcation and Chaos*, vol. 7, no. 3, pp. 645–664, 1997.
- [21] L. Kocarev, K. Halle, K. Eckert, L. Chua, and U. Parlitz, "Experimental demonstration of secure communications via chaotic synchronization," *International Journal of Bifurcation and Chaos*, vol. 2, no. 3, pp. 709–713, 1992.
- [22] K. M. Cuomo and A. V. Oppenheim, "Circuit implementation of synchronized chaos with applications to communications," *Phys. Rev. Lett.*, vol. 71, no. 1, pp. 65–68, Jul 1993.
- [23] L. Kocarev and U. Parlitz, "General approach for chaotic synchronization with applications to communication," *Phys. Rev. Lett.*, vol. 74, no. 25, pp. 5028–5031, Jun 1995.

- [24] G. Kolumban, M. Kennedy, and L. Chua, “The role of synchronization in digital communications using chaos. i . fundamentals of digital communications,” *Circuits and Systems I: Fundamental Theory and Applications, IEEE Transactions on [see also Circuits and Systems I: Regular Papers, IEEE Transactions on]*, vol. 44, no. 10, pp. 927–936, Oct 1997.
- [25] ———, “The role of synchronization in digital communications using chaos. ii. chaotic modulation and chaotic synchronization,” *Circuits and Systems I: Fundamental Theory and Applications, IEEE Transactions on [see also Circuits and Systems I: Regular Papers, IEEE Transactions on]*, vol. 45, no. 11, pp. 1129–1140, Nov 1998.
- [26] I. Fischer, Y. Liu, and P. Davis, “Synchronization of chaotic semiconductor laser dynamics on subnanosecond time scales and its potential for chaos communication,” *Phys. Rev. A*, vol. 62, no. 1, p. 011801, Jun 2000.
- [27] A. Argyris, D. Syvridis, L. Larger, V. Annovazzi-Lodi, P. Colet, I. Fischer, J. Garcia-Ojalvo, C. R. Mirasso, L. Pesquera, and K. A. Shore, “Chaos-based communications at high bit rates using commercial fibre-optic links,” *NATURE*, vol. 7066, pp. 343–346, 2005.
- [28] M. P. Kennedy and G. Kolumbn, “Digital communications using chaos,” *Signal Processing*, vol. 80, no. 7, pp. 1307–1320, July 2000.
- [29] T. Hasler, M. Schimming, “Chaos communication over noisy channels,” *International Journal of Bifurcation and Chaos*, vol. 10, pp. 719–736, 2000.
- [30] S. Wang, J. Kuang, J. Li, Y. Luo, H. Lu, and G. Hu, “Chaos-based secure communications in a large community,” *Phys. Rev. E*, vol. 66, no. 6, p. 065202, Dec 2002.
- [31] A. Abel and W. Schwarz, “Chaos communications-principles, schemes, and system analysis,” *Ieee Institute of Electrical and Electronics*, vol. 90, no. 5, pp. 691–710, 2002.

- [32] G. Mazzini, G. Setti, and R. Rovatti, "Chaotic complex spreading sequences for asynchronous ds-cdma. i. system modeling and results," *Circuits and Systems I: Fundamental Theory and Applications, IEEE Transactions on [see also Circuits and Systems I: Regular Papers, IEEE Transactions on]*, vol. 44, no. 10, pp. 937–947, Oct 1997.
- [33] M. Sushchik, L. Tsimring, and A. Volkovskii, "Performance analysis of correlation-based communication schemes utilizing chaos," *Circuits and Systems I: Fundamental Theory and Applications, IEEE Transactions on [see also Circuits and Systems I: Regular Papers, IEEE Transactions on]*, vol. 47, no. 12, pp. 1684–1691, Dec 2000.
- [34] F. Lau, M. Yip, C. Tse, and S. Hau, "A multiple-access technique for differential chaos-shift keying," *Circuits and Systems I: Fundamental Theory and Applications, IEEE Transactions on [see also Circuits and Systems I: Regular Papers, IEEE Transactions on]*, vol. 49, no. 1, pp. 96–104, Jan 2002.
- [35] T. Schimming and M. Hasler, "Optimal detection of differential chaos shift keying," *Circuits and Systems I: Fundamental Theory and Applications, IEEE Transactions on [see also Circuits and Systems I: Regular Papers, IEEE Transactions on]*, vol. 47, no. 12, pp. 1712–1719, Dec 2000.
- [36] A. Kisel, H. Dedieu, and T. Schimming, "Maximum likelihood approaches for non-coherent communications with chaotic carriers," *Circuits and Systems I: Fundamental Theory and Applications, IEEE Transactions on [see also Circuits and Systems I: Regular Papers, IEEE Transactions on]*, vol. 48, no. 5, pp. 533–542, May 2001.
- [37] L. Kocarev and Z. Tasev, "Public-key encryption based on chebyshev maps," *Circuits and Systems, 2003. ISCAS '03. Proceedings of the 2003 International Symposium on*, vol. 3, pp. 28–31, May 2003.
- [38] L. Kocarev and M. Sterjev, "Public-key encryption with chaos," *Physica D: Nonlinear Phenomena*, vol. 14, no. 4, pp. 1078–1081, Nov 2004.

- [39] P. Bergamo, P. D'Arco, A. De Santis, and L. Kocarev, "Security of public-key cryptosystems based on chebyshev polynomials," *Circuits and Systems I: Regular Papers, IEEE Transactions on [Circuits and Systems I: Fundamental Theory and Applications, IEEE Transactions on]*, vol. 52, no. 7, pp. 1382–1393, July 2005.
- [40] J. Gleick, *Chaos: Making a New Science*. Penguin, December 1988.
- [41] W. Diffie and M. Hellman, "Multi-user cryptographic techniques," *AFIPS Proceedings 45*, p. 109C112, June 1976.
- [42] —, "New directions in cryptography," *IEEE Transactions on Information Theory*, vol. 22, no. 6, pp. 644–654, Nov. 1976.
- [43] R. Rivest, A. Shamir, and L. Adleman, "A method for obtaining digital signatures and public-key cryptosystems," *Communications of the ACM*, vol. 21, no. 2, p. 120C126, 1978.
- [44] C. Cocks, "A note on 'non-secret encryption'," *CESG Research Report*, November 1973.
- [45] O. Rössler, "An equation for continuous chaos," *Phys. Lett. A*, vol. 57, pp. 397–398, 1976.
- [46] G. Chen and T. Ueta, "Yet another chaotic attractor," *International Journal of Bifurcation and Chaos*, vol. 9, no. 7, pp. 1465–1466, July 1999.
- [47] H. Gottlieb, "Question #38. what is the simplest jerk function that gives chaos?" *American Journal of Physics*, vol. 64, no. 5, pp. 525– 525, May 1996.
- [48] K. Ikeda and K. Matsumoto, "High-dimensional chaotic behavior in systems with time-delayed feedback," *Physica D*, vol. 29, pp. 223–235, 1987.

- [49] A. Medio and M. Lines, *Nonlinear dynamics: a primer*. Cambridge, UK: Cambridge University Press, 2001.
- [50] C. Robinson, *Dynamical systems: stability, symbolic dynamics, and chaos*. Boca Raton, Florida: CRC Press, 1995.
- [51] V. Lakshmikantham, D. Bainov, and P. Simeonov, *Theory of impulsive differential equations*. Singapore: World Scientific, May 1989.
- [52] X. Liu, “Stability results for impulsive differential systems with applications to population growth models,” *Dynamical Systems*, vol. 9, no. 2, pp. 163–174, 1994.
- [53] T. Yang and L. Chua, “Secure communication via chaotic parameter modulation,” *Circuits and Systems I: Fundamental Theory and Applications*, vol. 43, pp. 817–819, 1996.
- [54] G. Ballinger and X. Liu, “Boundedness of solutions of impulsive systems,” *Nonlin. Stud.*, vol. 4, pp. 121–131, 1997.
- [55] A. Khadra, X. Liu, and X. Shen, “Robust impulsive synchronization and its application to communication security,” *Int. J. Dyn. Continuous Discr. Impulsive Syst.*, vol. 10, pp. 403–416, 2003.
- [56] ———, “Application of impulsive synchronization to communication security,” *IEEE Trans. Circuits Syst. I*, vol. 50, pp. 341–351, 2003.
- [57] X. Liu, “Stability of linear delay systems via impulsive control,” *Int. J. Dyn. Continuous Discr. Impulsive Syst. B*, vol. 13, pp. 791–803, 2006.
- [58] O. Rössler, “An equation for hyperchaos,” *Phys. Lett. A*, vol. 71, pp. 155–157, 1979.
- [59] J. Goedgebuer, L. Larger, and H. Porte, “Optical cryptosystem based on synchronization of hyperchaos generated by a delayed feedback tunable laser diode,” *Phys. Rev. Lett.*, vol. 80, pp. 2249–2252, 1998.

- [60] J. Peng, E. Ding, M. Ding, and W. Yang, “Synchronizing hyperchaos with a scalar transmitted signal,” *Phys. Rev. Lett.*, vol. 76, pp. 904–907, 1996.
- [61] G. Grassi and S. Mascolo, “Synchronizing hyperchaotic systems by observer design,” *Circuits and Systems II: Analog and Digital Signal Processing*, vol. 46, pp. 478–483, 1999.
- [62] C. Li and G. Chen, “Chaos and hyperchaos in the fractional-order rossler equations,” *Physica A*, vol. 341, pp. 55–61, 2004.
- [63] Y. Li, W. Tang, and G. Chen, “Generating hyperchaos via state feedback control,” *Int. J. Bifurc. Chaos*, vol. 15, pp. 3367–3375, 2005.
- [64] M. E. Yalcin, “Multi-scroll and hypercube attractors from a general jerk circuit using josephson junctions,” *Chaos, Soliton & Fractals*, vol. 34, pp. 1659–1666, 2007.
- [65] Z. Yan and P. Yu, “Hyperchaos synchronization and control on a new hyperchaotic attractor,” *Chaos, Soliton & Fractals*, vol. 35, pp. 333–345, 2008.
- [66] J. Lu, F. Han, X. Yu, and G. Chen, “Generating 3-d multi-scroll chaotic attractors: a hysteresis series switching method,” *Automatica*, vol. 40, pp. 1677–1687, 2004.
- [67] A. Elwakil and S. Ozoguz, “Multi-scroll chaotic oscillators: the nonautonomous approach,” *IEEE Trans. Circuits Syst., II: Analog Digital Signal Process*, vol. 53, pp. 862–866, 2006.
- [68] Y. Li, X. Liu, and H. Zhang, “Dynamical analysis and impulsive control of a new hyperchaotic system,” *Mathematical and Computer Modelling*, vol. 42, pp. 1359–1374, 2005.
- [69] J. Lu, X. Yu, and G. Chen, “Switching control for multi-scroll chaos generation: an overview,” *Physics and Control*, vol. 2, pp. 420–428, 2003.

- [70] J. Lu, G. Chen, X. Yu, and H. Leung, "Generating multi-scroll chaotic attractors via switching control," *Control Conference*, vol. 3, pp. 1753–1761, 2004.
- [71] X. Liu, K. Teo, H. Zhang, and G. Chen, "Switching control of linear systems for generating chaos," *Chaos, Solitons & Fractals*, vol. 30, pp. 725–733, 2006.
- [72] T. Hartley, C. Lorenzo, and H. K. Qammer, "Chaos in a fractional order chua's system," *IEEE Trans. Circuits Syst. I*, vol. 42, pp. 485–490, 1995.
- [73] W. Ahmad and J. Sprott, "Chaos in fractional-order autonomous nonlinear systems," *Chaos, Solitons & Fractals*, vol. 16, pp. 339–351, 2003.
- [74] C. Li and G. Chen, "Chaos in the fractional order chen system and its control," *Chaos, Solitons & Fractals*, vol. 22, pp. 549–554, 2004.
- [75] L. Chua, C. Wu, A. Huang, and G. Zhong, "A universal circuit for studying and generating chaos. i. routes to chaos," *IEEE Trans. Circuits Syst. I*, vol. 40, pp. 732–744, 1993.
- [76] M. Yalcin, J. Suykens, J. Vandewalle, and S. Ozoguz, "Families of scroll grid attractors," *Int. J. Bifurc. Chaos*, vol. 12, pp. 23–41, 2002.
- [77] A. Elwakil and M. Kennedy, "Construction of classes of circuit-independent chaotic oscillators using passive-only nonlinear devices," *IEEE Trans. Circuits Syst. I*, vol. 48, pp. 289–307, 2001.
- [78] H. Lu and Z. H. Sprott, "Chaotic behavior in first-order autonomous continuous-time systems with delay," *IEEE Trans. Circuits Syst. I*, vol. 43, pp. 700–702, 1996.
- [79] A. Namajunas, K. Pyragas, and A. Tamasevicius, "An electronic analog of the mackey-glass system," *Phys. Lett. A*, vol. 201, pp. 42–46, 1995.

- [80] A. Tamasevicius, G. Mykolaitis, and S. Bumeliene, “Delayed feedback chaotic oscillator with improved spectral characteristics,” *Electron. Lett.*, vol. 42, pp. 736–737, 2006.
- [81] L. Wang, X. Yang, J. Vandewalle, and S. Ozoguz, “Generation of multi-scroll delayed chaotic oscillator,” *Electron. Lett.*, vol. 42, pp. 1439–1441, 2006.
- [82] M. Yalcin and S. Ozoguz, “N-scroll chaotic attractors from a first-order time-delay differential equation,” *CHAOS*, vol. 17, p. 033112, 2007.
- [83] J. Farmer, “Chaotic attractors of an infinite-dimensional dynamical system,” *Physica D*, vol. 4, pp. 366–393, 1982.
- [84] J. Hale and S. Lunel, *Introduction to Functional Differential Equations*. New York: Springer-Verlag, 1993.
- [85] G. Grassi and S. Mascolo, “Nonlinear observer design to synchronize hyperchaotic systems via a scalar signal,” *IEEE Trans. Circuits Syst. I (Special Issue on Chaos Synchronization, Control and Applications)*, vol. 44, pp. 1011–1013, 1997.
- [86] R. Amritkar and N. Gupte, “Synchronization of chaotic orbits: The effect of a finite time step,” *Phys. Rev. E*, vol. 47, pp. 3889–3895, 1993.
- [87] T. Stojanovski, L. Kocarev, and U. Parlitz, “Driving and synchronizing by chaotic impulses,” *Phys. Rev. E*, vol. 54, pp. 2128–2131, 1996.
- [88] L. M. Pecora, T. L. Carroll, G. Johnson, D. Mar, and K. S. Fink, “Synchronization stability in coupled oscillator arrays: Solution for arbitrary configurations,” *Int. J. Bifurc. Chaos*, vol. 10, no. 2, pp. 273–290, 2000.
- [89] C. W. Wu, “Perturbation of coupling matrices and its effect on the synchronizability in arrays of coupled chaotic systems,” *Phys. Lett. A*, vol. 319, no. 5-6, pp. 495–503, 2003.

- [90] X. Wang and G. Chen, "Synchronization in small-world dynamical networks," *Int. J. Bifurc. Chaos*, vol. 12, no. 1, pp. 187–192, 2002.
- [91] Z. Li and G. Chen, "Robust adaptive synchronization of uncertain dynamical networks," *Phys. Lett. A*, vol. 324, no. 2-3, pp. 166–178, 2004.
- [92] B. Liu, X. Liu, G. Chen, and H. Wang, "Robust impulsive synchronization of uncertain dynamical networks," *IEEE Trans. Circuits Syst. I*, vol. 52, no. 7, pp. 1431–1441, 2005.
- [93] S. H. Strogatz, "Exploring complex networks," *Nature*, vol. 410, no. 6825, pp. 268–276, 2001.
- [94] X. Wang and G. Chen, "Complex network: Small-world, scale-free and beyond," *IEEE Circuits Syst. Mag.*, vol. 3, no. 1, pp. 6–20, 2003.
- [95] J. Lü and G. Chen, "A time-varying complex dynamical network models and its controlled synchronization criteria," *IEEE Trans. Auto. Contr.*, vol. 50, no. 6, pp. 841–846, 2005.
- [96] E. Bai and K. Lonngren, "Sequential synchronization of two Lorenz systems using active control," *Chaos, Solitons & Fractals*, vol. 11, no. 7, pp. 1041–1044, 2000.
- [97] J. Park, "Synchronization of Genesio chaotic system via backstepping approach," *Chaos, Solitons & Fractals*, vol. 27, no. 5, pp. 1369–1375, 2006.
- [98] C. Wang and S. Ge, "Adaptive synchronization of uncertain chaotic systems via backstepping design," *Chaos, Solitons & Fractals*, vol. 12, no. 7, pp. 1199–1206, 2001.
- [99] M. Yassen, "Adaptive chaos control and synchronization for uncertain new chaotic dynamical system," *Phys. Lett. A*, vol. 350, no. 1, pp. 36–43, 2006.

- [100] C. Chen, G. Feng, and X. Guan, “Robust synchronization of chaotic lur’e systems via delayed feedback control,” *Phys. Lett. A*, vol. 321, no. 5-6, pp. 344–354, 2004.
- [101] T. Liao and N. Huang, “Control and synchronization of discrete-time chaotic systems via variable structure control technique,” *Phys. Lett. A*, vol. 234, no. 4, pp. 262–268, 1997.
- [102] H. Yau, “Design of adaptive sliding mode controller for chaos synchronization with uncertainties,” *Chaos, Solitons & Fractals*, vol. 22, no. 2, pp. 341–347, 2004.
- [103] J. Park, “Chaos synchronization between two different chaotic dynamical systems,” *Chaos, Solitons & Fractals*, vol. 27, no. 2, pp. 549–554, 2006.
- [104] M. Yassen, “Chaos synchronization between two different chaotic systems using active control,” *Chaos, Solitons & Fractals*, vol. 23, no. 1, pp. 131–140, 2005.
- [105] H. Chen, “Synchronization of two different chaotic systems: a new system and each of the dynamical systems lorenz, chen and lu,” *Chaos, Solitons & Fractals*, vol. 25, no. 5, pp. 1049–1056, 2005.
- [106] L. Huang, R. Feng, and M. Wang, “Synchronization of chaotic systems via nonlinear control,” *Phys. Lett. A*, vol. 320, no. 4, pp. 271–275, 2004.
- [107] H. Zhang, W. Huang, Z. Wang, and T. Chai, “Adaptive synchronization between two different chaotic systems with unknown parameters,” *Phys. Lett. A*, vol. 350, no. 5-6, pp. 363–366, 2006.
- [108] H. Salarieh and M. Shahrokhi, “Adaptive synchronization of two different chaotic systems with time varying unknown parameters,” *Chaos, Solitons & Fractals*, vol. 37, no. 1, pp. 125–136, 2008.
- [109] J. Zhou, J. Lu, and J. Lü, “Adaptive synchronization of an uncertain complex dynamical network,” *IEEE Trans. Auto. Contr.*, vol. 51, no. 4, pp. 652–656, 2006.

- [110] ———, “Pinning adaptive synchronization of a general complex dynamical network,” *Automatica*, vol. 44, no. 4, pp. 996–1003, 2008.
- [111] J. Suykens and G. Osipov, “Introduction to focus issue: synchronization in complex networks,” *CHAOS*, vol. 18, p. 037101, 2008.
- [112] A. Huang, L. Pivka, C. Wu, and M. Franz, “Chua’s equation with cubic nonlinearity,” *Int. J. Bifurcation Chaos*, vol. 6, no. 12, pp. 2175–2222, 1996.
- [113] E. Sanchez and J. Perez, “Input-to-state stability (iss) analysis for dynamic nn,” *IEEE Trans. Circuits Syst. I*, vol. 46, no. 11, pp. 1395–1398, 1999.
- [114] T. Huang, C. Li, and X. Liu, “Synchronization of chaotic systems with delay using intermittent linear state feedback,” *CHAOS*, vol. 18, no. 3, p. 033122, 2008.
- [115] M. Gilli, “Strange attractors in delayed cellular neural networks,” *IEEE Trans. Circuits Syst. I*, vol. 40, no. 11, pp. 849–853, 1993.
- [116] H. Lu, “Chaotic attractors in delayed neural networks,” *Phys. Lett. A*, vol. 298, no. 2, pp. 109–116, 2002.
- [117] G. Chen, J. Zhou, and Z. Liu, “Global synchronization of coupled delayed neural networks and applications to chaotic cnn model,” *Int. J. Bifur. Chaos*, vol. 14, no. 7, pp. 2229–2240, 2004.
- [118] X. Liao, G. Chen, and E. Sanchez, “Delay-dependent exponential stability analysis of delayed neural networks: an lmi approach,” *Neural Networks*, vol. 15, no. 7, pp. 855–866, 2002.
- [119] J. Cao and J. Wang, “Global asymptotic and robust stability of recurrent neural networks with time delays,” *IEEE Trans. Circuits Syst. I*, vol. 52, no. 2, pp. 417–426, 2005.

- [120] J. Cao and J. Lu, "Adaptive synchronization of neural networks with or without time-varying delay," *CHAOS*, vol. 16, p. 013133, 2006.
- [121] J. Park, "Synchronization of cellular neural networks of neutral type via dynamic feedback controller," *Chaos, Solitons & Fractals*, vol. 42, no. 3, pp. 1299–1304, 2009.
- [122] J. Lu and G. Chen, "Global asymptotical synchronization of chaotic neural networks by output feedback impulsive control: An lmi approach," *Chaos, Solitons & Fractals*, vol. 41, no. 5, pp. 2293–2300, 2009.
- [123] P. Bergamo, P. D'Arco, A. D. Santis, and L. Kocarev, "Security of public-key cryptosystems based on chebyshev polynomials," *IEEE Trans. Circuits Syst. I*, vol. 52, no. 7, pp. 1382–1393, 2005.
- [124] L. Kocarev, J. Makraduli, and P. Amato, "Public-key encryption based on chebyshev polynomials," *Circuits, Systems, Signal Processing*, vol. 24, no. 5, pp. 497–517, 2005.
- [125] L. Kocarev, M. Sterjev, A. Fekete, and G. Vattay, "Public-key encryption with chaos," *CHAOS*, vol. 14, no. 4, pp. 1078–1082, 2004.